The Synthesis of Adipic Acid from Cyclohexene Utilising Green Procedures

Thesis submitted in accordance with the requirement of Cardiff University for the degree of Doctor of Philosophy

Owen Rogers

2017-2021

Abstract

The possibility of replacing cyclohexane in the adipic acid process with cyclohexene is assessed in this investigation. This is accomplished using green procedures such as low temperatures, solventless conditions and green oxidants. This cyclohexene-based process would proceed in 2 steps, in which the first step would be an epoxidation of cyclohexene to form cyclohexanediol (CHD), using O_2 or H_2O_2. The second step would be the aerobic oxidative cleavage of CHD to adipic acid.

The aerobic epoxidation of cyclohexene was achieved using Au supported on graphite or graphene. A comparison of the effect on reactivity between impregnation (WI) and sol immobilisation (SI) preparation methods was assessed and testing was conducted using solventless and radical initiator-free conditions. The selectivity to the epoxide could be enhanced using a WO_3 co-catalyst and subsequently hydrolysed to CHD with the addition of water, where a maximum yield of 17 % to the diol was achieved. The comparison of preparation methods showed that SI catalysts were more reproducible and far more active, however, selectivity towards CHD was lower than for the WI catalyst by 8.0 %. In addition, this study also reveals that the formation of CHD was limited by the formation of the allylic hydroperoxyl species where a maximum selectivity of 50 % was attainable. A further study showed the aerobic oxidation of cyclohexene could also be achieved using graphitic oxide catalysts in a non-metal approach with selectivity observed towards allylic products. To improve selectivity to CHD, H_2O_2 was utilised alongside Au / $Cs_3PW_{12}O_{40}$ and Au / $Cs_4SiW_{12}O_{40}$ catalysts, where the phosphotungstic acid supports displayed significantly more activity than their Si counterparts. Using solventless conditions and a sequential addition of H_2O_2, a conversion of 14.4 % and 100 % selectivity to CHD was reached after 8 h. However, the effect of Au was found to be minimal, with an increase of 5.4 % and 3.4 % conversion observed for Au / $Cs_2PW_{12}O_{40}$ and Au / $Cs_3PW_{12}O_{40}$ respectively.

For the oxidative cleavage of CHD to adipic acid (AA) $Na_2V_6O_{15}$, $Cu_xV_2O_6$ (x = 0.25, 0.3 0.5) and $AgVO_3$ were prepared. The addition of sodium, copper or silver to the vanadium oxide structure was to reduce the leaching observed when compared to V_2O_5. Leaching could be decreased to 5% for $AgVO_3$ and was also significantly reduced with $Cu_{0.33}V_2O_5$, compared to 88.4% with V_2O_5. Na was less successful in stabilising the material with 36.8 % of the total V found to leach into solution. However, despite significant stabilisation of vanadium in the bronze structures, we show that as little as 7.6 ppm of a homogeneous vanadium species in the reaction solution can cause the selective oxidation of 2-hydroxycyclohexanone to AA, with a yield of 1.5 %. The homogeneous vanadium species was discovered to be in the +5 oxidation state and ^{51}V NMR studies determined that the predominant species was a decavanadate molecule which was unbound to other reaction products or metal

Acknowledgements

This thesis is a culmination of work that I would not have been able to achieve without the input of several people. My four years as part of the catalysis CDT and doctorate years at Cardiff University have helped develop and mould me as a chemist and person. This research would not have been possible without the funding from the EPSRC and Invista, which has also allowed me to attend and present my work at conferences in Bangkok, Aachen and Loughborough.

I would like to thank my supervisors Graham Hutchings, Stu Taylor and Keith Whiston for their knowledge, support and guidance throughout my PhD. Also instrumental in my work was Sam Pattisson who was always available for advice and discussion and was key in my development as a chemist and kept me focused on the task at hand. My thanks also go to Rebecca Engel who was a very helpful influence on my studies.

Aspects of this work have also been reliant on the expertise of some of the technical staff at Cardiff University, namely, Dave Morgan for XPS, Tom Davies for TEM, Nia Richards for in situ XRD and finally Greg Shaw for training and ensuring the smooth running of equipment.

The office has seen many people come and go who have made my doctorate entertaining, namely, Joe and Matt, who make up the CDThree, and have both impacted on my life inside and outside of chemistry. If it wasn't for this time, I wouldn't have met my girlfriend, Annie, who has managed to put up with me even when isolating together in lockdown and helped keep me focused on finishing my thesis. Finally, I would like to thank my family who have supported me and provided me with guidance during stressful time.

Publication list

1. O. Rogers, S. Pattisson, J. Macginley, R. Engel, K. Whiston, S. Taylor and G. Hutchings, Catalysts., 2018, DOI:https://doi.org/10.3390/catal8080311.

2. S. Pattisson, O. Rogers, K. Whiston, S. H. Taylor and G. J. Hutchings, Catal. Today, 2019, DOI:https://doi.org/10.1016/j.cattod.2019.04.053.

3. O. Rogers, S. Pattisson, R. V. Engel, R. L. Jenkins, K. Whiston, S. H. Taylor and G. J. Hutchings, Catal. Sci. Technol., 2020, DOI:10.1039/d0cy00914h.

Table of Contents

1 Introduction

1.1 Project aims

The aim of this project is to investigate new methods for producing adipic acid (AA) from cyclohexene, which can compete with the current cyclohexane-based process. Presently, AA is produced from a feedstock of cyclohexane which is oxidised using nitric acid leading to the formation of N_2O.[1] The emission of N_2O can cause ozone depletion, acid rain, and global warming.[2] However, it is common for the N_2O to be catalytically abated in the waste gas streams.[3]

The synthesis of AA could be achieved using green procedures. For example, by using cyclohexene as a starting material, greener oxidants such as molecular oxygen (O_2) or hydrogen peroxide (H_2O_2) could be used.[4,5] Scheme 1-1 shows a basic schematic of the target reaction.

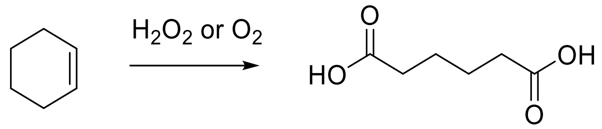

Scheme 1-1 Basic schematic of overall targeted reaction

1.2 Project overview

Chapter 3: Initiator-free solventless oxidation of cyclohexene using O_2.

Chapter 4: Oxidation of cyclohexene to cyclohexanediol using H_2O_2.

Chapter 5: Oxidation of cyclohexanediol to adipic acid.

1.3 Industrial production of adipic acid

AA is a bulk chemical used predominantly to produce nylon-6,6 as well as in coatings, plasticisers, detergents, footwear, textiles and electronics. Nylon-6,6 is a copolymer consisting of the monomers AA and hexamethylenediamine.[6] The use of AA in automobile production as tyre reinforcements and in lightweight auto parts production is expected to spur growth on in this area, which is projected to reach 8 billion pounds by 2022. The main production base is China, which held a 32.99 % production share in 2015. China, North America, EU and Asia (ex. China) are the main consumption bases, while China holds 28.83 % consumption share, North America holds 23.92 %, EU holds 23.45 %, and Asia (ex. China) holds 14.34 % consumption share in 2015.[7] AA is produced at quantities of around 4 million metric tonnes annually.[8]

The majority of AA is produced using a feedstock of cyclohexane.[6,9,10] The most common approach, which is illustrated in Scheme 1-2, requires cyclohexane to be heated to between 125 - 165 °C in air, at pressures of 6 – 15 atm. This is achieved alongside a homogeneous cobalt naphthenate catalyst. The reaction proceeds at low conversions around 4-8 % to achieve a high selectivity of 80 % to a cyclohexanone and cyclohexanol mixture, known as KA (ketone alcohol) oil.[11] The unreacted cyclohexane fraction can then be distilled for reuse. The KA oil is then oxidised in a second-step using an excess amount of nitric acid in the presence of a copper (II) and ammonium metavanadate catalyst.[11] This oxidation by nitric acid produces AA at a high conversion and high selectivity but is accompanied by the release of N_2O. In industry, this release of N_2O is subsided by the catalytic treatment of waste gases with around 95 % efficiency.[12] However, the production of nitric acid also provides an indirect source of N_2O emissions from AA synthesis. Nitric acid production represents the largest source of N_2O emission in the chemical industry, with a global annual emission of 400 kt.[13]

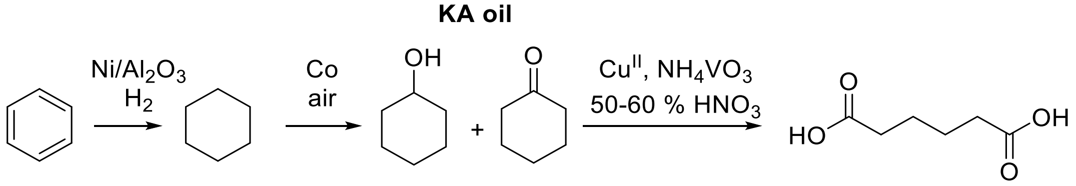

Scheme 1-2 Current process for industrial production of adipic acid using cyclohexane.

There are two processes which contribute significantly to the anthropogenic emissions of N_2O, nitric acid production and AA production. Combined, these processes contribute to 0.2 % of global emissions of N_2O.[1] Major AA producers have researched into various abatement technologies to control the levels of emission, with even some industrial companies looking at the reuse of the N_2O stream. One example is the use of the N_2O-containing stream for the hydroxylation of benzene to phenol, which can then undergo hydrogenation into cyclohexanol.[14,15] In addition, a vast amount of research has gone into the search for alternative feedstocks of which cyclohexene is one of these "greener" alternatives.[16] Currently, the only industrialised production process for cyclohexene is via the partial hydrogenation of benzene, developed by Asahi Chemical Industry Co., employing a Ru-Zn catalyst.[17] However, further improvements to this process have made cyclohexene a viable alternative.[18] This is achieved by design of the catalyst and reaction conditions to separate cyclohexene from the Ru-Zn catalytic surface. Such an effect can be provoked by the difference in solubilities between cyclohexene and benzene, notably in water.[19] Therefore a hydrophilic environment around the catalyst particles can help decrease further reduction of cyclohexene.[20] These improvements could see the price of cyclohexene decrease to an economically sustainable amount and the utilisation of air as an oxidant could also be an attractive prospect for an alternative AA process.

1.4 Principles of green chemistry

The principles of green chemistry were developed to address some of the problems caused by scientists and engineers in trying to improve standards of living, such as improving crop protection, designing new medicines and commercial products. In the early 1960s with the publication of Rachel Carson's *Silent Spring*,[21] the realisation of the negative impact of synthetic chemicals became apparent and a movement to understanding the effects that various synthetic chemicals were having on the environment was started. Carson emphasised the effect of pesticides but over the next few decades the effect of other synthetic chemicals on the environment has become increasingly apparent.

The solution to these problems was coined as "green chemistry" by Paul Anastas and John Warner and is defined as: "The utilisation of a set of principles that reduces or eliminates the use or generation of hazardous substances in the design, manufacture and application of chemical products". The list below gives an outline of the points which would make a process or reaction greener.[22]

1. **Waste prevention** – it is more efficient not to produce waste than to clean it up.
2. **Atom economy** – synthetic methods should be designed to maximise the incorporation of all materials used in the process.
3. **Less hazardous synthesis** – whenever possible, synthetic methodologies should be designed to use and generate substances that possess little or no toxicity to your health and the environment.
4. **Design benign chemicals** – chemical products should be designed to preserve efficacy of the function while reducing toxicity.
5. **Benign solvents and auxiliaries** – the use of auxiliary substances should be avoided whenever possible and should be harmless.
6. **Design for energy efficiency** – energy requirements should be recognised for their environmental and economic impact and should be minimised.
7. **Use of renewable feedstocks** – raw materials and feedstocks should be renewable when possible.
8. **Reduce derivatives** – unnecessary derivatisation should be avoided when possible.
9. **Catalysis (vs. Stoichiometric)** – catalytic reagents reduce energy demands, increase rate of reaction and increase selectivity to desired product.
10. **Design for degradation** – chemical products should be designed so that they do not persist in the environment and degrade into benign products.

11. **Real-time analysis for pollution prevention** – analytical methodologies need to be further developed to allow for real-time in-process monitoring and control prior to the formation of hazardous substances.
12. **Inherently benign chemistry for accident prevention** – substances should be chosen as to minimise the potential for chemical accidents.

These points outline the principles of green chemistry. In summary, processes should be designed to minimise the amount of waste produced through prevention, processes should be atom and energy efficient, use renewable energy resources and materials, and avoid using toxic or hazardous solvents.

A problem with oxidations is they are usually performed using stoichiometric amounts of highly damaging oxidants such as nitric acid, chromium salts, chlorates, permanganates or organic peroxides.[23,24] The use of these oxidants can result in the production of large amounts of waste and can they also be expensive. The use of more a benign oxidant, such as molecular oxygen or air is a much cheaper alternative and offers a more sustainable alternative to stoichiometric reactants. In addition, H_2O_2, is a reagent which is more benign as it produces only water as a by-product.[25] Its drawbacks are that it is associated with safety risks for transportation and in its expense. The development of new processes aims to eliminate the production of waste at its source and down-stream of production, which are key aspects of the principles of green chemistry and a goal that catalysis can have a role in achieving.

1.5 The role of catalysis

The application of catalysts in the chemical industry is ubiquitous, ranging from pharmaceuticals to polymers and in petroleum processing. More than 90 % of all industrial processes are based on catalysis.[22] Therefore, the future development of catalysts plays a massive role in the pursuit of green chemistry and creating a sustainable environment. The careful design of catalysts that can activate inert starting materials as well as enhance reaction rates will decrease the current dependence on reactive and toxic reagents. A movement towards catalytic processes instead of methods which require stoichiometric reagents/oxidants will benefit the progression towards more sustainable atom economies. This can be extended to the use of catalysts in the design of new polymers and materials that remove the need for additives such as plasticisers and flame retardants, which will allow the materials to be reused in a high value-retaining manner.[26]

1.6 Gold-based catalysis

1.6.1 History of gold

Gold, as a bulk material, has always been important in history and been treasured as a symbol of wealth and religious devotion. Other historic uses of gold exist as a method of exchanging money and date back as far as Egyptian Pharaohs commissioning gold tokens around 2700 BCE.[27] Many of its qualities that made it so important then, such as its resistance to corrosion and scarcity, still lend it much importance today for many of the same reasons, among others. The first uses of gold nanoparticles only came much later and existed mainly as method for the coloration of glass in the seventeenth century. This use of it in glass was made by Johann Kunckel (c. 1637 – 1703) and discovery to create the nanoparticles to add to the melted glass was made by Andreas Cassius in 1685.[28] This was achieved by the dissolution of gold metal in *aqua regia* and then precipitation of metallic gold by a mixture of stannous and stannic chloride.[29]

The use of gold nanoparticles in catalysts only came in the 1970s and 80s when it was discovered that very small Au nanoparticles exhibited activity for alkene hydrogenation and in CO oxidation particularly when supported on metal oxides.[30,31] In 1987 Haruta and co-workers discovered that small nanoparticles below 3 nm supported on a reducible support such as TiO_2 catalysed the oxidation of CO at ambient temperatures igniting an interest in the Au catalysis debate.[30]

1.6.2 Commercialisation of gold catalysts in hydrochlorination of acetylene

Gold has since shown increasing importance in other environmentally significant reactions and in some has become commercially exploited. The hydrochlorination of acetylene is a key example of the commercialisation of gold catalysts.[32,33] The industrial catalyst used for this process was traditionally a 5–12 wt. % $HgCl_2$ supported on high surface area activated carbon.[34] Acetylene itself was mainly produced in coal-rich countries until the development of what is known as the balanced reaction which uses natural gas to form vinyl chloride monomer (VCM), however, this is mainly used in western societies. China still uses the process from coal due to their abundance of this resource and produces about 13 million tons of VCM using a mercury catalyst. The main drawbacks from using a mercury catalyst arose from its volatility at the reaction temperature leading to a loss of mercury and short catalyst lifetimes.[35] This loss of mercury to the environment also creates environmental problems which are unsustainable.

Shinoda et al.[36] correlated the activity of metal chlorides supported on activated carbons with their electron affinity. This provided the foundations for Hutchings to make a prediction that Au would be the best catalyst,[37] which was then proved experimentally for this reaction. This was achieved by plotting the reaction rate of acetylene hydrochlorination with the electrode potential of the reaction of M^{2+} + 2 e^-.[38,39] The success of the gold catalyst owed much to the preparation method whereby the Au precursor was dissolved in *aqua regia* and then impregnated onto the carbon support. This resulted in small nanoparticles of the size of 4.8 nm in diameter. The Hg and Au catalyst showed deactivation under the reaction with the Au catalyst deactivating at a slower rate. However, unlike in the Hg catalyst where the metal was lost to the gaseous phase, the Au stayed on the support. A rise in nanoparticle diameter was observed but not attributed to the loss in activity. Instead this loss in activity was attributed to the change in the electronic state of the Au atoms with a higher majority of Au(III) compared to Au(0) in the fresh catalysts. Beneficially, the Au catalyst could be also be regenerated using Cl_2, HCl, or NO when introduced into the reaction feed unlike a Hg-based catalyst.[40] The deactivation of the catalyst could also be reduced by using Au precursors containing soft donor ligands such as thiocyanates which have a greater stability meaning reduction of Au(III) to Au(0) became more difficult. The greater stability of S-containing Au complexes meant water could be used as a medium for catalyst preparation instead of *aqua regia* which is environmentally hazardous and a stumbling block when it comes to making a process industrially viable. As a result, Johnson Matthey built a plant in Shanghai dedicated to the production of Au/C catalysts for VCM production.[32]

The study of Au for the hydrochlorination of acetylene represents an interesting case because unlike in most catalytic systems it is the cationic species of Au that is active for the reaction rather than the metallic species.[41–43] Au monometallic and Au alloy catalysts have already been commercialised in other reactions notably in the manufacture of methyl acrylate where a Au-Ni catalyst is used and also in Au-Pd alloys which are active for CO oxidation in automobile applications and in the manufacture of the vinyl acetate monomer.[44–47]

1.6.3 Gold in hydrogen peroxide synthesis

A further application of Au nanoparticles is in the synthesis of hydrogen peroxide, which is produced on a scale of about 2 million tonnes a year.[48] H_2O_2 is a high value commodity chemical which has applications across industry and in household cleaning goods. Currently, H_2O_2 is produced through the anthraquinone process (Scheme 1-3) which was developed by BASF in 1939 and is only economically viable when carried out in large scale.[49,50] This makes synthesising H_2O_2 through the direct reaction between H_2 and O_2 and attractive proposition. This is a very complex reaction due to the instability of H_2O_2 either by further hydrogenation or by decomposition, which is accompanied by the release of O_2, both processes result in the formation of water. Recent advances have shown development in using Au nanoparticles and in its alloy with Pd for this purpose.[51,52]

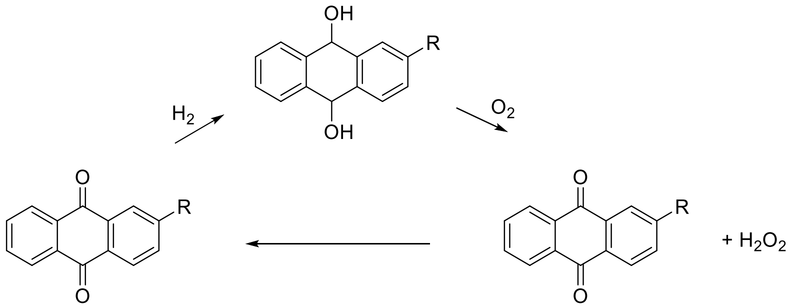

Scheme 1-3 Production of H_2O_2 through the anthraquinone process

Work on the direct synthesis of H_2O_2 has been extensively studied by the Hutchings group.[42,52–55] The first report that explored the use of Au nanoparticles was reported by Landon et al. in 2002.[56] In this study a Au/Al_2O_3 catalyst showed activity for the direct synthesis of H_2O_2 owing to its ability as an oxidation catalyst and also as a hydrogenation catalyst. This same report also was the first to document the alloying of Au and Pd to give an enhanced activity.[56] This was followed up by work by Ishihara et al. in 2005.[57] In this investigation a 1 % Au/SiO_2 catalyst exhibited promising activity compared to its monometallic Pd counterpart when they were tested without halide promoters. However, it was shown that the addition of a 1 wt % Pd to the Au/SiO_2 gave much improved rates.[57] The importance of using bimetallic materials to direct selectivity towards H_2O_2 has been extensively reported in the Hutchings group and was notably studied by Edwards et al. where a Pd-Au alloyed catalyst showed greater efficiency for H_2O_2 production than its monometallic counterparts.[55,58,59] It was also noted that when these bimetallic catalysts were placed onto a TiO_2 or Al_2O_3 support core-shells structures were formed. This research was followed up by Howe et al. where microwaves were used to prepare a Au-Pd alloy catalyst supported on TiO_2 reducing the preparation time for these catalysts and producing a catalyst which was stable for four reaction cycles.[60]

Additives also play a key role in this reaction. The addition of acids helps to suppress the base-catalysed decomposition of H_2O_2. The addition of acids such as nitric, sulfuric, phosphoric, and hydrochloric acids shown to be essential in achieving high yields of H_2O_2 in Pd and AuPd systems.[61] These additives led to this process being more expensive and less industrially viable. The use of recoverable solid acids to this reaction can increase its feasibility, for this purpose Cs-exchanged phosphotungstic acids have shown potential. In studies by Park et al. an insoluble $Cs_{2.5}H_{0.5}PW_{12}O_{40}$ heteropolyacid supported on Pd/MCF (mesostructured cellular foam) showed high catalytic activity for this reaction.[62] These heteropolyacids were investigated further by Lewis et al. showing that a solid acid additive has a promotional effect on H_2O_2 formation and stabilisation.[53] In the same group, work by Ntainjua et al. has shown that these polyacids can also be substituted with Au and Pd giving more efficient catalysts than Au-Pd/C catalysts previously reported by the group.[63] These polyacids acids were studied in further depth by Freakley et al. with a 5 % Au /2.5 % Pd/$Rb_{2.5}H_{0.5}PW_{12}O_{40}$ showing the greatest activity under their conditions.[64]

The nature of the support has a significant impact on the catalyst activity and selectivity. The most common supports in the direct synthesis of H_2O_2 have been carbon, SiO_2, Al_2O_3 and TiO_2 when using metallic Au-Pd catalysts. Much like the use of polyoxometalates an acidic support can have beneficial effects on the activity of catalysts. Park and co-workers noticed a volcano-shape trend when increasing the ZrO_2 content of their Pd/TZ-75 catalysts, the catalyst with the highest surface acidity was also the one with the highest activity.[65] This acidity is reported to prevent the decomposition of H_2O_2 and inhibit the formation of water. Gemo et al. came to similar conclusions in research focused on the Al doping of mesoporous SBA-15. In this research it was demonstrated that the use of Al as a dopant led to increased catalytic productivity and selectivity, which was due to the number of Bronsted acid sites available.[66] This effect of Bronsted acid sites was investigated further by Park and co-workers who varied the Si:Al ratio with H-ZSM-5 catalysts showing that the greater the amount of acid sites led to the highest H_2O_2 yield.[67] Developments in flow reactor technology and the collaboration between experimental and theoretical chemists to developing new catalysts could see this commercialised by the end of the 21st century.[52]

1.6.4 Liquid phase oxidation of alcohols

Liquid phase oxidation over heterogeneous catalysts is an area of great importance for the synthesis of organic chemicals. A significant area of research in liquid phase is the oxidation of alcohols.[68–70] Research by Prati et al. in 1998 showed the catalytic potential of Au for the oxidation of vicinal diols to α-hydroxy carboxylates with O_2 in a basic solution. High selectivities (90-100 %) and conversions (80-94 %) were achieved for the oxidation of ethan-1,2-diol and propane-1,2-diol to glycolic acid and hydroxyacetone respectively. This was achieved with Au/C and Au/Al_2O_3 catalysts.[71] This was followed up by later research in the same group with the oxidation of glycol to glycolate with Au catalysts showing the highest selectivity compared to Pd or Pt counterparts. The catalysts in this research were prepared through sol immobilisation techniques and deposited onto carbon or oxide supports (alumina or titania). Interestingly it was also noted that larger nanoparticles of 7-8 nm achieved high conversions with the carbon supports which contrasted with the oxide supports where small nanoparticles below 4 nm were favoured.[72]

1.6.4.1 Oxidation of cinnamyl alcohol to cinnamaldehyde

Among heterogeneously catalysed oxidations, the use of cinnamyl alcohol as a substrate is widely used. The interest in cinnamyl alcohol is due it being a constituent in lignin and due to its simple aromatic allylic alcohol. The product formed from its oxidation is cinnamaldehyde (Scheme 1-4), which is an important intermediate in organic transformations and has applications across the food industry and perfume industries.

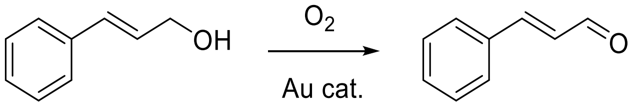

Scheme 1-4 Oxidation of Cinnamyl Alcohol to Cinnamaldehyde

Corma and co-workers investigated a Au/CeO_2 catalyst, showing their high activity for the aerobic oxidation of cinnamyl alcohol.[73] Their high activity was due to the high density of positive Au atoms which could act as Lewis acid sites. Cerium nanoparticles in this example has a significant role in the support as it facilitated oxygen activation and the reoxidation of metal hydrides. The support also provided the stability for these positive Au atoms by its strong interactions with the support and achieved 99 % selectivity and 98 % converison.[73] This work was followed up by Dimitratos et al. in 2006 using a bimetallic 1 % Au/Pd/C catalyst.[74] It was found that using that bimetallic Au-Pd catalysts significantly enhanced the liquid-phase oxidation of cinnamyl alcohol with the Au-Pd providing a synergistic effect. However, Au-Pt alloying was found to be detrimental.[74] Since the deactivation of heterogeneous catalysts can be difficult to investigate in batch reactors, Au-Pd/TiO_2 catalysts were examined in packed bed capillary microreactors by Wu et al.[75] Through this investigation it was discovered that catalyst deactivation was more severe at high reaction temperature and high oxygen concentration.[75] A higher deactivation rate was noted when oxygen concentration was higher and when higher Pd leaching was observed.[75] More recently in 2018, Rucinska et al. investigated the autoxidation of cinnamyl alcohol using Au/Pd catalysts.[76] In addition to investigating the auto-oxidation in this reaction, preparation methods of catalysts were also analysed.[76] In this investigation the effect of sol immobilisation and impregnation catalysts were analysed.[76] Sol immobilisation catalysts were shown to prevent the auto-oxidation catalyst by splitting the peroxides/hydroperoxides caused by the autoxidation process thereby enabling a high selectivity to cinnamaldehyde.[76] The larger particles prepared via an impregnation method are less active for the oxidation and results suggested that both autoxidation and catalytic mechanisms occurred simultaneously.[76]

1.6.4.2 Oxidation of alcohols and aldehydes to carboxylic acids

Aliphatic and aromatic aldehydes can be converted to carboxylic acids under mild reaction conditions using H_2O_2, peracids, NaOCl, or O_3 as oxidants.[77,78] Homogeneous systems are common with the use of metal salts, such as, Mn(II), Cu(II) or Ni(II) alongside O_2 and have been used on industrial scales.[79] Heterogenous catalysts have also shown potential, with high yields of carboxylic acids reported for the liquid phase oxidation of aromatic aldehydes using O_2 at atmospheric pressure with an organic solvent alongside Pt or Pd catalysts.[80] However, the first use of a Au catalyst for this reaction was in 2005 by Corma et al. where Au/CeO_2 was reported as a highly active and selective catalyst for the oxidation of aliphatic and aromatic aldehydes to the corresponding carboxylic acids.[81] Similarly, Au/MgO was also reported with high yields to corresponding carboxylic acids and achieved in the absence of a base.[82] Biella et al. showed that Au/C was also active for oxidising aldehydes and carboxylic acids in aqueous solution under mild conditions. This catalyst also maintained this activity after five repeated tests.[83]

The oxidation of alcohols to carboxylic acids the absence of a base is also an area of interest. This reduces the number of reaction steps and a neutralisation post-reaction would be unnecessary leading to more benign by-products. However, Au catalysts when used for this purpose often require the use of bases and reports of base-free oxidation of alcohols to carboxylic acids are rare. In 2006, Christensen et al. reported the first oxidation of an alcohol to carboxylic acid using a Au catalyst reporting a yield of 83 % and a conversion of 97 %.[84] The catalyst used in this research was Au/$MgAl_2O_4$.[84] In this same study Pt and Pd were also substituted for Au but showed significantly lower yields, with 16 % and 60 % yield for Pt and Pd respectively.[84] Work by Christensen and co-workers followed up this research by comparing the activity of a Au/TiO_2 catalyst with the Au/$MgAl_2O_4$ catalyst.[85] These catalysts were found to exhibit similar activities and with careful selection of the reaction conditions, yields of 90-95 % selectivity to acetic acid could be achieved.[85] This investigation also offered insight into the reaction pathway and the authors proposed that the rate-determining step was found to be the dehydrogenation of ethanol to produce acetaldehyde (Scheme 1-5).[85] Other Au/MO_x reported to have high selectivities in this reaction are Au/ZnO,[86] Au/SiO_2[87] and Au/$NiCuO_x$.[88]

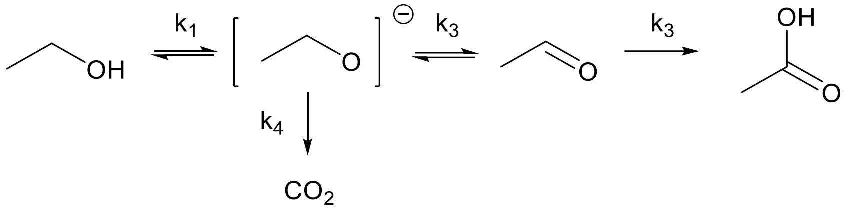

Scheme 1-5 Reaction pathway suggested by Jørgensen et al. where CH_3CH_2O is the dehydrogenation intermediate.[85]

The oxidation of long-chain aliphatic alcohols is more difficult because they are less reactive than the previous examples using ethanol. The first report of the base-free oxidation of an aliphatic alcohol to carboxylic acid was using unsupported platinum nanoparticles.[89] The first example of Au in this reaction was reported by Ishida et al. when oxidising 1-octanol as a model substrate using Au/NiO, achieving selectivities to octanoic acid of 87 % and full conversion.[90] This contrasted with

Au/CeO_2 which selectively produced octyl octanoate to 82 % selectivity in the same study.[90] More recently work has shown that Au/Mg-doped $ZnAl_2O_4$[91] and Au/NiTi-LDH[92] can also perform this base-free oxidation at a selectivity of 99 % and also a conversion of 99 %.

1.6.5 Epoxidation of linear and cyclic alkenes

1.6.5.1 Linear alkenes

The epoxidation of alkenes is an important process industrially and in organic synthesis. Epoxidation can be achieved with various oxidants but is commonly accomplished using stoichiometric oxidants, however this can be expensive and lead to poor atom economies.[93] Extensive research has focused on the oxidation of propene to propene oxide (PO) which is an important bulk chemical intermediate and has applications in the production of a range of commercial commodities. Several processes are carried out on an industrial scale but suffer from some drawbacks (Scheme 1-6), such as, the production of hazardous waste (chlorohydrin process),[94–96] the dependence on the economics of a co-product (styrene monomer process), the requirement of multiple processing steps (chlorohydrin, styrene monomer, hydrogen peroxide process) and the use of an expensive reactant (hydrogen peroxide process).[97–103] It is to this end that the one-step synthesis of PO from propene remains a key area of scientific interest.[104]

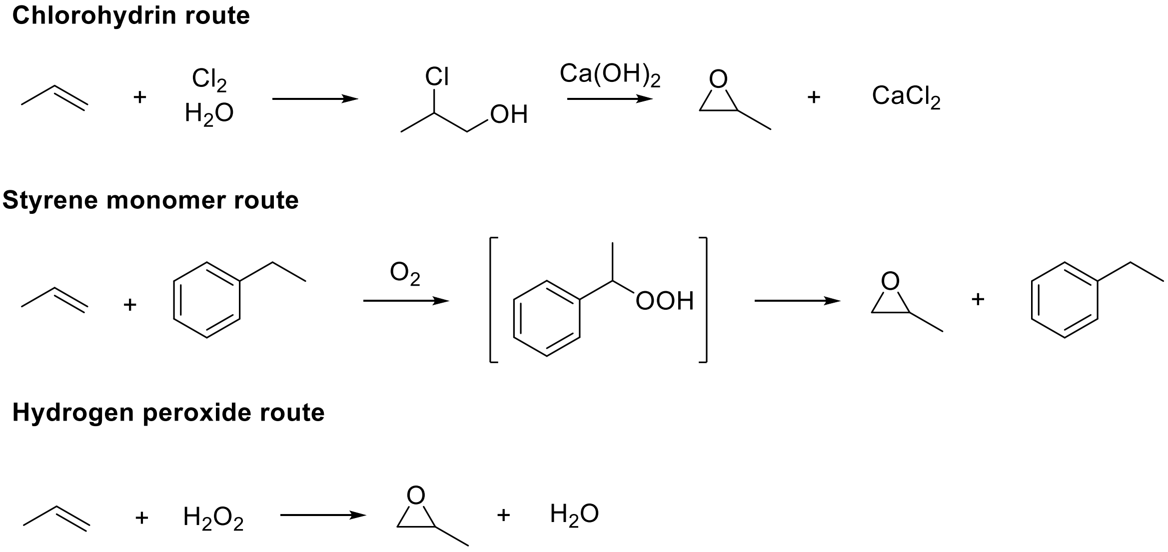

Scheme 1-6 Industrial processes for the production of propylene oxide (PO).

Of the more promising catalysts for this process are Au nanoparticles coupled with Ti, either as titania or an isolated Ti species supported on silica. H_2 can then be introduced into the system as a sacrificial reducing agent which has been demonstrated to improve conversion (5-10 %) and obtain a high PO selectivity (>85 %). The use of H_2 as a sacrificial reagent, which permits the activation of O_2 at relatively lower temperatures was discovered by Haruta and co-workers.[105] Some examples of active catalysts are gold dispersed on TS-1, Ti-SiO_2, Ti-MCM-41 and Ti-SBA-15.[106–111] However, this approach can be hindered by the excessive amount of water that is produced from the oxidation of H_2. Overall, the low H_2 efficiency represents a major economic hurdle. Although, it has been reported that water can replace H_2, even if propene conversion and PO selectivity then become very low.[112,113] It is generally accepted that propene oxidation takes place at the interface between Au nanoparticles and Ti sites. The formation of radical OOH species on the Au surface caused by interactions between O_2 and H_2 are key in driving selectivity to PO.[114]

PO formation using O_2 and H_2 produces by-products such as propanal, acetone, acrolein and CO_2. The formation of these by-products can be alleviated by the modification of support structures and surfaces. For example, the neutralisation of acid sites by a base, such as trimethylamine (TMA), has been demonstrated to improve PO selectivity with titanosilicate supports. The concept behind this is that TMA would poison the Lewis acid sites of the support, manly isolated Ti^{4+} centers, which are responsible for forming PO by-products that cause catalyst deactivation.[115] Work in 2004 by Haruta and co-workers[116] showed that further modification of titanosilicate supports could lead to good yields and slow deactivation. In this study, gold nanoparticles were supported on 3D mesoporous, silylated titanosilicates with large (> 7 nm) pores giving efficient catalysts together with the addition of an alkaline-metal promoter. This addition of $Ba(NO_3)_2$ also enhanced conversion by promoting the formation of a hydroxide like species from H_2 and O_2. The addition of TMA as a strong Lewis base in low concentrations would also improve the catalytic performance of Au nanoparticles.[115]

The epoxidation of longer chain linear and terminal alkenes has also been studied with the use of H_2O_2 as the oxidant.[117–119] This approach can be expensive, therefore it would be beneficial to achieve the epoxidation aerobically. It was demonstrated by Alshammari et al. that the oxidation of hex-2-ene could be achieved using Au/C catalysts with a catalytic amount of *tert*-butyl hydroperoxide (TBHP) as an initiator.[120] However, despite selectivity being directed towards allylic components it was subsequently discovered that the presence of stabilisers within the starting materials were inhibiting oxidation. Therefore, removal of the stabilisers made the requirement for a peroxide initiator obsolete for cyclic and internal alkenes. However, for terminal alkenes, such as, dec-1-ene the initiator has been required with Au/C as catalyst enhancing selectivity to 1,2-epoxydecane. A mechanism for this epoxidation has been depicted in Scheme 1-7. The reaction is started by the radical initiator removing an allylic hydrogen forming a dec-1-enyl radical which subsequently reacts with oxygen to form the peroxy-radical species. The peroxy-radical can then react in the presence of Au nanoparticles to form a 3-dec-1-enyloxy radical. with dec-1-ene to produce equimolar amounts of hydroperoxide and dec-1-ene radical thus forming a cycle to produce a peroxy-radical by interacting with oxygen. This molecule can then react with dec-1-ene and form the epoxide and another allylic dec-1-enyl radical via an intramolecular reaction. The presence of Au is vital for this reaction pathway, providing a surface for the fragmentation of the peroxy species. In the absence of Au nanoparticles, there is an accumulation of the peroxy species which can then abstract an allylic proton from dec-1-ene to give the hydroperoxide molecule.[121] This can then subsequently form the allylic products through a Russell termination.[122]

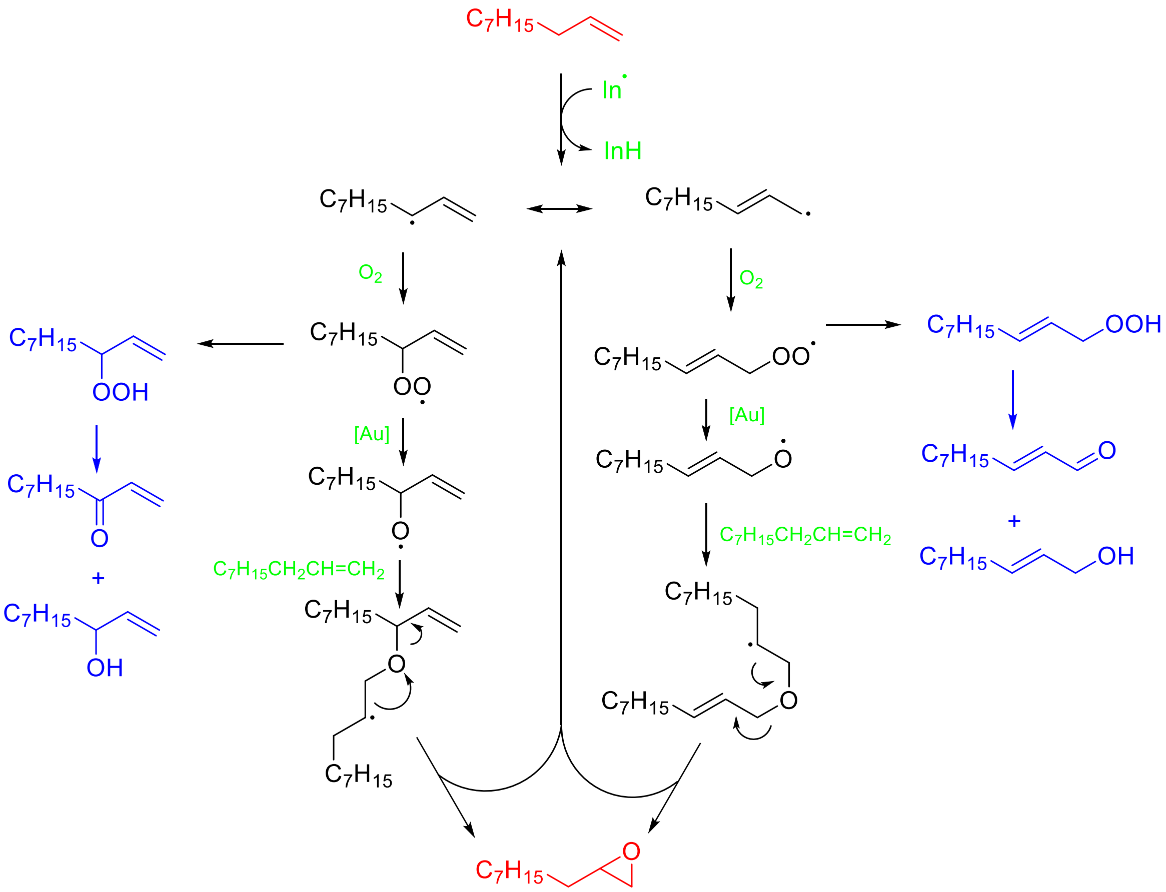

Scheme 1-7 Proposed mechanism of 1-decene epoxidation by Gupta et al.[123]

The epoxidation of dec-1-ene under initiator- and metal-free conditions was later achieved by Pattisson et al. using graphitic oxide catalysts.[124] These materials show an optimum level of oxidation (25 wt. %) with those prepared via a Hoffman potassium chlorate method exhibiting greater activity than the conventional potassium permanganate Hummers procedure. It was also found that sulphur acts as a deactivator in the formation of an active catalyst for the epoxidation. However, it is unavoidable in current chemical oxidation methods with sulfuric acid essential to the chemical oxidation of graphite due to its oxidising and intercalating nature.[125]

1.6.5.2 Cyclic alkenes

The aerobic epoxidation of cyclic alkenes using Au has been studied extensively.[126–130] In 2005, Kiely and co-workers focused on tuneable Au catalysts for selective hydrocarbon oxidation under mild conditions using TBHP as a radical intiator.[128] Their work showed that Au catalysts had the potential for selective epoxide formation rather than the favoured allylic oxidation, most notably with cyclohexene and cyclooctene. For cyclohexene, their most successful catalyst was a Bi-modified 0.5 % Au/C catalyst which achieved 49.6 % selectivity towards cyclohexene oxide (cy-oxide).[128] In this study it was also found that, under tuning of the catalyst and conditions, selective oxidation could be achieved using solventless conditions. The oxidation of cyclooctene can be achieved using a range of radical initiators in catalytic amounts. In work by Tsang et al. a continuation on the development of Au catalysts found that nanoparticles supported on Si nanowires (SiNWs) could successfully epoxidise cyclooctene in the presence of TBHP under mild reaction conditions. It was suggested that the high activity of the catalysts was due to the high surface area of the SiNWs giving them the ability to support high metal loadings (up to 20 wt %). However, this approach was less successful with cyclohexene as substrate. The reactions require an initiator, such as hydrogen peroxide or t-butyl hydroperoxide and, once started, the reaction can be maintained by molecular O_2. However, subsequent studies in the Hutchings group showed that an initiator was only required when the cyclic alkene contained a stabiliser molecule, such as 6-bis(*t*-butyl)-4-methylphenol (BHT) or 3-octadecyl-(3,5-di-*t*-butyl-4-hydroxyphenyl)-propanoate (irganox 1076). Upon removal of this stabiliser, the reaction with and without an initiator is identical.[121]

The importance of the ring size was subsequently assessed by Alshammari et al. demonstrating its importance in dictating whether an epoxidation or allylic oxidation was the dominant reaction pathway.[131] For cycloalkenes with ring sizes of C7 or smaller allylic oxidation was preferred and for larger ring sizes epoxidation was almost exclusively observed. One possible origin of the difference in energy for the C5 and C8 ring closure transition states is additional ring strain that may be expected when an epoxide is formed on a small (e.g. C5) alkene ring compared to that for the more flexible larger rings of C8 and greater.[131] A comparison of preparation techniques was also conducted with sol immobilisation catalysts proving to be more active than those prepared via impregnation, deposition-precipitation and incipient wetness impregnation.[131] This was in correlation to the method producing the narrowest particle size distribution between the techniques.[132,133]

A mechanism for the aerobic oxidation of cyclopentene was proposed by the same author and is displayed in Scheme 1-8, although the initiator, TBHP, was used in this instance.[131] The reaction is initiated by cleavage of the hydroperoxide bond in TBHP, over the surface of a Au particle to form surface bound radicals. The reaction can then be propagated by the abstraction of an allylic proton by the TBHP radical, to give **2**. **2** can then capture an oxygen molecule to form a peroxy radical, **3**, which can then abstract another proton from a cyclopentene molecule to produce the hydroperoxide, **4**, and another cyclopentene radical, **2**.

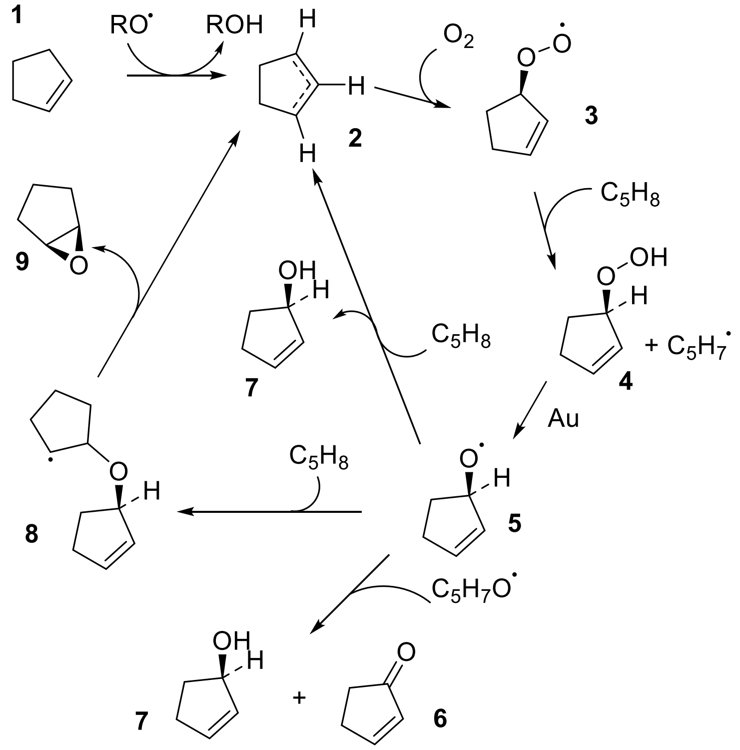

Scheme 1-8 Proposed mechanism for cyclopentene oxidation under aerobic conditions in the presence of an initiator.

The hydroxy radical, **5**, is then generated which creates a situation where there are three possibilities of reaction routes. In the first route 2 molecules of **5** react to produce the allylic ketone (**6**) and allylic alcohol (**7**), which acts as a termination step. Alternatively, an interaction between **5** and the double bond of cyclopentene to form the intermediate, **8**, which can ring close to form the epoxide product, **9**, and an allylic radical, **2**. A third route involves the reaction of **5** and further substrate with another H abstraction from the allylic position to produce the allylic alcohol and allylic radical, **2**. In the absence of an initiator, Donoeva et al. have proposed that the abstraction of the allylic proton is catalysed by metallic gold nanoparticles > 2 nm.[134]

1.7 Cyclohexene oxidation

1.7.1 Aerobic cyclohexene epoxidation

Shringarpure et al. used supported heteropolyacids for the solvent-free oxidation of cyclohexene with molecular oxygen, using TBHP as initiator.[135] In this catalyst Co was exchanged with the available protons of a supported 12-tungstophosphoric acid (TPA/ZrO_2).[135] In this investigation the authors were able to achieve 98 % conversion of cyclohexene with 57 % selectivity to cy-oxide.[135]

However, the use of an initiator provided a disadvantage due to its added cost and the additional waste contributed by the organic hydroperoxide. A similar approach using functionalised metal organic frameworks (MOFs) have shown promise in the aerobic oxidation of cyclohexene.[136,137] However, high selectivities to the epoxide are also accompanied by the presence of isobutylaldehde as co-oxidant.[137] The use of a coper incorporated gallium 2,2'-bipyridine-5,5'-dicarboxylate MOF was also investigated.[137] Using this catalyst, 49.0 % conversion and 89.0 % selectivity to cy-oxide was achieved.[137] This activity was consistent after 4 runs, where conversion reduced to 41.6 % and selectivity remained high at 89.2 %, showing leaching was negligible.[137] Despite the good selectivity shown by these examples of aerobic oxidation, they are still hindered by the use of co-oxidants and initiators which reduce the atom economy of these processes, making them less economically viable and impact their environmental sustainability.

In 2013, the Hutchings group studied the effect of ring size on the selective oxidation of cycloalkenes.[131] This study also investigated the effect of the choice of metal, notably Pd and Au.[131] In this study it was demonstrated that supported gold is superior to palladium or a gold palladium alloy.[131] These reactions were carried out in the presence of a catalytic amount of TBHP. The highest selectivity to cy-oxide was achieved with a 1 % Au/C catalyst at a temperature of 40 °C.[131] The use of Au nanoparticles was also applied by Golovko and co-workers in the solvent-free oxidation of cyclohexene.[134] In this investigation the effect of Au nanoparticles size was established, showing Au nanoparticles larger than 2 nm were beneficial for higher conversion of cyclohexene.[134] These catalysts were prepared using triphenylphosphine-stabilised Au clusters supported on SiO_2, which lost their structure during reaction, eventually forming particles of diameter ∼5−10 nm.[134] The same group later used these same catalysts to target the epoxidation of cyclohexene under initiator and solvent-free conditions (Scheme 1-9).[138]

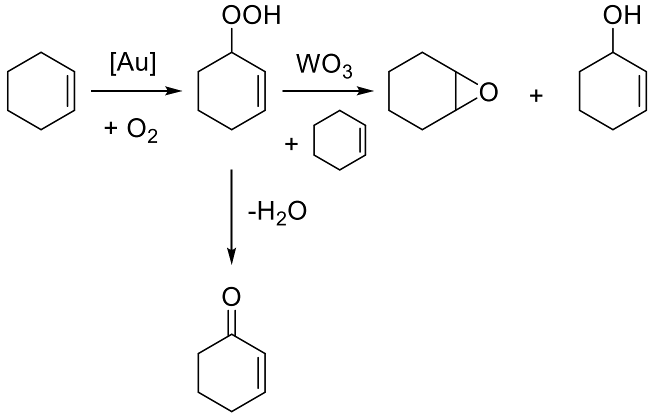

Scheme 1-9 Reaction scheme as reported by Ovoshchnikov et al. for the aerobic oxidation of cyclohexene.[138]

In this investigation WO_3 was used as a co-catalyst and also as a support for the triphenylphosphine-stabilised Au clusters. The Au clusters were also supported on SiO_2 for comparison.[138] It was found that the formation of cyclohexenyl hydroperoxide (cy-OOH) was catalysed by Au nanoparticles, which can then be converted to other products in the presence of other co-catalysts.[138] WO_3 catalysed the conversion of cy-OOH to cy-oxide.[138] However, the formation of cy-oxide is limited to 50 % selectivity as the hydroperoxide forms the epoxide and 2-cyclohexene-1-ol (cy-ol) in equal amounts.[138]

The formation of allylic components presents a major stumbling block in the aerobic epoxidation of cyclohexene. This problem arises from the lability of the allylic C-H bonds which have a bond dissociation energy of ～77 kcal mol^{-1} compared to the vinylic ethylene bond, which has a bond dissociation energy around ～112 kcal mol^{-1}.[139] However, the selective oxidation to form cy-ol and 2-cyclohexene-1-one (cy-one) remains an important process in the pharmaceutical and fragrance industry.[140,141] Due to its importance in these fields it is an area which has been extensively studied using noble metals such as gold, silver, platinum, and ruthenium, showing excellent results with the help of oxidant.[142–144] Recently, the focus has switched to non-noble metal based heterogeneous catalysts because of the advantage both in terms of economic and environmental perspective. This has resulted in the success of catalysts such as Fe_3O_4,[145,146] CuO,[147] N-doped carbon nanotubes[141] and MOFs.[148,149]

An alternative route to the epoxide was provided by Zhong et al., which utilised ethyl benzene as a sacrificial reductant, this route is displayed in Scheme 1-10.[150] This allows the electrophilic oxidation of oxygen-centred radicals to alkenes which is similar to the mechanistic feature of the "hydroperoxide" process.[150] For this route, a CoMo oxide catalyst was used.[150] In this system the less positive charge on the cobalt metal site, would be enough to render ethylbenzene fixation into ethylbenzene peroxide, the more positive charge on Mo would then favour EBHP activation for subsequent step of epoxidation.[150] The solvent would then also be recycled through a dehydration and hydrogenation process which would satisfy the requirements of green chemistry.[150] This synergy between the metal centres results in an epoxidation selectivity of 59 % with 33 % cyclohexene conversion, the ratio of Co(II) to Mo(III) was 2:1.[150] This reactivity was achieved under mild conditions with an oxygen pressure of 0.6 MPa and a temperature of 130 °C for 1 h.[150] Similarly, the use of Mn(III)- and Co(III)-containing molecular sieves exhibited high yields of epoxide (48.0 %) when utilised alongside the sacrificial reagent benzaldehyde.[151]

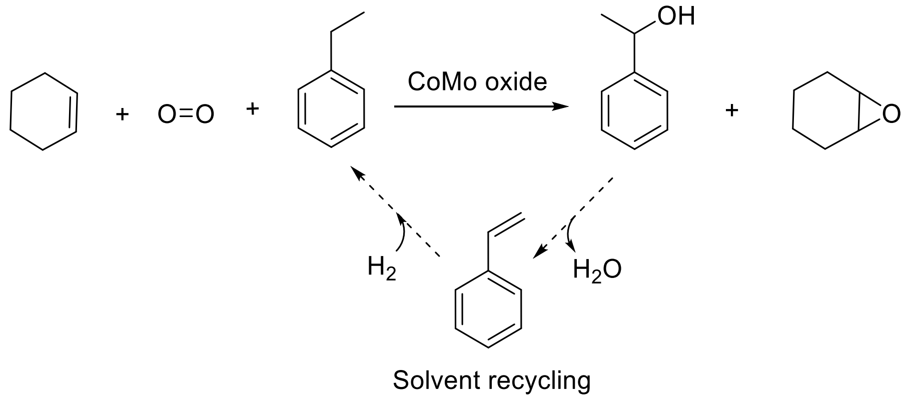

Scheme 1-10 Alternative cascade-type route for cyclohexene epoxidation as suggested by Zhong et al.[150]

Other approaches using photocatalytic,[152,153] biomimetic,[154] and enzymatic[155] systems have shown potential for the efficient aerobic epoxidation of cyclohexene. However, these reactions also required the use of additional solid base catalysts or sacrificial reagents to obtain high selectivities to the epoxide. Allylic oxidation and the limit to selectivity associated with cy-OOH formation represent the major problems associated with aerobic cyclohexene oxidation. However, these problems could be alleviated using H_2O_2 as an oxidant.

1.7.2 Cyclohexene oxidation via H_2O_2

Hydrogen peroxide is an environmentally benign oxidant which only water as a by-product of its decomposition. The drawbacks associated with H_2O_2 from an industrial perspective are that it is relatively expensive, particularly in cyclohexene oxidation where a 4:1 ratio of H_2O_2 to substrate would be necessary to form AA. In addition, H_2O_2 is an explosive chemical which would provide safety and logistical issues in a large-scale production of basic chemicals. Nonetheless, research into prospective routes to AA using H_2O_2 have been a large area of interest in homogeneous and heterogeneous catalysis.[156–164] In addition, another focus has been in the in situ and point of use synthesis of H_2O_2, which may provide a solution to the logistical and economic problems associated with this oxidant.[52,54,59,63,165,166]

In 1998, Sato et al. reported the clean synthesis of AA from aqueous 30 % H_2O_2 (Scheme 1-11).[4] This reaction was catalysed by small amounts of Na_2WO_2 and the phase transfer catalyst (PTC), $[CH_3(n\text{-}C_8H_{17})_3N]HSO_4$, achieving a 93 % yield after 9 h.[4] At the temperature of 75 to 90 °C, Na_2WO_2 is oxidised by H_2O_2 to form an anionic peroxo species which can then be extracted by the PTC into the organic phase.[167] A reaction with cyclohexene reduces the catalyst which then returns to the aqueous phase, completing the catalytic cycle.[168] However, this may be a relatively expensive route to implement industrially and the use of a quaternary ammonium salt is also not environmentally benign. Nonetheless, this research set the foundation for future research on the H_2O_2 mediated synthesis of AA and was quickly followed up by Deng et al. with a direct synthesis over a peroxytungstate-organic acid complex of the form, $[W(O)(O_2)_2L_{(2)}]^{2-}$ (where $L_{(2)}$ is an organic acid with double or multi-functional groups).[169] Using oxalic acid as the ligand a 96.6 % yield was attained after 24 h of reaction, however, catalyst reuse and separation was not investigated providing a drawback to this approach.

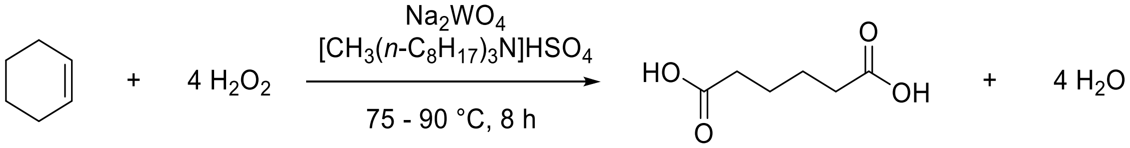

Scheme 1-11 Oxidation of cyclohexene to AA with H_2O_2.[4]

The problem with reactant incompatibility in 2-phase systems was considered by Bohström et al. In this approach a concentrated dispersion of mesoporous oxides containing immobilised WO_3 sites within the pores was prepared achieving high yields of AA with a recyclable catalyst.[170] Other alternatives to the use of a PTC have consisted of microemulsions made up of benzalkonium chloride surfactants, which offers a homogeneous reaction medium for cyclohexene as the organic phase and H_2O_2 as the aqueous phase.[25] W is a common metal for the one-pot oxidation of cyclohexene to AA and has been studied extensively with the differing constitutions including oxotungsten-containing SBA-15,[171] surfactant-type peroxotungstates,[172] $[BMIm]_2WO_4$ ionic liquid supported on silica sulphamic acid,[173] AgNps supported on WO_3,[164] $H_3PW_{12}O_{40}$[174] and combinations of Na_2WO_4 with H_2SO_4[175] or H_2WO_4 with acidic resins.[176] In addition, several patents exist implementing W-based technology, such as, peroxytungstate-organocarboxylic acid complexes,[177] polystyrene resin immobilized decatungstate[178] and tungstic acid,[179] therefore highlighting the substantial catalytic efficiency of tungstate in cyclohexene oxidation. The batch mode effectiveness of the biphasic reaction was reassessed by Freitag et al. using a microwave irradiation as an alternative heating approach.[180] This system was based on a Na_2WO_4 and $[CH_3(n\text{-}C_8H_{17})_3N]HSO_4$, as described previously in studies by Sato et al.[4] A high yield of 68 % after only 90 minutes demonstrated a significant reduction in reaction time and a good yield. However, this method still required the use of a PTC which was an issue that was addressed by Buonomenna et al. with the application of polymeric microporous membranes.[181] Succinic acid was added to favour contact at the membrane–aqueous interface between the catalytic active species, formed in the aqueous compartment, and the cyclohexene substrate. The purpose of the membrane was two-fold; firstly, to stabilise the contact between the two immiscible phases and secondly, to separate the cyclohexene from the AA. This enabled the attainment of a 90 % yield to AA, however, the high cost of implementing a membrane makes this unlikely to be industrially viable.

The mechanistic pathway of the oxidative cleavage reaction was studied further by Lee et al., using a titanium framework-substituted aluminophosphate (TAPO-5) and a combination of nuclear magnetic resonance (NMR) and gas chromatography coupled with mass spectrometry (GC-MS). Further insight into the formation of reaction intermediates using these techniques enabled a deeper understanding of the free radical mechanism and acid-catalysed ring-opening mechanism.[182] The observations contrasted with those made by Sato et al.,[4] revealing the formation of *trans*- and *cis*- stereoisomers of 1,2-cyclohexanediol (CHD) during the reaction (Scheme 1-12). The *trans*-diol was known to form from an acid-catalysed epoxide ring opening of cy-oxide, however, the *cis*-diol was found to proceed through a free-radical mechanism. In their catalytic studies it was also discovered that the TAPO-5 catalyst reacted faster with the *cis*-diol than its isomer.

The mechanistic insights made by Lee et al. formed the basis of rational design into bifunctional heterogeneous catalysts consisting of Brønsted acid and metal sites as the main factor in improving AA yields. An example of this was the incorporation of aluminium into the framework of a Ti grated SBA-15 catalyst for the "one-pot" synthesis of AA. Using mild, stoichiometric conditions and TBHP as oxidant an 80 % yield to AA was achieved.[183] A high Bronsted acid strength was also found to be critical to enabling a fast acid-catalysed ring opening epoxide using zeolite obstructed manganese diamine complexes.[184]

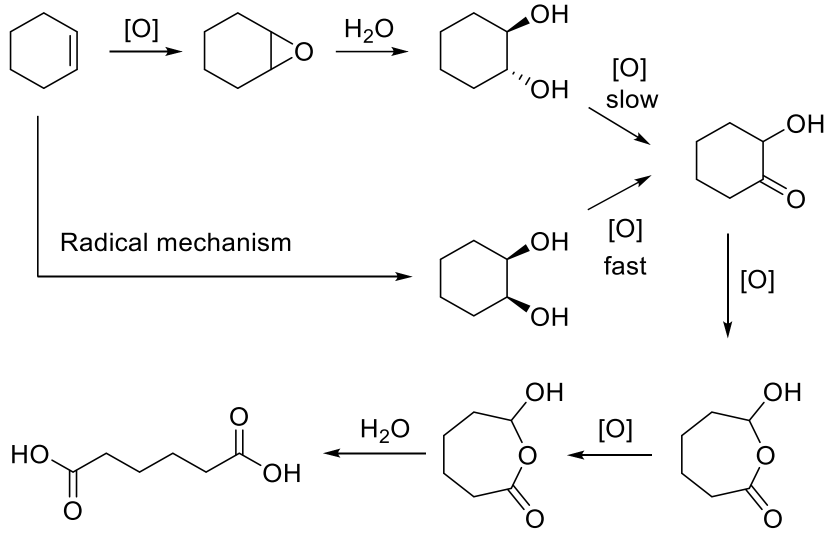

Scheme 1-12 Suggested mechanistic pathway for cyclohexene to AA over a TAPO-5 catalyst, adapted from Lee at al.[182]

The epoxidation step of the reaction can be improved by using Ti-grafted mesoporous silica catalysts. When using Ti catalysts, the leaching of Ti species are one of the main problems encountered by groups in this area.[185,186] Studies have also been conducted on the oxidant efficiency with the implementation of a dropwise addition of H_2O_2 to minimise local concentrations of oxidant near Ti sites.[185] A dropwise addition also aids in reducing the decomposition of H_2O_2 and may also be beneficial in promoting the more selective heterolytic reaction pathway over the homolytic pathway (Scheme 1-13).[187] Specifically with Ti-Si catalysts the lower water concentrations may also reduce the formation of less reactive TiO_2 clusters due to the hydrolytic cleavage of Ti-O-Si bonds.[188] Interestingly, the leaching of Ti species into the reaction medium from a mesoporous Ti-Si catalyst (Ti-MMM-2)[189] was attributed to the interaction of surface sites with the AA reaction product.[190]

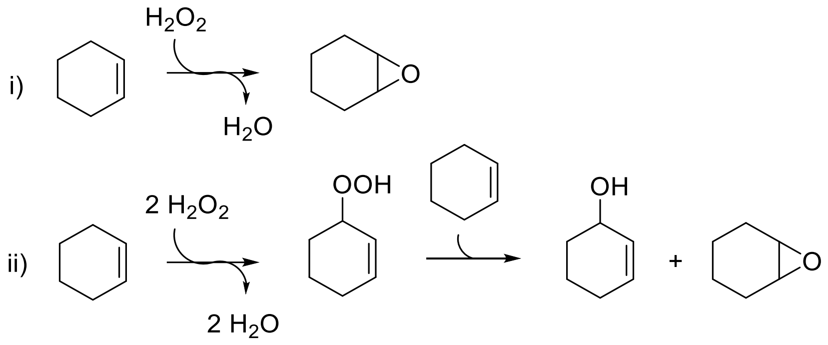

Scheme 1-13 Heterolytic (i) and homolytic (ii) reaction pathways for H_2O_2 oxidation of cyclohexene.[185]

1.7.3 Cyclohexene oxidation via ozone

The principal application of ozone is as a stoichiometric oxidant for the cleavage of alkenes to carbonyl compounds or alcohols,[191] occurring through the Criegee mechanism.[192] The ozonolysis of cyclohexene has been reported as early as 1906 by Harries et al.,[193] however subsequent efforts have often suffered from low yields and from the use of expensive reactants in the oxidative decomposition of ozonolysis products. A decreased cost in the production of ozone has made this route more commercially viable but post treatment processes remain complicated. The ozonolysis carried out in reactive solvents, such as alcohols and carboxylic acids, led to higher yields of useful products. A catalyst is not required in this reaction due to the reactivity of ozone with the alkene double bond. Bailey et al. demonstrated an ozonolysis of cyclohexene in a formic acid-acetic acid mixture at —10° C., after which the temperature was raised, and a molecular oxygen oxidation was carried out to from the cleaved carboxyl groups. The yield of AA was only 49 to 63 %.[194]

More recently, patents have reported high yields of AA,[195,196] using a system containing glacial acetic acid and cyclohexene with a post treatment reflux under oxygen to generate the product. Although no catalyst is required it is stated that the addition of a titanium silicon molecular sieve structure MFI (such as TS-1) can increase yields.[196]

1.8 Adipic acid synthesis via biomass-derived catalytic pathways

The conversion of biomass into cellulose, hemicellulose and lignin are areas of increased scientific interest. Thus, interest has also been evidenced by the ambition of numerous industrial companies to offer a biobased alternative to current AA production. One of these companies, Rennovia, developed bio-adipic acid through a chemo-catalytic process using D-glucose as a starting material (Scheme 1-14).[197] This process was made more sustainable using an excess supply of high fructose corn syrup as the initial feedstock. During this non-biotechnological two step process, glucose is first aerobically oxidised to saccharic acid, after which saccharic acid undergoes hydrodeoxygenation to produce AA. Although the process reached pilot scale, it resulted in a mixture of components and the yield obtained was around 60 %. The first step of this process is an oxidation of D-glucose catalysed by Pt / SiO_2. In the patent filed by Boussie et al., a screening of Pd or Pt supported on several supports, such as, carbon, alumina, silica, titania or zirconia was performed. The best results were obtained with Pt / SiO_2 with a 66 % yield to saccharic acid after 8 h at 90 °C for 5 h. However, the catalyst is commonly affected by pH and the deactivation of Pt which proved a concern.[198,199] The second step is a hydrodeoxygenation reaction which is achieved using a PdRh / SiO_2 catalyst. This was accomplished in the presence of HBr and acetic acid, generating yields between 50 and 77 % after 3 h of reaction at 140 °C and 49 bar of H_2.[197] The Rennovia process was scaled up to a mini-plant in 2015 with a collaboration also announced with Johnson Matthey providing catalyst development. The commercialisation of another process using a direct fermentation approach reached pilot plant scale. In this direct approach the raw material is directly converted to adipic acid using microbes. Such a process is used by the company Verdezyne which used a genetically modified yeast species for the conversion of fatty acids, such as coconut oil, into adipic acid.[200,201] However, due to an oil price crash in 2018, any financial benefit to investors dwindled and operations for both Verdezyne and Rennovia ceased.[202]

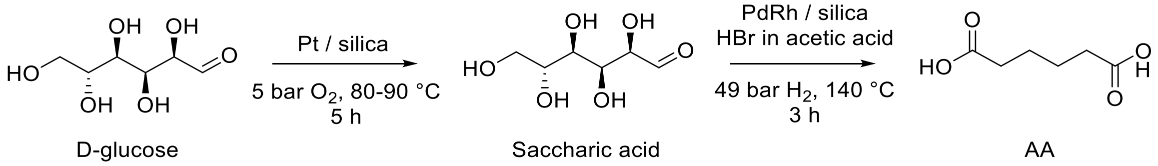

Scheme 1-14 Two-step process for the conversion of D-glucose to AA via the formation of saccharic acid.[197]

The use of D-glucose as a substrate was also studied by Deng et al., utilising Pt/CNT as an effective catalyst for the initial oxidation of glucose to glucaric acid, obtaining a yield of 82 %. This method also utilised a bifunctional Pd-ReOx/AC as a second catalyst. This removed the four OH groups in saccharic acid to form AA, reaching a yield of 99%. The highly dispersed ReOx species enabled the deoxydehydration (DODH) reaction, while Pd nanoparticles not only catalysed the hydrogenation of C=C bonds in the intermediates but also synergistically facilitated the DODH reaction by enhancing dispersion and reducing the ReOx species.[203]

Alternatively, the conversion of biomass derived glucose to 5-hydroxymethylfurfural (HMF) has offered another viable option (Scheme 1-15), which has been studied extensively in the past decades.[204,205] Pt- and Au-based catalysts are often the preferred option in this area, however, several nonprecious metals, such as, Co and Ni, have also emerged as promising alternatives for the oxidation of HMF to 2,5-furandicarboxylic acid (FDCA).[206,207] The ring opening of tetrahydrofuran-2,5-dicarboxylic acid (THFDCA) can be achieved by a non-metal approach, as described by Gilkey et al.,. In this work HI and H_2 are described to be capable of obtaining an AA yield of 89 %.[208] A later improvement to this work was focused on substituting the corrosive HI, which would provide a limitation in the scale-up of this process. Therefore, zeolites were employed as an effective proton source in combination with iodide salts (NaI), obtaining similar AA formation rates to the previous HI pathway.[209]

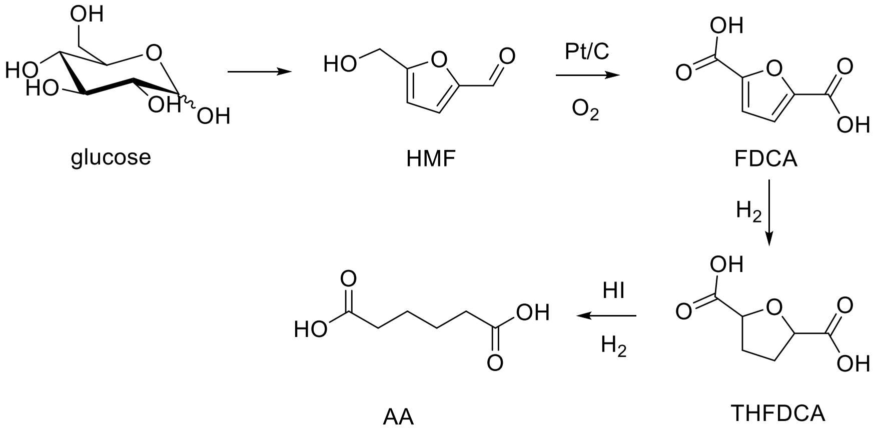

Scheme 1-15 Proposed pathway to AA from biomass derived HMF.[208]

Microbiological routes for adipic acid have been hindered by low yields and low concentrations. The search for a microbiological route is complicated by there being no known natural producer of AA.[201] Natural producers would benefit from lacking the necessity to be genetically engineered to obtain AA, weak acids are also often employed as food preservatives because they act as inhibitors.[210] Another disadvantage of natural producers is that they are incompatible with many reaction mediums and therefore reactors require special design.[211,212]

Metabolically engineered strains of *Escherichia coli*, *Corynebacterium glutamicum* and *Saccharomyces cerevisiae* have attracted significant interest for production of various dicarboxylic acids. These microorganisms have extensive characterisation data available and can be genetically modified to their environment.[213] The combination of *Escherichia coli* and a heterogeneous catalyst has also been utilised to produce AA from D-glucose.[214,215] However, this route also requires a heterogeneous catalyst as the enzymatic step only transforms the sugar into the intermediate catechol and *cis,cis*-muconic acid. A second-step to hydrogenate the intermediates with Pt/C is then required.[214] Recent breakthroughs have been made by industry and academia in the development of bio- and chemocatalytic routes for AA synthesis from biorefinery building blocks such as 5-hydroxymethylfurfural,[216–218] γ-valerolactone[219–221] and compounds representative of lignin and lignin-derived bio-oils.[222–224]

1.9 Aerobic oxidative cleavage of cyclic 1,2-diols

The oxidative cleavage of vicinal diols has drawn much interest across industry and academia, not just to produce AA but in organic synthesis and biochemistry. The cleavage of 1,2-diols is also an area of interest in biomass valorisation for renewal feedstocks. The Criegee oxidation in 1931[225] and the Malaprade reaction in 1934[226] offer the earliest examples of such a cleavage. This is also a reaction which is largely dominated using homogeneous catalysts, but many attempts have been hindered by poor substrate scope and a lack of reusability.[227,228] Another drawback is the use of stoichiometric oxidants, such as, high-valent iodine or lead which results in large amounts of toxic waste.[23,24]

The use of Ag(I) to homogeneously catalyse the cleavage of cyclic 1,2-diols has been reported by Huyser et al. in 1971.[229] This reaction is accompanied by the presence of the oxidant peroxydisulfate.[229] The substrate used in this reaction was *trans*-1,2-dimethylcyclohexane-1,2-diol and cleavage to the corresponding dione was achieved with good activity.[229] More recently in 2015, Li and co-workers showed the potential for the homogeneous Ag(I)-catalysed aerobic oxidation of aldehydes in water, giving the successful conversion of these aldehydes to the corresponding carboxylic acid.[230] Further work from this group expanded the substrate scope of these Ag(I) catalysts to the cleavage of aliphatic-, aromatic-, terminal-, internal-, and cyclic-1,2-diols.[231] This was also achieved while keeping reaction conditions mild, with atmospheric pressure and low temperature.[231] Using AgOTf as catalyst they can achieve high yields in the cleavage of a range of vicinal diols and can form AA in 88 % yield from CHD.[231] However, this result is achieved with the use of 3 equivalents of base and a solvent system consisting of THF/MeOH (5:1).[231] More common Ag salts such as Ag_2CO_3 were also examined in this study but showed inferior yields even with prolonged reaction times.[231]

Heterogenous catalysts have also been used for vicinal diol cleavage with some success using noble metals such as, Pt Ru and Au, however these catalysts usually suffer from low activity and a minimal substrate scope.[232–234] Polyoxometalates have shown potential for the aerobic oxidative cleavage of vicinal diols, however substrate scope is limited. In a study by Khenkin et al. a range of glycol substrates were investigated using an Anderson-Type polyoxometalate of the formula, $[IMo_6O_{24}]^{5\pm}$. Reaction data showed that aryl-substituted diols yielded the most carbon-carbon bond cleavage products, while CHD yielded cyclohexanone-2-ol and 1,2-cyclohexanedione. Only a 5 % yield to carbon-carbon bond cleavage products was observed with CHD.[234] Polyoxometalate catalysts were compared with $Ru(OH)_3$ catalysts in a study by Rozhko et al. where the reaction conditions were probed to obtain the greatest selectivity to AA.[235] In the former case, several side reactions were observed under the basic conditions leading to a low selectivity to AA. The Keggin type P/Mo/V polyoxometalate catalyst was selective to AA but under the acidic reaction conditions AA reacted with unconverted CHD to yield the corresponding ester. Ru-based catalysts have received interest in alcohol oxidations to the corresponding aldehyde or ketone. These oxidations are commonly performed in organic solvents, such as toluene, trifluorotoluene, acetonitrile and ethyl acetate, among others.[236–240] However, it was also reported that in aqueous media the ability of a homogeneous system of Ru^{2+}/Ru^{3+} acetate complexes or $[Ru(H_2O)_6](tosylate)_2$ can catalyse the aerobic oxidative cleavage of α-substituted cycloalkanones into oxo-acids. The cleavage of CHD using Ru-based pyrochlore oxides exhibit greater activity under basic conditions, which is a characteristic that is shared by Group VIII elements.[80,241–243]

The oxidative cleavage of 1,2-diols into aldehydes and ketones was achieved using a manganese layered mixed oxide as the catalyst.[244] This was accomplished in the absence of toxic solvents or reagents, with the use of mild reaction conditions and short reaction times. Another advantage of this approach was the recyclability of the catalyst. However, the substrate scope for this catalyst largely encompasses benzylic 1,2-diols and had no activity in diols substituted by two aliphatic moieties with no conversion observed for cis-1,2-CHD. Noble metals, such as, Au have also displayed an ability to oxidise alcohols, diols, and polyols.[41] Supported Au nanoparticles have been reported to be active in the oxidative cleavage of 9,10-dihydroxystearic acid to azelaic and pelargonic acids.[245–247] The oddity of Au catalysts is that the Au-based catalysts only coordinate to one hydroxyl group in vicinal glycols. This peculiarity is demonstrated in the oxidation of 1,2-propanediol where the Au NPs either oxidise the primary OH group to lactic acid or oxidises them in sequence producing pyruvic acid, which is then oxidised to acetic acid and CO_2.[248] Based on this capability of Au to oxidise alcohols, Solmi et al. investigated the reactivity of Au NPs for *trans*-1,2-CHD cleavage by placing them onto TiO_2 and MgO.[249] These reactions were run in equimolar ratios of substrate to base with 4 bar of O_2 flowed into the reactor. The catalysts proved to be active with a moderate CHD conversion and selectivity to AA of close to 70 %. However, deactivation of the catalyst was significant found to be due to the increase in NP size and the carbonaceous residue on the catalyst surface.[249] The key step of this oxidation was found to be the oxidation of the diol into 2-hydroxycyclohexanone which is then oxidised by air – even in the absence of catalyst – to AA and other by-products such as glutaric acid and succinic acid albeit in lesser amounts. This study also proposed a reaction mechanism (Scheme 1-16) involving 2-hydroxycyclohexanone (2-HCO) as the main reaction intermediate, which can undergo a variety of C-C scissions to produce several carboxylic acid products. These scissions are annotated by the red numbers indicating which scissions give rise to AA, GA or SA.

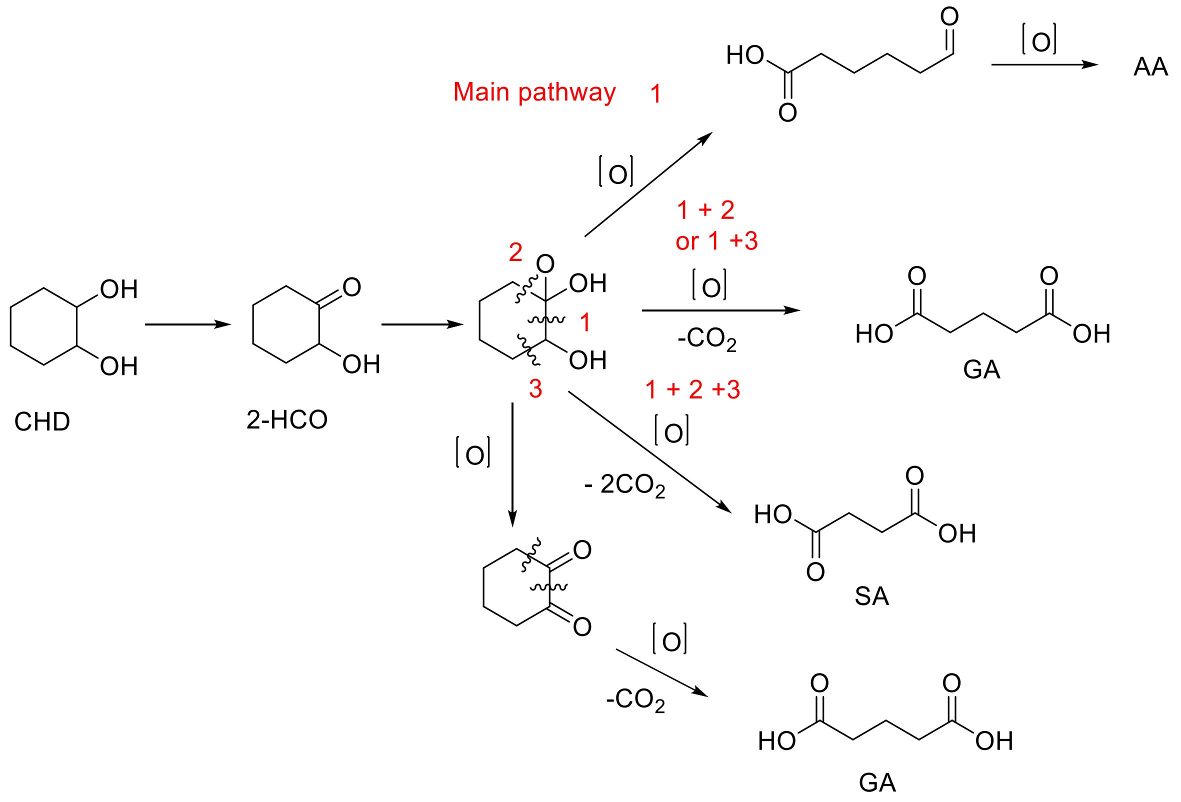

Scheme 1-16 Proposed mechanism by Solmi et al. illustrating the pathways through the 2-HCO reaction intermediate, leading to the observed products.[249]

The effectiveness of V compounds to aerobically cleave CHD to AA was studied by Obara et al.[250] This work utilised a 2-catalyst system of Pt/C and V_2O_5 to gain a 90 % yield to AA. This yield was achieved after 48 h at 353 K in acidic conditions. It was found that CHD was converted to 2-HCO over Pt/C alone, whereas CHD was not converted over V_2O_5 alone. These observations suggested the conversion of CHD to AA proceeded by Pt-catalysed oxidative dehydrogenation of CHD to 2-HCO and V-catalysed oxidative cleavage of 2-HCO to AA (Scheme 1-17). The Pt catalyst was gradually deactivated, and the activity was partially restored by treating the used Pt with H_2 at 573 K. In this study, alternatives to Pt were explored such as Pd and Ru but they showed low activities in contrast to their reported activities under basic conditions for vicinal diols.[5,241,251,252] It was also stated that about half of the V still remained in in the solid catalyst and the leaching reduced with each run. The solid V which remained was speculated to be responsible for the activity observed.[250] This observation could lead to a promising discovery if a stable V catalyst could be designed.

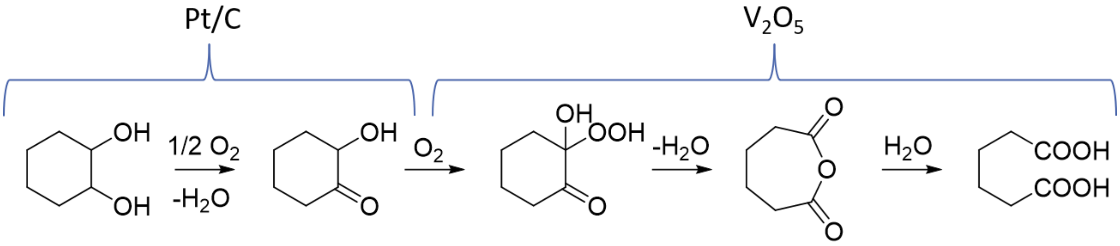

Scheme 1-17 Formation of AA from CHD over Pt/C and V_2O_5 as suggested by Obara et al.[250]

1.10 Vanadium oxides

Vanadium oxides have attracted a lot of attention due to their interesting catalytic properties, their structural flexibility, and electrochemical properties.[10,253–257] These nanostructured materials can take many different morphologies such as, nanobelts,[258,259] nanowires,[260,261] nanorods,[262,263] nanourchins,[264] nanocogs[265] and flower like nano shapes.[266] Vanadium oxide nanotubes were first discovered by Spahr et al.[267] and their use across a variety of applications notably in cathode materials for lithium batteries has since been reported. This success as a cathode material is seemingly due to the ease of intercalation of Li and various other metals into the lattice structure, which may stabilise the material in aqueous applications. Typically, vanadium oxide nanostructures are prepared via a hydrothermal treatment of aqueous solutions of vanadium (V) precursors.[268] The resulting morphology is reported to be dependent on the pH and temperature of the precursor mixture and thermal treatment.[266] Vanadium oxide nanostructures have been employed in a wide range of applications including field-effect transistors,[269,270] sensors,[259,271] spintronic devices[272] and nanolithography templates.[273,274]

The ability of vanadium atoms to exist in a multitude of oxidation states (+2, +3, +4 and +5) results in the easy conversion of oxides with different stoichiometry by oxidation and reduction and is believed to be an important factor for the oxide to function as a catalyst in selective oxidations.[275] Vanadium oxide-based catalysts are also reported to have success in the oxidative dehydrogenation of lower alkenes. This was reported by Mamedov et al. with an accepted reaction mechanism proceeding through a V^{5+} and V^{4+} redox cycle.[253] The effect of vanadium oxide supported monolayers were studied by Bond et al. for selective oxidations showing particular stability on supports such as TiO_2 and Al_2O_3.[254] However, these reactions were based in organic media such as *ortho*-xylene and 1,3-butadiene so this stability may not be transferable to an aqueous system. The selective epoxidation of alkenes by homogeneous polyoxovanadometalate catalysts, $[\gamma\text{-}1,2\text{-}H_2SiV_2W_{10}O_{40}]^{4-}$, was studied by Nakagawa et al. showing good efficiency of H_2O_2 uptake and a 90 % yield to the epoxide using a solvent system of MeCN and *t*BuOH.

The ability of vanadium compounds to perform aerobic oxidation has been reported by Vennat et al. showing the capability of monomeric vanadium species and polyoxometalate vanadium species to perform the oxidative cleavage of 2-HCO to form AA.[276]The potential of vanadium systems for oxidative cleavage of CHD was furthered by Obara et al.,[250] as described in section 1.9. The good yield to AA observed in these studies was accompanied by about 50 % leaching. Research into heterogenous vanadium catalysts has been impacted by their susceptibility to leach into aqueous solutions. The effect of the support and reaction conditions can alleviate leaching as shown in work by Masumoto et al.[277] However, the most successful catalyst in their studies still showed that 37.6 wt % of vanadium leached into the reaction when using V/Al_2O_3. Furthermore, leaching was also reported by Ziolek et al. in H_2O_2 liquid phase oxidations. In these investigations V/MCM-41 leached 71 wt. % of vanadium into the reaction solution, illustrating the difficulty in developing a stable vanadium catalyst.[278] Further investigations into vanadium incorporated in mesoporous silicas and vanadium xerogels, especially in combination with H_2O_2, gives an extremely unstable material.[279] “Ship-in-a-bottle” catalysts have also been investigated and their stability is reliant on a V-O-Si framework, however they still show a susceptibility to leahcing.[280–282] Leaching was similarly observed using a silica support[283] and a vanadomolybdophosphate polyoxometalate ($H_5PV_2Mo_{10}O_{40}$), supported on mesoporous MCM-41.[284] This latter example was used in a hydrocarbon oxidation with a combination of aldehyde and molecular oxygen but leaching was found to be dependent on the concentration of aldehyde.

The main application of vanadium oxides in aqueous systems remains in their utilisation for electrochemical purposes. Frequently, metals such as Na, Cu, Ag or Co are incorporated into the vanadium oxide structure and aimed at increasing their catalytic capabilities, however, under these applications the leaching of vanadium into aqueous media is not always reported.[285,286]

1.11 Aims and objectives

In summary, this investigation explores the use of cyclohexene as a starting material for the synthesis of adipic acid. The current industrial production of AA is achieved using cyclohexane, which has environmental limitations due to the emission of N_2O, either as a by-product or indirectly through the production of nitric acid as a reagent. Cyclohexene could provide a competing process whereby the C=C bond would allow greener oxidants such as O_2 and H_2O_2 to be utilised.

Au catalysts have exhibited promise for the aerobic epoxidation of linear and cyclic alkenes and will provide a starting point for this investigation. The use of atmospheric oxygen would be the most advantageous approach due to economic reasons and its high abundance. However, this approach can be limited by lower selectivities due to the reactivity of the allylic bond and alternative radical mechanistic pathways. Alternatively, the stoichiometric use of H_2O_2 could also provide an option with higher attainable selectivities to AA. However, this route has disadvantages associated with its relatively high cost and the logistical difficulties of using H_2O_2. Finally, in a two-step process, an aerobic oxidation of CHD to AA has shown promise using Pt/C and a V_2O_5 catalyst but there are improvements to be made to the stability of the vanadium catalyst in aqueous conditions, which may be achievable using vanadium bronzes, given their applications across aqueous media in electrochemical applications.

1.12 References

1 *IPCC, 5th AR, Working Group III Report "Climate Change 2014: Mitigation of Climate Change", Technical Summary,* 2014.

2 L. Donner and V. Ramanathan, *J. Atmos. Sci.*, 1980, **37**, 119–124.

3 F. Kapteijn, J. Rodriguez-Mirasol and J. A. Moulijn, *Appl. Catal. B Environ.*, 1996, **9**, 25–64.

4 K. Sato, M. Aoki and R. Noyori, *Sci. 281*, 1998, **281**, 1646–1648.

5 G.-J. ten Brink, I. W. C. E. Arends and R. A. Sheldon, *Science (80-.).*, 2000, **287**, 1636–1639.

6 A. Castellan, J. C. J. Bart and S. Cavallaro, *Catal. Today*, 1991, **9**, 237–254.

7 *Adipic Acid Market: Global Share, Size, Trends and Growth Analysis Forecast to 2019-2025*, 2019.

8 *Adipic acid - Market Analysis, Trends and Forecasts*, 2019.

9 A. F. Lindsay, *Chem. Eng. Sci.*, 1954, **3**, 78–93.

10 J. R. L. Smith, D. I. Richards, C. B. Thomas and M. Whittaker, *J. Chem. Soc. Perkin Trans. 2*, 1985, 1677–1682.

11 K. Weissermel and H. J. Arpe, *Industrial Organic Chemistry*, Wiley, 2008.

12 R. A. Reimer, C. S. Slaten, M. Seapan, M. W. Lower and P. E. Tomlinson, *Environ. Prog.*, 1994, **13**, 134–137.

13 J. Pérez-Ramírez, F. Kapteijn, K. Schöffel and J. A. Moulijn, *Appl. Catal. B Environ.*, 2003, **44**, 117–151.

14 P. Notté, *Top. Catal.*, 2000, **13**, 387–394.

15 V. N. Parmon, G. I. Panov, A. Uriarte and A. S. Noskov, *Catal. Today*, 2005, **100**, 115–131.

16 S. Van De Vyver and Y. Román-Leshkov, *Catal. Sci. Technol.*, 2013, **3**, 1465–1479.

17 H. Nagahara, M. Ono, M. Konishi and Y. Fukuoka, *Appl. Surf. Sci.*, 1997, **121**, 448–451.

18 T. Zhang, Z. Wang, Q. Zhao, F. Li and W. Xue, *J. Nanomater.*, 2015, **2015**, 670896.

19 L. Foppa and J. Dupont, *Chem. Soc. Rev.*, 2015, **44**, 1886–1897.

20 H. Sun, W. Guo, X. Zhou, Z. Chen, Z. Liu and S. Liu, *Chinese J. Catal.*, 2011, **32**, 1–16.

21 R. Carson and L. Darling, *Silent spring*, Houghton Mifflin Company ; The Riverside Press, Boston; Cambridge, [Mass.], 1962.

22 P. Anastas and J. Warner, *Green Chemistry: Theory and Practice*, Oxford University Press, New York, 1998.

23 F. J. Wolf and J. Weijlard, *Org. Synth.*, 1955, **35**, 18.

24 M. Frigerio and M. Santagostino, *Tetrahedron Lett.*, 1994, **35**, 8019–8022.

25 P. Blach, Z. Böstrom, S. Franceschi-Messant, A. Lattes, E. Perez and I. Rico-Lattes, *Tetrahedron*, 2010, **66**, 7124–7128.

26 P. T. Anastas, M. M. Kirchhoff and T. C. Williamson, *Appl. Catal. A Gen.*, 2001, **221**, 3–13.

27 J. Geller, *Am. Antiq.*, 1993, **58**, 594–595.

28 L. B. Hunt, *Gold Bull.*, 1973, **6**, 16–27.

29 C. Louis and O. Pluchery, *Gold nanoparticles for physics, chemistry and biology*, Imperial College Press, London, 2012.

30 M. Haruta, T. Kobayashi, H. Sano and N. Yamada, *Chem. Lett.*, 1987, **16**, 405–408.

31 G. C. Bond and P. A. Sermon, *Gold Bull.*, 1973, **6**, 102–105.

32 P. Johnston, N. Carthey and G. J. Hutchings, *J. Am. Chem. Soc.*, 2015, **137**, 14548–14557.

33 R. Ciriminna, E. Falletta, C. Della Pina, J. H. Teles and M. Pagliaro, *Angew. Chemie Int. Ed.*, 2016, **55**, 14210–14217.

34 G. Malta, S. J. Freakley, S. A. Kondrat and G. J. Hutchings, *Chem. Commun.*, 2017, 53, 11733–11746.

35 W. Ren, L. Duan, Z. Zhu, W. Du, Z. An, L. Xu, C. Zhang, Y. Zhuo and C. Chen, *Environ. Sci. Technol.*, 2014, **48**, 2321–2327.

36 K. Shinoda, *Chem. Lett.*, 1975, **4**, 219–220.

37 G. J. Hutchings, *J. Catal.*, 1985, **96**, 292–295.

38 B. Nkosi, N. J. Coville and G. J. Hutchings, *Appl. Catal.*, 1988, **43**, 33–39.

39 B. Nkosi, N. J. Coville and G. J. Hutchings, *J. Chem. Soc. Chem. Commun.*, 1988, 71–72.

40 B. Nkosi, M. D. Adams, N. J. Coville and G. J. Hutchings, *J. Catal.*, 1991, **128**, 378–386.

41 A. S. K. Hashmi and G. J. Hutchings, *Angew. Chemie Int. Ed.*, 2006, **45**, 7896–7936.

42 J. K. Edwards, S. J. Freakley, A. F. Carley, C. J. Kiely and G. J. Hutchings, *Acc. Chem. Res.*, 2014,

47, 845–854.

43 G. J. Hutchings and C. J. Kiely, *Acc. Chem. Res.*, 2013, **46**, 1759–1772.

44 K. Suzuki, T. Yamaguchi, K. Matsushita, C. Iitsuka, J. Miura, T. Akaogi and H. Ishida, *ACS Catal.*, 2013, **3**, 1845–1849.

45 7709414, 2010.

46 E. K. Hanrieder, A. Jentys and J. A. Lercher, *ACS Catal.*, 2015, **5**, 5776–5786.

47 M. Chen, D. Kumar, C.-W. Yi and D. W. Goodman, *Science (80-.).*, 2005, **310**, 291–293.

48 R. Hage and A. Lienke, *Angew. Chemie*, 2006, **118**, 212–229.

49 J. Kirchner, *Kirk-Othmer Encyclopedia of Chemical Technology*, Wiley New York, 1979.

50 G. Goor and W. Kunkel, *O. Weiberg in Ullmann s Encyclopedia of Industrial Chemistry, Vol. A13*, VCH, Weinheim, 1989.

51 S. Ranganathan and V. Sieber, *Catalysts*, 2018, **8**, 379.

52 J. K. Edwards, S. J. Freakley, R. J. Lewis, J. C. Pritchard and G. J. Hutchings, *Catal. Today*, 2015, **248**, 3–9.

53 R. J. Lewis, J. K. Edwards, S. J. Freakley and G. J. Hutchings, *Ind. Eng. Chem. Res.*, 2017, **56**, 13287–13293.

54 G. Li, J. Edwards, A. F. Carley and G. J. Hutchings, *Catal. Today*, 2006, **114**, 369–371.

55 J. K. Edwards, B. E. Solsona, P. Landon, A. F. Carley, A. Herzing, C. J. Kiely and G. J. Hutchings, 2005, **236**, 69–79.

56 P. Landon, P. J. Collier, A. J. Papworth, C. J. Kiely and G. J. Hutchings, *Chem. Commun.*, 2002, **18**, 2058–2059.

57 T. Ishihara, Y. Ohura, S. Yoshida, Y. Hata, H. Nishiguchi and Y. Takita, *Appl. Catal. A Gen.*, 2005, **291**, 215–221.

58 B. E. Solsona, J. K. Edwards, P. Landon, A. F. Carley, A. Herzing, C. J. Kiely and G. J. Hutchings, *Chem. Mater.*, 2006, **18**, 2689–2695.

59 J. K. Edwards, B. Solsona, P. Landon, A. F. Carley, A. Herzing, M. Watanabe, C. J. Kiely and G. J. Hutchings, *J. Mater. Chem.*, 2005, **15**, 4595–4600.

60 A. G. R. Howe, P. J. Miedziak, D. J. Morgan, Q. He, P. Strasser and J. K. Edwards, *Faraday Discuss.*, 2018, **208**, 409–425.

61 N. M. Wilson and D. W. Flaherty, *J. Am. Chem. Soc.*, 2016, **138**, 574–586.

62 S. Park, D. Ryul, J. Ho, T. Jin, Y. M. Chung, S. H. Oh, I. Kyu, D. R. Park, J. H. Choi, T. J. Kim, Y. M. Chung, S. H. Oh and I. K. Song, *J. Mol. Catal. A Chem.*, 2010, **332**, 76–83.

63 E. N. Ntainjua, M. Piccinini, S. J. Freakley, J. C. Pritchard, J. K. Edwards, A. F. Carley and G. J. Hutchings, *Green Chem.*, 2012, **14**, 170–181.

64 S. J. Freakley, R. J. Lewis, D. J. Morgan, J. K. Edwards and G. J. Hutchings, *Catal. Today*, 2015, **248**, 10–17.

65 S. Park, J. G. Seo, J. C. Jung, S. H. Baeck, T. J. Kim, Y. M. Chung, S. H. Oh and I. K. Song, *Catal. Commun.*, 2009, **10**, 1762–1765.

66 N. Gemo, P. Biasi, P. Canu, F. Menegazzo, F. Pinna, A. Samikannu, K. Kordás, T. O. Salmi and J.-P. Mikkola, *Top. Catal.*, 2013, **56**, 540–549.

67 S. Park, J. Lee, J. H. Song, T. J. Kim, Y. M. Chung, S. H. Oh and I. K. Song, *J. Mol. Catal. A Chem.*, 2012, **363**–**364**, 230–236.

68 Y. Hui, S. Zhang and W. Wang, *Adv. Synth. Catal.*, 2019, **361**, 2215–2235.

69 A. S. Sharma, H. Kaur and D. Shah, *RSC Adv.*, 2016, **6**, 28688–28727.

70 L. Liu and A. Corma, *Chem. Rev.*, 2018, **118**, 4981–5079.

71 L. Prati and M. Rossi, *Gold on Carbon as a New Catalyst for Selective Liquid Phase Oxidation of Diols*, 1998, vol. 176.

72 C. Bianchi, F. Porta, L. Prati, M. Rossi and oxide Al, *Selective liquid phase oxidation using gold catalysts*, 2000, vol. 13.

73 A. Abad, A. Corma and H. García, *Chem. - A Eur. J.*, 2008, **14**, 212–222.

74 N. Dimitratos, A. Villa, D. Wang, F. Porta, D. Su and L. Prati, *J. Catal.*, 2006, **244**, 113–121.

75 G. Wu, G. L. Brett, E. Cao, A. Constantinou, P. Ellis, S. Kuhn, G. J. Hutchings, D. Bethell and A. Gavriilidis, *Catal. Sci. Technol.*, 2016, **6**, 4749–4758.

76 E. Rucinska, P. J. Miedziak, S. Pattisson, G. L. Brett, S. Iqbal, D. J. Morgan, M. Sankar and G. J. Hutchings, *Catal. Sci. Technol.*, 2018, **8**, 2987–2997.

77 C. Venturello and M. Gambaro, *J. Org. Chem.*, 1991, **56**, 5924–5931.

78 P. L. Anelli, S. Banfi, F. Montanari and S. Quici, *J. Org. Chem.*, 1989, **54**, 2970–2972.

79 US Patent, 4487720, 1984.

80 M. Besson and P. Gallezot, *Catal. Today*, 2000, **57**, 127–141.

81 A. Corma and M. E. Domine, *Chem. Commun.*, 2005, 4042–4044.

82 V. R. Choudhary and D. K. Dumbre, *Catal. Commun.*, 2011, **13**, 82–86.

83 S. Biella, L. Prati and M. Rossi, *Gold catalyzed oxidation of aldehydes in liquid phase*, 2003, vol. 197.

84 C. H. Christensen, B. Jørgensen, J. Rass-Hansen, K. Egeblad, R. Madsen, S. K. Klitgaard, S. M. Hansen, M. R. Hansen, H. C. Andersen and A. Riisager, *Angew. Chemie - Int. Ed.*, 2006, **45**, 4648–4651.

85 B. Jørgensen, S. Egholm Christiansen, M. L. Dahl Thomsen and C. H. Christensen, *J. Catal.*, 2007, **251**, 332–337.

86 S. M. Tembe, G. Patrick, M. S. Scurrell and W. G. Org, *Acetic acid production by selective oxidation of ethanol using Au catalysts supported on various metal oxide*, 2009, vol. 42.

87 K.-Q. Sun, S.-W. Luo, N. Xu and B.-Q. Xu, *Catal. Letters*, 2008, **124**, 238–242.

88 T. Takei, J. Suenaga, T. Ishida and M. Haruta, *Top. Catal.*, 2015, **58**, 295–301.

89 T. Wang, H. Shou, Y. Kou and H. Liu, *Green Chem.*, 2009, **11**, 562–568.

90 T. Ishida, Y. Ogihara, H. Ohashi, T. Akita, T. Honma, H. Oji and M. Haruta, *ChemSusChem*, 2012, **5**, 2243–2248.

91 S. Li, W. Li, Y. Li, G. Fan and F. Li, *Chempluschem*, 2017, **82**, 270–279.

92 M. Liu, G. Fan, J. Yu, L. Yang and F. Li, *Dalt. Trans.*, 2018, **47**, 5226–5235.

93 Y. Nishiyama, Y. Nakagawa and N. Mizuno, *Angew. Chemie - Int. Ed.*, 2001, **40**, 3639–3641.

94 W. . Richey, Wiley, New York, 1993, p. 140.

95 D. H. R. Barton, A. E. Martell and D. . Sawyer, Eds., *The Activation of Dioxygen and Homogeneous Catalytic Oxidation*, Plenum, New York, 1993.

96 R. Sheldon and J. Kochi, in *Academic Press*, 1981.

97 B. Chowdhury, C. Santra, S. Mandal and R. Kumar, in *Advanced Materials for Agriculture, Food, and Environmental Safety*, John Wiley & Sons, Ltd, 2014, pp. 197–241.

98 T. A. Nijhuis, E. Sacaliuc and B. M. Weckhuysen, in *Mechanisms in Homogeneous and Heterogeneous Epoxidation Catalysis*, ed. S. T. Oyama, Elsevier, Amsterdam, 2008, pp. 339–354.

99 A. M. Joshi, B. Taylor, L. Cumaranatunge, K. T. Thomson and W. Nicholas Delgass, in *Mechanisms in Homogeneous and Heterogeneous Epoxidation Catalysis*, ed. S. T. Oyama, Elsevier, Amsterdam, 2008, pp. 315–338.

100 M. Haruta and J. Kawahara, in *Mechanisms in Homogeneous and Heterogeneous Epoxidation Catalysis*, ed. S. T. Oyama, Elsevier, Amsterdam, 2008, pp. 297–313.

101 J. Kawahara and M. Haruta, in *Nanoparticles and Catalysis*, John Wiley & Sons, Ltd, 2008, pp. 457–473.

102 C. Qi, *Gold Bull.*, 2008, **41**, 224–234.

103 T. A. Nijhuis, M. Makkee, J. A. Moulijn and B. M. Weckhuysen, *Ind. Eng. Chem. Res.*, 2006, **45**, 3447–3459.

104 J. Huang and M. Haruta, *Res. Chem. Intermed.*, 2012, **38**, 1–24.

105 T. Hayashi, K. Tanaka and M. Haruta, *J. Catal.*, 1998, **178**, 566–575.

106 C.-H. Liu, Y. Guan, E. J. M. Hensen, J.-F. Lee and C.-M. Yang, *J. Catal.*, 2011, **282**, 94–102.

107 S. Kanungo, K. S. Keshri, A. J. F. van Hoof, M. F. N. d'Angelo, J. C. Schouten, T. A. Nijhuis, E. J. M. Hensen and B. Chowdhury, *J. Catal.*, 2016, **344**, 434–444.

108 S. Kanungo, D. M. Perez Ferrandez, F. Neira d'Angelo, J. C. Schouten and T. A. Nijhuis, *J. Catal.*, 2016, **338**, 284–294.

109 W.-S. Lee, M. Cem Akatay, E. A. Stach, F. H. Ribeiro and W. Nicholas Delgass, *J. Catal.*, 2012, **287**, 178–189.

110 X. Feng, Y. Liu, Y. Li, C. Yang, Z. Zhang, X. Duan, X. Zhou and D. Chen, *AIChE J.*, 2016, **62**, 3963–3972.

111 X. Feng, N. Sheng, Y. Liu, X. Chen, D. Chen, C. Yang and X. Zhou, *ACS Catal.*, 2017, **7**, 2668–2675.

112 M. Ojeda and E. Iglesia, *Chem. Commun.*, 2009, 352–354.

113 J. Huang, T. Akita, J. Faye, T. Fujitani, T. Takei and M. Haruta, *Angew. Chemie Int. Ed.*, 2009, **48**, 7862–7866.

114 C. Sivadinarayana, T. V Choudhary, L. L. Daemen, J. Eckert and D. W. Goodman, *J. Am. Chem. Soc.*, 2004, **126**, 38–39.

115 B. Chowdhury, J. J. Bravo-Suárez, M. Daté, S. Tsubota and M. Haruta, *Angew. Chemie - Int. Ed.*, 2006, **45**, 412–415.

116 A. K. Sinha, S. Seelan, S. Tsubota and M. Haruta, *Angew. Chemie - Int. Ed.*, 2004, **43**, 1546–1548.

117 S. Ikeda, H. Nur, T. Sawadaishi, K. Ijiro, M. Shimomura and B. Ohtani, *Langmuir*, 2001, **17**, 7976–7979.

118 F. Figueras, H. Kochkar and S. Caldarelli, *Microporous Mesoporous Mater.*, 2000, **39**, 249–256.

119 K. Sato, M. Aoki, M. Ogawa, T. Hashimoto and R. Noyori, *J. Org. Chem.*, 1996, **61**, 8310–8311.

120 H. Alshammari, P. J. Miedziak, S. Bawaked, D. W. Knight and G. J. Hutchings, 2012, 1565–1571.

121 H. Alshammari, P. J. Miedziak, T. E. Davies, D. J. Willock, D. W. Knight and G. J. Hutchings, *Catal. Sci. Technol.*, 2014, **4**, 908–911.

122 R. Sheldon and J. Kochi, in *Metal-catalyzed Oxidations of Organic Compounds*, Academic Press, 1981, pp. 17–32.

123 U. N. Gupta, N. F. Dummer, S. Pattisson, R. L. Jenkins, D. W. Knight, D. Bethell and G. J. Hutchings, *Catal. Letters*, 2015, 689–696.

124 S. Pattisson, E. Nowicka, U. N. Gupta, G. Shaw, R. L. Jenkins, D. J. Morgan, D. W. Knight and G. J. Hutchings, *Nat. Commun.*, 2016, **7**, 12855.

125 Y. Hong, Z. Wang and X. Jin, *Sci. Rep.*, 2013, **3**, 3439.

126 S. Bawaked, Q. He, N. F. Dummer, A. F. Carley, D. W. Knight, D. Bethell, C. J. Kiely and G. J. Hutchings, *Catal. Sci. Technol.*, 2011, **1**, 747–759.

127 S. Bawaked, N. F. Dummer, D. Bethell, D. W. Knight and G. J. Hutchings, *Green Chem.*, 2011, **13**, 127–134.

128 M. D. Hughes, Y.-J. Xu, P. Jenkins, P. Mcmorn, P. Landon, D. I. Enache, A. F. Carley, G. A. Attard, G. J. Hutchings, F. King, E. H. Stitt, P. Johnston, K. Griffin and C. J. Kiely, *Nature*, 2005, **437**, 1132–1135.

129 S. Bawaked, N. F. Dummer, N. Dimitratos, D. Bethell, Q. He, C. J. Kiely and G. J. Hutchings, *Green Chem.*, 2009, **11**, 1037–1044.

130 M. Álvaro, C. Aprile, A. Corma, B. Ferrer and H. García, *J. Catal.*, 2007, **245**, 249–252.

131 H. Alshammari, P. J. Miedziak, D. W. Knight, D. J. Willock and G. J. Hutchings, *Catal. Sci. Technol.*, 2013, **3**, 1531–1539.

132 J. A. Lopez-Sanchez, N. Dimitratos, P. Miedziak, E. Ntainjua, J. K. Edwards, D. Morgan, A. F. Carley, R. Tiruvalam, C. J. Kiely and G. J. Hutchings, *Phys. Chem. Chem. Phys.*, 2008, **10**, 1921–1930.

133 P. J. Miedziak, Q. He, J. K. Edwards, S. H. Taylor, D. W. Knight, B. Tarbit, C. J. Kiely and G. J. Hutchings, *Catal. Today*, 2011, **163**, 47–54.

134 B. G. Donoeva, D. S. Ovoshchnikov and V. B. Golovko, *ACS Catal.*, 2013, **3**, 2986–2991.

135 P. Shringarpure and A. Patel, *J. Mol. Catal. A Chem.*, 2010, **321**, 22–26.

136 Y. Qin, B. Wang, J. Li, X. Wu and L. Chen, *Transit. Met. Chem.*, 2019, **44**, 595–602.

137 Y. Y. Liu, K. Leus, T. Bogaerts, K. Hemelsoet, E. Bruneel, V. Van Speybroeck and P. Van Der Voort, *ChemCatChem*, 2013, **5**, 3657–3664.

138 D. S. Ovoshchnikov, B. G. Donoeva, B. E. Williamson and V. B. Golovko, *Catal. Sci. Technol.*, 2014, **4**, 752.

139 S. J. Blanksby and G. B. Ellison, *Acc. Chem. Res.*, 2003, **36**, 255–263.

140 A. Dali, I. Rekkab-Hammoumraoui, A. Choukchou-Braham and R. Bachir, *RSC Adv.*, 2015, **5**, 29167–29178.

141 Y. Cao, H. Yu, F. Peng and H. Wang, *ACS Catal.*, , DOI:10.1021/cs500187q.

142 R. Burch, D. J. Crittle and M. J. Hayes, *Catal. Today*, 1999, **47**, 229–234.

143 J. A. Labinger and J. E. Bercaw, *Nature*, 2002, **417**, 507–514.

144 R. G. Bergman, *Nature*, 2007, **446**, 391–393.

145 X. Cai, H. Wang, Q. Zhang, J. Tong and Z. Lei, *J. Mol. Catal. A Chem.*, 2014, **383**–**384**, 217–224.

146 M. Sarkheil, M. Lashanizadegan and M. Ghiasi, *J. Mol. Struct.*, 2019, **1179**, 278–288.

147 D. D. Mal, J. Kundu and D. Pradhan, *ChemCatChem*, 2021, **13**, 362–372.

148 A. Dhakshinamoorthy, M. Alvaro and H. Garcia, *J. Catal.*, 2012, **289**, 259–265.

149 Y. Fu, D. Sun, M. Qin, R. Huang and Z. Li, *RSC Adv.*, 2012, **2**, 3309–3314.

150 W. Zhong, M. Liu, J. Dai, J. Yang, L. Mao and D. Yin, *Appl. Catal. B Environ.*, 2018, **225**, 180–196.

151 R. Raja, G. Sankar and J. Meurig Thomas, *Chem. Commun.*, 1999, 829–830.

152 K. Teramura, K. Ogura, T. Sugimoto, H. Tsuneoka, T. Shishido and T. Tanaka, *Chem. Lett.*, 2009, **38**, 1098–1099.

153 K. Teramura, H. Tsuneoka, K. Ogura, T. Sugimoto, T. Shishido and T. Tanaka, *ChemCatChem*, 2014, **6**, 2276–2281.

154 X. Zhou and H. Ji, *Chem. Eng. J.*, 2010, **156**, 411–417.

155 A. D. N. Vaz, D. F. McGinnity and M. J. Coon, *Proc. Natl. Acad. Sci. U. S. A.*, 1998, **95**, 3555–3560.

156 H. Jiang, H. Gong, Z. Yang, X. Zhang and Z. Sun, *React. Kinet. Catal. Lett.*, 2002, **75**, 315–321.

157 W. Zhu, H. Li, X. He, Q. Zhang, H. Shu and Y. Yan, *Catal. Commun.*, 2008, **9**, 551–555.

158 Z. Bohström, I. Rico-Lattes and K. Holmberg, *Green Chem.*, 2010, **12**, 1861–1869.

159 M. Vafaeezadeh, C. Wilhelm, P. Breuninger, S. Ernst, S. Antonyuk and W. R. Thiel, *ChemCatChem*, 2020, **12**, 2695–2701.

160 M. Vafaeezadeh and M. Mahmoodi Hashemi, *Catal. Commun.*, 2014, **43**, 169–172.

161 C.-Y. Cheng, K.-J. Lin, M. R. Prasad, S.-J. Fu, S.-Y. Chang, S.-G. Shyu, H.-S. Sheu, C.-H. Chen, C.-

H. Chuang and M.-T. Lin, *Catal. Commun.*, 2007, **8**, 1060–1064.

162 J. Gui, D. Liu, X. Cong, X. Zhang, H. Jiang, Z. Hu and Z. Sun, *J. Chem. Res.*, 2005, 520–522.

163 G. Lapisardi, F. Chiker, F. Launay, J. P. Nogier and J. L. Bonardet, *Catal. Commun.*, 2004, **5**, 277–281.

164 S. Ghosh, S. S. Acharyya, S. Adak, L. N. S. Konathala, T. Sasaki and R. Bal, *Green Chem.*, 2014, **16**, 2826–2834.

165 T. García, R. Murillo, S. Agouram, A. Dejoz, M. J. Lázaro, L. Torrente-Murciano and B. Solsona, *Chem. Commun.*, 2012, **48**, 5316–5318.

166 T. García, S. Agouram, A. Dejoz, J. F. Sánchez-Royo, L. Torrente-Murciano and B. Solsona, *Catal. Today*, 2015, **248**, 48–57.

167 R. Noyori, M. Aoki and K. Sato, *Chem. Commun.*, 2003, 1977–1986.

168 F. Cavani and S. Alini, in *Sustainable Industrial Chemistry*, John Wiley & Sons, Ltd, 2009, pp. 367–425.

169 Y. Deng, Z. Ma, K. Wang and J. Chen, *Green Chem.*, 1999, **1**, 275–276.

170 Z. Bohström, I. Rico-Lattes and K. Holmberg, *Green Chem.*, 2010, **12**, 1861–1869.

171 C.-Y. Cheng, K.-J. Lin, M. R. Prasad, S.-J. Fu, S.-Y. Chang, S.-G. Shyu, H.-S. Sheu, C.-H. Chen, C.-H. Chuang and M.-T. Lin, *Catal. Commun.*, 2007, **8**, 1060–1064.

172 W. Zhu, H. Li, X. He, Q. Zhang, H. Shu and Y. Yan, *Catal. Commun.*, 2008, **9**, 551–555.

173 M. Vafaeezadeh, M. M. Hashemi and M. Shakourian-Fard, *Catal. Commun.*, 2012, **26**, 54–57.

174 K. Fujitani, T. Mizutani, T. Oida and T. Kawase, *J. Oleo Sci.*, 2009, **58**, 37–42.

175 P. Jin, Z. Zhao, Z. Dai, D. Wei, M. Tang and X. Wang, *Catal. Today*, 2011, **175**, 619–624.

176 H. Wei, H. Li, Y. Liu, P. Jin, X. Wang and B. Li, *ACS Appl. Mater. Interfaces*, 2012, **4**, 4106–4112.

177 Y. Deng, *CN1087012C*, China, 1999.

178 Z. Yingwei, *CN102614920B*, China, 2012.

179 K. Guo, *CN110407684A*, China, 2019.

180 J. Freitag, M. Nüchter and B. Ondruschka, *Green Chem.*, 2003, **5**, 291–295.

181 M. G. Buonomenna, G. Golemme, M. P. De Santo and E. Drioli, *Org. Process Res. Dev.*, 2010, **14**, 252–258.

182 S.-O. Lee, R. Raja, K. D. M. Harris, J. M. Thomas, B. F. G. Johnson and G. Sankar, *Angew. Chemie Int. Ed.*, 2003, **42**, 1520–1523.

183 G. Lapisardi, F. Chiker, F. Launay, J. P. Nogier and J. L. Bonardet, *Microporous Mesoporous Mater.*, 2005, **78**, 289–295.

184 P. P. Knops-Gerrits, F. Thibault-Starzyk and P. A. Jacobs, in *Zeolites and Related Microporous Materials: State of the Art 1994 - Proceedings of the 10th International Zeolite Conference, Garmisch-Partenkirchen, Germany, 17-22 July 1994*, eds. J. Weitkamp, H. G. Karge, H. Pfeifer and W. Hölderich, Elsevier, 1994, vol. 84, pp. 1411–1418.

185 M. Guidotti, C. Pirovano, N. Ravasio, B. Lázaro, J. M. Fraile, J. A. Mayoral, B. Coq and A. Galarneau, *Green Chem.*, 2009, **11**, 1421–1427.

186 M. Guidotti, E. Gavrilova, A. Galarneau, B. Coq, R. Psaro and N. Ravasio, *Green Chem.*, 2011, **13**, 1806–1811.

187 J. M. Fraile, J. I. García, J. A. Mayoral and E. Vispe, *J. Catal.*, 2001, **204**, 146–156.

188 S. Van De Vyver and Y. Román-Leshkov, *Catal. Sci. Technol.*, 2013, **3**, 1465–1479.

189 O. A. Kholdeeva, M. S. Mel'gunov, A. N. Shmakov, N. N. Trukhan, V. V Kriventsov, V. I. Zaikovskii, M. E. Malyshev and V. N. Romannikov, *Catal. Today*, 2004, **91**–**92**, 205–209.

190 M. N. Timofeeva, O. A. Kholdeeva, S. H. Jhung and J.-S. Chang, *Appl. Catal. A Gen.*, 2008, **345**, 195–200.

191 W. P. Griffith, *Coord. Chem. Rev.*, 2001, **219**–**221**, 259–281.

192 R. Criegee, *Angew. Chem., Int. Ed. Engl.*, 1975, **14**, 745–752.

193 C. Harries and H. Neresheimer, *Berichte der Dtsch. Chem. Gesellschaft*, 1906, **39**, 2846–2850.

194 P. S. Bailey, *Ind. Eng. Chem.*, 1958, **50**, 993–996.

195 L. Xuebing, *CN109761796A*, China, 2019.

196 L. Min, *CN102766038B*, China, 2011.

197 T. R. Boussie, E. L. Dias, Z. M. Fresco, V. J. Murphy, J. Shoemaker, R. Archer and H. Jiang, *2010/ 0317823 A1*, US Patent, 2010.

198 A. Abbadi and H. van Bekkum, *J. Mol. Catal. A Chem.*, 1995, **97**, 111–118.

199 J. M. H. Dirkx and H. S. van der Baan, *J. Catal.*, 1981, **67**, 1–13.

200 T. Beardslee and S. Picataggio, *Lipid Technol.*, 2012, **24**, 223–225.

201 E. Skoog, J. H. Shin, V. Saez-Jimenez, V. Mapelli and L. Olsson, *Biotechnol. Adv.*, 2018, **36**, 2248–2263.

202 J. Lane, *Biofuels Dig. Newsl.*, 2018.

203 W. Deng, L. Yan, B. Wang, Q. Zhang, H. Song, S. Wang, Q. Zhang and Y. Wang, *Angew. Chemie - Int. Ed.*, 2021, **60**, 4712–4719.

204 X. Kong, Y. Zhu, Z. Fang, J. A. Kozinski, I. S. Butler, L. Xu, H. Song and X. Wei, *Green Chem.*, 2018, **20**, 3657–3682.

205 L. Hu, L. Lin, Z. Wu, S. Zhou and S. Liu, *Renew. Sustain. Energy Rev.*, 2017, **74**, 230–257.

206 S. Zhang, X. Sun, Z. Zheng and L. Zhang, *Catal. Commun.*, 2018, **113**, 19–22.

207 M. Ventura, F. Lobefaro, E. de Giglio, M. Distaso, F. Nocito and A. Dibenedetto, *ChemSusChem*, 2018, **11**, 1305–1315.

208 M. J. Gilkey, A. V. Mironenko, D. G. Vlachos and B. Xu, *ACS Catal.*, 2017, **7**, 6619–6634.

209 M. J. Gilkey, H. J. Cho, B. M. Murphy, J. Wu, D. G. Vlachos and B. Xu, *ACS Appl. Energy Mater.*, 2020, **3**, 99–105.

210 Z. Gu, B. A. Glatz and C. E. Glatz, *Enzyme Microb. Technol.*, 1998, **22**, 13–18.

211 M. Sauer, D. Porro, D. Mattanovich and P. Branduardi, *Trends Biotechnol.*, 2008, **26**, 100–108.

212 R. Mazzoli, F. Bosco, I. Mizrahi, E. A. Bayer and E. Pessione, *Biotechnol. Adv.*, 2014, **32**, 1216–1236.

213 M. Zhao, D. Huang, X. Zhang, M. A. G. Koffas, J. Zhou and Y. Deng, *Metab. Eng.*, 2018, **47**, 254–262.

214 W. Niu, K. M. Draths and J. W. Frost, *Biotechnol. Prog.*, 2002, **18**, 201–211.

215 K. M. Draths and J. W. Frost, *J. Am. Chem. Soc.*, 1994, **116**, 399–400.

216 N. K. Gupta, S. Nishimura, A. Takagaki and K. Ebitani, *Green Chem.*, 2011, **13**, 824–827.

217 T. R. Boussie, E. L. Dias, Z. M. Fresco and V. J. Murphy, *US 2010/0317822 A1* , US Patent, 2010.

218 M. Chia, Y. J. Pagán-Torres, D. Hibbitts, Q. Tan, H. N. Pham, A. K. Datye, M. Neurock, R. J. Davis and J. A. Dumesic, *J. Am. Chem. Soc.*, 2011, **133**, 12675–12689.

219 European Patent Office, 1994.

220 US Patent, 1992.

221 J. Q. Bond, D. Martin Alonso, R. M. West and J. A. Dumesic, *Langmuir*, 2010, **26**, 16291–16298.

222 J. B. J. H. van Duuren, B. Brehmer, A. E. Mars, G. Eggink, V. A. P. M. dos Santos and J. P. M. Sanders, *Biotechnol. Bioeng.*, 2011, **108**, 1298–1306.

223 T. Nimmanwudipong, R. C. Runnebaum, D. E. Block and B. C. Gates, *Catal. Letters*, 2011, **141**, 779–783.

224 R. C. Runnebaum, T. Nimmanwudipong, D. E. Block and B. C. Gates, *Catal. Letters*, 2010, **141**, 817.

225 R. Criegee, *Berichte der Dtsch. Chem. Gesellschaft*, 1930, **64**, 260–266.

226 L. Malaprade, *Bull. Soc.Chim. Fr*, 1934, **3**, 833–852.

227 Z. Wang, Y.-T. Cui, Z.-B. Xu and J. Qu, *J. Org. Chem.*, 2008, **73**, 2270–2274.

228 E. Takezawa, S. Sakaguchi and Y. Ishii, *Org. Lett.*, 1999, **1**, 713–715.

229 E. S. Huyser and L. G. Rose, *J. Org. Chem.*, 1972, **87**, 1546.

230 M. Liu, H. Wang, H. Zeng and C. J. Li, *Sci. Adv.*, , DOI:10.1126/sciadv.1500020.

231 Z. Z. Zhou, M. Liu, L. Lv and C. J. Li, *Angew. Chemie - Int. Ed.*, 2018, **57**, 2616–2620.

232 J. M. Bregeault, B. El Ali, J. Mercier, J. Martin and C. Martin, *C. R. Acad. Sci. Paris*, 1989, **309**, 459.

233 K. Fujitani, T. Mizutani, T. Oida and T. Kawase, *J. Oleo Sci*, 2009, **58**, 323–328.

234 A. M. Khenkin and R. Neumann, *Adv. Synth. Catal.*, 2002, **344**, 1017–1021.

235 E. Rozhko, K. Raabova, F. Macchia, A. Malmusi, P. Righi, P. Accorinti, S. Alini, P. Babini, G. Cerrato, M. Manzoli and F. Cavani, *ChemCatChem*, 2013, **5**, 1998–2008.

236 M. H. Robbins and R. S. Drago, *J. Chem. Soc., Dalt. Trans.*, 1996, 105–110.

237 A. S. Goldstein, R. H. Beer and R. S. Drago, *J. Am. Chem. Soc.*, 1994, **116**, 2424–2429.

238 C.-X. Yin and R. G. Finke, *Inorg. Chem.*, 2005, **44**, 4175–4188.

239 R. Neumann and M. Dahan, *Nature*, 1997, **388**, 353–355.

240 J. T. Groves and R. Quinn, *J. Am. Chem. Soc.*, 1985, **107**, 5790–5792.

241 T. R. Felthouse, *J. Am. Chem. Soc.*, 1987, **109**, 7566–7568.

242 T. Pasini, M. Piccinini, M. Blosi, R. Bonelli, S. Albonetti, N. Dimitratos, J. A. Lopez-Sanchez, M. Sankar, Q. He, C. J. Kiely, G. J. Hutchings and F. Cavani, *Green Chem.*, 2011, **13**, 2091–2099.

243 R. Garcia, M. Besson and P. Gallezot, *Appl. Catal. A Gen.*, 1995, **127**, 165–176.

244 V. Escande, C. H. Lam, P. Coish and P. T. Anastas, *Angew. Chemie - Int. Ed.*, 2017, **56**, 9561–9565.

245 A. Köckritz and A. Martin, *Eur. J. Lipid Sci. Technol.*, 2011, **113**, 83–91.

246 A. Kulik, A. Janz, M.-M. Pohl, A. Martin and A. Köckritz, *Eur. J. Lipid Sci. Technol.*, 2012, **114**, 1327–1332.

247 A. Kulik, A. Martin, M.-M. Pohl, C. Fischer and A. Köckritz, *Green Chem.*, 2014, **16**, 1799–1806.

248 Y. Ryabenkova, P. J. Miedziak, N. F. Dummer, S. H. Taylor, N. Dimitratos, D. J. Willock, D. Bethell, D. W. Knight and G. J. Hutchings, *Top. Catal.*, 2012, **55**, 1283–1288.

249 S. Solmi, E. Rozhko, A. Malmusi, T. Tabanelli, S. Albonetti, F. Basile, S. Agnoli and F. Cavani, *Appl. Catal. A Gen.*, 2018, **557**, 89–98.

250 N. Obara, S. Hirasawa, M. Tamura and Y. Nakagawa, *ChemCatChem*, 2016, **8**, 1732–1738.

251 Y. Uozumi and R. Nakao, *Angew. Chemie Int. Ed.*, 2003, **42**, 194–197.

252 S. J. H. F. Arts, F. van Rantwijk and R. A. Sheldon, *J. Carbohydr. Chem.*, 1996, **15**, 317–329.

253 E. A. Mamedov and V. Cortds Corberfin, *Appl. Catal. A, Gen.*

254 G. C. Bond and S. F. Tahir, *Appl. Catal.*, 1991, **71**, 1–31.

255 T. Allersma, R. Hakim, T. N. Kennedy and J. D. Mackenzie, *J. Chem. Phys.*, 1967, **46**, 154–160.

256 F. D. Hardcastle and I. E. Wachs, *J. Phys. Chem.*, 1991, **95**, 5031–5041.

257 A.-M. Cao, J.-S. Hu, H.-P. Liang and L.-J. Wan, *Angew. Chemie Int. Ed.*, 2005, **44**, 4391–4395.

258 G. Li, S. Pang, L. Jiang, Z. Guo and Z. Zhang, *J. Phys. Chem. B*, 2006, **110**, 9383–9386.

259 J. Liu, X. Wang, Q. Peng and Y. Li, *Adv. Mater.*, 2005, **17**, 764–767.

260 A. Holsteen, I. S. Kim and L. J. Lauhon, *Nano Lett.*, 2014, **14**, 1898–1902.

261 Z. Chen, Y. Qin, D. Weng, Q. Xiao, Y. Peng, X. Wang, H. Li, F. Wei and Y. Lu, *Adv. Funct. Mater.*, 2009, **19**, 3420–3426.

262 R. Ostermann, D. Li, Y. Yin, J. T. McCann and Y. Xia, *Nano Lett.*, 2006, **6**, 1297–1302.

263 K. Takahashi, S. J. Limmer, Y. Wang and G. Cao, *J. Phys. Chem. B*, 2004, **108**, 9795–9800.

264 G. Li, K. Chao, C. Zhang, Q. Zhang, H. Peng and K. Chen, *Inorg. Chem.*, 2009, **48**, 1168–1172.

265 Z.-S. Wu, W. Ren, L. Wen, L. Gao, J. Zhao, Z. Chen, G. Zhou, F. Li and H.-M. Cheng, *ACS Nano*, 2010, **4**, 3187–3194.

266 C. Wu, Y. Xie, L. Lei, S. Hu and C. OuYang, *Adv. Mater.*, 2006, **18**, 1727–1732.

267 M. E. Spahr, P. Bitterli, R. Nesper, M. Müller, F. Krumeich and H. U. Nissen, *Angew. Chemie - Int. Ed.*, 1998, **37**, 1263–1265.

268 J. Livage, *Materials (Basel).*, 2010, **3**, 4175–4195.

269 J. Muster, G. T. Kim, V. Krstić, J. G. Park, Y. W. Park, S. Roth and M. Burghard, *Adv. Mater.*, 2000, **12**, 420–424.

270 S. Myung, M. Lee, G. T. Kim, J. S. Ha and S. Hong, *Adv. Mater.*, 2005, **17**, 2361–2364.

271 P. Liu, S.-H. Lee, H. M. Cheong, C. E. Tracy, J. R. Pitts and R. D. Smith, *J. Electrochem. Soc.*, 2002, **149**, H76–H80.

272 L. Krusin-Elbaum, D. M. Newns, H. Zeng, V. Derycke, J. Z. Sun and R. Sandstrom, *Nature*, 2004, **431**, 672–676.

273 M. G. Ancona, S. E. Kooi, W. Kruppa, A. W. Snow, E. E. Foos, L. J. Whitman, D. Park and L. Shirey, *Nano Lett.*, 2003, **3**, 135–138.

274 R. Šordan, M. Burghard and K. Kern, *Appl. Phys. Lett.*, 2001, **79**, 2073–2075.

275 J. Haber, M. Witko and R. Tokarz, *Appl. Catal. A Gen.*

276 M. Vennat, P. Herson, J.-M. Brégeault and G. B. Shul, *Vanadium-Catalysed Aerobic Cleavage of CC Bonds in Substituted Cyclohexanones To Afford Carboxylic Acids: Two Model Complexes with Tetrahedral Geometry around Vanadium(V)*, .

277 Y.-K. Masumoto, R. Hamada, K. Yokota, S. Nishiyama and S. Tsuruya, *Liquid-phase oxidation of benzene to phenol by vanadium catalysts in aqueous solvent with high acetic acid concentration*, 2002, vol. 184.

278 M. Ziolek, in *Catalysis Today*, 2004, vol. 90, pp. 145–150.

279 R. Neumann and M. Levin-Elad, *Appl. Catal. A, Gen.*, 1995, **122**, 85–97.

280 A. N. Kozlov and L. A. Maksimov, *Phys. Lett. Sect. A Gen. At. Solid State Phys.*, 1999, **253**, 223–226.

281 I. W. C. E. Arends, M. P. Birelli and R. A. Sheldon, *Stud. Surf. Sci. Catal.*, 1997, **110**, 1031–1040.

282 R. A. Sheldon, I. W. C. E. Arends and H. E. B. Lempers, *Collect. Czechoslov. Chem. Commun.*, 1998, **63**, 1724–1742.

283 M.-A. Ishida, Y. Masumoto, R. Hamada, S. Nishiyama, S. Tsuruya and M. Masai, *J. Chem. Soc. Perkin Trans. 2*, 1999, 847–853.

284 A. M. Khenkin, R. Neumann, A. B. Sorokin and A. Tuel, *Catal. Letters*, 1999, **63**, 189–192.

285 C. Xia, J. Guo, P. Li, X. Zhang and H. N. Alshareef, *Angew. Chemie*, 2018, **130**, 4007–4012.

286 R. Konta, H. Kato, H. Kobayashi and A. Kudo, *Phys. Chem. Chem. Phys.*, 2003, **5**, 3061–3065.

2 Experimental

2.1 Introduction

This section provides information on the procedures to analyse reaction products and characterise catalysts. Details of chemical lists, catalyst testing, and catalyst preparations are separated into their respective chapters.

2.2 Analysis of reaction products

2.2.1 Gas chromatography (GC)

2.2.1.1 Theory

Gas chromatography (GC) is a form of chromatography in which the gas is the moving phase. A typical gas chromatograph consists of a carrier gas, flow controller, injector, column, detector, and data system, as shown in Figure 2-1. The column is typically made from fused silica and are open tubes (OT) in which the solid phase is coated with a liquid phase.[1]

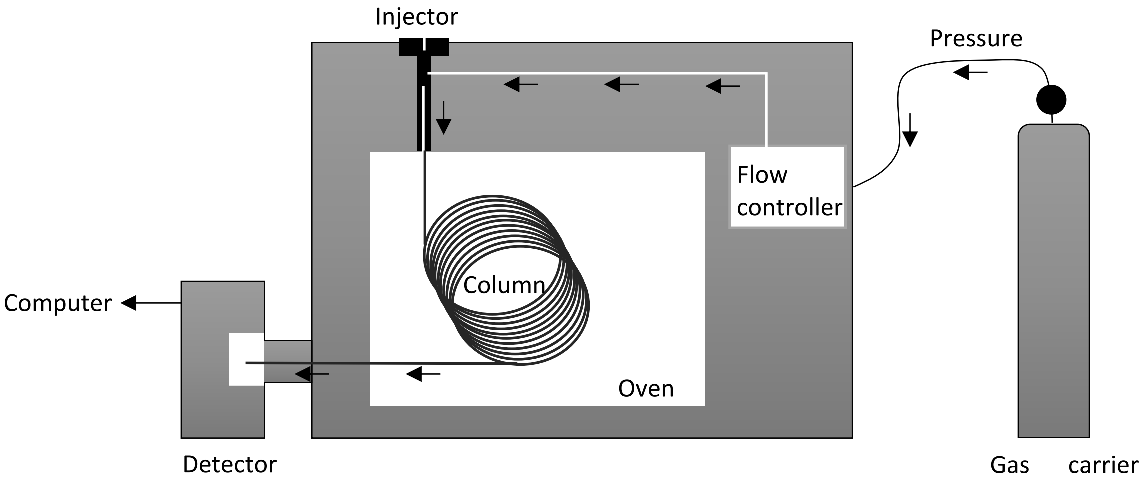

Figure 2-1 Basic setup of a gas chromatograph adapted from reference.[1]

The mobile phase is generally made up of an inert gas such as He or N_2, which passes through an inlet and is passed through the column which contains the stationary phase. This carrier gas does not interact with the analytes and the choice of carrier gas is usually limited by the choice of detector and availability. N_2 can generally offer the best resolution but is hindered by the slow linear velocities required to achieve this. He is the carrier gas chosen for the analysis of reaction products within this project due to efficiency in analysis time and resolution.[1]

The sample is injected through a septum into a glass liner in which the sample is brought into the gas phase through flash vaporisation. The sample can then be introduced to the column by either split or splitless injection. A splitless injection would involve the entire sample being introduced onto the column. This technique has its advantages in terms of increased sensitivity of the detector to the analyte because of the amount of sample introduced but has its disadvantages with tailing of the chromatogram and diminishing resolution. Split injection allows the introduction of only a small proportion of the sample to the column by dividing the carrier gas flow inside the inlet into a split flow and a column flow. A basic schematic of a split/splitless injector is shown in Figure 2-2. The split ratio is defined by equation 2-1 and has typical ratios within the range of 20 : 1 and 80 : 1.[1]

$$Split\ ratio = \frac{Split\ flow}{Column\ flow} \tag{2-1}$$

The split flow is then evacuated to the atmosphere via a vent while the column flow is introduced to the chromatographic column. This column (CP-wax 52CB) is an open-tubular (OT) column where a liquid stationary phase is coated on the inside wall of the column and the mobile phase flows through the tube. The choice of column is based entirely on the samples to be analysed and this decision is made regarding four variables: the chemical nature of the stationary phase, its thickness, column length and diameter. The most important variable to consider is the interaction of the analyte with the stationary phase as it must have enough affinity to separate effectively. The column is contained inside an oven and is set to a temperature that the user requires. [1]

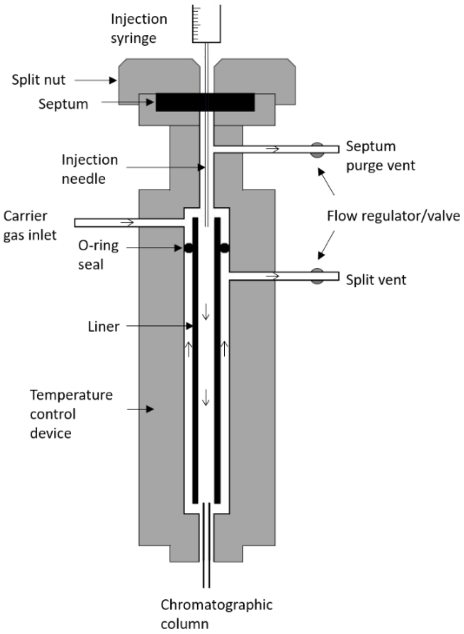

Figure 2-2 Typical configuration of a split/splitless injector adapted from reference.[1]

Chromatographic separation of substances within the sample then takes place within the column. As sample leaves the column an electronic signal is provided by a detector which is proportional to the amount of substance eluting. The detector equipped onto the 7820A GC Agilent system and used for the purpose of this project was a flame ionisation detector (FID), which has a sensitivity of 10 – 100 pg and is generally the most common detector due to its ability to detect organic compounds. This detector is illustrated in Figure 2-3. The FID responds to compounds containing carbon and hydrogen and its operation is dependent on the conversion of eluting compounds to a current. Upon elution of compounds from the column they enter the FID where they are burnt by a hydrogen-red flame. When combustion takes place ions are formed, which enter a collector. Contained within the collector are 2 plates through which a potential difference is applied. As the ions pass through the space between these plates a current is established and detected.[1]

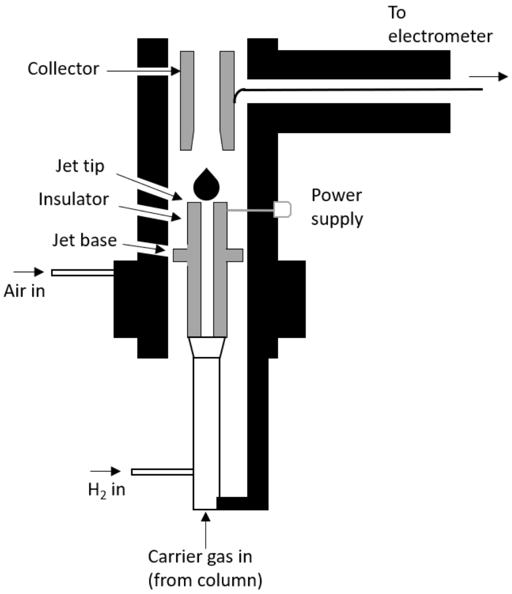

Figure 2-3 Schematic of a flame ionisation detector (FID) adapted from reference.[1]

2.2.1.2 Experimental

Analysis of products was achieved using an Agilent Technologies 7820 A gas chromatograph fitted with a CP-wax 52 CB capillary column and a flame ionization detector. The detector temperature was set to 250 °C and injector at 220 °C. The initial temperature of the column was 60 °C, which was ramped at 5 °C min^{-1} until a temperature of 200 °C was reached. The ramp rate was increased to 20 °C min^{-1} until a temperature of 240 °C was reached and held for 10 min. Quantification was achieved by calibration against bought analytical standards.

2.2.2 Gas chromatography mass spectrometry (GC-MS)

2.2.2.1 Theory

GC-MS combines two powerful analytical techniques to separate and structurally identify components within a mixture. As described in Section 2.2.1 the components are first separated by a column, which then passes through into a mass spectrometer. The most common ionisation technique in GC-MS is electron ionisation (EI). In this method electrons are bombarded into the gas phase molecules to produce ions. This bombardment causes the molecule to fragment, which can then be used to identify unknown compounds by use of the fragmentation pattern. The separated ions are displayed in the form of a mass spectrum, which plots the ions using their mass-to-charge ratio (*m/z*) against their relative abundance in the sample. The most ubiquitous device to produce the data is a transmission quadrupole analyser also known as a quadrupole mass filter (QMF). However, these devices can be limited due to producing data with an integer *m/z* value. This has led to the increase in popularity of time of flight (TOF) analyser, which can provide more accurate mass measurements and has lower detection limits.[2]

2.2.2.2 Experimental

Samples were analysed by the Cardiff university GC-MS service and analysed by Dr. Simon Waller. Analysis was performed using a Waters GC-TOF equipped with a BPX-5 column. The ionisation method utilised in this study was electron ionisation.

2.2.3 High-performance liquid chromatography (HPLC)

2.2.3.1 Theory

Separation for a mixture of components is resolved into its constituent parts by its passage through a chromatographic column. A mobile phase, containing the mixture of components, is carried through the stationary phase, which consists of a column packed with solid particles. The physical and chemical interactions between the two phases are responsible for the retention of solutes on the chromatographic column.[3]

HPLC instrumentation generally consists of 8 basic components (Figure 2-4): mobile phase/solvent reservoir, solvent delivery system, autosampler, column, detector, data collection and output system, post-detector eluent processing, and connective tubing and fittings.[4] The mobile phase reservoir is where the mobile phase is stored and can be any clean, inert container. Many separations can be done isocratically, which means that solvent being delivered to the column is not changing in composition over the course of the separation. For more complex separations a gradient elution can be performed which alters the proportion of the eluents over the course of the separation. Multiple solvents may be applied as the mobile phase and the selection is crucial to obtaining accurate quantitative data. The purpose of the pump is to deliver a precise, accurate, reproducible, constant, and pulse-free flow of mobile phase to the column. The purpose of the pump is to deliver a precise, accurate, reproducible, constant, and pulse-free flow of mobile phase to the column. To improve precision autosamplers are typically utilised and offer greater reproducibility between injections.

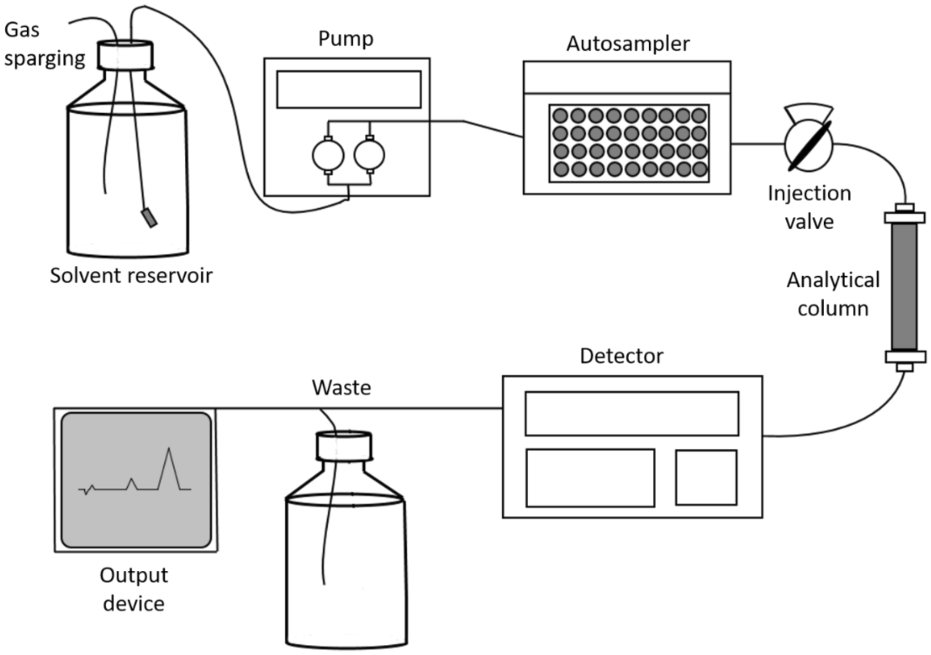

Figure 2-4 Schematic of a typical HPLC setup adapted from reference.[3]

The Metacarb 67 H column used in this investigation uses a column containing a 0.65 x 30 cm bed packed with a cation-exchange resin in the H^+ ionic form. Only an aqueous mobile phase is required to achieve separation of a variety of acids. The primary mode of separation is ion exclusion although steric exclusion and partitioning mechanisms may also be involved. The HPLC detectors are classified by their ability to either respond to the bulk properties of the eluent (refractive index detector, RID) or the solute property, which means it responds to some property of the analyte (diode array detector, DAD). The solute property detectors tend to be more sensitive than the bulk property detectors, on the order of 1000 times or more. In UV-vis detectors, such as DAD, the mobile phase is passed through a small-volume flow cell, where the radiation beam of a UV-vis photometer or spectrometer is located. However, the samples must consist of molecular components, which absorb light. For this reason, detection is limited to compounds containing unsaturated, aromatic or carbonyl compounds. RI detectors monitor the difference in RI between the column eluent containing analyte and a reference stream containing only the mobile phase.

The sensitivity of the RI detector is poor relative to other methods, since the difference in refractive indices between substances is small.[3]

2.2.3.2 Experimental

The analysis was carried out using an Agilent HPLC with ultraviolet and refractive index detectors. Reactants and products were separated using a Metacarb 67 H column. The eluent was an aqueous solution of H_3PO_4 (0.01 M) and the flow was 0.5 ml min^{-1}. Products were identified by comparison with bought samples. For the quantification of resulting compounds, an external calibration method was used.

2.3 Catalyst characterisation techniques

2.3.1 Electron Microscopy

2.3.1.1 Theory

An electron microscope uses a beam of electrons to create an image of a sample. This allows much greater resolutions and magnifications than with a regular light microscope. An electromagnetic lens is created by inducing a magnetic field in a solenoid (metal wire coil), which can carry an electric current. An electron beam passes through the centre of the solenoid, this electron beam can be easily controlled by changing he current through the solenoid. The faster the electrons travel the shorter the wavelength of the electrons. A smaller wavelength increases the resolving power of the microscope. This can be altered by increasing the voltage, which provides greater resolution.[5]

2.3.1.2 Transmission Electron Microscopy (TEM)

TEM uses a high voltage electron beam emitted by a cathode and then passes through an electromagnetic lens. The electron beam is partially transmitted through the thin sample, this interaction between the beam and the atoms can be used to observe features in the sample. An objective aperture can be used to enhance the contrast and block out high-angle diffracted electrons. The transmitted portion of this beam is then focused by an objective lens into an image on a phosphor screen or a charge coupled device (CCD). When the beam hits this phosphor screen light is created showing an image. In this image the dark areas represent places where the electrons could not pass through the sample and light areas where high proportions of electrons could pass through.[6]

2.3.1.3 Scanning Transmission Electron Microscopy (STEM)

STEM differs from TEM in that it scans only a very small probe over the sample. The STEM consists of an electron source, several lenses to focus these electrons into a small probe, a scanning unit to scan this probe across the sample and a detector that collects a signal after the electrons have interacted with the specimen. The microscope focuses this illumination to a single spot which is then scanned across the surface. An image is formed by recording a signal of interest as a function of the probe position. The image therefore relates to the part of the sample that the probe interacts with at each position. As in Figure 2-5, the convergent cone (with semi-angle α) defines a bright-field (BF) disk on a detector below, whole electrons scattered outside this cone arrive at an annular dark-field (ADF) detector. STEM relies on selecting collection angles, which may be varied using the diffraction projector lens and adjusting the "camera length".[5]

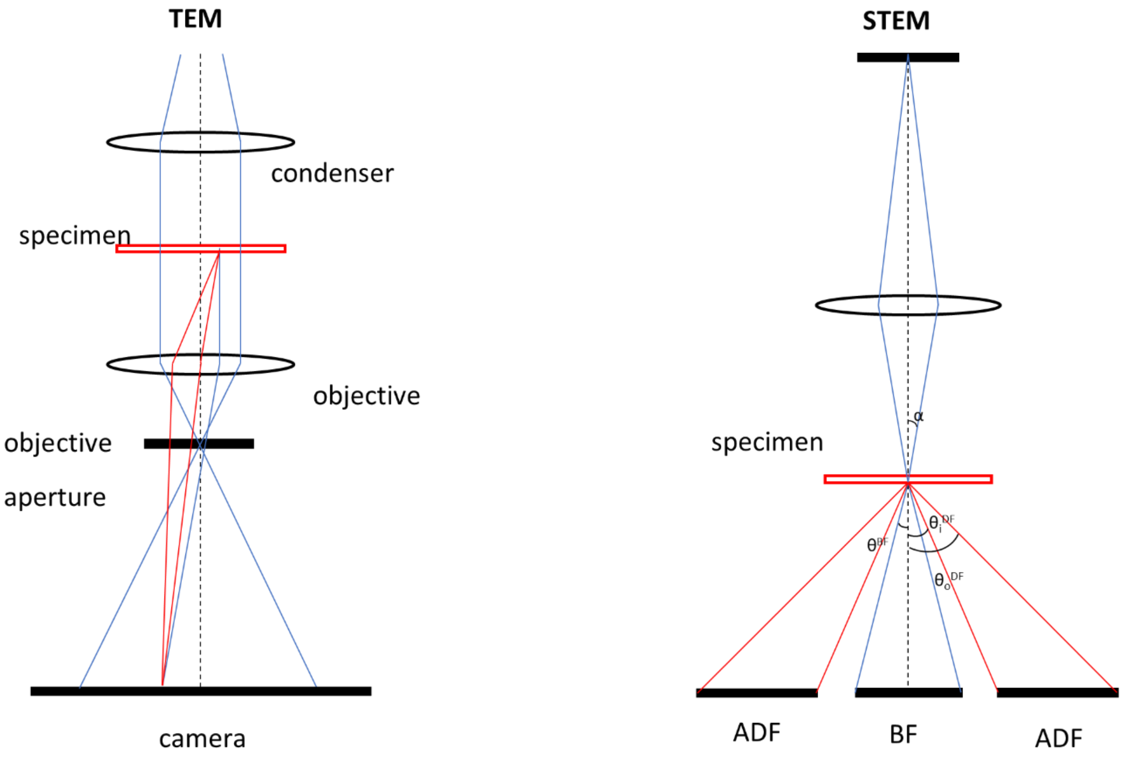

Figure 2-5 Basic microscope layout for TEM and STEM adapted from reference.[7]

Experimental

Scanning transmission electron microscopy (STEM) was performed on a Tescan MAIA 3 field emission gun scanning electron microscope (FEG-SEM) fitted with secondary and backscattered electron detection. Transmission electron microscopy (TEM) was performed on a Jeol JEM 2100 LaB6 microscope operating at 200 kV. Samples were suspended in ethanol and then deposited on holey carbon-coated copper grids. At least 150 particles were measured to plot size distributions.

2.3.2 Microwave plasma atomic emission spectroscopy (MP-AES)

2.3.2.1 Theory

Atomic spectroscopy includes several techniques, which can determine the elemental composition of a sample by measuring its electromagnetic spectrum. These techniques include inductively coupled plasma atomic emission spectroscopy (ICP-AES), which is capable of rapid multi-element analysis at and below nanograms per gram levels and flame atomic absorption spectroscopy (FAAS). MP-AES is an analytical technique aimed at improving analytical performance and productivity whilst also increasing accessibility and reducing running costs. MP-AES works on the principle that once an atom from a specific element is excited it emits a wavelength of light which is characteristic for that element as it returns to its ground state. The microwave plasma acts as the source of emission and this nitrogen fuelled plasma can reach temperatures close to 5000 K. This high temperature leads to a high population of excited states.[8]

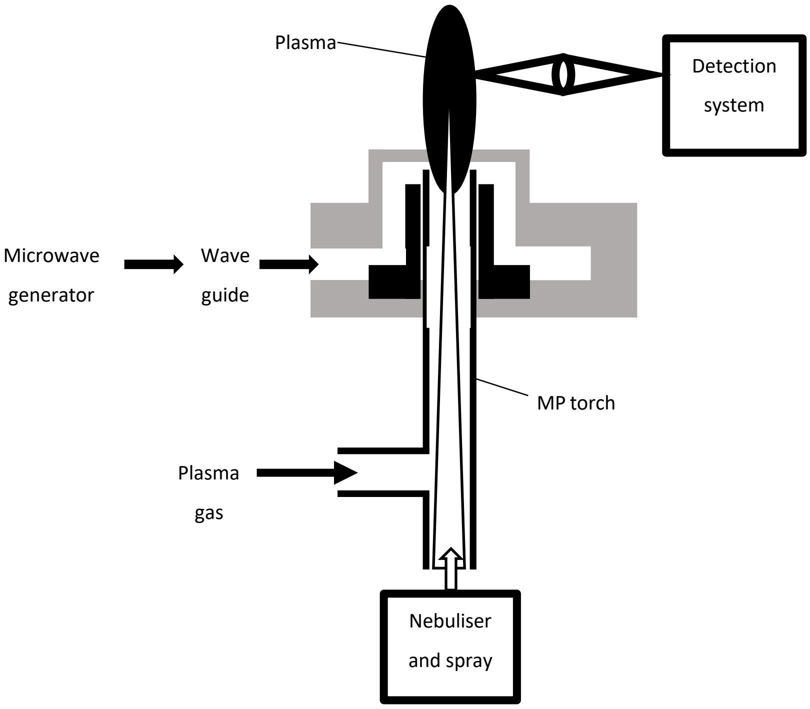

Figure 2-6 Schematic of a sample introduction system for MP-AES, adapted from reference.[8]

The MP-AES runs on a microwave induced plasma using a magnetron and N_2, which has been extracted from a compressed air source. In an MP-AES a microwave waveguide creates an optimised magnetic field at the torch using an axial magnetic field and a radial electromagnetic field to focus and contain the microwave energy to create a plasma. The sample is introduced to the plasma from a liquid sample using a nebuliser and a spray chamber, as depicted in Figure 2-6. This aerosol is introduced to the plasma where it is quickly atomised. The atoms are then excited and emit a characteristic wavelength of light. This emission is then directed at a fast-scanning monochromator. The required wavelength is then imaged onto a CCD detector. The element is quantified by comparing it to the emission of known concentrations of that element, plotted in a calibration curve.[8]

2.3.2.2 Experimental

Samples of the reaction solution were tested without dilution. If samples exceeded 100 ppm then samples were diluted as required using deionised water and then filtered using PTFE syringe filters (0.45 µm). For solid samples, 10 mg of catalyst was dissolved in freshly prepared *aqua regia* (5 ml) and left for 24 h. The solution was then diluted up to 50 ml using deionised water. Elemental composition was determined using an Agilent MP-AES 4100, quantification was achieved by calibration of the instrument using commercial calibration standards.

2.3.3 Powder X-ray diffraction (XRD)

2.3.3.1 Theory

XRD is a common technique for the characterisation of solid materials. The technique is based on the constructive interference arising from monochromatic x-rays and a crystalline sample. A cathode ray tube produces the X-rays which are filtered to produce monochromatic radiation which are then collimated and then directed at the sample. The sample will interact with the incident rays and cause constructive inference when the conditions satisfy Bragg's law (equation 2-2). A schematic representation of Braggs' Law is shown in figure 2-7.[9]

$$n\lambda = 2\ d \sin\theta \tag{2-2}$$

Where:

n = an integer and the "order" of reflection

λ = wavelength of the incident X=rays

d = interplanar spacing of the crystal

θ = angle of incidence

The diffracted X-rays are then collected and analysed. The sample is scanned through a range of 2θ angles so that all possible orientations for the diffraction pattern are collected for the crystalline sample due to the random orientation of the powder. The diffraction pattern can then be converted to d-spacings, which can be compared with a reference.

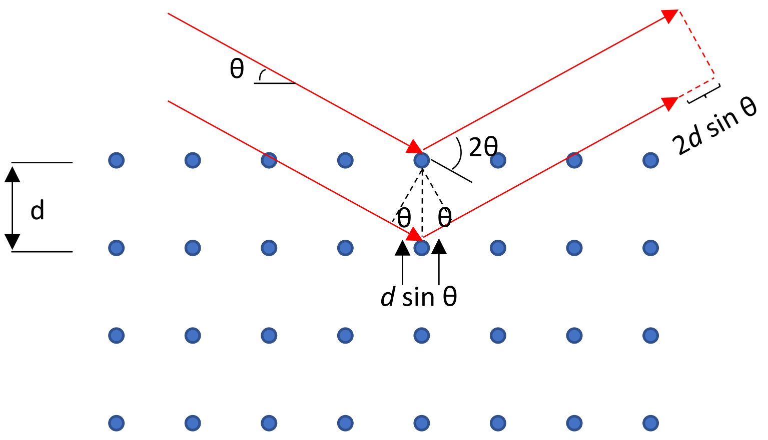

Figure 2-7 Representation of Bragg's law and diffraction of X-rays from a crystalline surface

From an XRD experiment you can learn to what extent the sample is crystalline, in addition to how many and which crystalline phases are present. Further evaluation can give you the relative amounts of crystalline components that are present and the crystal structures can be refined. Furthermore, some microstructural parameters such as crystallite size and lattice strain will affect the diffraction pattern and can be derived by line profile analysis.[10]

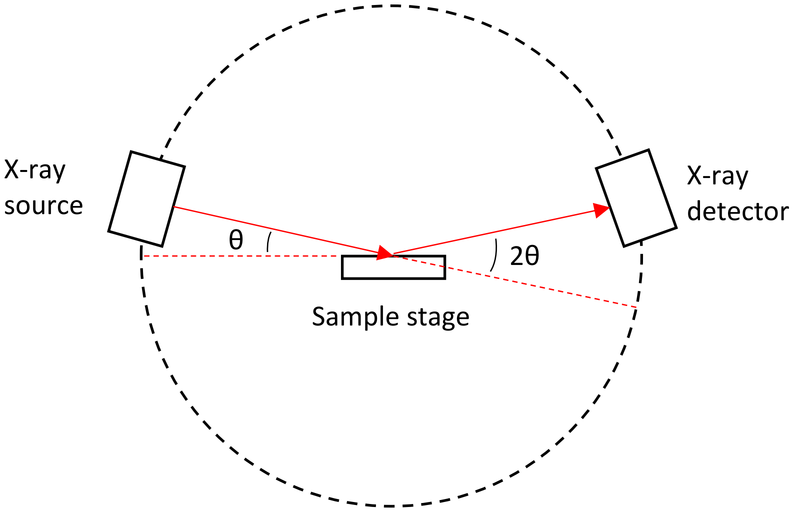

Figure 2-8 Schematic setup of an X-ray diffractometer

An X-ray diffractometer consists of an X-ray tube, a sample holder, and an X-ray detector as shown in figure 2-8. The X-rays are directed towards a target and when the electrons have enough energy to dislodge an inner-shell electron a characteristic X-ray spectrum is produced. The X-rays are then collimated and directed onto the sample, which is rotated along with the detector using a goniometer. The detector then records the peak intensity generated from the X-rays and converts the signal to a count rate which gives a quantifiable value.

In situ XRD allows you to heat the sample in a cell, which can withstand heat and is transparent to X-rays. The changes in structure of the catalyst as temperature increases can then be measured. In addition, the effect of different heating rates and gases on the phase produced can then also be observed.

2.3.3.2 Experimental

Powder X-ray diffraction was carried out using a Panalytical X'Pert diffractometer equipped with a Cu X-ray source operating at 40 kV and 40 mA. The ICDD standard database was used for phase identification where possible or checked against examples in the literature.

2.3.4 X-ray photoelectron spectroscopy (XPS)

2.3.4.1 Theory

In XPS, the sample is irradiated with low-energy (≈ 1.5 keV) X-rays, to provoke the photoelectric effect. The energy of the emitted photoelectrons is then determined by use of a high-resolution electron spectrometer. The analysis is conducted under vacuum, which is typically ≈ 10^{-10-} torr. The vacuum allows the transmission of the emitted photoelectrons to the analyser and minimises any contamination of the sample surface. This is important as XPS is a surface sensitive technique with a sampling depth of a few nanometres.[11]

When an atom or molecule is irradiated by the X-rays, an electron can be ejected (Figure 2-9). The kinetic energy (KE) of the of the electron is dependent upon the photon energy (hν) and the binding energy (BE) of the electron, which is the energy required to remove the electron from the surface. The equation which governs the photoemission process is detailed in equation 2-3.

$$KE = h\nu - BE \tag{2-3}$$

The kinetic energy of the emitted electron will allow the user to determine which elements are near the material's surface, their chemical states, and the binding energy of the electron. The binding energy can be affected by a few factors; the elements from which the electron is emitted, the chemical environments of the original atom the electron was emitted from, and the orbital from which the electron was emitted.

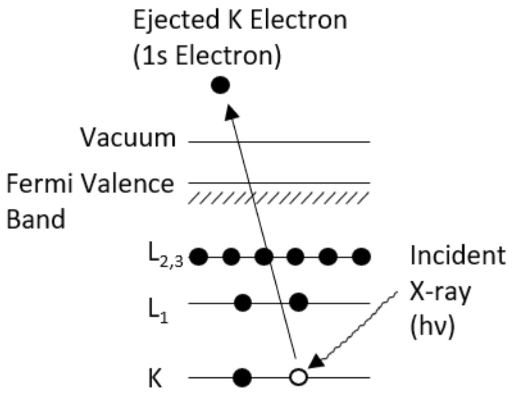

Figure 2-9 Photoemission process involved for XPS surface analysis

2.3.4.2 Experimental

All XPS was carried out by Dr David Morgan and analysed using a Thermo Scientific K-Alpha XPS spectrometer utilising monochromatic Al Kα radiation operating at an energy of 120 W (10 x 12 kV). The relative binding energies were standardised against a C 1s reference (284.7 eV) unless stated. The data was analysed using CasaXPS.

2.3.5 Nuclear magnetic resonance (NMR)

2.3.5.1 Theory

NMR is one of the most effective methods in obtaining information on chemical structure and dynamics. It is a unique technique in that there is a direct relationship between signal intensity and the number of atoms in a sample. The information gained in an NMR spectrum can also give straightforward insights into the relationship between spectral features and chemical structures.[12]

When certain nuclei are placed in an external magnetic field and are perturbed by a weak oscillating field, a magnetic dipole moment is generated. The angular momentum of this spinning charge can be described by its quantum spin number, *I*. Nuclei with an even mass and atomic number (e.g. ^{12}C), I = 0, which means their nuclei are not detectable. Nuclei with a spin number of I = ½ have a uniform spherical charge distribution and therefore a NMR spectra can be obtained. The most commonly utilised of these nuclei are ^{13}C and ^{1}H because of their abundance in organic structures.[12]

Only V nuclei are analysed in this investigation. The range of oxidation states which encompass V are -III to +V. Of these, 3 oxidation states (-III, -I, +V) where V intrinsically is diamagnetic and is thus susceptible to NMR. There are also 3 oxidation states where the nuclei is only diamagnetic under certain circumstances; +I (d^4 low spin), +III (d^2, low spin), and +IV (d^1, dinuclear anti-ferromagnetically coupled). V has two magnetic nuclei, ^{50}V and ^{51}V. The ^{51}V has a higher abundance (99.76 %) and is almost exclusively used in analytical V NMR. The ^{51}V NMR nucleus has a spin of 7/2, for which relaxation times are short. This becomes a disadvantage with respect to line widths and thus resolution in solution. This is overcome by some favourable properties of this nuclei, notably, its broad shift range, high natural abundance, and small quadrupole moment. In addition, the resonance frequency is close to that of ^{13}C, which makes the ^{51}V nucleus more accessible to conventional NMR methods.[13]

2.3.5.2 *Experimental*

NMR spectroscopy was conducted on a Bruker Avance III 500 MHz (11.7 Tesla) spectrometer equipped with a Prodigy cryoprobe, chemical shifts are reported in ppm. When required, reaction samples were diluted by 10 % with D_2O and ^{51}V NMR measurements acquired over 512 scans at a frequency of 131.55 MHz over the spectral range -100 ppm to -900 ppm.

2.3.6 Fourier transform infrared spectroscopy (FTIR)

2.3.6.1 *Theory*

FTIR analysis is used for identification of organic, inorganic, and polymeric materials. It utilises infrared light to scan the samples with alterations in the characteristic pattern of absorption bands indicating a change in the material composition. Infrared radiation, generally about 10 000 – 100 cm^{-1} is passed though the sample causing some of the radiation to be absorbed. This absorbed radiation causes a change in dipole moment of sample molecules This causes the vibrational energy of the material to transfer from ground state to excited state. The frequency of the absorption peak is determined by the vibrational energy gap and the number of absorption peaks is related to the number of vibrational freedoms of the molecule. In addition, the intensity of the absorption peak can be associated with the change of dipole moment and possibility of transitions between energy levels. A signal is then generated by the detector usually from 4000 – 400 cm^{-1}, which represents the materials molecular 'fingerprint'. This fingerprint is unique to the molecule making FTIR an important tool in chemical identification.[14] For a vibration to absorb infrared radiation and become excited, a change in dipole must occur. Therefore, homonuclear diatomic molecules such as N_2 and O_2 are not infrared active.

2.3.6.2 *Experimental*

All samples were analysed using a Agilent Cary 630 Fourier transform infrared spectrometer. All scans were conducted between 650 and 4000 cm^{-1}.

2.3.7 Raman

2.3.7.1 Theory

Raman spectroscopy is a vibrational spectroscopy technique, which is useful for investigating the vibrational, rotational, and other low-frequency modes in a specimen.[15] In this technique a sample is illuminated with a laser using a certain wavelength, the light interacts with the sample molecules and get either absorbed or scattered. The majority of light will be scattered elastically (Rayleigh scattering), where no change in wavelength occurs. However, 1 photon in 10^5-10^7 photons will be scattered inelastically, which results in a change of wavelength, known as Raman scattering. A weaker signal is obtained due to the significantly reduced number of scattered photons resulting in Raman scattering compared to Rayleigh scattering. This reduced sensitivity is a drawback of this approach as is interference from fluorescence of some samples.[16] The fluorescence of carbon samples can sometimes be overcome by using a lower intensity ultraviolet laser, which shifts any signals out of the visible range where fluorescence would be prominent.

The interaction between the incident photon and the sample results in an exchange of energy. The energy of the scattered photon can be either higher or lower than the energy of the incident photon (Figure 2-10). Stokes radiation occurs at lower energy (longer wavelength) than the Rayleigh radiation, and anti-Stokes radiation has greater energy.[17] This change in energy is directly linked to the change in rotational or vibrational energies in the examined molecule. These rotational or vibrational energies are specific to the chemical bond or constituent of the molecule and can therefore provide a unique signature of the molecule.

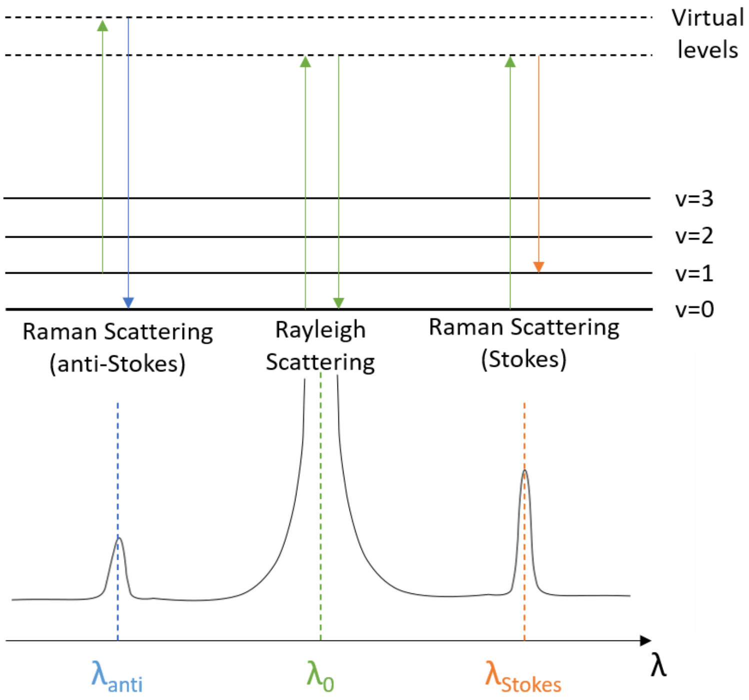

Figure 2-10 Stokes and anti-Stokes Raman scattering.

2.3.7.2 Experimental

Raman spectroscopy of SBA-15 GX materials was conducted using a Renishaw Inin-s confocal Raman microscope using an Ar ion green laser at a power of 20 mW. Spectra were generally obtained in the region of 850-2000 cm^{-1} to incorporate the D (sp^3) and G (sp^2) bands of sp^2 hybridised carbons.

2.3.8 Ultra-violet visible (UV-vis) spectroscopy

2.3.8.1 Theory

UV-vis spectroscopy is a technique which can be used for the quantitative determination of different analytes, such as transition metal ions, highly conjugated organic compounds, and biological macromolecules. The setup for the UV-vis spectrophotometer is relatively straightforward and consists of a light source, a wavelength dispersive element, sample, and detector. It is usually applied to liquid samples but can also be utilised for solids and gases. Solutions of transition metal ions can be coloured because they absorb light in the visible region (uv = 200-400 nm, visible = 400-800 nm). This is due to the excitation of d electrons from one electronic state to another.[18]

The lowest energy transition is between the highest occupied molecular orbital (HOMO) and the lowest unoccupied molecular orbital (LUMO). In transition metal complexes the energy required to excite an electron from the LUMO to the HOMO can depend on a number of factors: the oxidation state of the metal ion, nature of the metal ion (3d, 4d, 5d), number and geometry of ligands, and finally the nature of the ligands. The most common excitations are either ligand to metal charge transfers (LMCT) or metal to ligand charge transfers (MLCT). Charge transfers such as d-d can be observed in UV-vis spectrometry but are forbidden by selection rules so appear weak.[18]

2.3.8.2 Experimental

All samples were diluted with deionised water if necessary and analysed using a AvaSpec-USB2 Fiber Optic Spectrometer. All scans were conducted between 200 and 1100 nm.

2.3.9 Surface area and porosity analysis

2.3.9.1 Theory

A common method to determine the surface area of a material is using the Brunauer-Emmett-Teller (BET) theory. This theory was initially used to describe the multilayer adsorption of gas molecules on a solid surface and is typically used to calculate surface areas. The adsorption of gases is performed using the adsorption isotherms of non-reactive gases, such as, N_2 or Ar at 77 K and 87 K respectively. The pressure is the changed to include the monolayer coverage of molecules. The obtained isotherms can then be plotted into a linearised BET graph where the monolayer coverage can be calculated.[19] Equation 2-4 describes the isotherm:

$$\frac{\frac{P}{P_0}}{V\left(1-\frac{P}{P_0}\right)}=\frac{1}{V_mC}+\frac{C-1}{C}\frac{\frac{P}{P_0}}{V_m} \tag{2-4}$$

This is where V is the volume of absorbed at pressure P and absolute temperature T; P_0 is the vapour pressure of the gas at temperature T; V_m is the volume of gas absorbed at monolayer coverage. The constant C is mathematically derived from the heat of adsorption. When the function $(P / P_0) / V(1 - P / P_0)$ is plotted against P / P_0, a straight line is obtained where the slope and intercept give the values of V_m and C, respectively. Since it is the ratio of gases adsorbed (*i.e.* V/V_m) at a given relative pressure (P/P_0), a slight rearrangement of equation 2-5 gives:

$$\frac{\frac{P}{P_0}}{1-\frac{P}{P_0}}=\frac{V}{V_m}\left(\frac{1}{C}+\frac{C-1}{C}\frac{P}{P_0}\right) \tag{2-5}$$

The specific surface area can then be calculated from the obtained V_m using equation 2-6:

$$S_{BET}=\frac{(V_m)(N)(s)(a)}{V} \tag{2-6}$$

Where S_{BET} is the specific surface area; N is Avogadro's number; V_m is the molar volume of gas to form a complete monolayer; s is the cross-sectional area of adsorbent gas, which for nitrogen this is 16 Å^2.

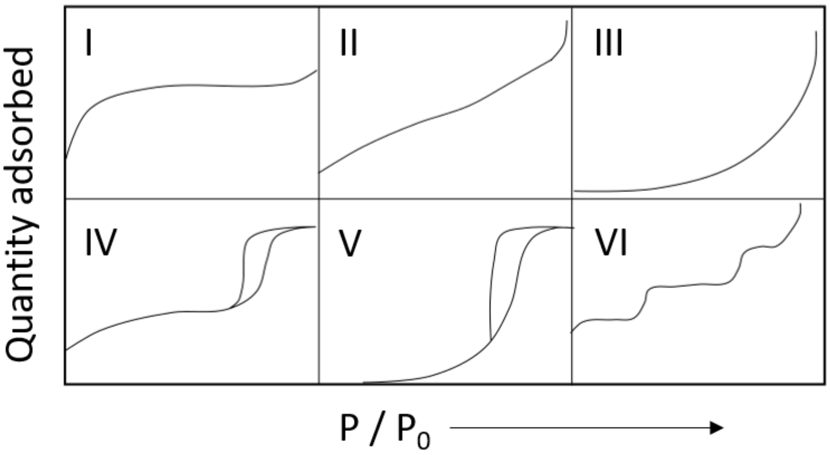

Figure 2-11 Adsorption isotherms showing the 6 IUPAC categorised types

The adsorption isotherm can give information on the pore characteristics of a material and the strength of adsorbate/adsorbent interactions. These isotherms are labelled from I through to VI according to an established by Branauer et al. and have been categorised by IUPAC (Figure 2-11).[20] Type I isotherm illustrates adsorption on a microporous material. Type II represents adsorption on macroporous material with strong adsorbent and adsorbate interactions, while type III occurs with weak interactions. Type IV and V isotherms are characteristic of mono- and multilayer adsorption with capillary condensation.[21]

Hysteresis loops obtained from the adsorption and desorption of inert gases can be classified into 4 groups, H1-H4 (Figure 2-12). These groups were designated by the IUPAC committee and can give information regarding the pore structure. The hysteresis loops can be interpreted as follows: H1 indicates a regular pore structure without interconnecting channels; H2 represents a pore structure with narrow and wide sections and possible interconnecting channels; H3 indicates that the pores developed are irregular and open with good connectivity between intragranular pores with shapes of parallel, slit-like, and open-ended tubes; H4 may suggest the presence of mesopores and narrow slit pores.

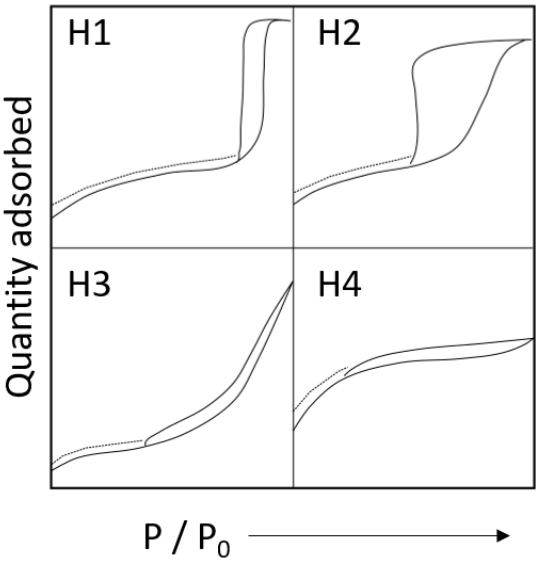

Figure 2-12 Hysteresis loops with 4 IUPAC recognised types

The Barrett-Joyner-Halenda (BJH) analysis is generally applied to calculate the pore size distribution of mesoporous materials.[22] It uses the modified Kelvin equation to relate the amount of adsorbate removed from the pores of the material, as the relative pressure (P/P_0) is decreased from a high to low value, to the size of the pores.

2.3.9.2 Experimental

Samples were analysed using the Micrometric 3Flex Surface Characterisation instrument. Samples were weighed to allow at least 50 m^2 for analysis and degassed at 250 °C for 6 h. Pore size was analysed using the BJH desorption plot obtained from the Micrometrics software.

2.4 References

1 E. Stauffer, J. A. Dolan and R. Newman, in *Fire Debris Analysis*, eds. E. Stauffer, J. A. Dolan and R. Newman, Academic Press, Burlington, 2008, pp. 235–293.

2 O. D. Sparkman, Z. E. Penton and F. G. Kitson, in *Gas Chromatography and Mass Spectrometry (Second Edition)*, eds. O. D. Sparkman, Z. E. Penton and F. G. Kitson, Academic Press, Amsterdam, Second Edition., 2011, pp. 2–13.

3 A. Fallon, R. F. G. Booth and L. D. Bell, Eds., in *Applications of HPLC in Biochemistry*, Elsevier, 1987, vol. 17, pp. 8–22.

4 M. E. LaCourse and W. R. LaCourse, in *Liquid Chromatography (Second Edition)*, eds. S. Fanali, P. R. Haddad, C. F. Poole and M.-L. Riekkola, Elsevier, Second Edition., 2017, pp. 417–429.

5 M. Omidi, A. Fatehinya, M. Farahani, Z. Akbari, S. Shahmoradi, F. Yazdian, M. Tahriri, K. Moharamzadeh, L. Tayebi and D. Vashaee, in *Biomaterials for Oral and Dental Tissue Engineering*, eds. L. Tayebi and K. Moharamzadeh, Woodhead Publishing, 2017, pp. 97–115.

6 B. Misof, P. Roschger and P. Fratzl, in *Comprehensive Biomaterials*, ed. P. Ducheyne, Elsevier, Oxford, 2011, pp. 407–426.

7 https://www.jic.ac.uk/microscopy/intro_EM.html.

8 *Microwave Plasma Atomic Emission Spectroscopy (MP-AES)*, 2021.

9 P. Debye, *Nature*, 1934, **134**, 303–305.

10 M. Che and J. C. Vedrine, *Characterization of Solid Materials and Heterogeneous Catalysts - From Structure to Surface Reactivity*, Wiley-VCH Verlag GmbH & Co. KGaA, 2012.

11 T. Asefa and V. Dubovoy, in *Comprehensive Supramolecular Chemistry II*, ed. J. L. Atwood, Elsevier, Oxford, 2017, pp. 157–192.

12 P. L. Rinaldi, X. Li, L. Li, L. Paudel and E. B. Twum, in *Polymer Science: A Comprehensive Reference*, eds. K. Matyjaszewski and M. Möller, Elsevier, Amsterdam, 2012, pp. 111–184.

13 D. Rehder, T. Polenova and M. Bühl, *Annu. Reports NMR Spectrosc.*, 2007, **62**, 49–114.

14 D. Titus, E. James Jebaseelan Samuel and S. M. Roopan, in *Green Synthesis, Characterization and Applications of Nanoparticles*, eds. A. K. Shukla and S. Iravani, Elsevier, 2019, pp. 303–319.

15 P. Graves and D. Gardiner, *Practical raman spectroscopy*, Springer, 1989.

16 A. K. Adya and E. Canetta, in *Animal Biotechnology*, eds. A. S. Verma and A. Singh, Academic Press, San Diego, 2014, pp. 247–263.

17 J. Ferraro, *Introductory raman spectroscopy*, Elsevier, 2003.

18 H. H. Perkampus, *UV-VIS Spectroscopy and Its Applications*, Springer, 1992.

19 D. Dollimore, P. Spooner and A. Turner, *Surf. Technol.*, 1976, **4**, 121–160.

20 J. Cortés, *Adv. Colloid Interface Sci.*, 1985, **22**, 151–176.

21 A. Chakraborty and B. Sun, *Appl. Therm. Eng.*, 2014, **72**, 190–199.

22 E. P. Barrett, L. G. Joyner and P. P. Halenda, *J. Am. Chem. Soc.*, 1951, **73**, 373–380.

3 The initiator-free solventless oxidation of cyclohexene using O_2

3.1 Introduction

Epoxidations are an important class of reactions within the chemical industry from pharmaceuticals to plastics.[1–3] Molecular oxygen is considered a cheap waste-free alternative and is generally the most desired oxidant from an environmental perspective.[4–6] Molecular oxygen lies in a stable paramagnetic state (two unpaired electrons in the ground state). Therefore, its electrophilic addition to alkene bonds (diamagnetic) is forbidden by spin selection rules.[7] Another challenge in alkene epoxidation arises from the lability of the allylic C-H bonds which have a bond dissociation energy of ~77 kcal mol^{-1} compared to the vinylic ethylene bond, which has a bond dissociation energy around ~112 kcal mol^{-1}.[8]

This investigation follows on from work by Ovoshchnikov et al. published in 2014 showing the effectiveness of Au catalysts for the oxidation of cyclohexene under solvent-free and initiator-free conditions.[9] The selectivity between allylic and epoxide products could be shifted depending on the choice of support or co-catalyst. Within this investigation it was observed that using WO_3 as a co-catalyst or support was able to shift selectivity towards the epoxide (Scheme 3-1). In contrast, the metal organic framework, MIL-101, was noted to catalyse the conversion of the cyclohexenyl hydroperoxide (cy-OOH) intermediate into 2-cyclohexen-1-one (cy-one).

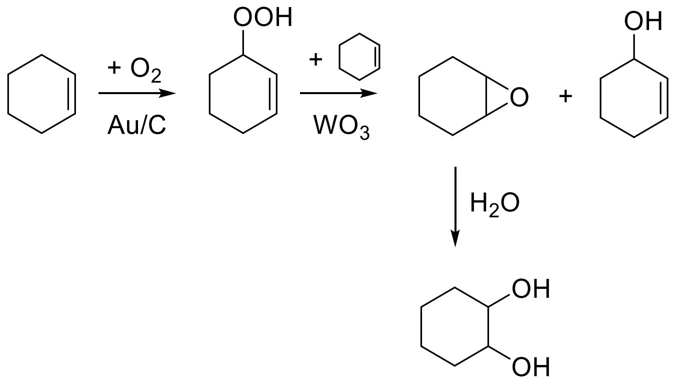

Scheme 3-1 Reaction scheme proposed by Ovoshchnikov et al. for the aerobic oxidation of cyclohexene[9]

Previous work in the Hutchings group has focused on the oxidation of cyclic alkenes using molecular oxygen.[10–12] Studies have shown that hydrogen peroxide or t-butyl hydroperoxide (TBHP), are required as initiators in a reaction which can then be maintained by molecular O_2. However, studies showed that an initiator was only required when the cyclic alkene contained a stabiliser molecule, such as 6-bis(*t*-butyl)-4-methylphenol (BHT) or 3-octadecyl-(3,5-di-*t*-butyl-4-hydroxyphenyl)-

propanoate (irganox 1076). Upon removal of this stabiliser reaction with and without an initiator is identical.[13] In the absence of an initiator, Donoeva et al. have proposed that the abstraction of the allylic proton is catalysed by metallic gold nanoparticles > 2 nm, this cyclohexnyl radical can then propagate the reaction.[14]

In the following investigation the initiator-free epoxidation of cyclohexene to *trans*-cyclohexanediol (CHD) is studied. Green principles such as solventless conditions and low temperatures are applied. The activities of Au/C catalysts prepared by sol immobilisation (SI) and wet impregnation (WI) are compared. The effect of using either graphite or graphene as the support was also investigated. A second part of this investigation also focuses on the impact of graphitic oxides (GOs) on the allylic oxidation of cyclohexene in a metal-free system. These GOs have previously exhibited good activity for the low-temperature aerobic epoxidation of linear alkenes in the absence of initiator or metal.[15] An optimum level of oxidation was necessary, with GOs prepared from Hoffmann procedures showing greater activity than those prepared from more conventional permanganate-based methods.

3.2 Experimental

3.2.1 Materials

Gold precursor ($HAuCl_4$, 99.8%) was purchased from Strem; hydrochloric acid (HCl, 37%) and nitric acid (HNO_3, 65%) were purchased from Fisher; sodium borohydride ($NaBH_4$, >97%), poly vinyl alcohol (PVA, 80% hydrolysed), sulfuric acid (H_2SO_4, 95–98%), n-decane ($C_{10}H_{22}$, 99%), cyclohexene (C_6H_{10}, 99%, inhibitor-free), 2-cyclohexen-1-ol ($C_6H_{10}O$, 95%), 2-cyclohexen-1-one (C_6H_9O, 98%), and cyclohexene oxide ($C_6H_{10}O$, 98%) were purchased from Sigma-Aldrich. The graphite and tungsten (VI) oxide (WO_3, nanopowder, <100 nm particle size) were purchased from Sigma-Aldrich. Graphene nanoplatelets aggregates (<1 µm) were purchased from Alfa Aesar. All materials were used without further purification.

3.2.2 Catalyst preparation

3.2.2.1 Impregnation

$HAuCl_4$ (0.816 ml, 12.25 mg/ml) was added to graphite or graphene (0.99 g) in a vial with enough water to create a thick slurry. This mixture was then heated to 80 °C and stirred for 30 min or until the stirrer bar became immobilised. The resulting paste was then dried for 17 h at 110 °C, yielding a black powder.

3.2.2.2 Sol Immobilisation

$HAuCl_4$ (0.816 ml, 12.25 mg/ml) was diluted in de-ionised water (400 ml) and stirred for 15 min. PVA (0.65 ml, 1 mM) was added to the mixture and stirring was continued for 15 min. $NaBH_4$ (1.269 ml, 0.2 M) was then added to the solution, causing a colour change from pale yellow to red. This mixture was then stirred for 30 min. Graphite or graphene (0.99 g) was then added to the solution with five drops of H_2SO_4 to turn the solution to pH 2. This mixture was then stirred for 1 h and filtered and washed with de-ionised water (1 L). The resulting powder was dried for 17 h at 110 °C, yielding a black powder.

3.2.3 Catalyst characterisation

Scanning transmission electron microscopy (STEM) was performed on a Tescan MAIA 3 field emission gun scanning electron microscope (FEG-SEM) fitted with secondary and backscattered electron detection. Transmission electron microscopy (TEM) was performed on a Jeol JEM 2100 LaB6 microscope operating at 200 kV. Samples were suspended in ethanol and then deposited on holey carbon-coated copper grids. At least 150 particles were measured to plot size distributions.

3.2.4 Catalyst testing

Cyclohexene oxidation was performed in a Colaver reactor heated using an oil bath. Typically, a mixture of cyclohexene (10 ml), catalyst (0.1 g), and n-decane (1 ml, as an internal standard) was magnetically stirred (900 rpm) at 60 °C. If required, WO_3 (0.1 g) and deionised water (1 ml) were also added to the mixture. The system was flushed with O_2 and remained connected to the O_2 line throughout the reaction to maintain a constant pressure (3 bar). After 24 h, the reactor was cooled down to room temperature and the reaction mixture was separated from the solid catalyst by centrifugation. Where two phases were formed, isopropanol (1 ml) was added to solubilise both layers. The liquid samples were analysed via gas chromatography (GC). Quantification of conversion and selectivity was conducted using n-decane as an internal standard with calibrations against commercial analytical samples. Selectivity was found in most cases to be largely to the allylic ketone (cy-one) and alcohol (cy-ol), cyclohexene oxide (cy-oxide), and cyclohexane diol (CHD). However, because of the high activity of the catalysts, there were many unknowns. Gaseous products were not analysed because of the use of a Colaver reactor, however, this contribution is likely to be negligible. The presence of cy-OOH was not confirmed as mentioned in the literature,[9] despite the use of GC-MS. The conversion, selectivity and mass balance were calculated as follows:

$$Conversion = \frac{(total\ mol\ of\ products)}{(total\ mol\ of\ products) + (total\ mol\ of\ unreacted\ substrate)} \times 100$$

$$Selectivity = \frac{(mol\ of\ product)}{(mol\ of\ observed\ products)} \times 100$$

$$Mass\ balance = \frac{(mol\ of\ product\ final)\ +(mol\ of\ final\ substrate)}{(mol\ of\ initial\ substrate)} \times 100$$

3.3 Results and discussion

3.3.1 Auto-oxidation of cyclohexene under aerobic conditions

Reaction conditions have been chosen to closely correlate those used in studies by Ovoshchnikov et al. to give a reasonable comparison. These reactions were carried out at a low temperature of 60 °C for 24 h without the use of a radical initiator and under solvent-free conditions. The main aim of this investigation was to improve the yield of epoxidation products such as, cy-oxide and CHD, as illustrated in Scheme 3-2. The greatest yield exhibited in the studies by Ovoshchnikov et al. was for a Au / WO_3 catalyst achieving a yield of 13 % after 16 h at 65 °C under 1 atm O_2.

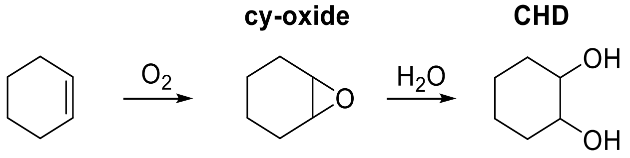

Scheme 3-2 Epoxidation products of cyclohexene oxidation

Initial tests were conducted to determine the auto-oxidation temperature of cyclohexene. This is important to ensure that the observed reaction products are a result of catalysis. These reactions were carried out under mild conditions with temperatures within the range of 50 to 70 °C and the oxygen pressure maintained at 3 bar for 24 h. The data shown in Table 3-1 clearly shows that a reaction does not occur at 50 or 60 °C, with only 1.0 and 2.0 % conversion displayed, respectively. At 70 °C a noticeable increase in conversion to 49 % is observed, this indicates that the temperature at which auto-oxidation can occur has been achieved. At a temperature of 70 °C, the oxidation can proceed without the involvement of a catalyst. Notably, there are four main products in this reaction: cyclohexene oxide (cy-oxide), 2-cyclohexen-1-one (cy-one), 2-cyclohexen-1-ol (cy-ol) and CHD. The compounds denoted as others do not accumulate to a significant degree but include cyclohexanol, cyclohexanone and 1,2-cyclohexanedione.

Table 3-1 Blank aerobic oxidation of cyclohexene under solventless initiator free conditions. Reaction conditions: 3 bar O_2, 10 ml cyclohexene, 1 ml decane (internal standard), 24 h

Entry	**Temp. / °C**	**Conv. / %**	**Selectivity / %**						**M. B / %**
			Cy-oxide	Cy-one	Cy-ol	CHD	Others	Unknowns	
1	50	1.0	21	35	30	0.0	2.0	11	92
2	60	2.0	3.0	48	42	2.0	2.0	3.0	97
3	70	49	8.0	55	17	8.0	5.0	9.0	55

The mass balance (M. B) under increased conversion is also seen to decrease significantly to 55 %, this decrease in mass balance occurs with increasing polymeric species in the reaction caused by the formation and build-up of radical species. Generally allylic oxidation is the dominating route, formation of cy-one and cy-ol occur through the reaction of cyclohexenyl peroxy intermediates as illustrated in Scheme 3-3. This route is favoured due to the lability of the allylic proton.

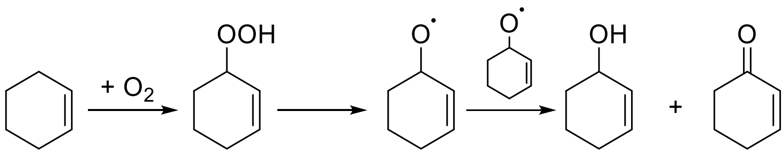

Scheme 3-3 Formation of allylic products occurs from generation of radical species

The selectivity profile for cyclic alkenes has been previously shown to be heavily influenced by the ring size. In work by Alshammari et al. ring sizes of C6 and below resulted in high selectivity to allylic products, whereas cyclic alkenes of C7 and above showed high selectivity to the epoxide. A suggestion for the difference in the selectivity profiles between C5 and C8 ring closure was associated with the additional ring strain on the transition state when the epoxide is formed. DFT calculations confirmed that the barrier to ring closure of radical intermediates is much greater for the smaller ring sizes.[16]

3.3.2 Aerobic oxidation of cyclohexene using Au/C catalysts

The aim of this work was to modify reaction conditions used by Ovoshchnikov et al. to achieve greater selectivity to the epoxide and subsequently to CHD. The catalysts focused on in this investigation were Au/Graphite and Au/Graphene. The catalysts were prepared via sol immobilisation and wet impregnation, with the results displayed in Table 3-2. For all catalysts, the Au content was maintained at 1 wt % with either a graphite or graphene support. Unless otherwise stated, all reactions were run at 3 bar O_2, 60 °C for 24 h, with 0.1 g of catalyst (5.08×10^{-6} Au mol %). The carbon supports show only a small amount of conversion. Graphite (entry 2) was inactive and had a comparable conversion to the blank reaction (entry 1), with 1.0 and 2.0 % conversion, respectively. The graphene support (entry 3) displayed a small increase of conversion to 4.0 % which may indicate some activity in this reaction, but it is still only a low amount and may be within error. WO_3 (entry 4) which is used as a co-catalyst in these reactions to promote the epoxidation route shows a small conversion of 10 %. This is accompanied by a selectivity of 37 % to cyclohexene epoxide and 5.0 % to CHD. Work from Ovoshchnikov et al. postulates that cy-OOH was a main product achieving 32 % selectivity with WO_3, however, this product is not stable enough to be identified by gas chromatography alone as it decomposes to form allylic products so is unlikely to be observed in these reactions. At higher conversions, as observed in entry 7 with 73 %, the main products are the allylic products, cy-ol and cy-one. Other main products are the epoxidation products, cy-oxide and CHD. Minor products such as cyclohexanol and cyclohexanone are not shown as their contributions were negligible.

Table 3-2 Aerobic oxidation results for cyclohexene and Au/C. Reaction conditions: 60 °C, 3 bar O_2, 0.1 g catalyst, 10 ml cyclohexene, 1 ml decane (internal standard), 24 h

Entry	**Catalyst**		**Conv. / %**	**Selectivity / %**					**M.B / %**
				Cy-oxide	Cy-one	Cy-ol	CHD	Unknowns	
1	Blank		2.0	3.0	48	42	2.0	3.0	97
2	Graphite		1.0	4.0	29	20	3.0	0.0	95
3	Graphene		4.0	13	49	27	0.0	8.0	96
4	1% Au/Graphite	WI	9.0	14	38	17	1.0	29	80
5		SI	62	4.0	55	16	5.0	17	78
6	1% Au/Graphene	WI	26	10	53	18	3.0	13	64
7		SI	73	0.0	56	19	8.0	12	70

The 1 % Au / Graphite (WI) catalyst shows a low conversion of 9.0 % resulting in a product distribution with main contributions attributed to allylic components, giving a total of 56 % selectivity to allylic species. The selectivity towards epoxydic products, namely, cy-oxide and CHD was low, with a total of 15 % selectivity to these components. Notably, this reaction suffers from a high selectivity towards unknowns. At a low conversion of 9.0 % it was unusual to observe this relatively high selectivity to unknowns as these are generally formed at high conversion when polymeric species are produced. When compared to the same catalyst prepared via SI, we observe a much greater conversion of 61 % which led to two phases being produced. This is due to the formation polar products and because of the generation of water, which is created as a by-product from the reaction of the cy-OOH to form the cy-one as shown in Scheme 3-4. The formation of two phases limits the total conversion due to increased mass transfer limitations. However, the water produced can also be used in the reaction for the hydrolysis of cyclohexene oxide to CHD, which is a non-catalytic step of the reaction and can occur at mild temperatures.[17] For analysis of biphasic mixtures, isopropanol was added to solubilise both layers and it was then quantified by GC.

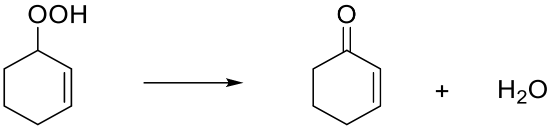

Scheme 3-4 Decomposition of cylohexenyl hydroperoxide (cy-OOH) to 2-cylohexen-1-one (cy-one) and water.

The results from various batches of 1 % Au / Graphite are displayed in Table 3-3 and a difference can clearly be seen between the batches of prepared impregnation catalysts. These reactions were run in Radley Carousel reactors as opposed to those previously run in Colaver reactors. This accounts for discrepancy observed between these values and those in Table 3-2. The selectivity between the various batches is consistent, however, the amount of conversion differs significantly among the batches. There is a 10 % difference in conversion between batch 3 and 4. Each catalyst was prepared with the same graphite source so any discrepancies would most likely be a result of the dispersion and size distribution of Au nanoparticles on the carbon surface which is notoriously unpredictable for WI catalysts.[18–20]

Table 3-3 Aerobic oxidation of cyclohexene showing batch variation in the preparation method between 1 % Au / C WI and SI catalysts Reaction conditions: 60 °C, 3 bar O_2, 0.1 g 1 % Au / C, 10 ml cyclohexene, 1 ml decane (internal standard), 24 h

Entry	**Catalyst**	**Batch**	**Conv. / %**	**Selectivity / %**					**M.B / %**
				Cy-oxide	Cy-one	Cy-ol	CHD	Unknowns	
1	WI	1	20	13	35	13	4.0	10	80
2		2	23	14	37	14	4.0	12	82
3		3	25	14	34	14	1.0	8.0	83
4		4	26	12	34	13	4.0	9.0	73
5	SI	1	74	0.0	50	18	9.0	17	78
6		2	71	2.0	48	16	7.0	16	73
7		3	73	0.0	44	17	8.0	23	78
8		4	70	0.0	44	19	7.0	22	69

For SI catalysts, also shown in Table 3-3, the difference between batches is less considerable. The largest change in conversion between these catalysts can be seen between batches 1 and 4, which are entries 5 and 8, respectively. This change in conversion is only 4.0 % compared to the 10 % difference observed with the WI catalysts. This reproducibility with the catalyst would be predominantly due to the narrower size distribution achieved with a SI method, where the PVA acts as a stabiliser around the Au nanoparticles which helps obtain a narrow size distribution. The most active catalyst for aerobic oxidation proved to be Au/Graphite (SI). Table 3-4 displays data for its reuse with 2 successive reactions. The conversion remains consistent during each run showing a stability of the Au nanoparticles when exposed to these mild reaction conditions and when subjected to the organic species in the reaction. Leaching is also not observed under these conditions when analysed by ICP-MS.

Table 3-4 Catalyst reuse results for Au/Graphite (SI) catalysts Reaction conditions: 60 °C, 3 bar O_2, 0.1 g 1 % Au / C, 10 ml cyclohexene, 1 ml decane (internal standard), 24 h

Entry	**Catalyst**	**Reuse**	**Conv. / %**	**Selectivity / %**					**M.B / %**
				Cy-oxide	Cy-one	Cy-ol	CHD	Unknowns	
1	SI	1	61	2.0	34	10	3.0	11	72
2		2	60	1.0	30	14	2.0	15	68
3		3	61	2.0	30	16	0.0	14	56

3.3.3 Microscopy images of Au/C

Au nanoparticle mean diameter sizes were analysed by TEM bright-field imaging and STEM techniques to establish a relationship between Au nanoparticle size and selectivity to desired products. Where it became difficult to observe nanoparticles, particularly in the case of WI catalysts, a back-scattered electron (BSE) approach was used. The size distribution plots in Figure 3-1 (c, f, i) illustrate the nanoparticle sizes determined from TEM and BSE. The images demonstrate that mean diameters from SI catalysts are much lower than those obtained from a WI preparation as would be expected. SI catalysts (a, b, c, g, h, i) have a mean nanoparticle size of 4 nm with a standard deviation of 1.2 nm compared to WI catalysts (d, e, f) which have a mean diameter of 20 nm and a standard deviation of 6 nm. The effect of the choice of carbon support, between graphite and graphene, on nanoparticle size appears to be negligible. This can be observed with the Au / Graphite (a, b, c) and Au/ Graphene SI (g, h, i) catalysts which display the same mean particle size and standard deviation of 4.5 nm and 1.2 nm, respectively.

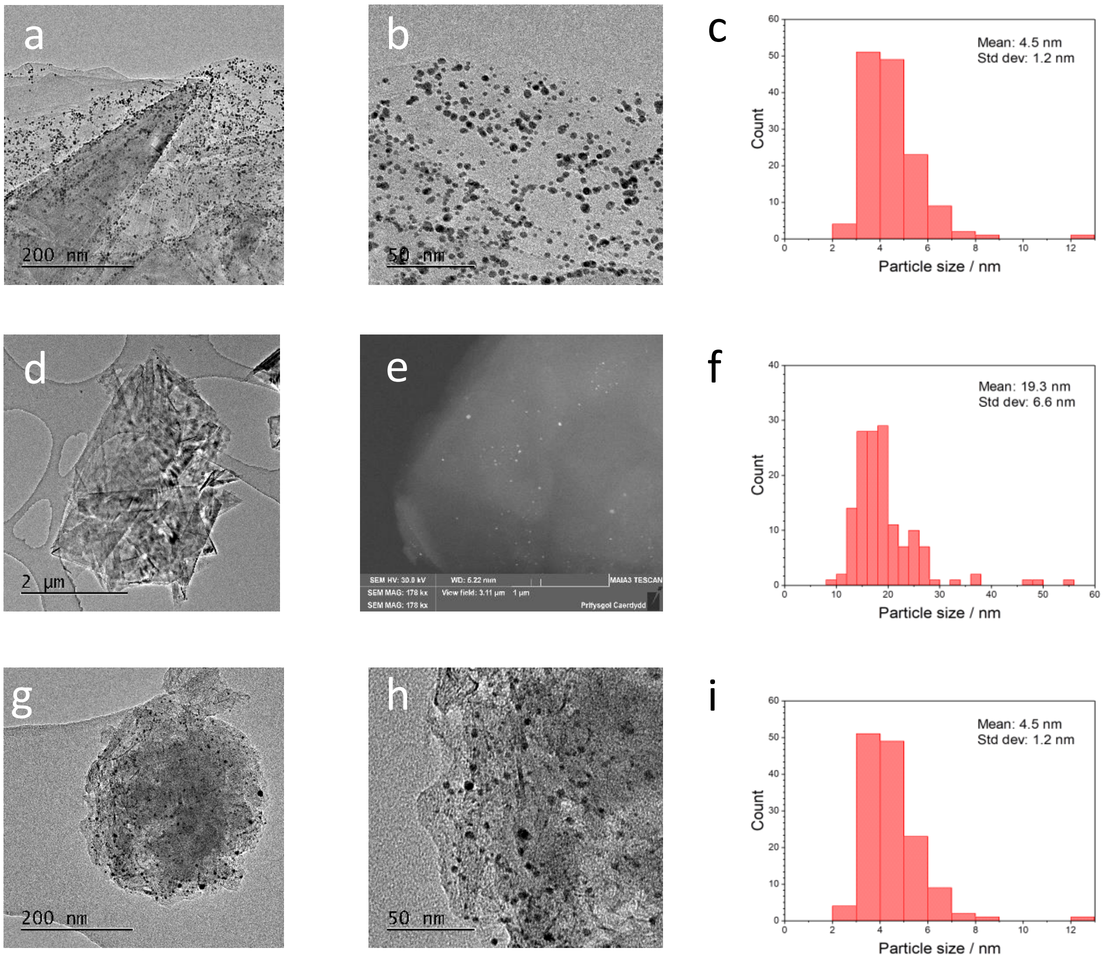

Figure 3-1 Bright field transmission electron microscopy (TEM) images of 1% Au / graphene via SI (a, b) show mean particle diameter of 4.5 nm, standard deviation of 1.2 nm shown in (c). TEM (d) and Back-scattered electrons (BSE) images (e) of 1 % Au / graphite prepared by impregnation show mean particle size of 19.3 nm and a standard deviation of 6.6 nm shown in (f). Bright field TEM images (g, h) of 1 % Au / graphite via SI show mean particle diameter of 4.2 nm, standard deviation of 1.1 nm shown in (i).

The mean nanoparticle size of Au / Graphene (WI) was unable to be determined because a large enough sample size could not be found. Figure 3-2 displays 2 of the images obtained in which 2 nanoparticles can be observed of 62 nm in Figure 3-2 (a) and 90 nm in Figure 3-2 (b). However, a particle size distribution similar to Au / Graphite (WI) would be expected, where large Au nanoparticles such as these would be visible.

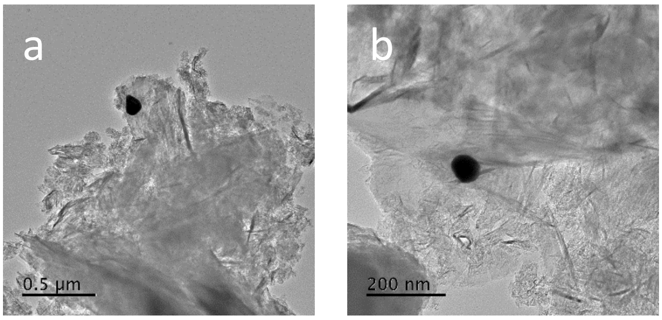

Figure 3-2 Bright field TEM imaging of Au / Graphene (WI) displaying large nanoparticles typical of an impregnation preparation technique

The Au wt. % as determined by energy dispersive X-ray (EDX) analysis is illustrated in Table 3-5. Since this is a surface sensitive technique and dependent on the area of analysis, these values tend to overestimate the Au content. These values differ significantly from the intended 1 wt. %, with the largest deviation of 11.4 %, which was a product of 1 % Au / Graphene (WI). This may result from the area chosen, possibly containing a large nanoparticle as shown in Figure 3-2. However, these results do confirm the presence of Au in these catalysts.

Table 3-5 EDX analysis of Au / C catalysts to determine Au wt. %

Catalyst	Preparation method	Au Wt. %
1 % Au / Graphite	SI	5.8
1 % Au / Graphite	WI	3.7
1 % Au / Graphene	SI	2.3
1 % Au / Graphene	WI	11.4

3.3.4 Aerobic oxidation of cyclohexene with Au/C and WO_3

Ovoshchnikov et al. demonstrated that use of WO_3 in aerobic solventless conditions could improve selectivity to epoxidation products.[9] The addition of WO_3 as a co-catalyst with 1 % Au / Graphite (WI) results in an increase in conversion to 18 % from 9.0 %, due to the additional activity contributed by WO_3. The effect of adding WO_3 (Table 3-6) also markedly increases selectivity to cyclohexene oxide with a total of 35 % selectivity to either epoxide or CHD. The total selectivity towards allylic species is 53 % which is always expected to be above 50 % due to the formation of equimolar amounts of allylic alcohol and epoxide as mentioned previously. However, the benefit of adding WO_3 to the 1 % Au / Graphite (SI) catalyst is not observed to the same extent, due to the increased activity obtained using a SI catalyst.

Table 3-6 Aerobic oxidation results with WO_3 co-catalyst to increase conversion to epoxide. Reaction conditions: 60 °C, 3 bar O_2, 0.1 g 1 % Au / C, 0.1 g WO_3, 10 ml cyclohexene, 1 ml decane (internal standard), 24 h

Entry	**Catalyst**		**Conv. / %**	**Selectivity / %**					**M.B / %**
				Cy-oxide	Cy-one	Cy-ol	CHD	Unknowns	
1	WO_3	-	10	37	12	40	5.0	3.0	98
2	Au / Graphite + WO_3	WI	18	30	22	31	5.0	10	85
3		SI	75	0.0	37	16	14	28	93
4	Au / Graphene + WO_3	WI	42	7.0	46	21	5.0	17	65
5		SI	76	0.0	49	17	9.0	20	78

The 1 % Au / Graphene (WI) catalyst shows greater conversion compared to the identical catalyst prepared with graphite. Reasons for this increased activity could be related to the increased surface area of graphene compared to graphite. There could also be an increased level of dispersion of Au nanoparticles across the graphene surface, which would increase the accessible active sites. Another explanation for this increased activity may result from the stabilisation of radical intermediates across the graphene surface due to a better electron mobility on graphene compared to graphite, this effect was observed by Yang et al. for cyclohexane oxidation.[21] The 1 % Au / Graphene (SI) catalyst demonstrates a much higher conversion at 73 %, which is comparable to the graphite catalyst. As observed previously, there is a correlation with conversion and selectivity to unknowns. This is attributed to the further oxidation of products, to form oligomers and other polymeric species.[22] In addition, due to the radical nature of the reaction there can be several different reaction pathways resulting in a variety of reaction products.

Table 3-7 shows the effect of adding de-ionised water to these reactions. The purpose of the addition of water is to hydrolyse the epoxide to form CHD, which is a non-catalytic step. For 1 % Au / Graphite (WI) we observe a comparable conversion to that observed without WO_3 or water. Under those conditions, a total of 15 % selectivity to either cy-oxide or CHD was observed, and in this instance a total combined selectivity of 19 % to either of the epoxidation products is observed. The graphite SI equivalent shows a higher conversion but lower levels of CHD. The total conversions of all these reactions are lower compared to the equivalent reactions run without water. This is evidence for water being detrimental to these reactions most likely due to the formation of a biphasic system and mass transfer limitations associated with this. The number of unknowns in this reaction generally increases with conversion, however the individual contributions of these compounds are not considered significant.

Table 3-7 Aerobic oxidation results with water added to convert cy-oxide to CHD. Reaction conditions: 60 °C, 3 bar O_2, 0.1 g 1 % Au / C, 0.1 g WO_3, 10 ml cyclohexene, 1 ml H_2O, 1 ml decane (internal standard), 24 h

Entry	**Catalyst**		**Conv. / %**	**Selectivity / %**					**M. B / %**
				Cy-oxide	Cy-one	Cy-ol	CHD	Unknowns	
1	Au/Graphite + WO_3 + H_2O	WI	12	2.0	46	23	17	10	74
2		SI	27	0.0	49	24	9.0	14	73
3	Au/Graphene + WO_3 + H_2O	WI	40	0.0	40	25	14	19	110
4		SI	57	0.0	33	19	11	34	110

3.3.5 Time-online for aerobic oxidation

Figure 3-3 demonstrates the relationship between the reaction time and yield to products in the aerobic oxidation of cyclohexene. Notably there is a significant induction period associated with this reaction with a relatively slow reaction rate from 0 – 10 h, which then accelerates between 10 – 15 h. An acceleration of the reaction occurs at around 10 h and the conversion reaches a maximum of 74 % after 23 h which is maintained even after 48 h. The increase in conversion may stop because of mass transfer limitations caused by an increase in viscosity of the reaction mixture and the formation of a biphasic mixture. This biphasic mixture forms due to the presence of polar compounds and water generated in the reaction. Selectivity over the course of the reaction is predominantly directed towards allylic products. Cy-one remains the most dominant product over the duration of the reaction with selectivity reaching 51 % after 20 h. This selectivity is largely maintained throughout the reaction with it being its lowest at 33 % after 1 h of reaction. Furthermore, this allylic product is also the only product which increases in yield significantly over the reaction. CHD reaches the highest selectivity of 7.0 % after 23 h, this increase in yield to CHD coincides with a similar decrease in yield to cy-oxide as would be expected when the epoxide is hydrolysed to the diol with an increased presence of in situ water in the mixture. However, these products formed through the epoxidation route remain minor products relative to allylic species.

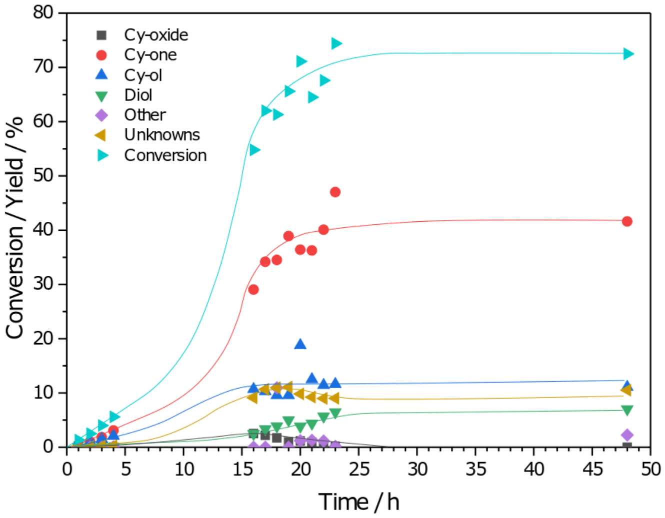

Figure 3-3 Time online data for the aerobic oxidation of cyclohexene for Au/C (SI) ***Reaction conditions:*** *60 °C, 3 bar O_2, 0.1 g 1 % Au / C, 10 ml cyclohexene, 1 ml decane (internal standard)*

A mechanism was proposed by Alshammari et al. and an adapted version is displayed in Scheme 3-5, although the initiator, TBHP, was used in this instance.[16] The proposed mechanism differs from that suggested by Ovoshchnikov et al. because a high selectivity to cy-oxide (**9**) should be attainable, since its formation does not result in termination. In this example, the reaction is propagated by the abstraction of an allylic proton by a TBHP radical, to give **2**. Without the presence of a radical initiator, the abstraction of an allylic H^+, is reported to be catalysed by Au nanoparticles > 2 nm, which was also proposed by Donoeve et al.[14] The cyclohexenyl radical can then capture an oxygen molecule to form a peroxy radical, **3**, which can then abstract another proton from a cyclohexene molecule to produce the cy-OOH, **4**, and another cyclohexene radical, **2**. The hydroxy radical, **5**, is then generated which creates a situation where there are three possibilities of reaction routes. In the first route 2 molecules of **5** react to produce cy-one (**6**) and cy-ol (**7**), which acts as a termination step. Alternatively, an interaction between **5** and the double bond of cyclohexene to form the intermediate, **8**, which can ring close to form cy-oxide, **9**, and an allylic radical, **2**. A third route involves the reaction of **5** and further substrate with another H abstraction from the allylic position to produce the allylic alcohol and allylic radical, **2**. In ring sizes of C6 and smaller allylic products are favoured due to the ring strain caused by the formation of the epoxide, which may explain the selectivity profile of these reactions.[16]

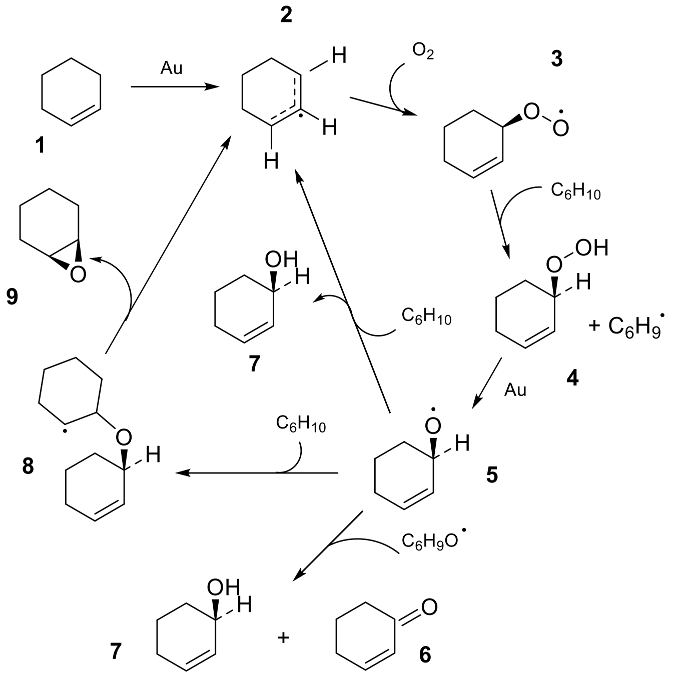

Scheme 3-5 Proposed mechanism for aerobic oxidation of cyclohexene which would lead to observed products, adapted from Alshammari et al.[16]

The WI catalyst, in Figure 3-4, illustrates that a much longer induction period is required for the reaction to achieve the same conversion as the SI catalyst. This is most likely due to the larger Au nanoparticles having a lower capability to abstract the allylic H^+. This catalyst required 48 h to reach a conversion of 58 % compared to the SI catalyst which required 16 h to reach 55 %. Selectivity to the various products in the reaction seems to be unaffected by the catalyst preparation method used. Similarly, the allylic components of the reaction generate the highest yields with cy-one achieving the greatest selectivity at 58 %. Epoxidation products are also minor products when using a WI catalyst over extended reaction times. CHD is obtained in a 3.0 % yield after 16 h, which only increases to 7.0 % after 48 h.

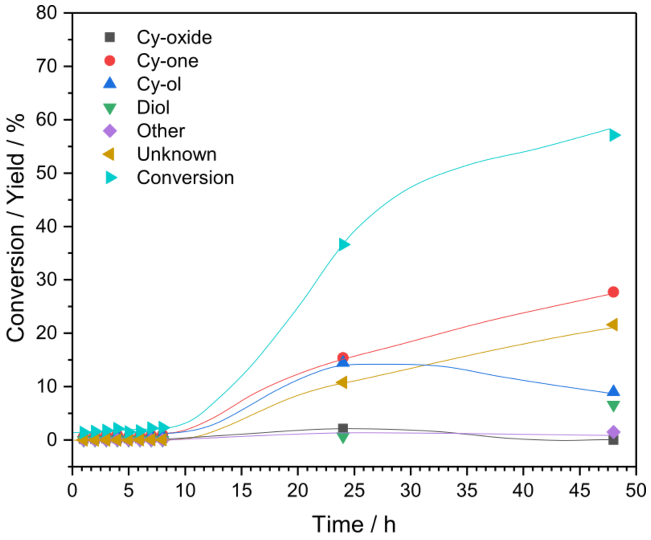

Figure 3-4 Time online data for the aerobic oxidation of cyclohexene for Au/C (WI) ***Reaction conditions:*** *60 °C, 3 bar O_2, 0.1 g 1 % Au / C, 10 ml cyclohexene, 1 ml decane (internal standard)*

At conversions above 30 % there is a noticeable decrease in mass balance. Figure 3-5, illustrates this relationship between mass balance and conversion. When conversion increases there is likely an increase in polymeric species which typical of this type of radical reaction.[23] This increase in polymeric species is accompanied by a rise in viscosity, which decreases the mass transfer and slows any conversion associated with the starting material. A high mass balance is only observed at low conversions, below 10 %. At high conversions of around 70 % a biphasic reaction mixture forms, owing to the water that is produced by the decomposition of the cy-OOH species and due to the formation of polar products. When a biphasic mixture was formed, isopropanol was added to the reaction mixture to homogenise the organic and aqueous layers so GC analysis could be performed.

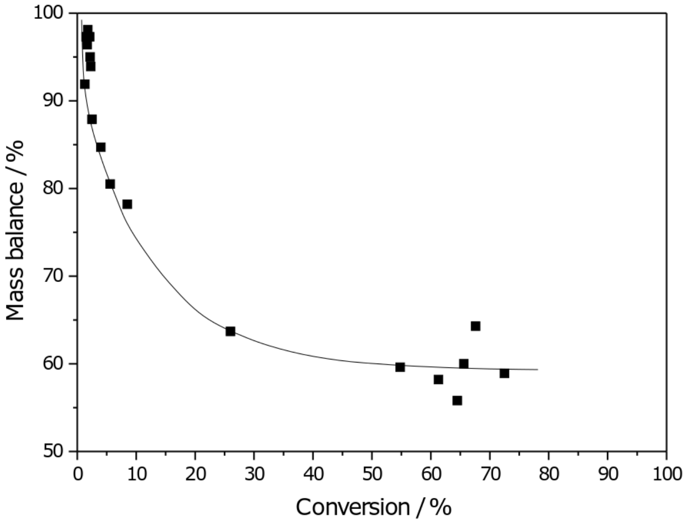

Figure 3-5 Plot of mass balance vs. conversion. ***Reaction conditions:*** *60 °C, 3 bar O_2, 0.1 g 1 % Au / C, 10 ml cyclohexene, 1 ml decane (internal standard)*

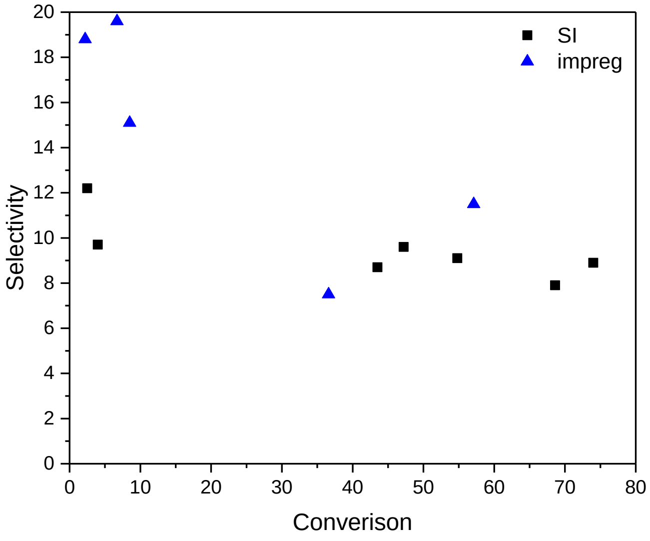

Figure 3-6 Conversion of cyclohexene versus selectivity to epoxidation products (cy-oxide and CHD. ***Reaction conditions:*** *60 °C, 3 bar O_2, 0.1 g 1 % Au / C, 10 ml cyclohexene, 1 ml decane (internal standard)*

The selectivity to epoxidation products can be seen to favour low conversions with SI catalysts as shown in Figure 3-6. At high conversions and long reaction times the thermodynamic product of the reaction would be favoured meaning more allylic products are formed. This increase in allylic products then dwarves any epoxide products that are formed. It is also postulated that the generation of any cy-oxide also results in an equimolar production of cy-ol. There is also a difference between the selectivity to epoxidation products from the WI catalyst and SI catalyst. At conversions between 0-10 % there is a selectivity of 20 % and 7.0 % conversion to epoxidation products. This is higher than for the SI catalyst which at a similar conversion only produces 10 % selectivity to epoxidation products. However, at high conversions this difference between the catalysts becomes negligible as allylic products become the major products in both catalysts.

3.3.6 Allylic oxidation of cyclohexene by graphitic oxides

In this study the use of a range of graphitic oxides (GO) was investigated to understand their efficacy for the solventless oxidation of cyclohexene. These GOs were initially prepared and characterised in work by Pattisson et al.[24] Interestingly, it was demonstrated that these carbocatalysts were active for the epoxidation of a range of linear alkenes, despite the absence of supported metal or an initiator. This previous study found that the activity of these the surface of the GOs were highly sensitive to the amount of oxidant used in the preparation and tuning of the surface could be achieved by tailoring the preparation method. The conventional Hummers (HU) based materials produced using permanganate as oxidant were less active when compared to a Hofmann (HO) series of GOs which utilise chlorate as the oxidant.[15]

Table 3-8 describes a selection of the studied GOs detailing the amount and type of oxidant used, with the oxygen wt. % as obtained from XPS analysis. These materials were selected to offer a varying degree of oxidation and to represent each of the preparation techniques. The naming system of the GOs (GO-XX##) corresponds to whether a Hofmann or Hummers method was utilised and to represent the amount of oxidant (g) used per 5 g of graphite. The oxygen wt. % does not correlate linearly with the amount of oxidant used, therefore it was more meaningful to relate catalyst activity to oxygen wt. %.

Table 3-8 Range of graphitic oxides prepared by Hofmann and Hummers methods and the obtained oxygen wt %.

Catalyst	**Oxidant used per 5 g Graphite (G)**	**Oxygen wt. %**
GO-HO1	1	9.0
GO-HO2	2	8.9
GO-HO4	4	14.6
GO-HO15	15	18.6
GO-HO20	20	21.1
GO-HO30	30	25.0
GO-HU15	15	33.2

Similarly, to the previous work with Au / C catalysts this work was also performed at a low temperature of 60 °C to assess the catalytic activity of the GOs and minimise auto-oxidation. The surface oxygen wt. % can be observed to correlate with conversion (Figure 3-7). This effect was also observed with linear alkenes displaying an optimum oxygen surface wt. % of 25 % for the highest catalytic activity. The surface of the GOs is mostly covered with hydroxyl, epoxide, and carboxylic acid functional groups among other more minor moieties. The GO-HU15 shows that there is no significant benefit of this preparation method on conversion, despite its higher surface oxygen content of *ca.* 33.2 wt. % oxygen. The selectivity is largely dominated towards allylic oxidation products cy-one and cy-ol and is unaffected by the surface oxygen content of the GOs (Figure 3-8). The selectivity to epoxidation products (cy-oxide and CHD) is mostly stable at around 10 %. In previous work focused on linear alkenes, a high initial selectivity to allylic compounds was observed which then diminished to give the epoxide as the major product. This was a reproducible trend across a range of linear alkenes. However, this effect is more difficult to replicate in cyclic alkenes of ring size C7 and below, with a high preference to from allylic compounds. This is suggested to result from the greater energy associated with ring closure of the radical intermediate in smaller ring sizes.

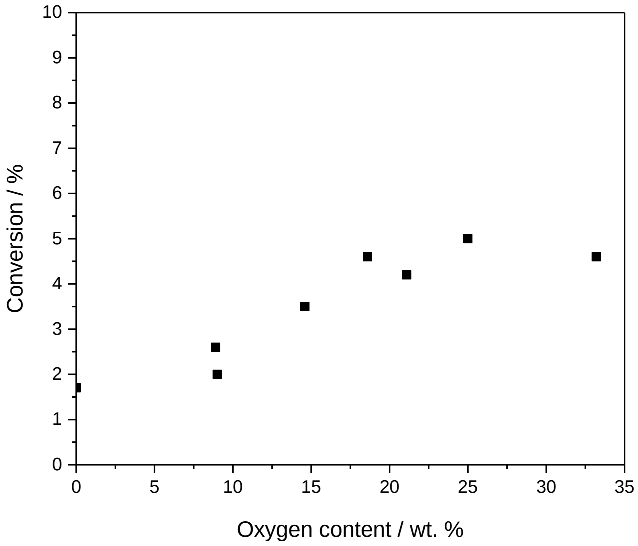

Figure 3-7 Catalytic activity of graphitic oxides and their reactivity in cyclohexene oxidation ***Reaction conditions:*** *60 °C, 3 bar O_2, 0.1 g catalyst, 10 ml cyclohexene, 1 ml decane (internal standard)*

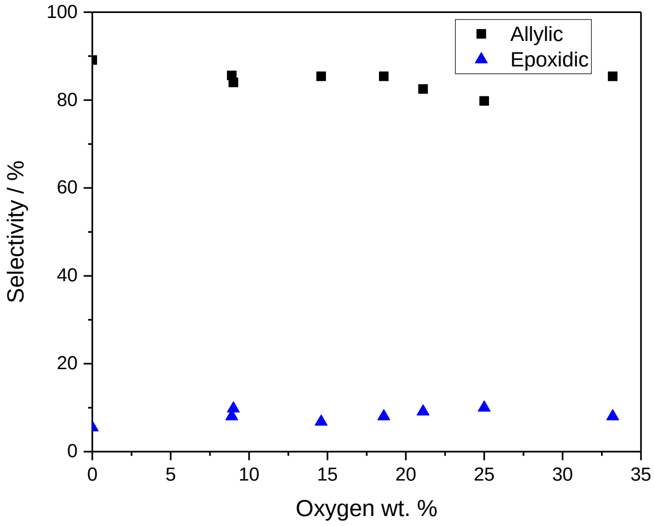

*Figure 3-8 Selectivity to epoxidation products (▲, cy-oxide and CHD) and combined allylic products (■) across GOs **Reaction conditions:** 60 °C, 3 bar O_2, 0.1 g catalyst, 10 ml cyclohexene, 1 ml decane (internal standard)*

A time online study was conducted to study selectivity at higher conversions, this was examined using the highest active catalyst containing *ca*. 25 wt. % oxygen (GO-HO30) with a blank reaction for comparison (Figure 3-9). The blank reaction was observed to require an induction period of 40 h before conversion increased significantly. The catalysed reaction required a shorter induction period with higher conversions observed earlier in the reaction, this difference was more noticeable at 36 h. The difference in conversion between blank and catalysed reaction later converged at the end of a 72 h period. This limit to conversion is possibly due to the formation of a biphasic mixture which limits the diffusion of reactants as described previously. The limit to conversion seen in the catalysed reaction is not due to deactivation of the catalyst through loss of oxygen, as the amount of oxygenated products far exceeds the surface oxygen species. Interestingly, even at high conversions, and long reaction times, a selectivity to allylic oxidation products is maintained. This relationship can be observed in Figure 3-10. Epoxidation products is only seen in small quantities and is calculated as a combination of cy-oxide and CHD. Over longer reaction times, cy-oxide is completely hydrolysed to the diol due to the significant presence of water that is generated.

The selectivity profile of both the catalysed and blank reaction appear to be very similar with a minimal difference between selectivity to allylic oxidation products in the reaction at early stages (Figure 3-10). Selectivity to allylic products decreases over longer reaction times but was not observed to increase in any other known products. Selectivity to epoxydic products was also similar in both catalysed and blank reaction over the reaction time. This selectivity decreased at longer reaction times, also possibly owing to its conversion into unknown compounds.

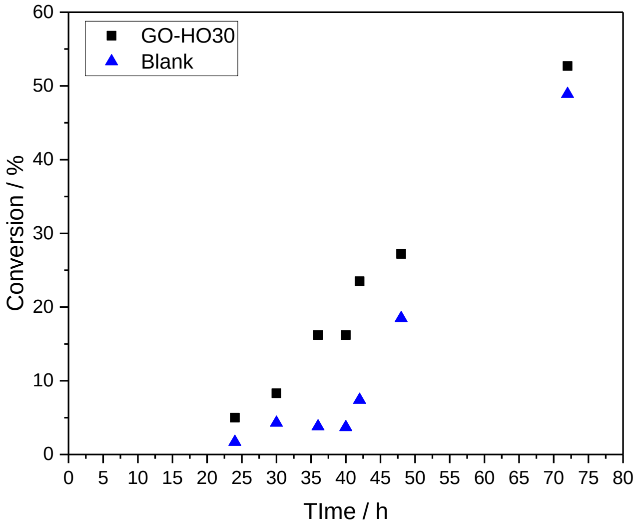

Figure 3-9 ***Reaction conditions:*** *60 °C, 3 bar O_2, 0.1 g catalyst, 10 ml cyclohexene, 1 ml decane (internal standard)*

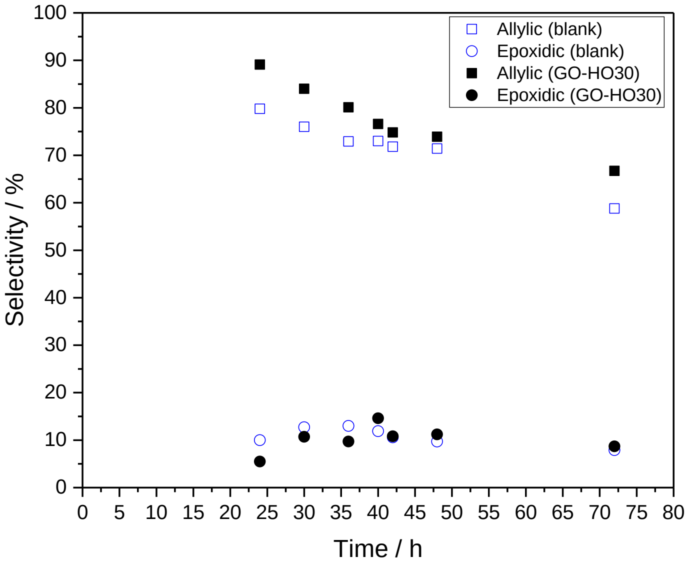

Figure 3-10 ***Reaction conditions:*** *60 °C, 3 bar O_2, 0.1 g catalyst, 10 ml cyclohexene, 1 ml decane (internal standard)*

A plot of selectivity as a function of conversion (Figure 3-11) demonstrates that the reaction profile of both catalysed and uncatalysed reaction follow almost identical profiles for allylic products. The GO carbocatalyst has no effect on the selectivity of the reaction and acts as an initiator to shorten the induction period required for the build-up of peroxy species. This was suggested in work by Dhakshinamoorthy et al. when studying the effects of doping on graphene catalysts for the oxidation of benzylic hydrocarbons.[25] In this work it was suggested that the presence of surface peroxy species are vital in the propagation of radical mechanisms. The existence of these species was confirmed by FT-Raman which clarified the presence of peroxy species at 100 °C, which then disappeared when the atmosphere was switched to N_2. The GOs in this study could be behaving in a similar way to the materials analysed by Navalon et al.[26] The importance of surface oxygen groups was further highlighted by reports on cyclohexane oxidation, emphasising the necessity of these groups for the radical mechanism.[27] Other reports also correlate the presence of carboxylic acid groups with the generation of superoxide ($\bullet O_2^-$) radicals.[28] However, in this study the material containing the highest carboxylic acid content was the Hummers material which did not demonstrate the highest activity. The carboxylic acid content of these GOs was analysed by XPS in previous work in by Pattisson et al.[15,24] Due to this material not exhibiting the highest activity a different functional group is suspected to be responsible for the observed activity, it is more likely in the form of an epoxy or hydroxy moiety. There is also an observed decrease in selectivity over longer conversions. This is not due to the formation of any known compounds. Rather it is a response likely due to the formation of higher molecular weight polymeric species, which create a more viscous reaction mixture. This effect is also observed in the reaction with Au / C as well as in the uncatalysed reaction. The effect that the formation of higher molecular weight species have on the mass balance is also illustrated in Figure 3-12. At around 5 % conversion, a mass balance of approximately 85 % is observed for both catalysed and uncatalysed reactions. This drops to below 48 % at 49 % conversion for the blank and 41 % at 53 % conversion for the catalysed reaction. This similarity in reaction profiles suggests the process is unaffected by the presence of the GO.

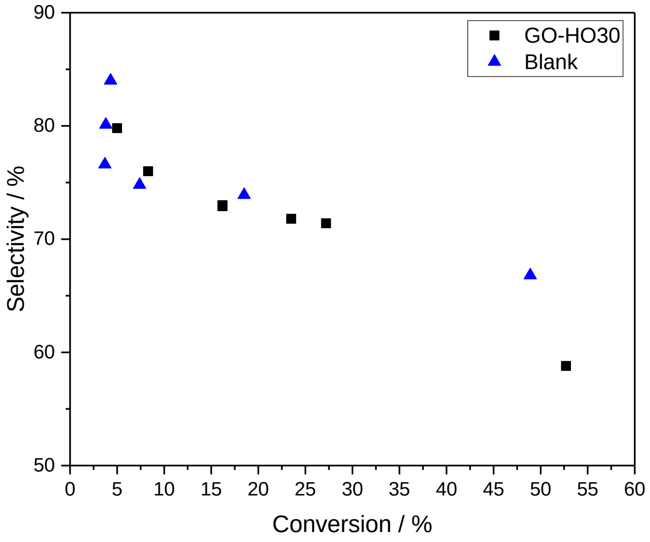

*Figure 3-11 Conversion of cyclohexene versus selectivity to allylic products. A comparison of GO-HO30 (■) and the blank reaction (▲). **Reaction conditions:** 60 °C, 3 bar O_2, 0.1 g catalyst, 10 ml cyclohexene, 1 ml decane (internal standard)*

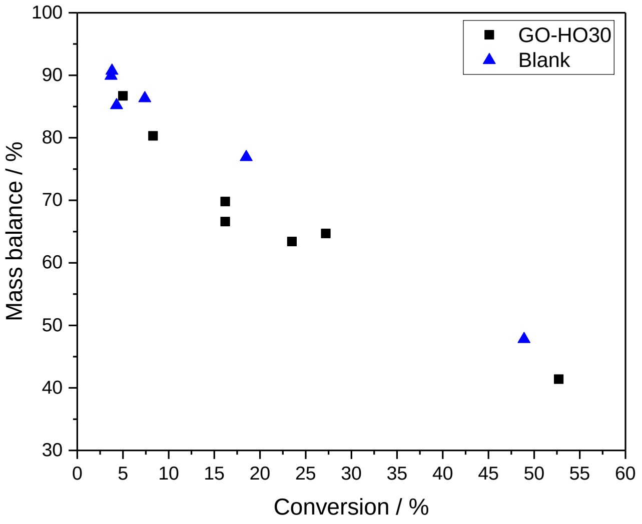

*Figure 3-12 Conversion of cyclohexene versus mass balance A comparison of GO-HO30 (■) and the blank reaction (▲). **Reaction conditions:** 60 °C, 3 bar O_2, 0.1 g catalyst, 10 ml cyclohexene, 1 ml decane (internal standard)*

3.4 Conclusions

This study shows the high activity of Au catalysts supported on graphite or graphene for cyclohexene oxidation. This study also highlights the effect that a WO_3 co-catalyst can have on the selectivity, to CHD under addition of water, which was not presented in previous work by Ovoshchnikov et al. The results from this work have shown that a catalyst prepared via sol-immobilisation can be highly active for cyclohexene oxidation, most likely because of the narrow size distribution and high dispersion, as shown by TEM imaging. The results highlight that there is a large degree of tuning required for efficient formation of epoxide and diol from cyclohexene, because of the large differences observed between WI and SI catalysts. Problems associated with limitation of selectivity via production of the allylic alcohol, and the lack of water formed in the reaction, required for hydrolysis to CHD ultimately limit the application of this system.

Graphitic oxide has also shown great potential as a metal-free catalyst for the low temperature allylic oxidation of cyclohexene. The activity of these catalysts correlates strongly with the amount of surface oxygen across their surface, which was also proved in previous work on linear alkenes. Similarly, the most active catalyst was demonstrated to be a GO with 25 wt. % oxygen. However, this relationship between activity and oxygen content is less pronounced in cyclohexene oxidation compared to the original work on linear alkene oxidation. This difference can be linked to the lower temperature used in the cyclohexene oxidation with could result in a lower proportion of surface peroxy formation. The resemblance between the blank and catalysed reaction suggest that these materials were acting as initiators and reducing the lengthy induction period associated with the reaction. The differences between the blank reaction and catalysed reaction become more pronounced over longer reaction periods with the GOs achieving higher conversions. A reason for this would be due to the initiation of a radical mechanism by the presence of surface oxygen species. The mass balance of both blank and catalysed reactions suffer at high conversions due to the formation of high molecular weight polymeric species which have been observed in previous studies into cyclohexene oxidation.

3.5 Future work

There are limitations in selectivity to CHD in this reaction. The mechanistic constraints, which limit selectivity, make an industrially viable solution using a solventless aerobic oxidation unlikely. A solution may be considered using metal cobalt catalysts which are reported to catalyse the selective aerobic oxidation of alkanes and alkylbenzenes to organic oxygenates. The Co (II) sites have been noted to form Co (III)-(O^{-2}) species, thus binding and activating oxygen. Commonly, these Co catalysts are successfully used with a limited substrate scope. However, a recent approach has combined Co with a second positively charged metal which is capable of stabilising activated oxygen intermediates because of increased basicity of the catalyst. In the example of styrene, this increased basicity reduces the decomposition to benzaldehyde and formaldehyde thereby increasing yield to the epoxide.[29] This approach was applied to a cyclohexene system using a CoMo oxide catalyst and ethylbenzene solvent. Interestingly, high epoxide selectivity is achieved through a peroxidation of the solvent which is catalysed by Co (II) centres. The oxygen atom of the ethylbenzenehydroperoxide is then transferred to cyclohexene in a reaction catalysed by Mo sites. In this system a cy-oxide selectivity of 59 % at 33 % conversion was obtained. It is possible a similar process could be developed using a tungsten oxide catalyst, which has proved to be an effective epoxidation catalyst, and may achieve better yields than the Mo basesd catalyst.[23] If an aerobic oxidation is going to be achievable it would require an additive such as ethylbenzene, however, this would affect the atom economy which was one of the targets of improvement when using solventless conditions.

Hydrogen peroxide possibly offers the best alternative to an aerobic oxidation. This first step to produce CHD could be achieved selectively with H_2O_2. This would facilitate epoxidation of the alkene substrate, followed by hydrolysis to CHD. A second step to form adipic acid from CHD could then be achieved aerobically as in studies by Obara et al.[30] The selective oxidation of cyclohexene using H_2O_2 has been achieved using homogeneous and heterogeneous catalysts. Most notably by Sato et al. using a homogeneous tungsten catalyst, reaching a yield of 93 % of adipic acid.[31] Polyoxometalates have been reported as effective oxidation catalysts in the presence of H_2O_2.[32–36] Their success is partly due to multi-metal sites which are more efficient than conventional mono-metal catalysts, when in combination with H_2O_2 as described by Mizuno et al.[33] Generally, when heteropolyacids are used in epoxidation reactions, the primary products formed are the diols, as the result of the electrophilic attack on the epoxide ring by the Keggin acid anion.[37] The use of polyoxometalates, specifically, Cs-substituted phosphotungstic acid acids is studied further in the following chapter.

3.6 References

1 R. Sheldon and J. Kochi, in *Academic Press*, 1981.

2 N. Mizuno, K. Yamaguchi and K. Kamata, *Coord. Chem. Rev.*, 2005, **249**, 1944–1956.

3 N. Dimitratos, J. A. Lopez-Sanchez and G. J. Hutchings, *Chem. Sci.*, 2012, **3**, 20–44.

4 B. S. Lane and K. Burgess, *Chem. Rev.*, 2003, **103**, 2457–2474.

5 J.-M. Brégeault, *Dalt. Trans.*, 2003, 3289–3302.

6 R. Noyori, M. Aoki and K. Sato, *Chem. Commun.*, 2003, 1977–1986.

7 O. Laporte and W. F. Meggers, *J. Opt. Soc. Am.*, 1925, **11**, 459.

8 S. J. Blanksby and G. B. Ellison, *Acc. Chem. Res.*, 2003, **36**, 255–263.

9 D. S. Ovoshchnikov, B. G. Donoeva, B. E. Williamson and V. B. Golovko, *Catal. Sci. Technol.*, 2014, **4**, 752.

10 S. Bawaked, N. F. Dummer, D. Bethell, D. W. Knight and G. J. Hutchings, *Green Chem.*, 2011, **13**, 127–134.

11 S. Bawaked, Q. He, N. F. Dummer, A. F. Carley, D. W. Knight, D. Bethell, C. J. Kiely and G. J. Hutchings, *Catal. Sci. Technol.*, 2011, **1**, 747–759.

12 M. D. Hughes, Y.-J. Xu, P. Jenkins, P. Mcmorn, P. Landon, D. I. Enache, A. F. Carley, G. A. Attard, G. J. Hutchings, F. King, E. H. Stitt, P. Johnston, K. Griffin and C. J. Kiely, *Nature*, 2005, **437**, 1132–1135.

13 H. Alshammari, P. J. Miedziak, T. E. Davies, D. J. Willock, D. W. Knight and G. J. Hutchings, *Catal. Sci. Technol.*, 2014, **4**, 908–911.

14 B. G. Donoeva, D. S. Ovoshchnikov and V. B. Golovko, *ACS Catal.*, 2013, **3**, 2986–2991.

15 S. Pattisson, E. Nowicka, U. N. Gupta, G. Shaw, R. L. Jenkins, D. J. Morgan, D. W. Knight and G. J. Hutchings, *Nat. Commun.*, 2016, **7**, 12855.

16 H. Alshammari, P. J. Miedziak, D. W. Knight, D. J. Willock and G. J. Hutchings, *Catal. Sci. Technol.*, 2013, **3**, 1531–1539.

17 Q. Yang, X. Yang, Y. Wang, H. Wang and Q. Cheng, *Res. Chem. Intermed.*, 2012, **38**, 2277–2284.

18 S. Schimpf, M. Lucas, C. Mohr, U. Rodemerck, A. Brückner, J. Radnik, H. Hofmeister and P. Claus, *Catal. Today*, 2002, **72**, 63–78.

19 S. Carrettin, P. McMorn, P. Johnston, K. Griffin, C. J. Kiely and G. J. Hutchings, *Phys. Chem. Chem. Phys.*, 2003, **5**, 1329–1336.

20 D. I. Enache, J. K. Edwards, P. Landon, B. Solsona-Espriu, A. F. Carley, A. A. Herzing, M. Watanabe, C. J. Kiely, D. W. Knight and G. J. Hutchings, *Science (80-.).*, 2006, **311**, 362–365.

21 X. Yang, H. Yu, F. Peng and H. Wang, *ChemSusChem*, 2012, **5**, 1213–1217.

22 J. Büker, B. Alkan, Q. Fu, W. Xia, J. Schulwitz, D. Waffel, T. Falk, C. Schulz, H. Wiggers, M. Muhler and B. Peng, *Catal. Sci. Technol.*, 2020, **10**, 5196–5206.

23 W. Zhong, M. Liu, J. Dai, J. Yang, L. Mao and D. Yin, *Appl. Catal. B Environ.*, 2018, **225**, 180–196.

24 S. D. Pattisson, Cardiff University, 2015.

25 S. Navalon, A. Dhakshinamoorthy, M. Alvaro and H. Garcia, *Chem. Rev.*, 2014.

26 S. Navalon, A. Dhakshinamoorthy, M. Alvaro, M. Antonietti and H. García, *Chem. Soc. Rev.*, 2017, **46**, 4501–4529.

27 Y. Xiao, J. Liu, K. Xie, W. Wang and Y. Fang, *Mol. Catal.*, , DOI:10.1016/j.mcat.2017.01.020.

28 H. Yu, F. Peng, J. Tan, X. Hu, H. Wang, J. Yang and W. Zheng, *Angew. Chemie - Int. Ed.*, 2011, **50**, 3978–3982.

29 J. Sebastian, K. M. Jinka and R. V. Jasra, *J. Catal.*, 2006, **244**, 208–218.

30 N. Obara, S. Hirasawa, M. Tamura and Y. Nakagawa, *ChemCatChem*, 2016, **8**, 1732–1738.

31 K. Sato, M. Aoki and R. Noyori, *Sci. 281*, 1998, **281**, 1646–1648.

32 J. Alcañiz-Monge, G. Trautwein and A. Garcia-Garcia, *J. Mol. Catal. A Chem.*, 2014, **394**, 211–216.

33 K. and Y. K. Mizuno Noritakaand Kamata, in *Bifunctional Molecular Catalysis*, ed. M. Ikariya Takaoand Shibasaki, Springer Berlin Heidelberg, Berlin, Heidelberg, 2011, pp. 127–160.

34 P. Zhao, M. Zhang, Y. Wu and J. Wang, *Ind. Eng. Chem. Res.*, 2012, **51**, 6641–6647.

35 X.-K. Li, J. Zhao, W.-J. Ji, Z.-B. Zhang, Y. Chen, C.-T. Au, S. Han and H. Hibst, *J. Catal.*, 2006, **237**, 58–66.

36 Y. Sasaki, K. Ushimaru, K. Iteya, H. Nakayama, S. Yamaguchi and J. Ichihara, *Tetrahedron Lett.*, 2004, **45**, 9513–9515.

37 J. C. S. Soares, A. H. A. Gonçalves, F. M. Z. Zotin, L. R. R. de Araújo and A. B. Gaspar, *Catal. Today*, , DOI:10.1016/j.cattod.2020.07.052.

4 Oxidation of cyclohexene to cyclohexanediol using H_2O_2

4.1 Introduction

In 1998 the use of H_2O_2 to convert cyclohexene to adipic acid (AA) in a highly selective process was published for the first time (Scheme 4-1).[1] This pioneering research has formed the benchmark of many investigations into the suitability of H_2O_2 as an oxidant for cyclohexene. This work represented an environmentally conscious, non-nitric acid alternative route to AA. However, the expensive use of H_2O_2 in a 4.0 to 4.4 mol ratio with substrate, provided an unattractive proposition for industrial applications.[2]

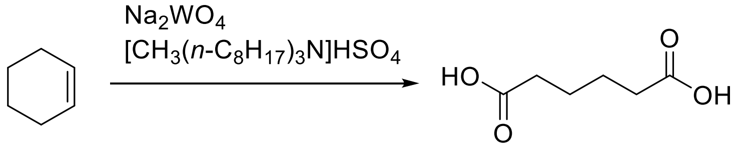

Scheme 4-1 Direct oxidation of cyclohexene to adipic acid with aqueous H_2O_2[1]

Multiple attempts have been made to improve the process first demonstrated by Sato et al. These have focused on creating a heterogenous alternative[3–9] to the sodium tungstate catalyst and omitting the use of the environmentally harmful phase transfer catalyst.[10–13] However, a solventless oxidation of cyclohexene to cyclohexanediol (CHD) using a stoichiometric amount of oxidant is a rarer topic of study. Although the use of H_2O_2 in an oxidation of cyclohexene to AA in a selective “one-pot” process is an attractive prospect, it would be more economically viable if a stoichiometric oxidation to CHD could be achieved first, with a second oxidation to AA using molecular oxygen. This chapter focuses on the first step described above and the overall approach is illustrated in Scheme 4-2.

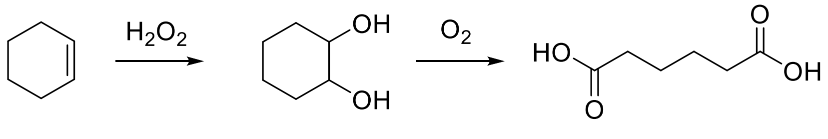

Scheme 4-2 Proposed two step oxidation to adipic acid from cyclohexene

Heteropolyacids (HPAs) have shown great potential as epoxidation catalysts, particularly with respect to cyclohexene.[14–19] Of these, 12-tungstophosphoric acid ($H_3PW_{12}O_{40}$), denoted as HPW, has been studied extensively as a solid acid catalyst due to its remarkably strong Brönsted acidity.[20] However, these materials are beset by problems associated with rapid deactivation and poor stability.[21] One method to possibly enhance the stability of these clusters is to prepare a catalyst in the form of a tungstophosphoric salt. Heteropolyacid (HPA) salts, are formed from the partial exchange of protons with large cations such as Cs^+. These Keggin type HPAs have the general formula of $[XM_{12}O_{40}]^{n-}$, where X is a heteroatom (most commonly P^{3+}, S^{4+}, B^{3+}), M is the addenda atom (most commonly used are Mb and W). These structures self-assemble in acidic aqueous solutions with a structure that is composed of a central tetrahedron of (XO_4), surrounded by 12 MO_6 octahedrons arranged in four groups of the type M_3O_{13}.[22] The oxidation of cyclohexene to AA using homogeneous (HPMo, HPW) and heterogeneous catalysts (PFeMo, PCoMo, PNiMo, VPMo, $(N(C_3H_7)_4)_3PMo_{12}O_{40}$, $(NH_4)_3PMo_{12}O_{40}$, $Cs_3PMo_{12}O_{40}$ and $Cs_3PW_{12}O_{40}$) was studied by Alcañis-Monge et al. This reaction was accomplished in a batch reactor at 75 °C and autogenous pressure. A yield of 80 % to AA was achieved with other products observed, such as, CHD, cyclohexene oxide (cy-oxide) and 1,2-cyclohexanedione. The selectivity to AA reduced under successive runs and was reached using a 5:1 ratio of H_2O_2 to substrate and $Cs_3PMo_{12}O_{40}$ as the catalyst. Acetic acid was also included in the reaction medium which has been shown to act positively on the epoxidation with a reduction to 13 % yield AA when not present.[14] In 2018, studies by Soares et al. into the effect of the acidity of a range of heteropolysalts with $K_3PW_{12}O_{40}$ exhibiting the best performance with 77 % yield to AA. This increase in yield was correlated with increasing acidity of the catalysts but was also achieved with a 5:1 ratio of H_2O_2 to cyclohexene. These results were obtained without the use of an organic acid additive.[15]

This investigation focuses on the effect of Au / $Cs_{3-x}H_xPw_{12}O_{40}$ for the oxidation of cyclohexene to CHD under solventless biphasic conditions. In this study an equimolar ratio of H_2O_2 to cyclohexene is utilised to improve efficiency and increase the industrial viability of this process. Au nanoparticles were also immobilised onto the polyoxometalates to study their impact on the reaction. Au nanoparticles were applied due to their significant applications in the selective epoxidation of alkenes utilising H_2O_2.[23–25] Finally, the replacement of the environmentally harmful phase transfer catalyst is explored with the use of silica-carbon hybrids to form a Pickering emulsion.

4.2 Experimental

4.2.1 Chemicals

Gold precursor (99.8%) was purchased from Strem. Tungstophosphoric acid ($H_3PW_{12}O_{40} \cdot xH_2O$), hydrochloric acid (HCl, 37%), caesium carbonate (Cs_2CO_3, 99.9 %), urea ($CO(NH_2)_2$, 99.0-100.5%), tungstosilicic acid ($H_4SiW_{12}O_{40} \cdot xH_2O$, $\geq$99.9%), Pluronic® P-123 ($M_n \approx 5,800$,), tetraethyl orthosilicate (TEOS, 98 %), 1-butanol (C_2H_5OH, anhydrous, 99.8 %), acetonitrile (MeCN, anhydrous, 99.8 %), hydrogen peroxide (H_2O_2, 30 %), cyclohexane (C_6H_{12}, anhydrous, 99.5 %), Aliquat 336, sodium sulfate (Na_2SO_4, , ACS reagent, $\geq$99.0%), chloroform ($CHCl_3$, anhydrous, $\geq$99%), n-decane

(99%, anhydrous, ≥99%), cyclohexene (C_6H_{10}, 99%, inhibitor-free), and cyclohexene oxide (98%) were purchased from Sigma-Aldrich. All materials were used without further purification.

4.2.2 Catalyst preparation

4.2.2.1 Au / $Cs_{3-x}H_x[P(W_3O_{10})_4]$

The Cs salts of Keggin-type tungstophosphoric acid with different Cs content (x=1.0-3.0) were prepared by a reaction between $H_3PW_{12}O_{40}$ and Cs_2CO_3 in aqueous solution.[26] Cs_2CO_3 (0.2 mol dm^{-3}) in de-ionised water was added dropwise to a solution of $H_3PW_{12}O_{40}$ (0.08 mol dm^{-3}). The precipitates were recovered by centrifugation and washed with de-ionised water 3 times. The solid sample was then dried at 373 K for 16 h. Au was supported on the polyoxometalates using a deposition-precipitation method with urea.[26] Urea (300 mg) was added into an aqueous solution of $HAuCl_4$ (0.12 mmol L^{-1}) with a molar ratio of urea: Au of 100:1. The polyoxometalate (1.0 g) was added and the solution was heated to 80 °C and stirred for 5 h. The product was recovered by centrifugation and washed with de-ionised water to remove chloride ions. The resulting product was dried under vacuum for 16 h at 40 °C, and thermally reduced in H_2 at 523 K for 2 h. The target Au loading in each catalyst was 1.0 wt. %. Au supported heteropolyacid salts are labelled AuCsXPW (X=1, 2, 3) for brevity.

4.2.2.2 Au / $Cs_{4-x}H_x[Si(W_3O_{10})_4]$

The Cs salts of Keggin-type tungstosilicic acid with different Cs contents (x=1.0-4.0) were prepared in a similar preparation to those described for $Cs_{3-x}H_x[P(W_3O_{10})_4]$.[27] Cs_2CO_3 (0.2 mol dm^{-3}) in de-ionised water was added dropwise to a solution of $H_4SiW_{12}O_{40}$ (0.08 mol dm^{-3}). The precipitate was then filtered by centrifugation and the solid washed with de-ionised water 3 times. The resulting solid powder was then dried for 16 h at 373 K. Au was supported onto the polyoxometalate using a urea deposition-precipitation technique.[26] Urea (300 mg) was added into an aqueous solution of $HAuCl_4$ (0.12 mmol L^{-1}) with a molar ratio of urea / Au of 100:1. The polyoxometalate (1.0 g) was added and the solution was heated to 80 °C and stirred for 5 h. The product was recovered by centrifugation and washed with de-ionised water to remove chloride ions. The resulting product was dried under vacuum for 16 h at 40 °C, and thermally reduced in H_2 at 523 K for 2 h. The target Au loading in each catalyst was 1.0 wt. %. Au supported heteropolyacid salts are labelled AuCsXSiW (X=1, 2, 3, 4) for brevity.

4.2.2.3 HPA / SBA-15 Gx

Graphitic oxide (GO) was prepared previously by Dr Samuel Pattisson, according to a modified Hummer's method with 15 g of permanganate used per 5 g graphite.[28] GO was suspended in de-ionised water (10 ml) and sonicated for 3 h. To synthesise SBA15-Gx, where x represents the wt.

% of carbon (x=5, 15, 25), the desired amount of a 1 wt. % aqueous solution of sonicated GO was combined with P-123 (4.0 g) and 3 wt. % HCl (140 ml). The mixture was stirred for 2 h, tetraethoxysilane (TEOS) (8.4 g) was added dropwise and the mixture was heated to 40 °C with stirring for an additional 24 h. The temperature was increased to 80 °C for 16 h and the resulting powder was centrifuged and washed with de-ionised water until neutral. The powder was dried in an oven at 110 °C for 16 h and subsequently heat treated at 600 °C under N_2.

The polyoxometalates were supported onto the SBA-15 Gx supports according to a two step incipient wetness impregnation procedure.[29] SBA-15 Gx (400 mg) was soaked with a Cs_2CO_3 (6 mg) solution and then left to adsorb the solution for 16 h. The powder was then dried overnight under vacuum at 40 °C. The sample was soaked in a $H_3PW_{12}O_{40}$ (39.4 mg) solution, left to adsorb the solution overnight and then dried under vacuum for 16 h at 40 °C. POM / SBA-15 Gx was then calcined at 300 °C under N_2. The target polyoxometalate loading was 10.0 wt. %.

4.2.3 Catalyst testing

4.2.3.1 Solvated reactions in 1-butanol or MeCN

Solvated cyclohexene oxidations were performed in a Colaver reactor heated using an oil bath. The system was flushed with N_2 and remained connected to an N_2 line throughout the reaction to maintain a constant pressure (3 bar). Typically, a mixture of cyclohexene (1 ml, 1 M in 1-butanol or MeCN), catalyst (0.1 g), H_2O_2 (30 %, 1.02 ml) and n-decane (0.195 ml, as an internal standard) was magnetically stirred (900 rpm) at 60 °C. Reactions in 1-butanol were conducted for 4 h while those in MeCN were 6 h. After completion of the respective reactions, the reactor was cooled down to room temperature and the reaction mixture was separated from the solid catalyst by centrifugation. The liquid samples were analysed via gas chromatography (GC). Quantification of conversion and selectivity was conducted using n-decane as an internal standard with calibrations against commercial analytical samples. Gaseous products were not analysed because of the use of a Colaver reactor, however, this contribution is likely to be negligible.

4.2.3.2 Solventless reactions

Solventless cyclohexene oxidation was performed in a Colaver reactor heated using an oil bath. The system was flushed with N_2 and remained connected to an N_2 line throughout the reaction to maintain a constant pressure (3 bar). Typically, a mixture of cyclohexene (5.0 ml), catalyst (50 mg with HPAs, 300 mg with HPA / SBA-15 Gx), H_2O_2 (30 %, 5.0 ml), Aliquat 336 (10 mg when required) and cyclohexane (0.250 ml, as an internal standard) was magnetically stirred (900 rpm) at 60 °C. For sequential additions of H_2O_2, 0.625 ml was added every hour to total a reaction time of 8 h. For each H_2O_2 addition, the reactor was cooled to room temperature and depressurised. H_2O_2 was added and the reactor was re-pressurised and purged with N_2. For batch addition of H_2O_2, reactions were conducted for 16 h. After the appropriate reaction time the reactor was cooled down to room temperature and the reaction mixture was separated from the solid catalyst by centrifugation. The organic products were separated from the aqueous layer in 2 extractions with $CHCl_3$. In the first extraction $CHCl_3$ (10 ml) was added, and 1.5 ml of the organic layer was removed for GC analysis. In the second extraction Na_2SO_4 (0.9 g) and $CHCl_3$ (20 ml) were added to the reactor with stirring after which another sample was taken for GC analysis. Quantification of conversion and selectivity was conducted using cyclohexane as an internal standard, with calibrations against bought analytical samples. Gaseous products were not analysed because of the use of a Colaver reactor; however, this contribution is likely to be negligible. The conversion, selectivity and mass balance were calculated as follows:

$$Conversion = \frac{(total\ mol\ of\ products)}{(total\ mol\ of\ products) + (total\ mol\ of\ unreacted\ substrate)} \times 100$$

$$Selectivity = \frac{(mol\ of\ product)}{(mol\ of\ observed\ products)} \times 100$$

$$Mass\ balance = \frac{(mol\ of\ product\ final)\ + (mol\ of\ final\ substrate)}{(mol\ of\ initial\ substrate)} \times 100$$

4.3 Results and discussion

4.3.1 Solvated reactions

4.3.1.1 Cyclohexene oxidation in 1-butanol

Solvated epoxidations in 1-butanol have been successfully demonstrated by Hammond et al.[30] in the epoxidation of cyclooctene and served as the starting point for testing of synthesised HPAs. The catalytic tests for Cs-substituted tungstosilicic acid and tungstophosphoric acid are presented in Table 4-1. Products that are entitled ‘other’ include cyclohexanone, cyclohexanol and 1,2-cyclohexanedione, however their contributions are generally low. Au-supported tungstosilicic acid catalysts have been proven to exhibit high activity for the oxidation of CO, showing excellent stability and full conversion at 0 °C.[27] Despite Keggin-type HPAs generally showing promise in epoxidations, the Au / $Cs_xH_{4-x}[Si(W_3O_{10})_4]$ (abbreviated to Au / CsXSiW where X=1, 2, 3, 4) catalysts were largely inactive and with minimal selectivity to the desired products of either cy- oxide or CHD.

The highest conversion was observed for Au / Cs3SiW which reached 3.0 % after 4 h. This selectivity profile was largely favoured by allylic species with 73 % for a combined selectivity of 2-cyclohexen-1-ol and 2-cyclohexen-1-one. Unknown products were responsible for the vast majority of other products and the main contribution was attributed to a single compound appearing on the GC/FID chromatogram. However, since conversion was only between 2.0 and 3.0 % there was a large error associated with the selectivities to these compounds. This low conversion is also comparable to the blank reaction indicating that these tungstosilicic catalysts are largely inactive.

Tungstophosphoric catalysts show significantly higher conversions than their silicon counterparts (Table 4-1). Au / CsXPW (X=1, 2, 3) displayed conversions of 16, 19 and 20 % conversion with increasing Cs substitution. This conversion increased with higher Cs content, potentially due to the lower acidity associated with increasing substitution. The higher acidity of these catalysts may have a stabilising effect on H_2O_2 contributing to the lower conversions observed.[31] The mass balance is consistent over the set of reactions tested with an average of 76 %. This loss of mass balance is considered mainly to be a result of evaporation of cyclohexene; a common problem associated with oxidations of volatile materials which is rarely reported. CHD is the predominant product of the known compounds; although, cy-oxide is not detected due to the presence of water, which causes its hydrolysis to CHD.

Table 4-1 Oxidation of cyclohexene in 1-butanol using caesium substituted heteropolyacids. ***Reaction conditions:*** *60 °C, 1 M cyclohexene in butanol, 4 h, 0.1 g catalyst, cyclohexene/H_2O_2 molar ratio = 1*

Catalyst		Selectivity / %					Conv. / %	M. B / %
		Cy-oxide	Allylic	CHD	Other	Unknowns		
	Blank	0.0	100	0.0	0.0	0.0	1.0	76
CsSiW	Au / Cs1SiW	0.0	63	5.0	0.0	32	3.0	76
	Au / Cs2SiW	0.0	75	2.0	0.0	23	2.0	73
	Au / Cs3SiW	0.0	73	4.0	0.0	23	3.0	75
	Au / Cs4SiW	0.0	87	2.0	0.0	10	2.0	73
CsPW	Au/ Cs1PW	2.0	9.0	33	7.0	51	16	75
	Au/ Cs2PW	2.0	10	33	6.0	50	19	78
	Au / Cs3PW	1.0	8.0	35	6.0	50	20	83

A significant proportion of a single unknown compound is still observed even at these higher conversions. Experiments proceeded to identify the composition of this unknown compound. Further oxidation of CHD to AA and 1,2-cyclohydroxyketone were ruled out after extraction of the reaction material into water and analysis by HPLC displayed no presence of either of these compounds. GC-MS analysis of the reaction material identified the unknown product as having a molecular mass of 172 g mol^{-1}. This molecular mass corresponds to a product that would form via the nucleophilic attack of butanol on cy-oxide (Scheme 4-3). The presence of this compound was also confirmed by an experiment using cy-oxide as the starting material without the addition of hydrogen peroxide, under an inert atmosphere of N_2 without the presence of a catalyst. Using a reaction temperature of 60 °C and reaction time of 4 h a small proportion of the substituted product is observed. A conversion of 1.0 % is achieved and no other products are detected by the GC. The product displayed on the chromatogram also has the same retention time as the unknown compound confirming that it is formed from nucleophilic attack of the solvent. Strangely, this compound is not noticed in the blank reaction reactions where a conversion of 2.0 % and selectivity of 62 % to cy-oxide is achieved. However, this may be due to the low concentration of cy-oxide in this reaction so a reaction between the solvent does not proceed to a noticeable degree. This epoxide ring-opening may only occur in acidic conditions as documented in studies by Guidotti et al.[8] when using *tert*-butanol as a solvent. This solvent-initiated epoxide ring opening has also been publicised by other groups.[32,33]

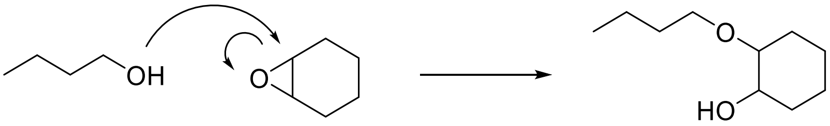

Scheme 4-3 Nucleophilic attack of butanol on cyclohexene oxide to form the unknown compound.

It has been postulated that the mechanism of epoxidation on HPW occurs through the formation of an active intermediate, $H_3PW_{12}(O)_nO_{40}$, forming through the H_2O_2 oxidation of the catalyst.[34] The difference between Si and P catalysts may be the inability of CsXSiW to form this intermediate. CsXPW catalysts also exhibit differences in activity depending on Cs-substitution, in addition to differences in acidity, a difference in activity could be due to discrepancies in Au content between catalysts. With the higher Cs-content catalysts possibly annealing Au more successfully in comparison to the lower Cs-content analogues. MP-AES analysis of the compounds gives the wt. % of Au deposited on the catalysts (Table 4-2). This was achieved after an *aqua regia* digestion of the catalysts. However, the polyoxometalate support could not be dissolved so the wt. % only shows the Au nanoparticles which been leached from the surface of the catalyst, and therefore may not give an accurate representation. A 1 wt. % Au loading was targeted and the data suggests that a values close to this were achieved in most cases. Entries 1-3 give the Au loadings of Au / CsXSiW. The Au content of Au / Cs2SiW and Au / Cs4SiW was measured to be 0.2 % lower than was targeted, however this could be due to incomplete leaching of the Au from the polyoxometalate. Entries 4 and 5 show the Au loadings for Au/ CsXPW and display an increasing Au loading, 0.92 to 1.01 %, in correlation with increasing Cs-substitution. This increase in Au loading also correlates with the increased activity of Au / Cs3PW related to Au / Cs2PW. However, the data obtained from these MP-AES studies would be too inaccurate to be conclusive in determining the difference in activity between catalysts. A full HF digestion of the entire catalyst would be a more conclusive method for obtaining Au loading.

Table 4-2 Percentage Au loading of heteropolyacids as determine by MP-AES

Entry	Catalyst	Wt %
1	Au/Cs2SiW	0.80 %
2	Au/Cs3SiW	1.11 %
3	Au/Cs4SiW	0.80 %
4	Au/Cs2PW	0.92 %
5	Au/Cs3PW	1.01 %

Further analysis of the post-reaction material demonstrated that the Au nanoparticles did not leach into the reaction solution. ICP-MS analysis of the reaction material revealed that there were minimal amounts of Au, W and Cs in the reaction mixture (0.006mg Au, 1.6mg W, 0.9mg Cs). This corresponds to 0.006 %, 2.4 % and 7.4 % for the wt. % of leached Au, W and Cs respectively.

FTIR analysis of catalysts was conducted to confirm the structure of Cs-substituted HPA and compare against their respective polyacid. This would also elucidate whether the structure of the HPA remained intact throughout the deposition of Au and thermal reduction. The FTIR spectra for the Au / CsXPW catalysts are illustrated in Figure 4-1, displaying four IR bands at 1080, 980, 884, 770 cm^{-1}, which were assigned as ν_{as}(P-O), ν_{as}(=O), ν_{as}(W–O–W), and ν_{as}(W–O–W), respectively, for Keggin-type $[PW_{12}O_{40}]^{3-}$. These bands are present in all Cs- substituted catalysts and are also present in the unsubstituted tungstophosphoric acid indicating an unchanged Keggin -type structure across the range of polyoxometalates. For Au / CsXSiW (Figure 4-2), four bands due to the Keggin structure were observed at 980, 926, 878, and 779 cm^{-1}, which were assigned as ν_{as}(W = O), ν_{as}(Si-O), ν_{as}(W–O–W), and ν_{as}(W–O–W), respectively. The unsubstituted $H_4SiW_{12}O_{40}$ displays some difference with a broadening of the peak at 926 cm^{-1} meaning the peak at 878 cm^{-1} is concealed. This peak broadening could be caused by increased hydrogen bonding in the polyoxometalate, possibly as a result of water present in the sample. Other samples were calcined possibly emitting water from the structure.

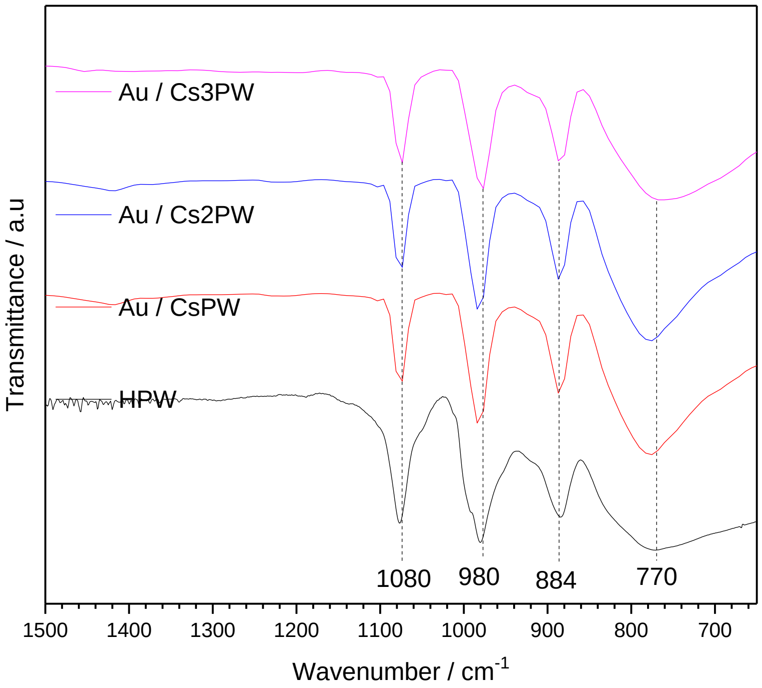

Figure 4-1 FTIR spectra for Au / CsxPW (x=1-3) catalysts

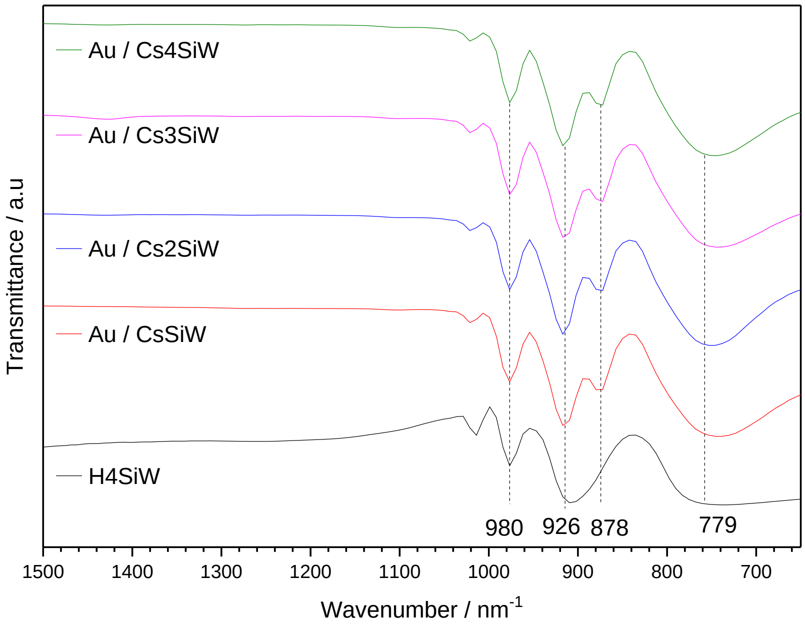

Figure 4-2 FTIR spectra for Au / CsxSiW (x=1-4) catalysts

XRD analysis also showed the correct synthesis of the phases and displayed the retention of the polyoxometalate structure after thermal reduction and incorporation of Cs. The substitution of Cs into the HPW acid lattice is illustrated in Figure 4-3. The pure acid had the triclinic (P-1) phase corresponding to the hydrate with 13 water molecules per Keggin unit. When protons are substituted for Cs, a new phase can be observed.[35] The diffraction pattern is characteristic of the

$Cs_3PW_{12}O_{40}$ cubic (Pn3m) phase.[36] This structure is consistent with that which would be expected before Au deposition so this process did not invoke any major structural changes. All peaks which are consistent with the cubic-structured Keggin-type polyoxometalate are indicated by the symbol in the diffraction pattern.

XRD analysis of the tungstosilicic acid catalysts is provided in Figure 4-4. The diffraction patterns for all CsSiW catalysts are similar and indicate a crystallisation of the cubic Pn3-m space group.[37] An increasing of phase purity is observed on addition of Cs and under heat treatment. The reflections in the XRD diffraction pattern are consistent with the Keggin-type polyoxometalate structure, indicating that the structures have good phase-purity. Neither diffraction pattern for CsPW or CsSiW show the presence of a diffraction peak for Au (111) (2θ = 38°) possibly due to overlap in this region or a small nanoparticle size.

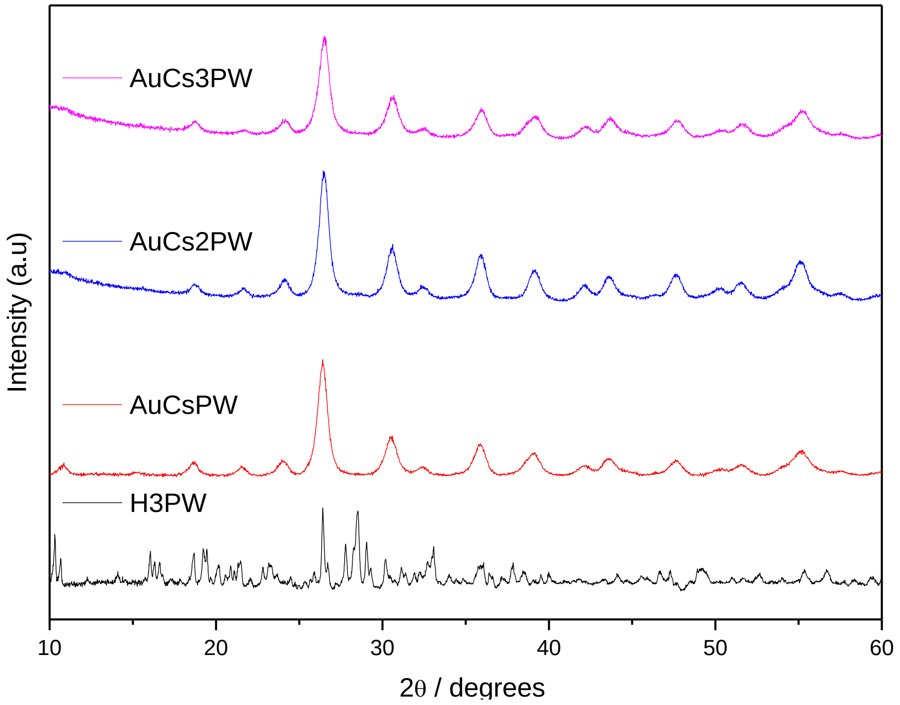

Figure 4-3 XRD diffraction patterns for tungstophosphoric acid catalysts

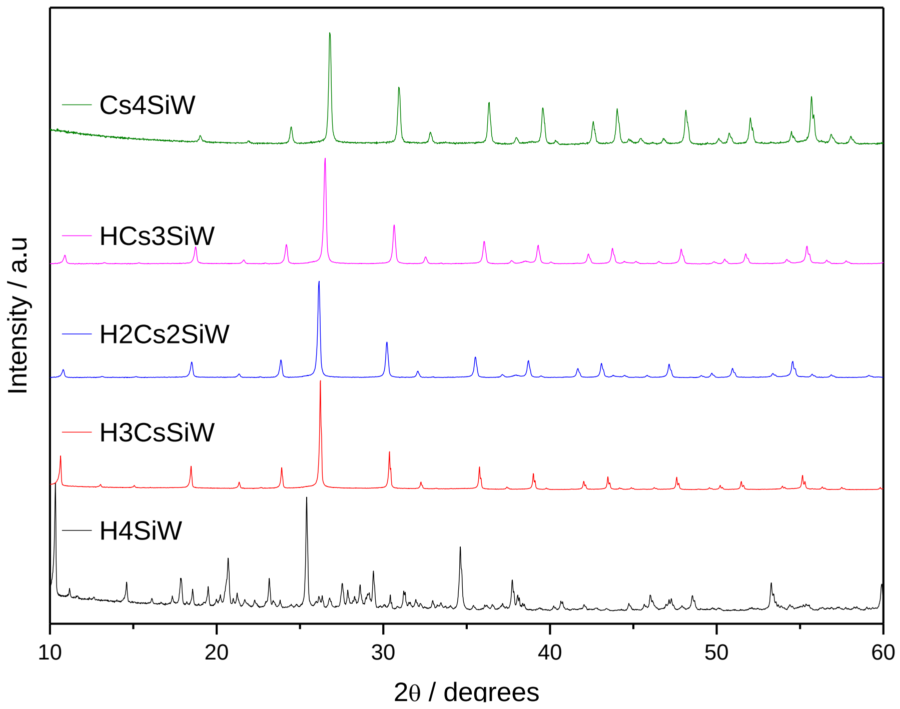

Figure 4-4 XRD diffraction patterns of silicatungstic acid catalysts

The benefit of adding Au to these polyoxometalate catalysts is more clearly illustrated in Table 4-3. Entries 1 and 2 display the reaction data for CsSiW and CsPW catalysts, respectively. The CsSiW polyoxometalate demonstrates minimal activity, as would be expected considering the Au supported analogue displayed in entry 3 also shows minimal activity. An increase in conversion of only 1.0 % is observed for these catalysts. In contrast, CsPW demonstrates 15 % conversion which is significantly higher than the Si equivalent. On addition of Au, an increase in conversion of 5.0 % is observed signifying that there is a benefit of adding Au. There does not appear to be any benefit in selectivity by having Au but the increase in conversion is clear. One possible explanation for this increase could be that the Au aids in the decomposition of H_2O_2 into its reactive counterparts, without further affecting the mechanism of oxidation.

Table 4-3 Comparison of reactivity of polyoxometalate supports with and without Au deposition. ***Reaction conditions:*** *60 °C, 1M cyclohexene in butanol, 4 hr, 0.1 g catalyst, cyclohexene/H_2O_2 molar ratio = 1*

	Catalyst	**Selectivity / %**					**Conv. / %**	**M. B / %**
		Cy-oxide	Allylic	CHD	Other	Unknowns		
1	Cs4SiW	0.0	79	2.0	0.0	19	1.0	72
2	Cs3PW	2.0	10	44	8.0	37	15	75
3	Au / Cs4SiW	0.0	88	2.0	0.0	10	2.0	73
4	Au / Cs3PW	1.0	8.0	35	6.0	50	20	83

4.3.2 Switch of solvent to MeCN

The use of MeCN in a solvated oxidation of cyclohexene is commonly used in literature and therefore makes this study more comparable to work from other groups.[4–9] In this investigation similar conditions were used to those used in the butanol study to give a better comparison of the solvents used. The use of MeCN allows the homogenisation of the aqueous H_2O_2 reagent and organic cyclohexene layer. H_2O_2 is commonly used in excess of a 4:1 ratio when AA is the required product.[15,38–40] An example of this is demonstrated by Soares et al. with a CsPW catalyst used and a 5:1 (H_2O_2: cyclohexene) molar ratio producing CHD with a yield of 47 % and AA with 20 % yield.[15] This reaction was performed over 24 h with a reaction composition of 0.21 mol of H_2O_2 (5 mL) and 0.023 mol (1.2 ml) of MeCN. MeCN was used to promote the higher stability of the heteropolysalt.[14] Nonetheless, the purpose of this study is to use an efficient equimolar ratio of H_2O_2 to cyclohexene to form CHD. As mentioned previously, 1-butanol was also found to react with cy-oxide to form a side product through a nucleophilic addition. Similarly, a conversion of only 2.0 % is noted in the MeCN reaction compared to the 1.0 % achieved in the 1-butanol reaction. For this study only the most active catalyst from the butanol investigation was used, therefore, omitting the tungstosilicic catalysts and Au / CsPW (x=1,2). In this investigation 2 methods of adding H_2O_2 were utilised: batch and sequential addition (Table 4-4). This study was initiated to determine if H_2O_2 usage could be more efficient and therefore achieve higher conversion and greater selectivity to CHD. It is evident from these reactions that cy-oxide is a predominant product under these conditions with 65 % selectivity seen when adding H_2O_2 in a batch system. The transformation of cy-oxide into CHD is possibly hindered by the presence of the solvent. The sequential addition of H_2O_2 was achieved by 10 aliquots of 0.1 ml staggered over the 6 h reaction in 36 min intervals. This approach displayed an increase in conversion of 6.0 %. This increase supports the hypothesis and a possible future requirement to feed H_2O_2 into the reactor at a slower rate. This approach has been successful for the oxidation of methane to methanol using H_2O_2.[41] Sequential addition of H_2O_2 also offers greater selectivity to the epoxidation products due to this greater efficiency of H_2O_2 uptake. However, the mass balance of the reactions is also affected by the 2 methods of H_2O_2 addition. The mass balance is significantly lower in the sequential addition compared to the batch addition. This can be explained by the frequent opening of the reactor vessel which would allow loss of cyclohexene due to its relatively low vapour pressure.

Table 4-4 Oxidation of cyclohexene using tungstophosphoric acid catalysts with a batch and sequential addition of H_2O_2 ***Reaction conditions:*** *60 °C, 1M cyclohexene in MeCN, 6 hr, 0.1 g catalyst, cyclohexene/H_2O_2 molar ratio = 1 cyclohexene/H_2O_2 molar ratio = 1 (sequential addition 0.1 ml added every 36 min)*

Catalyst		**Selectivity / %**					**Conv. / %**	**M. B / %**
		Cy-oxide	Allylic	CHD	Other	Unknowns		
Blank		62	20	17	0.0	0.0	2.0	76
HPW	Au / Cs3PW Batch addition	65	15	20	0.0	0.0	7.0	85
	Au / Cs3PW Seq. addition	70	7.0	23	0.0	0.0	13	59

4.3.3 Solventless oxidations with phase transfer catalyst

To improve the atom economy for this reaction a solventless system was employed with the addition of a phase-transfer catalyst. These conditions were similar to those used in the pioneering work by Sato et al. in 1998 with the exception being their utilisation of tetrabutylammonium hydrogensulfate instead of Aliquat 336 and the intended product being CHD instead of AA in this investigation.[42] The use of the phase transfer catalyst allows an emulsion to form and facilitates the migration of reactant from one phase to another.

Commonly with these reactions mass balances are not reported and reactions are analysed using GC. This is a difficulty with this reaction as the analysis of reaction products requires the evaluation of the aqueous and organic phase. Initial problems associated with the analysis of products culminated in low mass balances illustrated in Table 4-5. This table indicates the use of 2 extraction methods which resulted in low mass balances. The first method employed was an extraction of the products with 50 ml DCM. However, despite the reported high selectivity to CHD this was accompanied by a low mass balance of 26 % possibly owing to a large proportion of CHD remaining in the aqueous layer. This loss in mass balance is unlikely to be due to evaporation, as the blank reaction exhibits a mass balance of 89 % indicating a loss of around 10 % due to evaporation of cyclohexene. A subsequent method was employed whereby the aqueous layer was analysed by HPLC, and the organic layer diluted with DCM and analysed using GC. However, this technique also resulted in a low mass balance of 53 %. Since the evaporation of substrate would only account for around 10 % of mass lost. The other mass loss may be due to a sensitivity in the HPLC refractive index(RI) detector to differences in the reaction solution matrix and calibration solutions. Promisingly, selectivity to CHD is high using these conditions, however the problem associated with the low mass balance must be addressed.

Table 4-5 Solventless oxidation of cyclohexene with reaction work-up achieved by ***a)*** *a 50 ml extraction of aqueous phase into DCM.* ***b)*** *analysis of aqueous phase by HPLC and organic phase via GC.* ***Reaction conditions:*** *60 °C, 3 bar N_2, 5 ml cyclohexene, 5 ml H_2O_2 (30 %), 0.5 ml decane, 50 mg catalyst, Aliquat 336 20 mg, 16 h*

Entry	**Catalyst**	**Selectivity / %**					**Conv. / %**	**M. B / %**
		Cy-oxide	Allylic	CHD	Other	Unknowns		
1	Blank	0.0	0.0	0.0	0.0	0.0	0.0	89
2	Au / Cs2PW[a]	0.0	0.0	100	0.0	0.0	7.0	26
3	Au / Cs3PW[b]	1.0	0.0	99	0.0	0.0	4.0	53

Since the previous reaction work-up methods were ineffective in obtaining high mass balances, another approach using a salt solution to extract products from the aqueous phase was used. The outcome of a set of reactions using CsxPW catalysts is displayed in Table 4-5. In this method Na_2SO_4 was added to the reaction before analysis to obtain a concentration of 1 M, Na_2SO_4 being more effective as an extraction salt due to its harder ionic character.[43] The organic layer was then extracted with, initially 10 ml $CHCl_3$, and subsequently 30 ml $CHCl_3$. Products which had more affinity for the organic layer would be analysed after the 1st extraction while products which had an affinity for the aqueous layer would be analysed in the 2nd extraction (CHD). As observed in Table 4-6, selectivity to CHD is high, which is similar to values seen in Table 4-5. The significant difference between the data displayed in Table 4-5 and Table 4-6 is the better mass balance with an average of 79 % calculated for the 3 catalysts tested. This considerably higher mass balance suggest that this salt extraction is a more appropriate method for analysis of this reaction. This method was not successful in extracting all products but gave a far more accurate assessment of the activity of these catalysts. The blank reaction showed only 0.3 % conversion with full selectivity to CHD, which would be expected as cy-oxide would be quickly hydrolysed to CHD. This high selectivity towards CHD, and absence of cy-oxide, is consistent across the catalysts used with different Cs contents. The conversion of Au / Cs1PW is considerably lower than Au / Cs2PW and Au / Cs3PW suggesting that this reaction is favoured by the slightly lower acidity associated with these catalysts.

Table 4-6 Solventless oxidation of cyclohexene with 2 extractions into $CHCl_3$ and using Na_2SO_4 as extraction salt. ***Reaction conditions:*** *60 °C, 3 bar N_2, 5 ml cyclohexene, 5 ml H_2O_2 (30 %), 0.5 ml cyclohexane, 50 mg catalyst, Aliquat 336 20 mg, 16 h*

Entry	**Catalyst**	**Selectivity / %**					**Conv. / %**	**M. b / %**
		Cy-oxide	Allylic	CHD	Other	Unknown		
1	Blank	0.0	0.0	100	0.0	0.0	0.3	90
2	Au / Cs1PW	0.0	6.0	95	0.0	0.0	12	80
3	Au / Cs2PW	0.0	6.0	94	0.0	0.0	25	83
4	Au / Cs3PW	0.0	5.0	95	0.0	0.0	24	73

The reactivity of the HPAs is displayed in Table 4-7, giving an idea of the benefit of adding Au. The most active HPAs from Table 4-6 were used in this study. This study gives the indication that Au only has a minor effect on conversion. An increase of 5.0 % and 3.0 % are observed for Au / Cs2PW and Au / Cs3PW respectively, although the mass balances in these reactions are also higher. The minor benefit of adding Au to this catalyst would be unnecessarily expensive if industrial viability is considered. Although the activity of these catalysts is still too poor under these conditions to be deemed possible for industry.

Table 4-7 Reactivity of polyoxometalate support under solventless conditions ***Reaction conditions:*** *60 °C, 3 bar N_2, 5 ml cyclohexene, 5 ml H_2O_2 (30 %), 0.5 ml cyclohexane, 50 mg catalyst, Aliquat 336 20 mg, 16 h*

Entry	**Catalyst**	**Selectivity / %**					**Conv. / %**	**M. B / %**
		Cy-oxide	Allylic	CHD	Other	Unknowns		
1	Cs2PW	0.0	0.0	100	0.0	0.0	20	79
2	Cs3PW	0.0	0.0	100	0.0	0.0	21	70

Bright field TEM imaging could help indicate whether Au was successfully added to the catalysts and give an idea as to nanoparticle size. From the images of Au / Cs1PW (Figure 4-5a, b) and Au / Cs2PW (Figure 4-5 c,d) in Figure 4-5, it is unclear whether any Au was deposited onto the HPA surface. However, the EDX displayed in Table 4-8 denotes that 2.6 wt. % and 1.9 wt. % Au was detected on the surface. This may be possible if the Au was too small to observe at this magnification. The presence of Au was more obvious for Au / Cs3PW (Figure 4-5e, f) and can be seen clearly in Figure 4-5f, however, the Au nanoparticles appear to be large (around 10 nm). These observations may reveal why Au had such a minimal effect with Au nanoparticles either too small or too large to have an impact on the reaction. Au nanoparticle sizes of > 2 nm are described as being optimum for selective oxidations of alkenes using H_2O_2.[23–25]

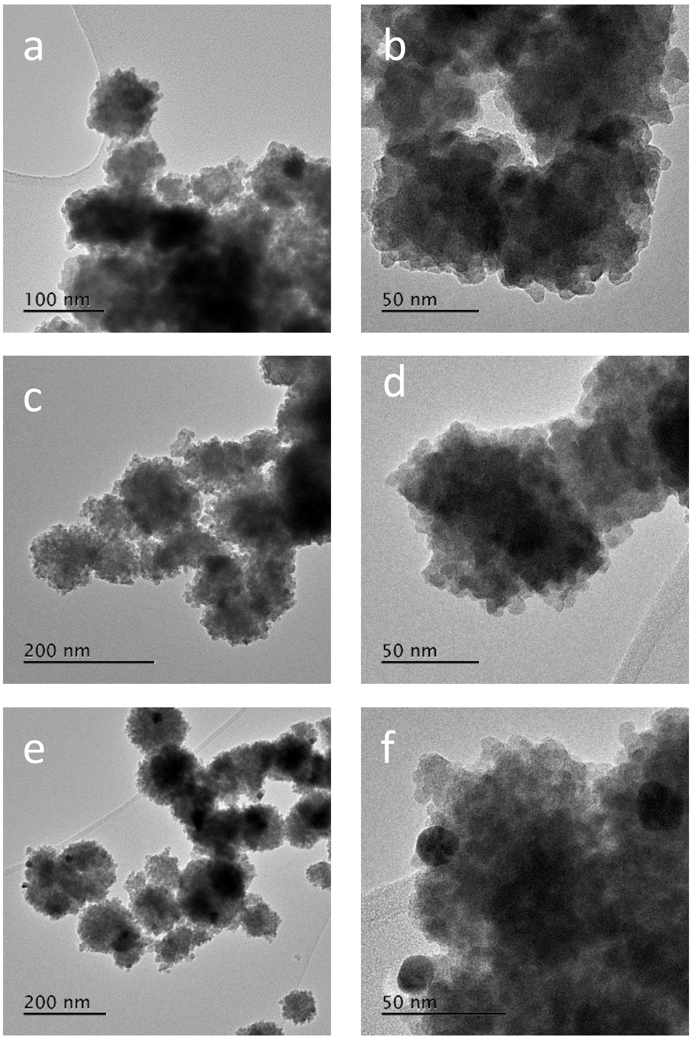

Figure 4-5 Bright field transmission electron microscopy (TEM) images of (a, b) 1 % Au / Cs1PW; (c, d) 1 % Au / Cs2PW; (e, f) 1 % Au / Cs3PW.

Table 4-8 EDX analysis of Au / CsXPW catalysts.

Catalyst	**Wt. %**		
	Au	Cs	W
Au / Cs1PW	2.6	9.2	70.2
Au / Cs2PW	1.9	10.3	75.1
Au / Cs3PW	2	12.7	71.1

To improve the yield of CHD under these conditions a sequential addition of H_2O_2 was utilised (Table 4-9). This reaction was conducted for 8 h compared to the 16 h reactions seen previously to allow H_2O_2 to be added in 8 aliquots with a 0.625 ml addition every hour. The benefit of this approach is validated by the increase in yield to CHD over the reaction time, showing an increase in yield of 5.0 % for CHD. This experiment provides a proof of concept that the sequential addition can improve H_2O_2 efficiency, delivering a step towards a stoichiometric use of oxidant. This approach could be further examined using a HPLC pump and autoclave which would allow a slower addition of H_2O_2 to the reaction. This approach would also limit the need to open the reactor, therefore reducing mass loss to evaporation. However, this has currently not been applied in this investigation.

*Table 4-9 Comparison of sequential addition and batch addition of H_2O_2. **Reaction conditions:** 60 °C, 3 bar N_2, 5 ml cyclohexene, 0.5 ml cyclohexane, 50 mg catalyst, Aliquat 336 20 mg, 8 h. **Batch:** 5 ml H_2O_2 (30 %). **Sequential:** 8 x 0.625 ml H_2O_2 (30 %) every hour.*

Entry	**Catalyst**	**Selectivity / %**					**Conv. / %**	**M. B / %**
		Cy-oxide	Allylic	CHD	Other	Unknowns		
1	Au / Cs3PW Batch addition	0.0	0.0	100	0.0	0.0	10	82
2	Au / Cs3PW Sequential addition	0.0	0.0	100	0.0	0.0	14	79

An important factor to consider is whether there is any leaching of the polyoxometalate into the reaction solution. This could be possible in either of the organic layer or aqueous layer. The substitution of Cs into the polyoxometalate is considered to stabilise the catalyst against leaching since tungstophosphoric acid is commonly used as homogeneous catalyst. W leaching into the reaction solutions is given in Table 4-10. No leaching of W was detected in the $CHCl_3$ phase. However, there was noticeable leaching of W into the aqueous phase illustrated by an average of 3.37 % of the total W leaching into the reaction mixture. Therefore, there could be some homogeneous influence on the reaction, with a highest concentration of 740 ppm in the mixture for Au / Cs1PW. However, as this reaction also produced a lower total conversion than the other 2 reactions, its influence on the reaction may be minimal.

Table 4-10 MP-AES data for leaching of polyoxometalate into solventless reactions

Entry	**Catalyst**	**Aqueous [W] / ppm**	**Organic [W] / ppm**	**% of total W**
1	Au / Cs1PW	740	0	3.7 %
2	Au / Cs2PW	668	0	3.3 %
3	Au / Cs3PW	616	0	3.1 %

4.3.4 Substitution for phase-transfer catalyst

A limitation of biphasic reactions is that they can require the use of phase transfer catalysts to achieve good yields. Phase transfer catalysts such as Aliquat 336 are harmful to the environment and alternative methods such as emulsion catalysis offer an environmentally benign approach.[44,45] The use of a silica-carbon hybrid has been reported to be successful by Wei et al. in an array of experiments (chloromethylation, hydrolysis of benzyl chloride, reduction of nitrobenzene, hydrogenation of vanillin and oxidative desulfurization).[46] These rGO-Silica hybrid materials stabilised the homogeneous dispersion of oil in water through the formation of a Pickering emulsion, therefore, increasing mass transfer through the phases. In the oxidative desulfurisation of dibenzothiophene, HPAs were integrated onto the surface of the materials via a two step incipient wetness impregnation. The catalysts investigated in this series are silica-carbon hybrid materials which have differing weight percentages of carbon signified by X in the label (SBA15 GX, where x = 5, 15, 25 wt. %). The weight loading of polyoxometalate adhered to these materials was kept constant at 10 wt. %. Table 4-11 displays the reaction data from this investigation, showing a low activity across the catalysts for this reaction. Conversion only reaches a maximum of 1.0 % which indicates these catalysts are largely inactive. The activity of these catalysts could be improved with a higher wt. % of HPAs or the addition of Au. However, previous experiments have indicated that adding Au only provides a small benefit. Selectivity towards CHD appears to be high with it being the only product observed. However, the error associated with this measurement would be high due to the low conversion registered.

Table 4-11 Substitution of Aliquat 336 for amphiphilic catalyst. ***Reaction conditions: 60 °C, 3 bar N_2, 5 ml cyclohexene, 5 ml H_2O_2 (30 %), 0.5 ml cyclohexane, 300 mg catalyst, 16 h***

Entry	**Catalyst**	**Selectivity / %**					**Conv. / %**	**M. b / %**
		Cy-oxide	Allylic	CHD	Other	Unknowns		
1	Blank	0.0	0.0	100	0.0	0.0	0.3	90
2	CsHPA / SBA-15G5	0.0	0.0	100	0.0	0.0	1.0	84
3	CsHPA / SBA-15G15	0.0	0.0	100	0.0	0.0	0.7	89
4	CsHPA / SBA-15G25	0.0	0.0	100	0.0	0.0	1.0	89

This set of reactions can be difficult to compare to the previous reactions involving Aliquat 336 because of the difference in weight loading of polyoxometalate in both studies. Reactions with CsHPA / SBA-15GX would have around 30 mg of polyoxometalate compared to 50 mg in reactions with Au / CsXPW. However, reactions in Table 4-11 exhibit significantly lower activities and the use of a higher weight loading of polyoxometalate may not have aided this. It could be that activity is considerably affected by the absence of a phase-transfer catalyst, but could also be explained if the polyoxometalate was not successfully adhered to the material. The mass balances calculated for this series of reactions are consistent with a 10 % mass loss of cyclohexene due to evaporation, which could occur during reaction analysis. To improve the mass balance, the internal standard used in previous reactions (decane) was substituted for cyclohexane, since the vapour pressures of cyclohexene and cyclohexane would be similar. Nevertheless, a 10 % mass loss is still observed.

MP-AES data (Table 4-12) for the leaching of W into the reaction mixture suggests a similar level of dissociation of W compared to the previous study using Aliquat 336. W is predominantly located in the aqueous phase and an average of 5.1 % of W used in the reaction was found to have leached. The low activities recorded despite leaching also implies that the leached W species are not catalytically active.

Table 4-12 MP-AES data for leaching of W in solventless reactions in the absence of a phase transfer catalyst

Entry	Catalyst	Aqueous [W] / ppm	Organic [W] / ppm	% of total W
1	CsHPA / SBA15G5	278	0	6.9 %
2	CsHPA / SBA15G15	128	0	3.0 %
3	CsHPA / SBA15G25	210	0	5.5 %

An inspection of the reaction progress also indicated that the catalyst was not creating a Pickering emulsion as intended. This was evident due to the catalyst displaying an affinity for the aqueous phase. This would also provide a reason for the lack of activity demonstrated by these catalysts. A reason for this could be that the graphitic oxide used in the preparation of the material was not sufficiently reduced by hydrazine in the preparation. Therefore, making the material hydrophilic and favouring the aqueous phase. Harsher conditions may have been needed to ensure full reduction of the GO to provide a hydrophobic material. Raman analysis is a common method to evaluate carbon materials and the extent of their oxidation. The Raman spectrum of graphite features 2 strong peaks at around 1600 and 1350 cm^{-1}, named the G and D bands, where the G label refers to graphite and D refers to defect. Therefore, the intensity of this D band is proportional to the amount of disorder in the sample, and the ratios between the intensity of the D band and the G band (I_D/I_G) provides a parameter to quantify the disorder.[47] As the sp^2 character of the carbon structure disappears the ratio of I_D/I_G also decreases. Therefore, as the level of oxidation increases and sp^3 character is exhibited by the material, an increase in the I_D/I_G ratio is observed.[48]

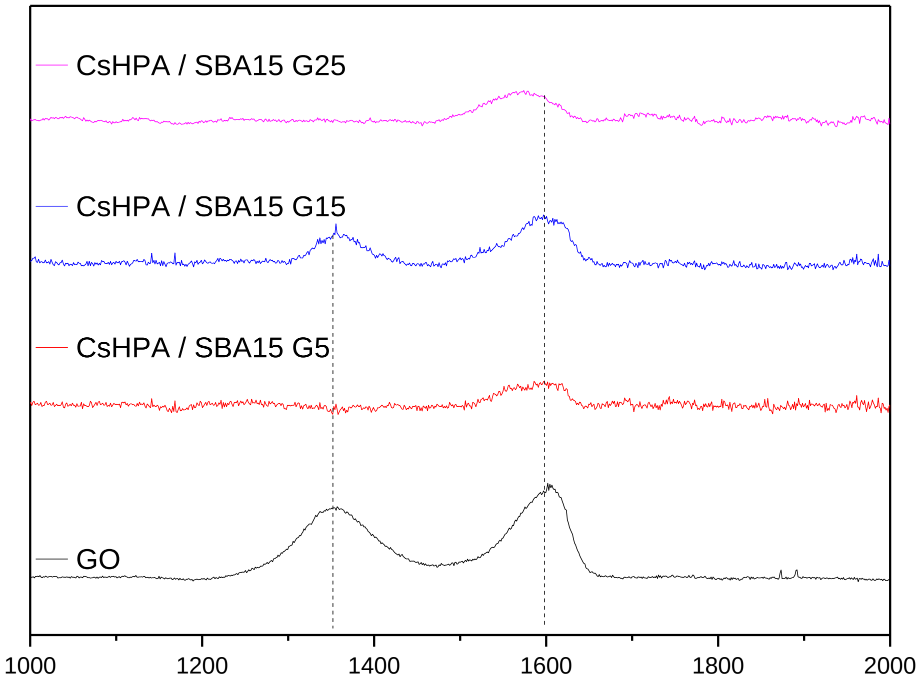

Figure 4-6 Raman spectra of CsHPA supported on silica-carbon hybrids in addition to the Hummers' prepared graphitic oxide starting material

The Raman spectra of the silica-carbon hybrid materials can be observed in Figure 4-6. The ratio of the D band (1350 cm^{-1}) and G band (1600 cm^{-1}) should provide an indication of the level of oxidation across the surface of the carbon. It can be seen in Figure 4-6that the carbon starting material (GO HU15, black) has an I_D/I_G ratio of 0.77. It is difficult to compare this with some of the other spectra owing to the weak signals received, possibly due to some fluorescence from the samples. However, CsHPA / SBA15 G15 (blue) exhibited a stronger signal which could provide a comparison. The I_D/I_G ratio in this spectrum was calculated to be 0.64 suggesting some reduction of the carbon in this sample. Whether the sample was reduced enough is unclear but a study implementing harsher reducing conditions may provide further insight. These harsher conditions may involve the use of a Parr reactor for the reducing step of the preparation or possibly a thermal reduction of the catalyst. In some of the SBA15 GX samples a clear Raman spectrum was difficult to achieve and analysis with XPS may provide some further understanding of the extent of oxidation in the material. The XPS spectra of GO and SBA15 GX catalysts is provided in Figure 4-7.

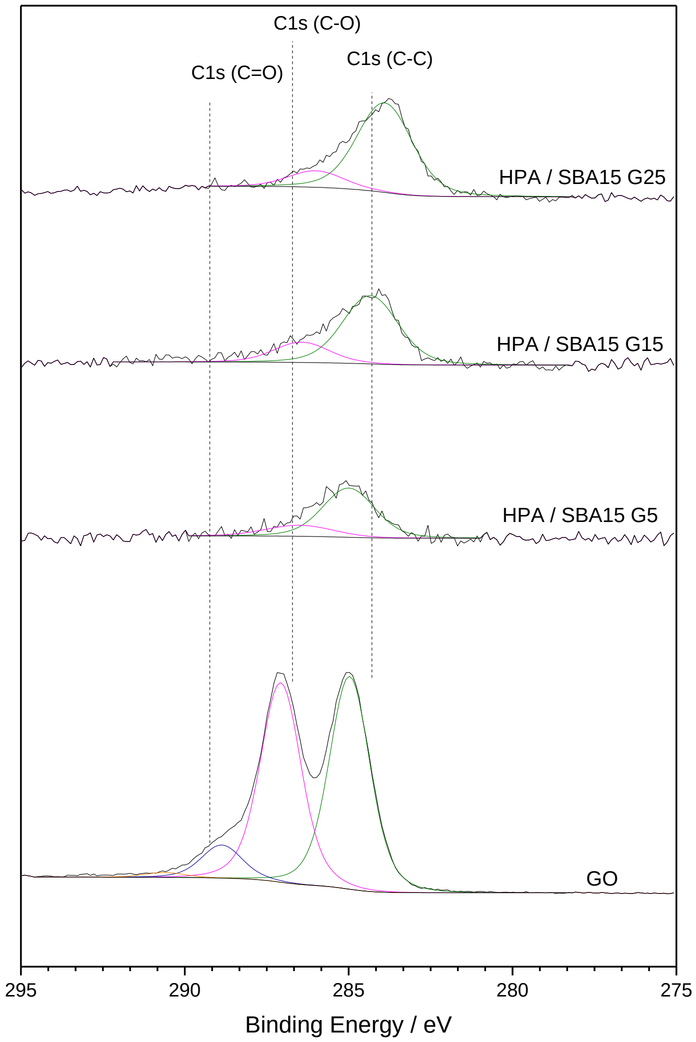

Figure 4-7 XPS spectra of SBA15 GX catalysts and GO

The XPS spectra of GO indicates the high degree of oxidation that would be expected with large contributions from C1s (C-O) and C1s (C-O). This contribution from C1s (C-O) is significantly decreased in SBA15 GX catalysts indicating the extensive reduction of the carbon. This is accompanied by the complete removal of contributions from C1s (C=O), signifying a largely successful reduction of the carbon entity of these catalysts. A further quantitative comparison is provided in Table 4-13 which reveals the stark difference between the C1s (C-C) and C1s (C-O) contributions in each sample. In the GO the ratio between C1s (C-C) and C1s (C-O) is almost equal. For the silica-carbon hybrids this ratio increases to 3.57, 5.43 and 3.36 in favour of C1s (C-C) for the SBA15 G5, SBA15 G15 and SBA15 G25 respectively. This does represent a significant reduction but there is still the presence of some level of oxidation within the catalysts. Therefore, this could be improved with harsher reduction conditions and may provide some evidence to the inability of the catalysts to form a Pickering emulsion.

Table 4-13 Spectral fitting parameters for C1s species, including peak area ratio between C1s species.

Catalyst	C1s (C-C) / eV	C1s (C-O) / eV	C1s (C=O) / eV	Peak area ratio, C1s (C-C) / C1s (C-O)
GO	285	287	289	1.07
HPA / SBA15 G5	285	287	-	3.57
HPA / SBA15 G15	284	286	-	5.43
HPA / SBA15 G25	284	286	-	3.36

The formation of a Pickering emulsion would require particles of SBA15 GX to exhibit the hydrophilic properties of silica and the hydrophobic properties of carbon. Bright-field TEM imaging, displayed in Figure 4-8, provides an insight into the microscopic properties of the material. Figure 4-8a, b and c display images for CsHPA / SBA15 G5, however from the images it is unclear whether the incorporation of carbon into the silica particles was successful. Evidence for carbon incorporation is provided by EDX analysis in Table 4-14, but it is not followed by the detection of W or CS, which would be prevalent in the CsHPA. Figure 4-8a shows rod-like granules of about 1 µm in diameter, which was analysed by EDX indicating the incorporation of 3.1 % carbon. These granules also seem to maintain an ordered structure that would be expected in SBA-15,[46] therefore the incorporation of carbon hasn't significantly affected the structure. Figure 4-8b shows graphene sheets which have not been incorporated into the SBA-15 structure. This is similarly shown in Figure 4-8d where graphene sheets have not been integrated with SBA-15. Furthermore, Figure 4-8e and h reveal an SBA-15 structure with significantly lower carbon percentages than would be expected. A solution to this could require harsher conditions, such as, a hydrothermal preparation and longer ageing times, which may allow full incorporation of carbon.

A further insight enabled by the TEM images is the invariable deposition of CsHPA particles. There only appears to be evidence of CsHPA clusters in Figure 4-8h, where the EDX analysis (Table 4-14) signifies a proportion of these clusters aggregating on the surface of SBA-15 particles. However, a larger proportion of particles would need to be analysed by EDX since it is conceivable that these CsHPAs would be too small to observe or could be located within the pore structure.

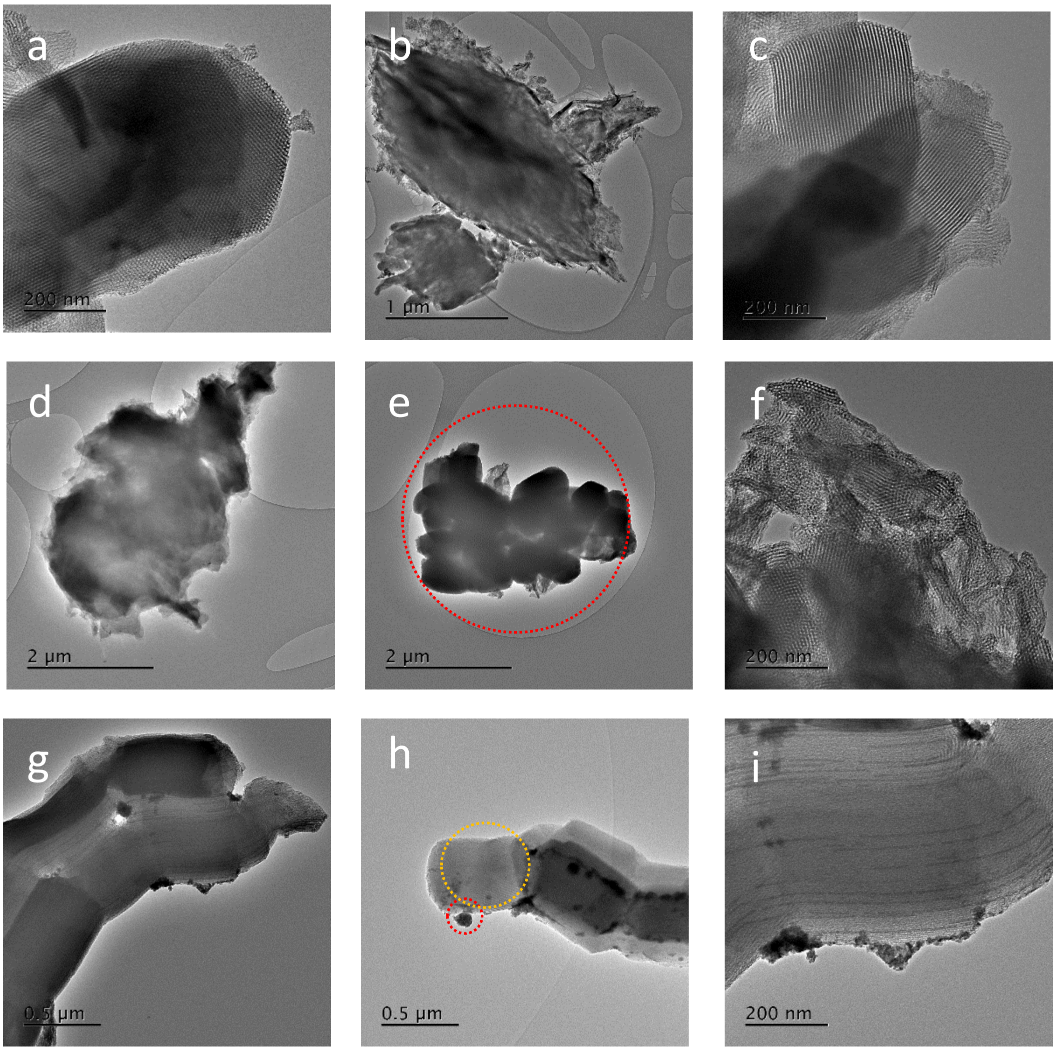

Figure 4-8 Bright field transmission electron microscopy (TEM) images of (top row: a, b, c) 10 % CsHPA / SBA15 G5; (d, e, f) 10 % CsHPA / SBA15 G15; (g, h, i) 10 % CsHPA / SBA15 G25. Coloured rings indicate areas of EDX analysis for Table 4-14.

Table 4-14 EDX analysis of CsHPA / SBA15 GX catalysts. Superscript letters directly refer to image labels in Figure 4-8 with the area highlighted if necessary, in the colour described.

Catalyst	**Wt. %**			
	C	Si	Cs	W
CsHPA / SBA15 G5	3.1	39.9	0.0	0.0
CsHPA / SBA15 G15^{d}	99.1	0.0	0.0	0.0
CsHPA / SBA15 G15^{e}	1.5	45.6	1.3	7.6
CsHPA / SBA15 G25$^{h(red)}$	1.2	28.3	4.3	31.2
CsHPA / SBA15 G25$^{h(yellow)}$	0.6	59.9	0.2	0.0

Figure 4-9 provides an FTIR spectrum of the supported HPAs against the tungstophosphoric acid precursor and could provide an indication on the extent of HPA immobilisation on the catalysts. Unfortunately, signals associated with the HPAs are overlapped by a strong, broad Si-O-Si stretch at 801 cm^{-1} and 1101 cm^{-1}, thus making it difficult to observe signals consistent with a HPA.[49] Evidence for the immobilisation of the HPA is provided by the XRD diffraction pattern of the materials in Figure 4-10. For SiO_2 spheres, a broad peak centred at $2\theta = 22°$ is observed which can be assigned to the SiO_2 microspheres.[49] This broad signal interferes with some of the peaks which would be assigned to the HPA. The diffraction pattern does bare similarities to the HPA (black) with many of the peaks displayed in the Cs3PW spectrum, also visible in the diffraction patterns of the supported catalysts. This implies that the HPA was present on the catalyst. A full quantification would require an acid digestion in HF followed by ICP analysis.

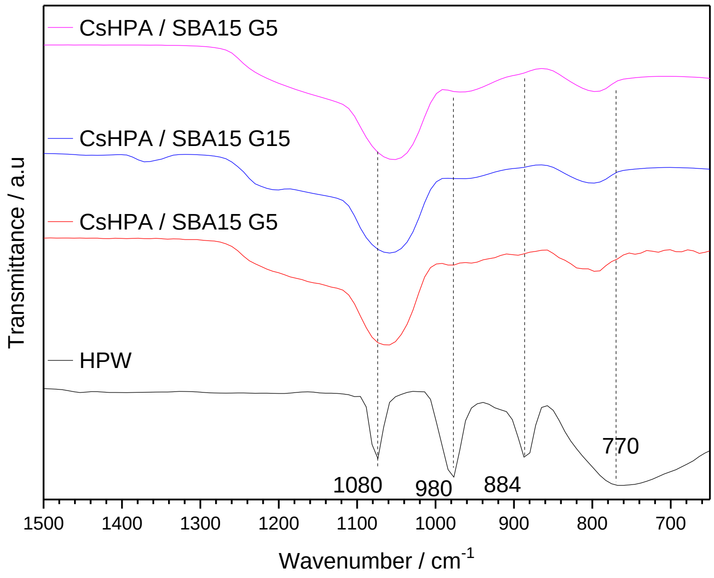

Figure 4-9 FTIR spectra for CsHPA / SBA-15 Gx catalysts

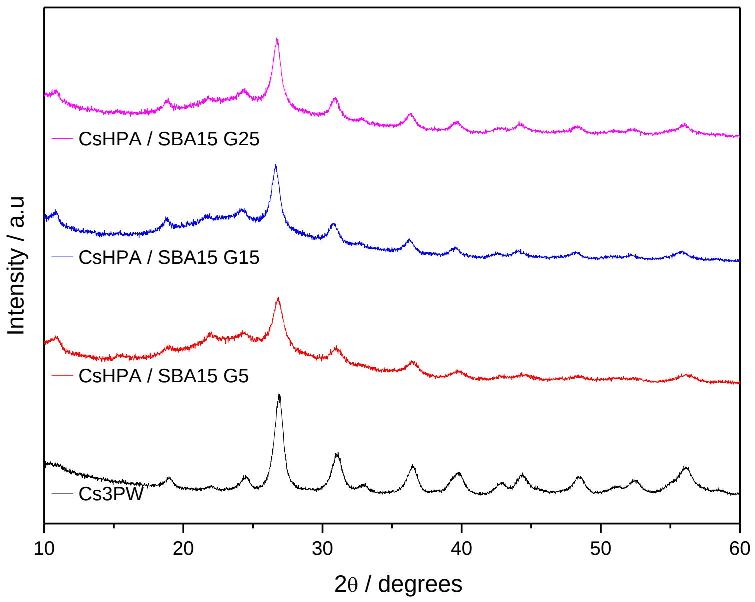

Figure 4-10 XRD spectra for CsHPA / SBA-15 Gx catalysts

The N_2 isothermal sorption analysis is provided in Figure 4-11 with selected structural parameters supplied in Table 4-15. According to the nitrogen sorption profile the hybrid materials present typical IV hysteresis curves, indicative of the mesoporous structure. The BET surface areas range from 475 m^2 to 595 m^2. The BJH pore volume and BJH average pore size are 1.14–1.16 $cm^3\ g^{-1}$ and 49–50 Å. These properties are similar to those of pure SBA-15 and suggest that the hybrids could act as ideal supports or catalysts due to the high surface area and mesopores.[46,50]

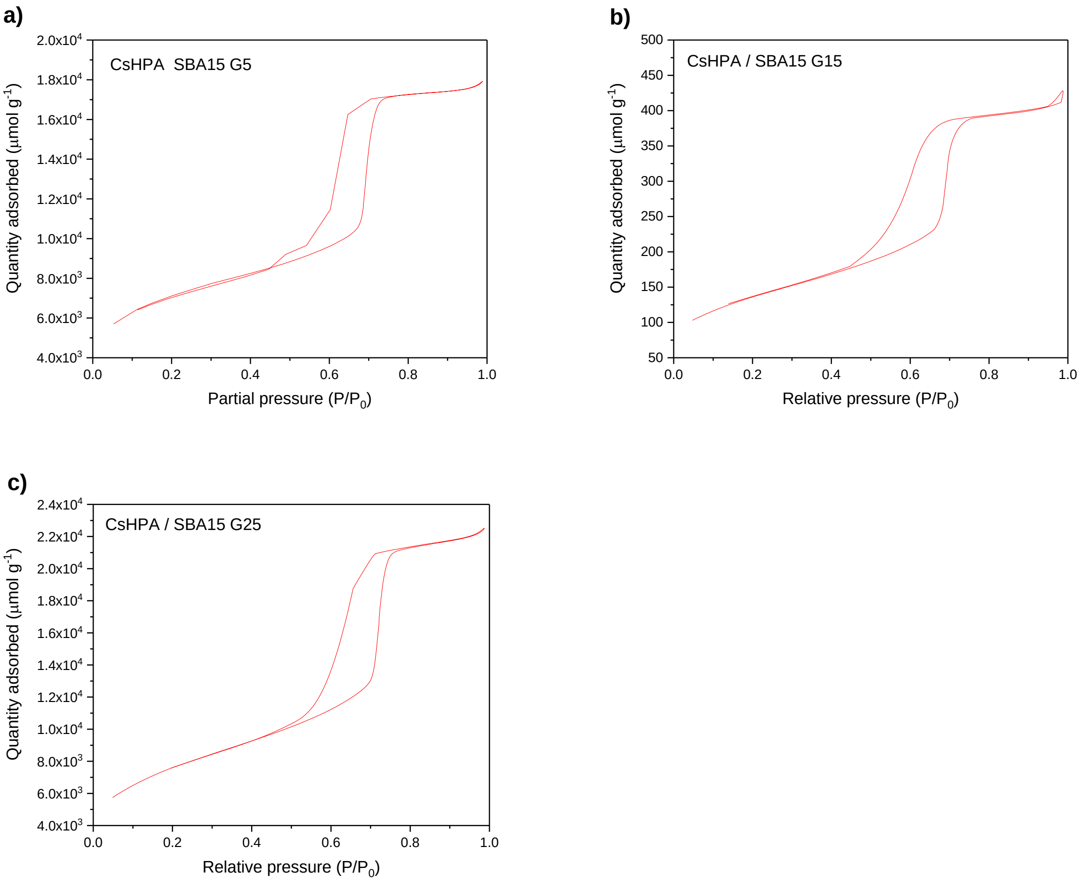

*Figure 4-11 Nitrogen sorption isotherms for CsHPA / SBA15 Gx materials **a)** CsHPA /SBA-25 G5 **b)** CsHPA /SBA-25 G15 **c)** CsHPA /SBA-25 G25*

Table 4-15 Surface area, pore size and pore volume of SBA-15-carbon hybrids and SBA-15[a]

Sample	**BET surface area (m^2g^{-1})**	**Pore size (Å)$_{BJH}$**	**Pore volume (cm^3g^{-1})**
CsHPA SBA-15 G5	550	50	0.61
CsHPA SBA-15 G15	500	50	0.63
CsHPA SBA-15 G25	600	50	0.76
SBA-15	550	50	0.60

[a] Pore sizes calculated using BJH desorption approach

4.4 Conclusions

Cs-substituted polyoxometalates have been shown to be active for the oxidation of cyclohexene to CHD using H_2O_2 as oxidant. Reactions were performed under mild conditions and using a stoichiometric amount of H_2O_2. The supporting of Au onto these catalysts has enabled an increased activity, although only modest. This study provides the first use of a Au/supported HPA in this reaction and also the first use of a HPA supported on a silica-carbon hybrid under biphasic conditions.

A number of experiments were commenced using solvated conditions. 1-Butanol was found to react with cy-oxide, which was proved through experiments using cy-oxide as starting material and reinforced through GC-MS. This product formed through a nucleophilic addition of butanol on the epoxide. Despite these drawbacks the higher substituted polyoxometalates exhibited higher activity, possibly owing to a higher surface area and lower acidity associated with these catalysts. Interestingly, the tungstosilicic acid showed very low activity compared to their phosphorus counterparts. The benefit of adding Au to the polyoxometalates was also realised in these studies with an increase in conversion from 15 % to 20 %. Further experiments were conducted in MeCN which did not cause any side reactions, and catalysts exhibited high selectivity to epoxidation products using this solvent. Experiments to assess the sequential addition of H_2O_2 through multiple aliquots of the oxidant proved that this method could improve its efficiency. However, this resulted in an impact on the mass balance where the increasing frequency of depressurisation resulted in an extended loss of cyclohexene.

To improve atom economy in line with the green principles of chemistry, a move to solventless conditions was commenced. A high selectivity to CHD was noticed and a sequential addition of H_2O_2 also showed an increased yield of CHD, which is similar to the observations made under solvated conditions. The benefit of Au in these experiments is also clear as evidenced by the increase in conversion from 21 % to 24 %, however the added expense of Au may make its inclusion impracticable for a small gain in CHD yield. Despite the improved atom economies that can be achieved under solventless conditions, this biphasic system still necessitates the need for a phase transfer catalyst. Aliquat 336 provides drawbacks in its use due to difficulties in separating it from the reaction mixture and because of its harm to the environment.

Work proceeded to finding a replacement for the phase transfer catalyst, through the development of a catalyst which could form a Pickering emulsion. However, activity of this silica-carbon hybrid was low even with a 10 % weight loading of POM on its surface. The catalyst was not observed to form a Pickering emulsion and favoured the aqueous phase possibly due to incomplete reduction of the graphitic oxide used in its preparation and an invariable incorporation of carbon into the SBA-15 structure.

4.5 Future work

The stoichiometric oxidation of cyclohexene with H_2O_2 offers a viable route to the selective formation of CHD. HPAs could offer a solution to achieving this, however greater yields of CHD would need to be achieved than has been accomplished here. There is an array of polyoxometalates which have not been utilised in this study but have also been demonstrated by other groups to be activity in oxidation reactions.[5,7,51–53] The use of some of these catalysts, notably molybdovanadates may enhance the activity we currently see or prove to be a better catalyst than the CsPW when immobilised onto the silica-carbon hybrid material. Materials such as these may exhibit some activity in the second oxidation step from CHD to AA as well. To try and understand the key differences between the POMs which may be attributed to the differences in activity observed, an ammonia TPD would be useful to plot the catalysts acidity against their conversion. By setting up an ammonia dosing experiment this may be possible to gain some accurate data with respect to their acidities which may help explain why the tungstosilicic catalysts were inactive and may also explain the discrepancy caused by differing Cs contents.

Further improvements to mass balance could be achieved, possibly through a longer extraction process. If Na_2SO_4 would be added to the reaction mixture and agitated for a longer time then more CHD would possibly migrate from the aqueous phase. Reaction with phase transfer catalyst and hybrid material to observe if activity is mostly dictated by Aliquat 336. A requirement for the success of the silica-carbon hybrid would be to ascertain the reduction of the graphitic oxide. To ensure this harsher reduction conditions in the material's preparation should be attempted with Raman studies to investigate the success of each approach. Firstly, an autoclave could be used which would enable the reduction using the hydrazine with an autogenous pressure, possibly over an extended time or alternatively via a thermal reduction. An area of improvement in this investigation could also be the implementation of reuse experiments as POMs are reported to lack reusability.

Some problems associated with this reaction were linked to mass balance issues. A solution to this would be to use an autoclave which allow analysis of the gaseous products. The use of an autoclave would also allow higher pressures of N_2 to be utilised which may also aid to keep cyclohexene in the liquid phase and limit that which is lost through evaporation. Another benefit of using an autoclave would be to use a HPLC pump to feed aqueous H_2O_2 into the reactor. This would enable a slower addition of H_2O_2 which could increase the oxidant efficiency even further than preliminary studies showed in this investigation. Adding H_2O_2 through a HPLC pump would also enable the reactor to remain a closed system and limit any mass loss through depressurisation. The prospect of forming H_2O_2 in situ would also be achievable when using an autoclave and the higher reactivity of cyclohexene may make it a more suitable substrate than previous work with cyclohexane. Pd and

Au can be substituted into the polyoxometalate structure and these materials have previously been used in the formation of H_2O_2.[54,55]

Ultimately, there is a lot of work required to make this reaction an industrially viable alternative and costs of H_2O_2 probably not making this an attractive solution against the current nitric acid process even if stoichiometric efficiency could be achieved.

4.6 References

1 K. Sato, M. Aoki and R. Noyori, *Sci. 281*, 1998, **281**, 1646–1648.

2 J. M. Campos-Martin, G. Blanco-Brieva and J. L. G. Fierro, *Angew. Chemie Int. Ed.*, 2006, **45**, 6962–6984.

3 S. Choi, Y. Wang, Z. Nie, J. Liu and C. H. F. Peden, *Catal. Today*, 2000, **55**, 117–124.

4 D. Hoegaerts, B. F. Sels, D. E. De Vos, F. Verpoort and P. A. Jacobs, *Catal. Today*, 2000, **60**, 209–218.

5 N. K. K. Raj, S. S. Deshpande, R. H. Ingle, T. Raja and P. Manikandan, *Catal. Letters*, 2004, **98**, 217–223.

6 C. Peng, X. H. Lu, X. T. Ma, Y. Shen, C. C. Wei, J. He, D. Zhou and Q. H. Xia, *J. Mol. Catal. A Chem.*, 2016, **423**, 393–399.

7 S. Boudjema, H. Rabah and A. Choukchou-Braham, *Acta Phys. Pol. A*, 2017, **132**, 469–472.

8 M. Guidotti, C. Pirovano, N. Ravasio, B. Lázaro, J. M. Fraile, J. A. Mayoral, B. Coq and A. Galarneau, *Green Chem.*, 2009, **11**, 1421–1427.

9 N. Maksimchuk, J. Lee, A. Ayupov, J.-S. Chang and O. Kholdeeva, *Catalysts*, 2019, **9**, 324.

10 L. Leclercq, R. Company, A. Mühlbauer, A. Mouret, J. M. Aubry and V. Nardello-Rataj, *ChemSusChem*, 2013, **6**, 1533–1540.

11 G. Lv, F. Wang, X. Zhang and B. P. Binks, *Langmuir*, 2018, **34**, 302–310.

12 P. Blach, Z. Böstrom, S. Franceschi-Messant, A. Lattes, E. Perez and I. Rico-Lattes, *Tetrahedron*, 2010, **66**, 7124–7128.

13 Y. Deng, Z. Ma, K. Wang and J. Chen, *Green Chem.*, 1999, **1**, 275–276.

14 J. Alcañiz-Monge, G. Trautwein and A. Garcia-Garcia, *J. Mol. Catal. A Chem.*, 2014, **394**, 211–216.

15 J. C. S. Soares, A. H. A. Gonçalves, F. M. Z. Zotin, L. R. R. de Araújo and A. B. Gaspar, *Mol. Catal.*, 2018, 0–1.

16 M. Jin, Q. Niu, Z. Guo and Z. Lv, *Appl. Organomet. Chem.*, , DOI:10.1002/aoc.5115.

17 R.-Z. Han, X.-H. Shi, H.-H. Ren and D.-G. Jiang, *Gao Xiao Hua Xue Gong Cheng Xue Bao/Journal Chem. Eng. Chinese Univ.*, 2012, **26**, 629–634.

18 Y. Ding, Q. Gao, G. Li, H. Zhang, J. Wang, L. Yan and J. Suo, *J. Mol. Catal. A Chem.*, 2004, **218**, 161–170.

19 M. N. Timofeeva, Z. P. Pai, A. G. Tolstikov, G. N. Kustova, N. V Selivanova, P. V Berdnikova, K. P. Brylyakov, A. B. Shangina and V. A. Utkin, *Russ. Chem. Bull.*, 2003, **52**, 480–486.

20 M. Misono, N. Mizuno, K. Katamura, A. Kasai, Y. Konishi, K. Sakata, T. Okuhara and Y. Yoneda, *Bull. Chem. Soc. Jpn.*, 1982, **55**, 400–406.

21 L. R. Pizzio, C. V Cáceres and M. N. Blanco, *Appl. Catal. A Gen.*, 1998, **167**, 283–294.

22 M. N. Timofeeva, *Appl. Catal. A Gen.*, 2003, **256**, 19–35.

23 N. S. Patil, B. S. Uphade, P. Jana, R. S. Sonawane, S. K. Bhargava and V. R. Choudhary, *Catal. Letters*, 2004, **94**, 89–93.

24 N. Linares, C. P. Canlas, J. Garcia-Martinez and T. J. Pinnavaia, *Catal. Commun.*, 2014, **44**, 50–53.

25 Y. Guo, L. Zhengwang, W. Guangjian, Y. Huang and F. Kang, *Appl. Surf. Sci.*, 2011, **258**, 1082–1090.

26 D. An, A. Ye, W. Deng, Q. Zhang and Y. Wang, *Chem. - A Eur. J.*, 2012, **18**, 2938–2947.

27 Y. Takuya, M. Toru, S. Norihito, O. Mitsutaka, I. Tamao and H. Masatake, *Angew. Chemie Int. Ed.*, **57**, 1523–1527.

28 S. Pattisson, E. Nowicka, U. N. Gupta, G. Shaw, R. L. Jenkins, D. J. Morgan, D. W. Knight and G. J. Hutchings, *Nat. Commun.*, 2016, **7**, 12855.

29 S. Soled, S. Miseo, G. McVicker, W. E. Gates, A. Gutierrez and J. Paes, *Catal. Today*, 1997, **36**, 441–450.

30 C. Hammond, J. Straus, M. Righettoni, S. E. Pratsinis and I. Hermans, *ACS Catal.*, 2013, **3**, 321–327.

31 R. J. Lewis, J. K. Edwards, S. J. Freakley and G. J. Hutchings, *Ind. Eng. Chem. Res.*, 2017, **56**, 13287–13293.

32 J. M. Fraile, J. I. García, J. A. Mayoral and E. Vispe, *J. Catal.*, 2001, **204**, 146–156.

33 J. M. Fraile, J. I. García, J. A. Mayoral and E. Vispe, *Appl. Catal. A Gen.*, 2004, **276**, 113–122.

34 M.-L. Wang and V. Rajendran, *Ultrason. Sonochem.*, 2007, **14**, 46–54.

35 M. Langpape, J. M. M. Millet, U. S. Ozkan and M. Boudeulle, *Study of Cesium or Cesium-Transition Metal-Substituted Keggin-TypePhosphomolybdic Acid as Isobutane Oxidation CatalystsI. Structural Characterization*, 1999, vol. 181.

36 G. M. Brown, M.-R. Noe-Spirlet, W. R. Busing and H. A. Levy, *Aeta Cryst*, 1977, **33**, 1038–1046.

37 Y. Ogasawara, S. Uchida, T. Maruichi, R. Ishikawa, N. Shibata, Y. Ikuhara and N. Mizuno, *Chem. Mater.*, 2013, **25**, 905–911.

38 G. Lapisardi, F. Chiker, F. Launay, J. P. Nogier and J. L. Bonardet, *Catal. Commun.*, 2004, **5**, 277–281.

39 S. Ghosh, S. S. Acharyya, S. Adak, L. N. S. Konathala, T. Sasaki and R. Bal, *Green Chem.*, 2014, **16**, 2826–2834.

40 J. C. S. Soares, A. H. A. Gonçalves, F. M. Z. Zotin, L. R. R. de Araújo and A. B. Gaspar, *Catal. Today*, , DOI:10.1016/j.cattod.2020.07.052.

41 N. Agarwal, S. J. Freakley, R. U. Mcvicker, S. M. Althahban, N. Dimitratos, D. J. Morgan, R. L. Jenkins, D. J. Willock, S. H. Taylor and C. J. Kiely, 2017, **6515**, 1–10.

42 K. Sato, M. Aoki and R. Noyori, *Science (80-.).*, 1998, **281**, 1646 LP – 1647.

43 A. M. Hyde, S. L. Zultanski, J. H. Waldman, Y. L. Zhong, M. Shevlin and F. Peng, *Org. Process Res. Dev.*, 2017, **21**, 1355–1370.

44 H. Zheng, Z. Sun, X. Chen, Q. Zhao, X. Wang and Z. Jiang, *Appl. Catal. A Gen.*, 2013, **467**, 26–32.

45 L. Lupa, L. Cocheci, R. Pode and I. Hulka, *Sep. Purif. Technol.*, 2018, **196**, 82–95.

46 X. R. Wei, J. Liu, Y. Yang and L. Deng, *RSC Adv.*, 2014, **4**, 35744–35749.

47 F. Tuinstra and J. L. Koenig, *J. Chem. Phys.*, 1970, **53**, 1126–1130.

48 M. S. Dresselhaus, A. Jorio, A. G. Souza Filho and R. Saito, *Philos. Trans. R. Soc. A Math. Phys. Eng. Sci.*, 2010, 368, 5355–5377.

49 Y. Liang, J. Ouyang, H. Wang, W. Wang, P. Chui and K. Sun, *Appl. Surf. Sci.*, 2012, **258**, 3689–3694.

50 D. Zhao, Q. Huo, J. Feng, B. F. Chmelka and G. D. Stucky, *J. Am. Chem. Soc.*, 1998, **120**, 6024–6036.

51 A. M. Khenkin and R. Neumann, *Adv. Synth. Catal.*, 2002, **344**, 1017–1021.

52 I. N. V., P. M. T. and K. Ulrich, *Angew. Chemie Int. Ed.*, **51**, 9492–9510.

53 A. N. Kharat, S. Moosavikia, B. T. Jahromi, A. Badiei, A. Nemati Kharat, S. Moosavikia, B. Tamaddoni Jahromi, A. Badiei, A. N. Kharat, S. Moosavikia, B. T. Jahromi, A. Badiei, A. Nemati Kharat, S. Moosavikia, B. Tamaddoni Jahromi and A. Badiei, *J. Mol. Catal. A Chem.*, 2011, **348**, 14–19.

54 E. N. Ntainjua, M. Piccinini, S. J. Freakley, J. C. Pritchard, J. K. Edwards, A. F. Carley and G. J. Hutchings, *Green Chem.*, 2012, **14**, 170–181.

55 S. J. Freakley, R. J. Lewis, D. J. Morgan, J. K. Edwards and G. J. Hutchings, *Catal. Today*, 2015, **248**, 10–17.

5 Oxidation of cyclohexanediol to adipic acid

5.1 Introduction

The low temperature oxidation of cyclohexene to adipic acid would likely require a 2-step process to achieve high yields. Under aerobic conditions the oxidation of cyclohexene to cyclohexanediol (CHD) is limited to a selectivity of 50 %,[1] this limitation was also mentioned in Chapter 3. This limitation is caused by the necessity to form a cyclohexenyl peroxide intermediate, which then reacts with cyclohexene to form the epoxide. Therefore, to achieve a high yield of CHD, H_2O_2 would need to be used as the oxidant.[2] A second-step to convert CHD to adipic acid (AA) could then be achieved aerobically as this would be unaffected by the mechanistic limitations of the first step. This second step could then be run in aqueous conditions, which would be a result of using aqueous H_2O_2 in the first step.

The ability of vanadium compounds to perform aerobic oxidation has been reported by Vennat *et al.* who used monomeric vanadium species and polyoxometalate vanadium species to perform the oxidative cleavage of 2-hydroxycyclohexanone (2-HCO) to form AA.[3] The potential of vanadium systems for oxidative cleavage of CHD was furthered by, Obara *et al.*[4] who achieved yields to AA of over 90 % when using O_2 as oxidant and H_2O as solvent (Scheme 5-1). However, it was reported that over 50 % of vanadium in this reaction was dissolved in the reaction solution. Therefore, offering a truly heterogeneous alternative to this catalyst would be a great advance in this field. Research into heterogenous vanadium catalysts has been impacted by their susceptibility to leach into aqueous solutions. This can be alleviated to some extent by changing the support and reaction conditions, as shown in work by Masumoto *et al.*[5] However, the most successful catalyst in their studies still demonstrated 37.6 wt % of vanadium leached into the reaction. The effect of leaching of vanadium catalysts in heterogeneous liquid phase reactions is also stated in studies by Ziolek *et al.*, whereby V/MCM-41 leaches 71 wt. % of vanadium into the reaction solution, illustrating the difficulty in developing a stable vanadium catalyst.[6]

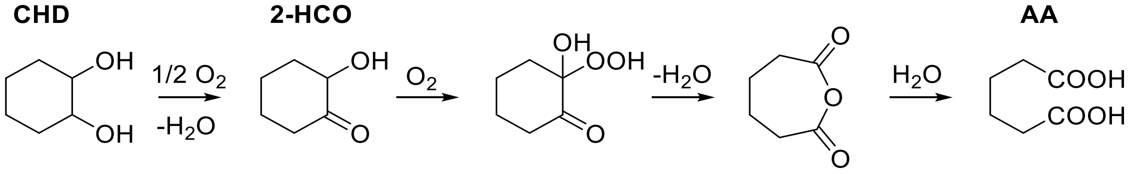

Scheme 5-1 Oxidation of cyclohexanediol to adipic acid

Vanadium bronzes have been reported to have many applications in aqueous media in areas such as photocatalysis and in electrochemical storage.[7–13] These bronzes often contain metals such as

Na, Cu, Ag or Co aimed at increasing their catalytic capabilities but their leaching into aqueous media is not always reported.[14,15] This chapter focuses on the preparation and catalytic properties of these bronzes in the oxidation of cyclohexanediol to adipic acid, and the role of any homogeneous species in the reaction solution.

5.2 Experimental

5.2.1 Materials

The following chemicals were used in this investigation without further purification. Vanadium oxide (V_2O_5 , 99.95 %), sodium chloride (NaCl, ≥99.0 %), sodium sulfate ($NaSO_4$, 99.99 %), copper(I) acetate (CuOAc, 97 %), hydrogen peroxide (H_2O_2, 30 wt. %), ammonium metavanadate (NH_4VO_3, 99.9 %), vanadium carbide (VC, 99 %), Silver nitrate ($AgNO_3$, ≥99.0 %), Cobalt chloride hexahydrate ($CoCl_2{\cdot}6H_2O$, 98 %), sodium orthovanadate ($NaVO_3$, 99.98 %), urea (CH_4N_2O, 99 %), *trans*-1,2-cyclohexanediol ($C_6H_{12}O_2$, 98 %), 5wt. % Pt/C, 2-hydroxycyclohexanone dimer ($C_6H_{12}O_2$, 97 %) were all sourced from Sigma-Aldrich. Hydrochloric acid (HCl, 37 %) and nitric acid (HNO_3, 70 %) were sourced from Fisher.

5.2.2 Catalyst preparation

5.2.2.1 $Na_2V_6O_{15}$ with NaCl

NaCl (25.7 mmol, 1.5 g) and V_2O_5 (2.0 mmol, 364 mg) were dissolved in deionised water (30 ml). H_2O_2 (5 ml, 30 %) was then added to this mixture and stirred at r.t for 2 h. This mixture was transferred to a 70 ml Teflon-lined stainless-steel autoclave and then placed in an oven for 72 h at 175 °C. The resulting precipitate was washed with deionised water several times and dried at 40 °C for 16 h in a vacuum oven. The sample was then calcined at 500 °C at 20 °C min^{-1} for 2 h under flowing air.

5.2.2.2 $Na_2V_6O_{15}$ with Na_2SO_4

Anhydrous Na_2SO_4 (3.6 mmol, 511 mg), V_2O_5 (1.8 mmol, 328 mg) and de-ionised water (45 ml) were loaded into a 70 ml Teflon-lined stainless-steel autoclave. The autoclave was then heated to 200 °C under autogenous pressure for 24 h and allowed to cool to room temperature. The precipitate was collected by vacuum filtration, washed with distilled water and ethanol. The solid was then dried in a vacuum oven at 60 °C for 16 h.

5.2.2.3 CuV_2O_6

CuOAc (0.5 – 1.0 mmol, 61.3 – 122.6 mg) and V_2O_5 (2.0 mmol, 364 mg) were dissolved in deionised water (30 ml). Cu/V molar ratios were varied from 0.25 – 0.5. H_2O_2 (5 ml, 30 %) was then added to this mixture and stirred at room temperature for 2 h. This mixture was then transferred to a 70 ml

Teflon-lined stainless-steel autoclave and placed in an oven for 72 h at 175 °C under autogenous pressure. The resulting solid was washed with deionised water and dried at 40 °C for 16 h in a vacuum oven. The dried solid was then heat-treated at 500 °C in flowng N_2 for 2 h at 10 °C min^{-1}.

5.2.2.4 *$AgVO_3$*

NH_4VO_3 (0.5 mmol, 58.5 mg) was dissolved in deionised water (30 ml). A solution of $AgNO_3$ (0.5 mmol, 84.9 mg, 10 ml) was added dropwise to the NH_4VO_3 solution. This mixture was stirred for 15 min and then transferred to a 70 ml Teflon-lined stainless-steel autoclave and heated at 180 °C under autogenous pressure for 18 h. The resulting precipitate was collected *via* vacuum filtration and rinsed with boiled deionised water and ethanol. The solid was then dried under vacuum at 60 °C.

5.2.2.5 *$Co_3V_2O_8$*

$CoCl_2 \cdot 6H_2O$ (3.0 mmol, 714 mg) was dissolved in deionised water (20 ml) and stirred at 70 °C. $NaVO_3$ (2.0 mmol, 244 mg) was suspended in deionised water (20 ml) and added dropwise to solution and stirred at 70 °C for 2 h. The resulting solid was filtered by vacuum and dried at 16 h at 110 °C. This was then transferred to a furnace and calcined in flowing air at 600 °C for 2 h at 5 °C min^{-1}.

5.2.2.6 *V-C_3N_4*

Urea (0.2 mol, 12.0 g) was dissolved in water (100 ml). Ammonium metavanadate (NH_4VO_3, 4.36 mmol, 510 mg) was then added to this mixture. The solution was heated to 100 °C to remove water. The dried catalyst underwent a heat treatment at 300 °C for 2 h at 3 °C min^{-1} under N_2. The temperature was subsequently increased to 550 °C for 4 h at 3 °C min^{-1} under flowing N_2.

5.2.2.7 *V-Pt/C*

5 % Pt/C (2.5 g) was stirred in water (300 ml) and V_2O_5 (0.137 mmol, 25 mg) was added and heated to 80 °C for 4 h. The solid was then filtered off under vacuum and dried at 110 °C for 16 h.

5.2.2.8 *Ag/AC*

Ag_2NO_3 (0.703 mol, 2.55 mg) was dissolved in *aqua regia* (3:1, HCl:HNO_3) and stirred for 30 mins. This was then added dropwise to activated carbon (DARCO 1.98 g) at 80 °C and stirred for 1 h. This mixture was dried by heating up to 110 °C for 16 h.

5.2.3 Catalyst testing

5.2.3.1 *Oxidation of cyclohexanediol to adipic acid under O_2*

A solution of cyclohexanediol (5 ml, 10000 ppm) was loaded into a low-pressure glass reactor. When required, Pt/C (10 mg) and the vanadium co-catalyst (2 mg) were added to the vessel. The reactor was purged with O_2 and then charged with 3 bar O_2. The reactor was stirred at 80 °C for 4 h. Samples were collected at regular intervals, centrifuged and filtered using PTFE syringe filters (0.45 µm) before HPLC analysis. After sampling, the reactor was purged with O_2 and charged once more with 3 bar O_2.

5.2.3.2 Oxidation of 2-hydroxycylohexanone to adipic acid under O_2

A stock solution of vanadium was prepared by stirring V_2O_5 (2.20 mmol, 400 mg) in water (50 ml) for 16 h. The resulting solution was centrifuged, and the supernatant was collected. After filtration using PTFE syringe filters (0.45 µm), an accurate concentration was determined by MP-AES analysis. A solution of 2-hydroxycyclohexanone (5 ml, 4000 ppm) was loaded into a low-pressure glass reactor. The required volume of vanadium solution was then added to the vessel. The reactor was purged with O_2 and then charged with 3 bar O_2. The reactor was stirred at 80 °C for 4 h. Samples were centrifuged and filtered using PTFE syringe filters (0.45 µm) before HPLC analysis.

5.2.3.3 HPLC analysis

Analysis was carried out using an Agilent 1260 Infinity HPLC equipped with ultraviolet and refractive index detectors. Reactants and products were separated using a Metacarb 67 H column. The mobile phase was an aqueous solution of H_3PO_4 (0.01 M) and the flow rate was 0.5 ml min^{-1}. For the quantification of the amounts of reactants consumed and products generated, an external calibration method was used against analytical standards. The conversion, selectivity and mass balance were calculated as follows:

$$Conversion\ (\%) = \frac{(\text{mol of consumed substrate})}{(\text{mol of initial substrate})} \times 100$$

$$Selectivity\ (\%) = \frac{(\text{mol of product})}{(\text{mol of consumed substrate})} \times 100$$

$$Mass\ balance\ (\%) = \frac{(\text{mol of final products } + \text{ mol of final substrate})}{(\text{mol of initial substrate})} \times 100$$

5.3 Results and discussion

5.3.1 Oxidation of cyclohexanediol

The combination of Pt/C and V_2O_5 has been demonstrated by Obara *et al.* to successfully catalyse the oxidation of cyclohexanediol to adipic acid in a highly selective one-pot reaction.[4] Table 5-1 shows a reproduction of the work from Obara *et al.* Firstly, the blank reaction (entry 1) gives no conversion at 80 °C, which is similar to when V_2O_5 (entry 2) is used as the sole catalyst where a conversion of 3.0 % is achieved and only 0.4 % selectivity towards unknowns can be observed. The use of Pt/C as the sole catalyst (entry 3), resulted in a drastic increase of selectivity to 2-HCO of 90 % and a conversion of 48%. This was accompanied by low selectivity to other oxidation products, such as glutaric acid (GA) and succinic acid (SA) at 3.0 % and 1.0 %, respectively. Interestingly, when V_2O_5 was used in tandem with Pt/C (entry 4), a switch of selectivity towards adipic acid of 76 % was observed, while conversion remained at 50 % which is a similar level to when using on Pt/C. V_2O_5 is soluble in aqueous conditions so this reaction was likely a homogeneous reaction, as 88.4 % of the V_2O_5 catalyst was measured by MP-AES to be dissolved in the reaction media. It was suggested in the work by Obara *et al.* that despite losing approximately half the solid vanadium on each use, the remaining solid catalyst was responsible for the activity observed.[4] The industrial viability of this reaction would be benefited by increasing the stability of this catalyst under aqueous conditions. The leaching of vanadium into the reaction would lead to possible contamination of the product with toxic vanadium species.[16] For this purpose, we therefore tested a range of vanadium bronzes incorporating Na, Cu or Ag to owing to their stability in aqueous reactions, however V leaching is rarely reported.[14,15,17,18]

Table 5-1 Reaction data for the oxidation of cyclohexanediol. **Reaction conditions:** 80 °C, 3 bar O_2, 4 h, 10 000 ppm cyclohexanediol in water (5 ml), 10 mg 5 % Pt/C, 2 mg V_2O_5

	Catalyst	**Conv. / %**	**Selectivity / %**					**V leaching / %**	**[V] / ppm**	**M. B / %**
			AA	2-HCO	GA	SA	Unknowns			
1	Blank	0.0	0.0	0.0	0.0	0.0	0.0	-	-	100
2	V_2O_5	3.0	0.0	0.0	0.0	0.0	0.4			98
3	Pt/C	39	0.0	59	2.0	1.0	9.0	-	-	90
4	Pt/C + V_2O_5	50	76	1.0	5.0	1.0	5.0	88	168	96

5.3.2 Sodium vanadium bronzes

The synthesis of heterogeneous alternatives for V_2O_5 started with the preparation of a sodium vanadium bronze (NaVO) and the results are presented in Table 5-2. Within this series both catalysts were prepared by a hydrothermal technique (Section 5.2.2.1 and 5.2.2.2). Entry 1 depicts the bronze prepared using a NaCl precursor and is henceforth denoted as NaVO1. Entry 2 shows the bronze prepared with a Na_2SO_4 precursor and is denoted NaVO2. The NaVO1 catalyst (entry 1) demonstrates a similar conversion and adipic acid selectivity to the Pt/C +V_2O_5 system, achieving 41 % and 70 % respectively. With the use of NaVO2, similar results to NaVO1 were obtained with 37 % and 70 % for conversion and selectivity to adipic acid, respectively. However, these promising results are accompanied by the large amount of leaching observed. MP-AES analysis of the NaVO1 and NaVO2 post reaction solution revealed a total of 60 and 67 ppm V respectively, which amounts to roughly 40 % of the overall vanadium present in these bronzes. This level of leaching was still distinctly lower than for a Pt/C + V_2O_5 catalytic reaction which leached 88.4 %, however it is still an unsustainable amount. The incorporation of sodium into the vanadium bronze structure was therefore not able to suppress the leaching of vanadium compounds in the mixed metal oxide.

Table 5-2 Reaction data for the oxidation of cyclohexanediol. **Reaction conditions:** 80 °C, 3 bar O_2, 4 h, 10 000 ppm cyclohexanediol in water (5 ml), 10 mg 5 % Pt/C, 2 mg sodium vanadium bronze

	Catalyst	**Conv. / %**	**Selectivity / %**					**V leaching / %**	**[V] / ppm**	**M. B / %**
			AA	2-HCO	GA	SA	Unknowns			
1	Pt/C +NaVO1	41	70	2.0	0.0	1.0	4.0	37	60	91
2	Pt/C +NaVO2	37	70	4.0	7.0	2.0	2.0	42	67	96

The XRD patterns for the two NaVO catalysts synthesised using NaCl and $NaSO_4$ are given in Figure 5-1. It is noticeable from the diffraction patterns that these two syntheses result in largely different phases. The preparation method for NaVO1 followed a protocol described by Liu *et al.*[12] This diffraction pattern did not exhibit a strong match to any diffraction patterns on the ICDD software or when compared to literature.[12,19,20]

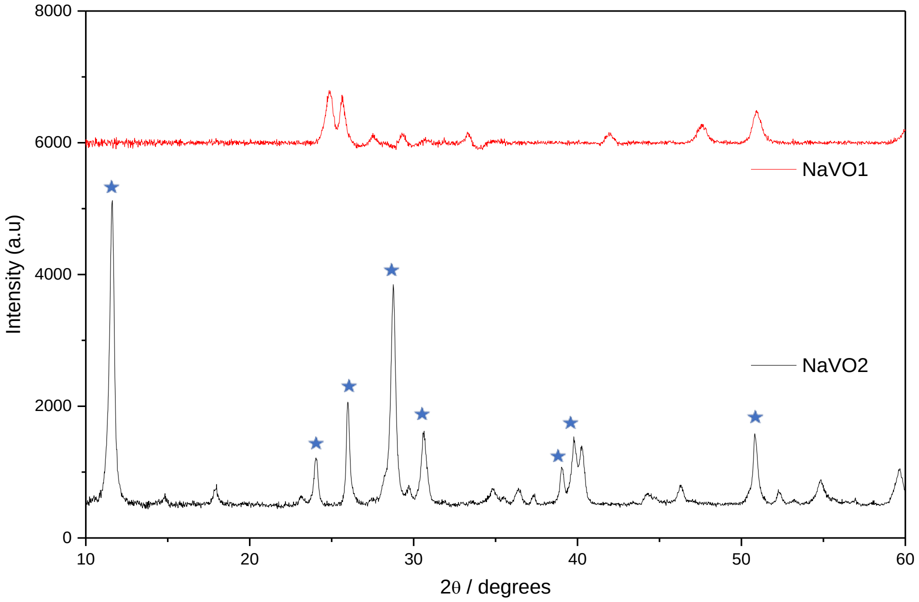

Figure 5-1 XRD pattern for NaVO bronzes, NaVO1 does not show a similarity to any phases on the ICDD database. NaVO2 has similarities to monoclinic $Na_2V_6O_{16}$ phase with the corresponding reflection illustrated (★)

Part of this difficulty in obtaining the correct phase may be due to the excess amount of NaCl used in the preparation method which may be necessary to ensure that Na is incorporated into the lattice. Another hypothesis is that the calcination temperature of 500 °C was not high enough to obtain the correct phase. Therefore, an *in-situ* XRD (figure 5-2) was performed to determine the effect of calcination temperature on the formed phase. The NaVO2 bronze was synthesised according to a previous method described by Zhou *et al.*[19] The XRD for NaVO2 is shown in figure 5-1 (black) and can be referenced to the monoclinic $Na_2V_6O_{16}$ phase with a P21/m space group with reflections at 2θ = 11.70, 25.93, 28.35, 29.77, 40.06, 46.26 and 50.83° being indicative of this phase. These reflections are signified by the stars (★) in the diffraction pattern.[19,20] This is accompanied by a high degree of crystallinity.

The first XRD pattern shown with the label 50 (1) represents the sample at 50 °C, before a temperature ramp has taken place. This diffraction pattern bares a similarity to the NaVO1 pattern and also did not show any matches on the ICDD database, possibly due to a low crystallinity. As the sample is heated to a temperature of 450 °C, an increase in crystallinity is observed. However the purity of this phase is questionable and matches to patterns in the ICDD database were low. It is evident that the diffraction pattern labelled as 450 is similar to the diffraction pattern obtained in Figure 5-1 for NaVO2, with the presence of refelections typical of the monoclinic $Na_2V_6O_{16}$ phase (★).[19,20] The purity of this phase is significantly lower than NaVO2 with additional unassigned peaks at 12.1, 18.7, 26.8, 27.4, 28.3, 29.9, 34.8 37.0 40.6 and 45.1 °. These additional peaks may be due to reproducibility errors in the hydrothermal preparation methods. The diffraction pattern largely remained the same from 450 to 600 °C, after which the sample lost its crystallinity, which may be explained by the sample melting at this temperature. The melting point of a $Na0_{.33}V_2O_5$ is reported to be 674 °C which is concurrent with the data shown.[21] The diffraction pattern labelled as 50 (2) shows the sample after it has cooled back down to 50 °C and shows that the sample regained its crystallinity. This diffraction pattern appears have greater purity and indexed to monoclinic layered NaV_6O_{15} nanorods (•), with reflections at 12.1, 18.8, 26.9, 27.5, 28.4, 29.9, 34.8, 37.1, 40.6 and 45.1 ° consistent with this.[12]

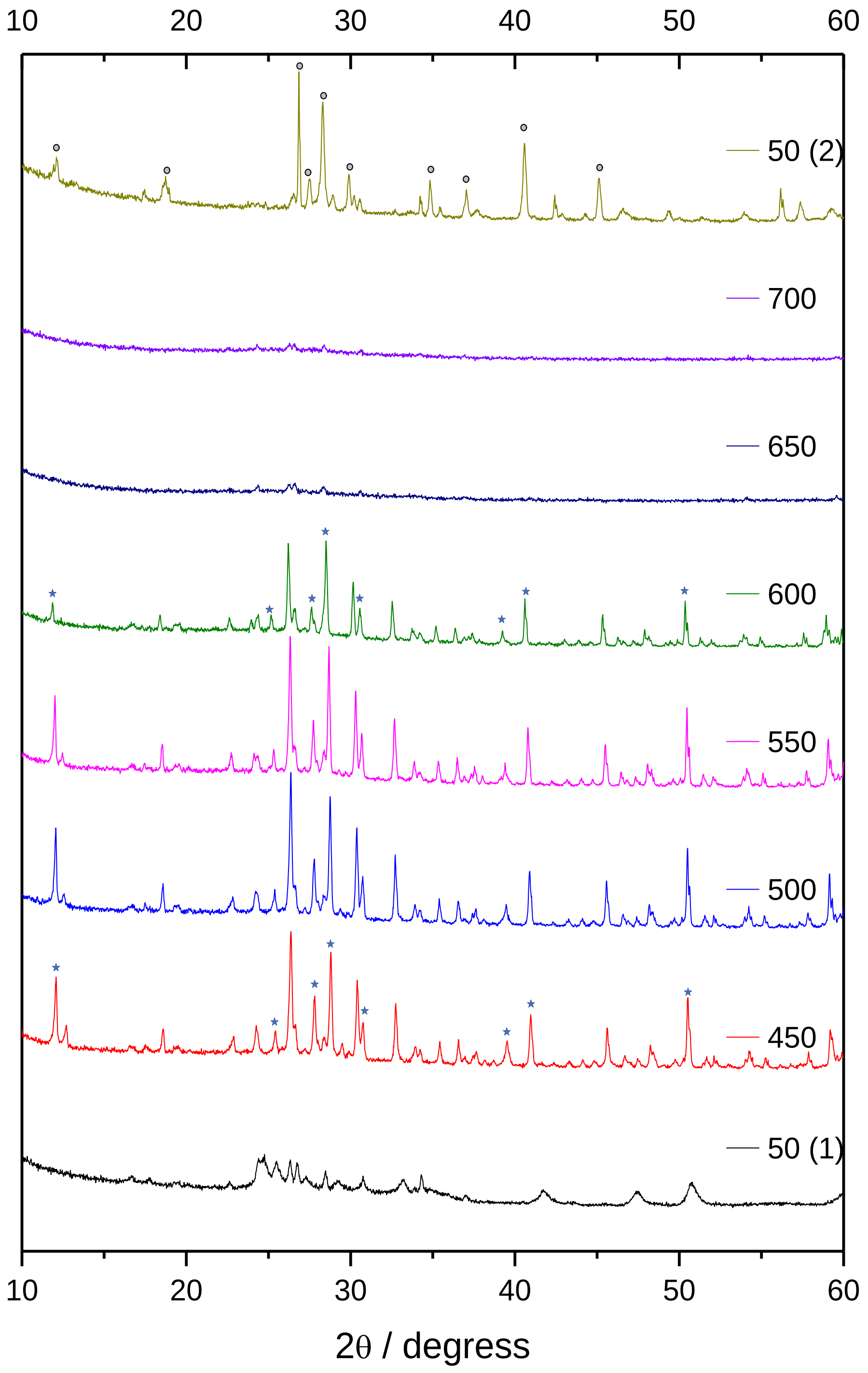

Figure 5-2 In-situ XRD of $Na_2V_6O_{16}$ prepared from NaCl, from the temperatures of 50 °C to 700 °C in 50 °C increments in air at 20 ml min^{-1}. 50 (1) denotes the sample before the calcination process and 50 (2) signifies that sample when it had cooled back down to 50 °C.

5.3.3 Copper vanadium bronzes

To further investigate the effect that other metals can have on the stability of vanadium bronzes, copper and silver were incorporated into the bronzes. Vanadium bronzes containing metals such as Cu, Ag and Co are commonly substituted into these materials. Their incorporation can result in enhanced electrochemical properties and increased activity, particularly in the oxidation of H_2S.[9,10,22-24] For the copper bronzes (CuVO), displayed in Table 5-3, molar ratios of 0.25, 0.33 and 0.50 copper to vanadium were prepared to investigate any effect that copper had on the stability of the bronze. Firstly, the reaction data from the CuVO, presented in Table 5-3 is similar to NaVO with selectivity towards AA of over 60 % in all cases. Conversion, which is largely dictated by the presence of Pt/C, is also very similar between bronzes with around 27 % conversion observed. It is therefore more relevant to compare the selectivity to AA, which is also very similar with around 60 % selectivity observed. It is evident that a lower selectivity to AA is achieved with CuVO compared to NaVO. Interestingly, it can also be seen that vanadium leaching, analysed by MP-AES, is reduced dramatically on inclusion of copper to 5.8 % for $Cu_{0.33}V_2O_6$. This low level of leaching contrasted with $Cu_{0.25}V_2O_6$ and $Cu_{0.5}V_2O_6$, which exhibited vanadium leaching of 16.6 % and 19.8 % respectively. Considering that the sodium vanadium bronzes showed leaching of around 40 %, these catalysts are significantly more stable, demonstrating that Cu successfully decreases the solubility of the bronze. This increase in stability may be due to Cu atoms occupying active sites at the surface of the catalyst, or due to the additional Cu affecting the electronic structure of V at the surface, making it more stable but potentially less reactive. This change in selectivity that is observed between the bronzes may be a result of less leaching in the reaction solution, highlighting the role of homogeneous V. However, $Cu_{0.33}V_2O_6$ displays a selectivity to AA of 60 %, which is comparable to the other Cu bronzes. This is accompanied by a lower concentration of V in the reaction solution, with only 11 ppm V present in this solution compared to 35 and 33 ppm V in the $Cu_{0.25}V_2O_6$ and $Cu_{0.50}V_2O_6$ reaction, respectively. However, this reaction may only require low concentrations of homogeneous V to have a marked effect on selectivity.

Table 5-3 Reaction data for the oxidation of cyclohexanediol. **Reaction conditions:** 80 °C, 3 bar O_2, 4 h, 10 000 ppm cyclohexanediol in water (5 ml), 10 mg 5 % Pt/C, 2 mg vanadium catalyst

	Catalyst	**Conv. / %**	**Selectivity / %**					**V leaching / %**	**[V] / ppm**	**M. B / %**
			AA	2-HCO	GA	SA	Unknowns			
1	Pt/C + $Cu_{0.25}V_2O_6$	32	64	5.0	0.0	0.0	4.0	17	35	91
2	Pt/C + $Cu_{0.33}V_2O_6$	27	60	9.0	0.0	0.0	0.0	6.0	11	91
3	Pt/C + $Cu_{0.5}V_2O_6$	25	64	10	0	2.0	5.0	20	33	96

The XRD patterns for $Cu_xV_2O_6$ catalysts are displayed in Figure 5-3. The diffraction pattern for V_2O_5 (black) is displayed giving an orthorhombic V_2O_5 phase (●), this pattern can be observed to maintain some presence even with a heat treatment and incorporated Cu. However, the inclusion of Cu leads to a partial transformation in the phase from V_2O_5 to a monoclinic β-$Cu_{0.261}V_2O_5$ (★), which is charactersied by peaks at 2θ = 12.15, 24.46, 26.39, 28.65, 31.16, 33.09, 37.25, 39.73, 40.93 and 46.23°.[9] This phase is present in all Cu bronzes but to a lesser extent in $Cu_{0.5}V_2O_6$ (pink). With a high Cu/V ratio the diffraction pattern is more indicative of a triclinic CuV_2O_6 phase (▼). The peaks which are typical with this phase are illustrated in Figure *5-3* at 2θ = 20.7, 26.7, 29.3, 31.7, 33.6, 42.1, 42.2 and 44.8°.[17,25] However, there also appears to be reflections which can be identified as related to the monoclinic β-$Cu_{0.261}V_2O_5$ but are much less visible. To conclude, it would appear that the main phase of $Cu_{0.25}V_2O_6$ and $Cu_{0.33}V_2O_6$ is the precursor orthorhombic V_2O_5 phase suggesting a further washing step would be required. However, there is still the presence of a monoclinic β-$Cu_{0.261}V_2O_5$ phase. This phase is still visible in $Cu_{0.5}V_2O_6$ but the main phase in this sample is the triclinic CuV_2O_6 phase with only minor contributions from V_2O_5.

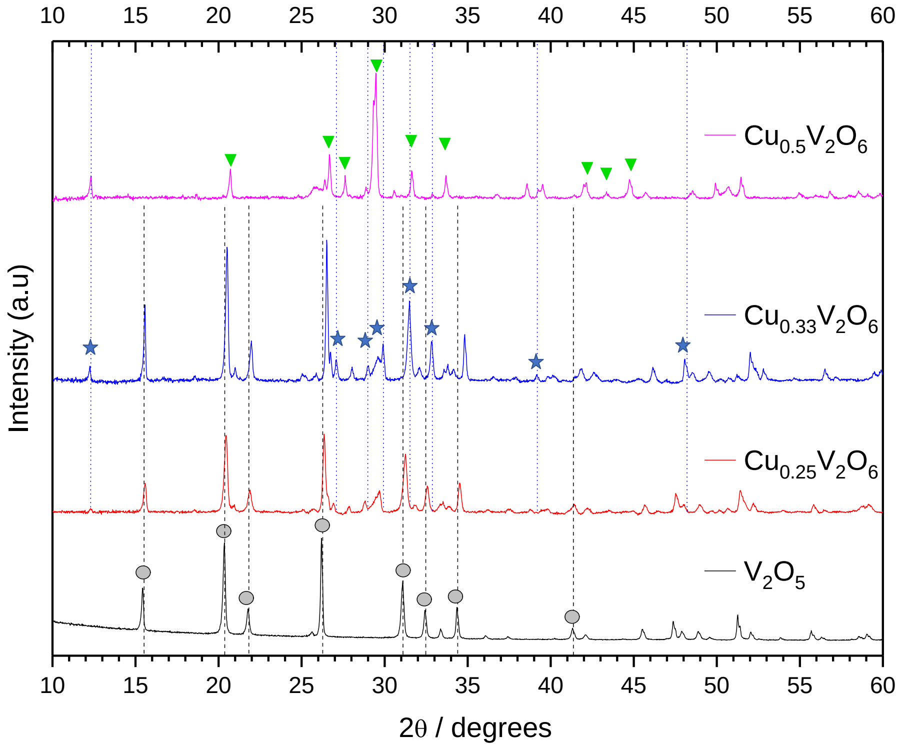

Figure 5-3 XRD pattern for $Cu_xV_2O_6$, showing orthorhombic V_2O_5 phase (●), monoclinic β-$Cu_{0.261}V_2O_5$ (★) and triclinic CuV_2O_6 phase (▼)

5.3.4 Silver and cobalt vanadium bronzes

The next bronzes to be tested for this reaction were silver vanadate and cobalt vanadate, with the results of these shown in Table 5-4. $AgVO_3$ were sleected due to their high aqueous stability in lithium battery anode applications.[22] Entry 1 shows the $AgVO_3$ has the highest stability of the catalysts tested with regards to V leaching, with only 5.0 % V observed. This level of leaching corresponded to a concentration of 9 ppm V in solution, which is substantially lower compared to the Na bronzes and is comparable to the $Cu_{0.33}V_2O_6$ catalyst. Unfortunately, this is also accompanied by the lowest activity of any of the catalysts. Selectivity to AA is still observed at 42 %, however, this is also lower than that of either the Cu or Na bronzes. In addition, there is also the presence of unconverted 2-HCO, with 21 % selectivity observed. The reason for high presence of 2-HCO may be due to the lower concentration of homogenous V present in the solution but could also be due to a lower number of reactive vanadium sites at the surface of the catalyst.

The final bronze of this series is a $Co_3V_2O_8$, a material which is predominantly used in aqueous media in the area of electrocatalysis.[24] For this reaction, 2-HCO was used as the starting material to remove the need for a Pt/C catalyst which controlled the amount of 2-HCO present. The $Co_3V_2O_8$ catalyst was not stable in aqueous solution with 42.5 % of the total V leaching, corresponding to a value of 67 ppm V being present in the reaction solution. It is notable that the conversion of this reaction remains low at 7.0 % but with a high selectivity to AA at 76 %.

Due to the leaching exhibited by most of the vanadium bronzes, a study was conducted using a carbon nitride (CN) support which has strong interactions with vanadium, as shown in previous studies by Ding et al.[26] In their investigations they demonstrated that vanadium supported on CN can be a promising catalyst in liquid phase reactions for the synthesis of phenol from benzene. CN was reported to exhibit a great affinity for vanadium because of the predominantly basic NH and NH_2 groups on the surface, which help to bind to the acidic vanadium species. In studies by Kharat *et al.*,[27] these acid-base interactions are also reportedly very effective in decreasing leaching to a negligible amount in vanadium-substituted molybdophosphoric acid, due to the strong interactions between the heteropolyacid and an amine functionalised SBA-15. The results for the V-C_3N_4 material in combination with Pt/C are shown in Table 5-4 for the oxidation of CHD. This catalyst was washed with 1 L boiling water prior to use but still exhibited significant leaching into the reaction. A percentage for the amount that was leached into solution could not be obtained due to the difficulty in dissolving the catalyst in *aqua regia* to obtain an accurate initial loading. In addition to the synthesised vanadium catalysts, a commercial vanadium carbide, was tested due to its reported insolubility in aqueous solutions.[28] This catalyst was tested for the oxidation of 2-HCO, however, on first use leaching was still evident for this catalyst with 3.0 % leaching observed. Leaching continued after a washing the catalyst with 5 L of boiling water, but was reduced to only 1.2 % of total vanadium leached from the catalyst, which was calculated empirically, giving a total concentration of 17.0 ppm vanadium in the reaction mixture.

Table 5-4 Reaction data for the oxidation of cyclohexanediol. **Reaction conditions:** 80 °C, 3 bar O_2, 4 h, 10000 ppm cyclohexanediol in water (5 ml), 10 mg 5 % Pt/C, 2 mg vanadium catalyst. ***Reaction conditions:** 80 °C, 3 bar O_2, 4 h, 4000 ppm 2-hydroxycyclohexanone

	Catalyst	**Conv. / %**	**Selectivity / %**					**V leaching / %**	**[V] / ppm**	**M. B / %**
			AA	2-HCO	GA	SA	Unknowns			
1	$AgVO_3$	18	42	21	0.0	2.0	0.0	5	9	93
2	CoV_2O_6*	7.0	76	-	6.0	0.0	4.5	43	67	99
3	V-C_3N_4	25	59	5.0	0.0	2.0	34	-	33	91
4	VC*	19	55	-	0.0	0.0	16	1.0	17	91

The XRD patterns for $AgVO_3$ and CoV_2O_6 are displayed in Figure 5-4. The diffraction pattern of $AgVO_3$ showed strong similarities to a β-$AgVO_3$ phase (●) with a monoclinic structure and I2/m space group. This phase is signified by reflections at 2θ = 20.6, 21.0, 23.0, 25.6, 28.6, 30.0, 33.8, 34.8, 40.1, 43.5, 44.3 and 51.2 °. There were no other detectable reflections in the sample suggesting the sample was mainly composed of this phase.[15,23] The XRD pattern of CoV_2O_6 was compred with literature and resembled a monoclinic crystal structure of space group C2/m (▼). The sample appeared to be highly crystalline and phase pure, with peaks at 2θ = 20.7, 27.8, 29.1, 29.6, 33.2, 39.3, 40.9, 41.7, 44.5, 49.0 ° indicative of this phase.[24,29]

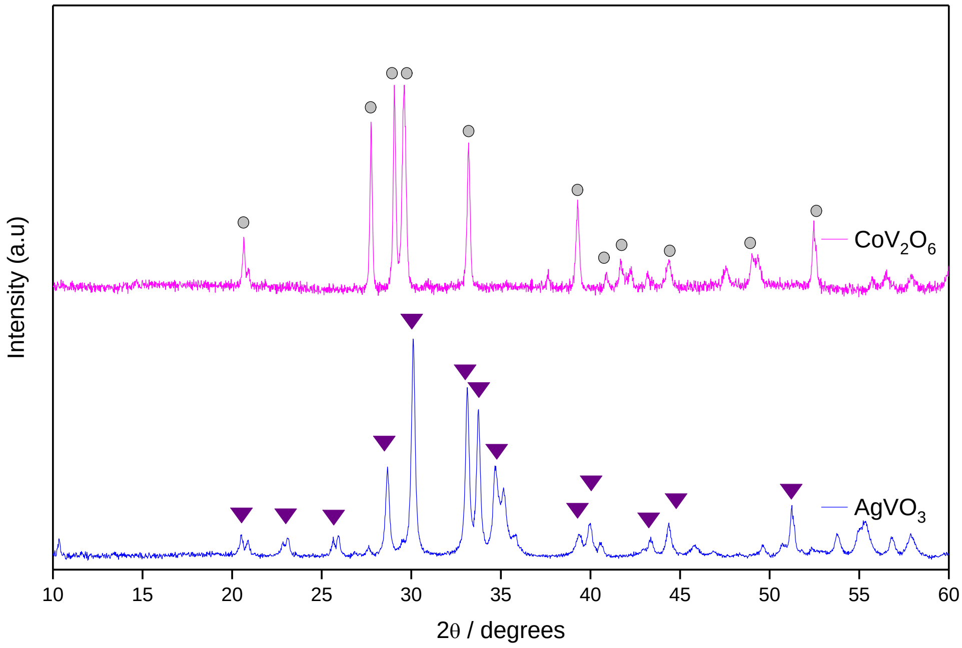

Figure 5-4 XRD pattern for $AgVO_3$ and CoV_2O_6.

5.3.5 MP-AES

Solid samples were dissolved in *aqua regia,* diluted and then analysed using MP-AES to give the elemental compositions given in Table 5-5. These compositions are used to calculate the amount of vanadium leached in subsequent reactions as they are more accurate than the chemical formula.

Table 5-5 Elemental compositions as calculated from MP-AES except for O which is calculated as the difference from the other given elements

Catalyst	**Elemental composition / wt. %**		
	Na/Cu/Ag/Co	V	O
NaVO1 (NaCl)	4.4	45.6	50
NaVO2 (Na_2SO_4)	4.0	44.3	51.7
$Cu_{0.25}V_2O_6$	6.5	55.2	38.3
$Cu_{0.33}V_2O_6$	13.5	44.7	41.8
$Cu_{0.5}V_2O_6$	22.2	42.1	35.1
$AgVO_3$	24.7	44.1	31.2
CoV_2O_6	20.6	39.1	40.3

5.3.6 XPS

The full XPS-derived surface atomic percentage for all vanadium bronze catalysts are shown in Table 5-6. The atomic concentrations for the NaVO catalysts attained from XPS analysis show that the material is closely related to the intended composition, indicating a successful integration of Na. The calculated atom percentages of $Cu_{0.25}V_2O_6$ display a similar atom composition to the targeted catalyst, indicating a successful incorporation of Cu into the structure. The increasing usage of Cu is also signified by the higher atom percentages received in the XPS studies, giving further proof that Cu was successfully integrated. There are differences in the intended composition of the catalyst and the calculated formulas which could be due to copper being situated in the bulk of the material. Strangely, for $AgVO_3$ and CoV_2O_6 a larger proportion of the alloying metal was detected, which may be caused by a greater density of the alloying metal at the surface of the material compared to the bulk.

Table 5-6 XPS data showing atom % of each elemental constituent of the bronzes, included is a chemical formula derived from the atom %

Catalyst	Atom %			Derived formula
	Na/Cu/Ag/Co	V	O	
NaVO1	9.4	27.5	63.1	NaV_3O_7
NaVO2	9.5	22.6	67.9	NaV_2O_7
$Cu_{0.25}V_2O_6$	3.1	28.8	68.1	CuV_9O_{22}
$Cu_{0.33}V_2O_6$	8.4	21.3	70.4	CuV_2O_6
$Cu_{0.5}V_2O_6$	9.6	21.6	68.8	CuV_2O_7
$AgVO_3$	20.8	14.8	64.4	$AgVO_4$
CoV_2O_6	17.9	10.2	71.8	Co_2VO_7

Curve fitting of the $V2p_{3/2}$ is shown in Figure 5-5. To quantify these regions, it was necessary to include the O1s signal in the extracted Shirley background. This is because this O1s region is close enough to the $V2p_{1/2}$ to have an influence on the background underneath the V2p signal. All binding energies have been given relative to the O1s(VO_x) core level, taken at 530.0 eV. Spectra were obtained using a Thermo Scientific K-Alpha XPS spectrometer equipped with a Al Kα source. The $V2p_{1/2}$ is broadened compared to the $V2p_{3/2}$ peak due to the Coster-Kronig effect,[30] which is described as a special form of the Auger process whereby the core hole in a shell with a certain principal quantum number is rapidly filled by an electron from a higher shell of the same principal quantum number.[31]

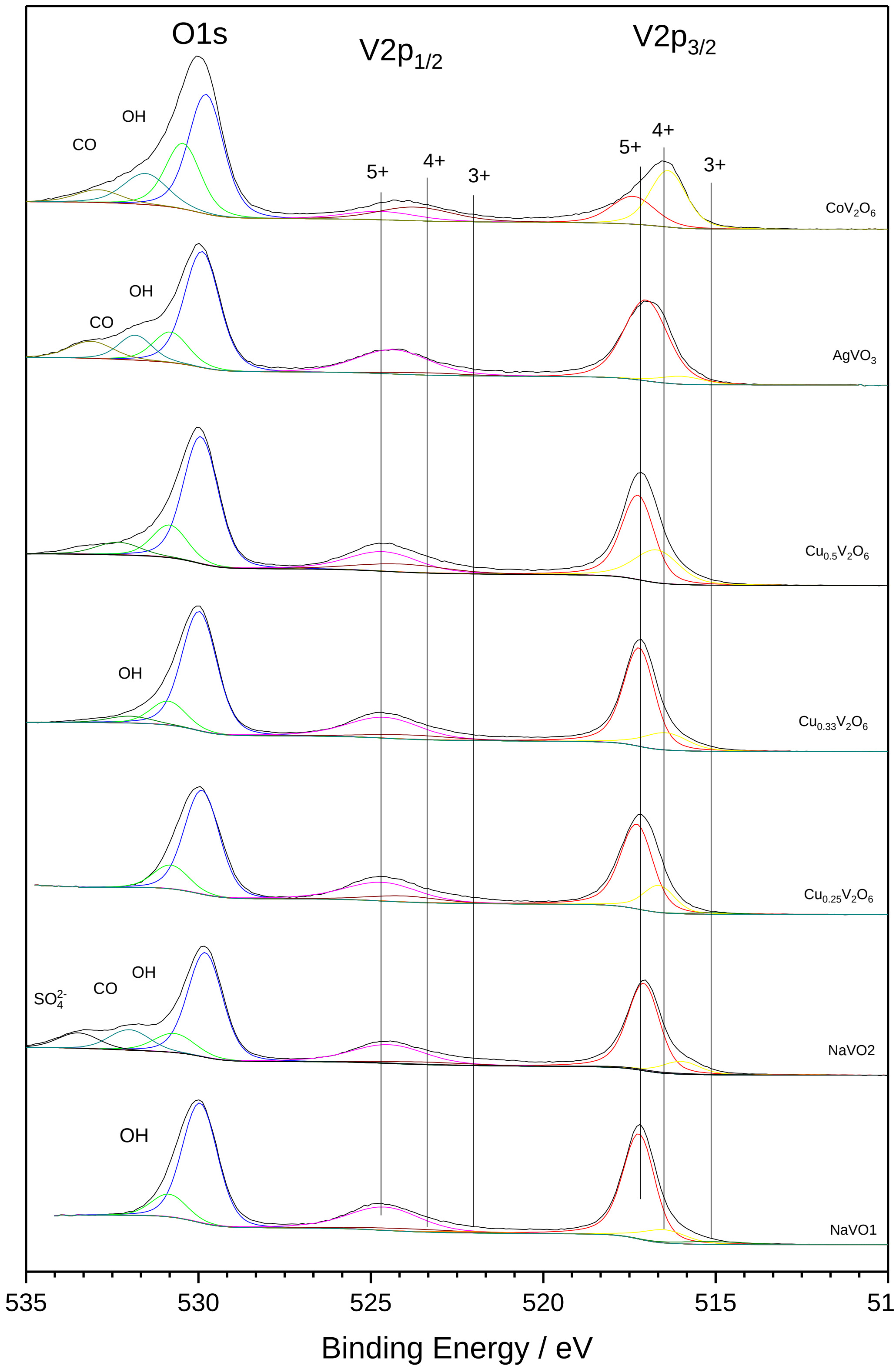

Figure 5-5 XPS spectra and fits for the vanadium bronzes. The binding energies are referenced to the O1s (VO_x) signal taken at 530.0 eV

Table 5-7 shows the spectral fitting parameters for the V2p species. The splitting between the V2p$_{1/2}$ and V2p$_{3/2}$ are typically reported at 7.3 eV for vanadium oxides and mixed metal vanadium oxides. FWHM values are also typically reported in the range of 1.0-1.5 eV for V(V) V2p$_{3/2}$ and 2.2-3.2 eV for V(IV) V2p$_{3/2}$.[32,33] The values reported for these bronzes are within this stated range giving an accurate fit of the expected contributions of each of these components. As expected, the majority of catalysts show significant contributions from V(V) species at 517.2-517.0 eV.[11,13,34] However, the $Cu_{0.25}V_2O_6$ shows the broadening of the V2p$_{3/2}$ peak at 516.4 eV, this broadening is due to the presence of an increased amount of V(IV) which may be due to photoreduction of the surface of these bronzes caused by the x-ray irradiation and could possibly result from a higher reducibility of the $Cu_{0.33}V_2O_6$ catalyst leading to the difference in spectra. This V(IV) peak is generally observed at around 516.2 eV so an increased presence of V(IV) is associated with a shift to lower binding energies.[33,35] Interestingly, with CoV_2O_6 a favouring of V(IV) species was observed as evidenced by a small shift in the V2p$_{3/2}$ to 516.5 eV. This was supplemented by a significant difference in the peak area ratios calculated from the peak components, this ratio was 1.6 in favour of V(IV). This is in comparison to values of around 0.2 for the other catalysts, showing a large change in the oxidation state of V depending on the alloying metal.

Table 5-7 Spectral fitting parameters for V2p species. Binding energy values are corrected to O1s (VO_x) set to 530.0 eV

Catalyst	V2p$_{3/2}$ (eV)	V2p$_{1/2}$ - V2p$_{3/2}$ splitting (eV)	FWHM (eV), V (V)		FWHM (eV), V (IV)		Peak area ratio, V (IV) / V(V)
			V 2p$_{1/2}$	V 2p$_{3/2}$	V 2p$_{1/2}$	V 2p$_{3/2}$	
NaVO1	517.2	7.3	2.5	1.1	2.4	1.1	0.30
NaVO2	517.1	7.4	2.5	1.1	2.5	1.4	0.17
$Cu_{0.25}V_2O_6$	517.2	7.3	2.4	1.1	3.7	1.5	0.17
$Cu_{0.33}V_2O_6$	517.2	7.5	2.5	1.1	3.2	1.5	0.20
$Cu_{0.5}V_2O_6$	517.2	7.4	2.3	1.1	2.9	1.5	0.50
$AgVO_3$	517.0	7.4	2.5	1.5	2.6	1.5	0.10
CoV_2O_6	516.5	7.6	2.5	1.5	2.7	1.2	1.6

5.3.7 Time on-line data

A time online study was conducted to further understand the source of the unknowns in these reactions. These reactions were run in parallel with V_2O_5 and Pt/C used as catalysts, and the results are given in Figure 5-6. Selectivity to AA is relatively high even after 1 h of reaction time where a selectivity of 67 % was achieved. The selectivity to AA increases gradually to 80 % over 3 h and maintains this level throughout the reaction, albeit with small fluctuations. These fluctuations may be due to the reactions being run in parallel so there is an error associated with each set of data as no further oxidation of AA would be expected. The presence of 2-HCO is low during the reaction with an initial concentration of 7.0 % after 1 h which is the highest selectivity that it reaches in the reaction. After 6 h, the concentration of 2-HCO becomes undetectable by the RID on the HPLC. The low concentrations of 2-HCO present in the reaction demonstrates that the second part of this oxidation to adipic acid occurs relatively quickly when vanadium is present.

A noticeable increase in conversion is observed after 16 h, where there is 68 % conversion and a selectivity to adipic acid of 80 %, the unknowns then also decrease in selectivity to 13 %. From conversion continues to increase and reaches the highest value of 87 % between 18 and 22h, with selectivity to adipic acid of 84 %. The unknowns also appear to decrease with longer reaction times with the lowest selectivity of 10 %. Although the unknowns are produced in low quantities, it is most likely that they consist of oxygenates with C4 and C5 carbon chains, formed in oxidations of 2-HCO, as described by Obara *et al.*[4]

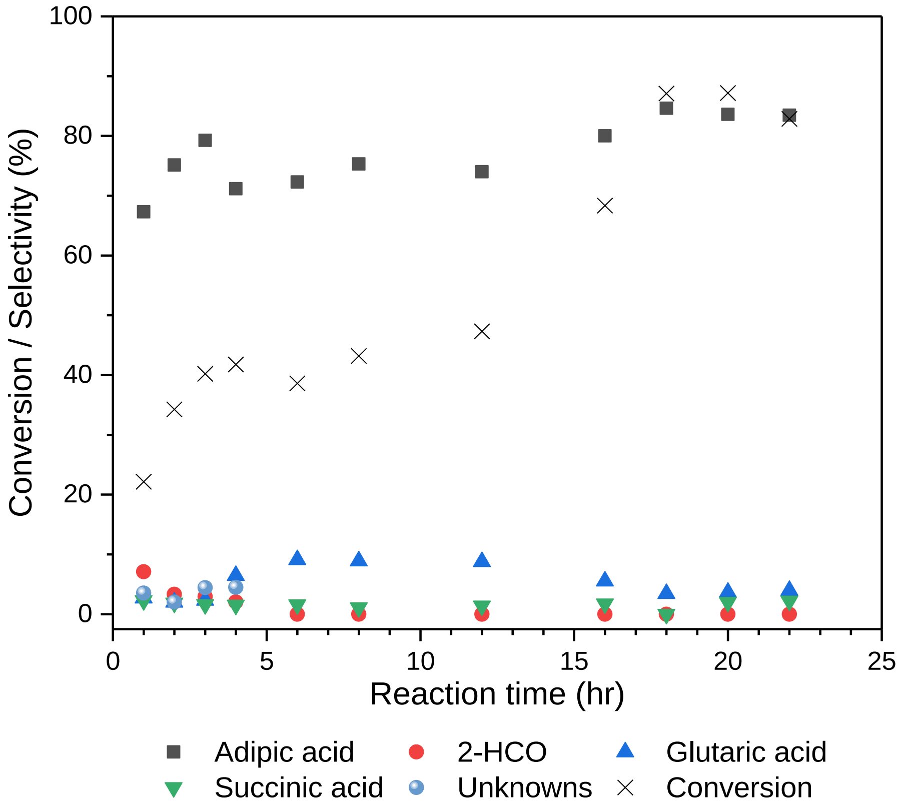

Figure 5-6 Time-online of oxidation of cyclohexanediol ranging from 1 h to 22 h. Reaction conditions: 80 °C, 3 bar O_2, 5 ml 10000 ppm cyclohexanediol in water, 10 mg Pt/C, 2 mg V_2O_5

5.3.8 Reactivity of side products

To determine whether any of these unknowns were the result of the further oxidation of the products in this reaction, additional experiments were carried out using AA and GA as the starting materials. The results of these reactions can be seen in Figure 5-7. The further oxidation of these substrates resulted in the formation of some unknown compounds of similar retention times as those in the oxidation reactions of cyclohexanediol. However, the conversion of these substrates is very low with 0.9 % and 0.7 % conversion for adipic acid and glutaric acid respectively. This low conversion makes these compounds difficult to identify as the amount produced in the reaction is small. These substrates are seemingly quite stable against further oxidation, so it is unlikely that the unknowns produced in the reaction are from this source. As mentioned previously, it is more likely the unknowns are side products, formed in the oxidation of 2-HCO.

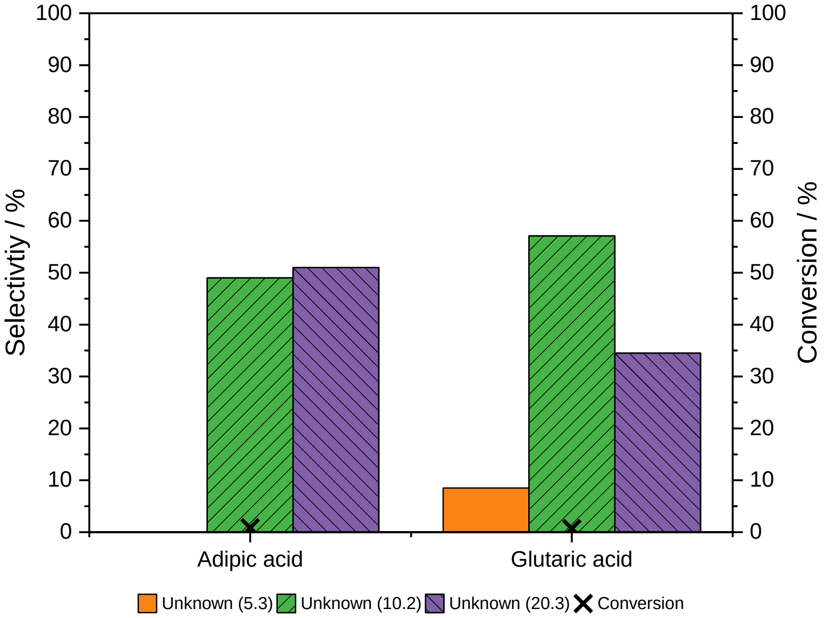

Figure 5-7 Reaction data for oxidation of adipic acid and glutaric acid to determine if their further oxidation results in unknowns observed. **Reaction conditions:** 80 °C, 3 bar O_2 4000 ppm substrate in water (5 mL), 4 hr, 10 mg 5% Pt/C, 2 mg V_2O_5.

5.3.9 Effect of homogeneous vanadium

5.3.9.1 Reaction filtrate

To determine the impact of leached species from the vanadium bronzes, the filtrate from a wash of NaVO2 and $Cu_{0.25}V_2O_6$ in water was reinserted into a reaction mixture of 10000 ppm CHD to determine any reactivity caused by these vanadium species. The result of these reactions is displayed in Table 5-8. Entry 1 shows that conversion of CHD is still achieved with the filtrate of a NaVO2 catalyst, alongside Pt/C, and is enough to cause further selectivity to AA with 67 % recorded and 36 % conversion. A similar outcome was obtained by using the filtrate of the $Cu_{0.25}V_2O_6$ bronze which, showed a selectivity of 64 % to adipic acid and a conversion of 33 %. The concentration of vanadium present in the reactions was 142 and 152 ppm for the NaVO2 and $Cu_{0.25}V_2O_6$ reactions, respectively.

Table 5-8 Reaction data for the oxidation of cyclohexanediol using the reaction filtrate from the NaVO2 and $Cu_{0.25}V_2O_6$ reactions. **Reaction conditions:** 80 °C, 3 bar O_2 10000 ppm cyclohexanediol in water (5 mL), 4 hr, 10 mg 5% Pt/C, 1 ml reaction filtrate.

	Catalyst	**Conv. / %**	**Selec. / %**					**[V] / ppm**	**M. B / %**
			AA	2-HCO	GA	SA	Unknowns		
1	Pt/C +NaVO2 filtrate	36	67	9.0	0.0	0. 0	0.0	142	91
2	Pt/C +$Cu_{0.25}V_2O_6$ filtrate	33	64	8.0	5.0	3.0	0.0	152	93

5.3.9.2 Reactivity of low concentrations of vanadium

To further understand the role of homogeneous vanadium species in this process, a series of reactions at low concentrations of vanadium were designed. Pt/C was omitted from these reactions because of the impact that it has on conversion. This effect can be more clearly seen in Figure 5-8a where data from the time on-line experiments and previous reactions with vanadium bronzes and Pt/C were combined to determine if there was a relationship between conversion and selectivity. Where conversions were similar, the data was collated in triplicate to give error bars, which were calculated using standard error. The error associated with selectivity is noticeably larger than conversion, however the error associated with both variables is more prominent at low conversions and selectivities. The statistically defined linear fit also clarifies a small relationship between conversion and selectivity with a gradient of 0.266. Since there is a relationship between the conversion and selectivity it was necessary to omit Pt/C from the reaction and use 2-HCO as substrate.

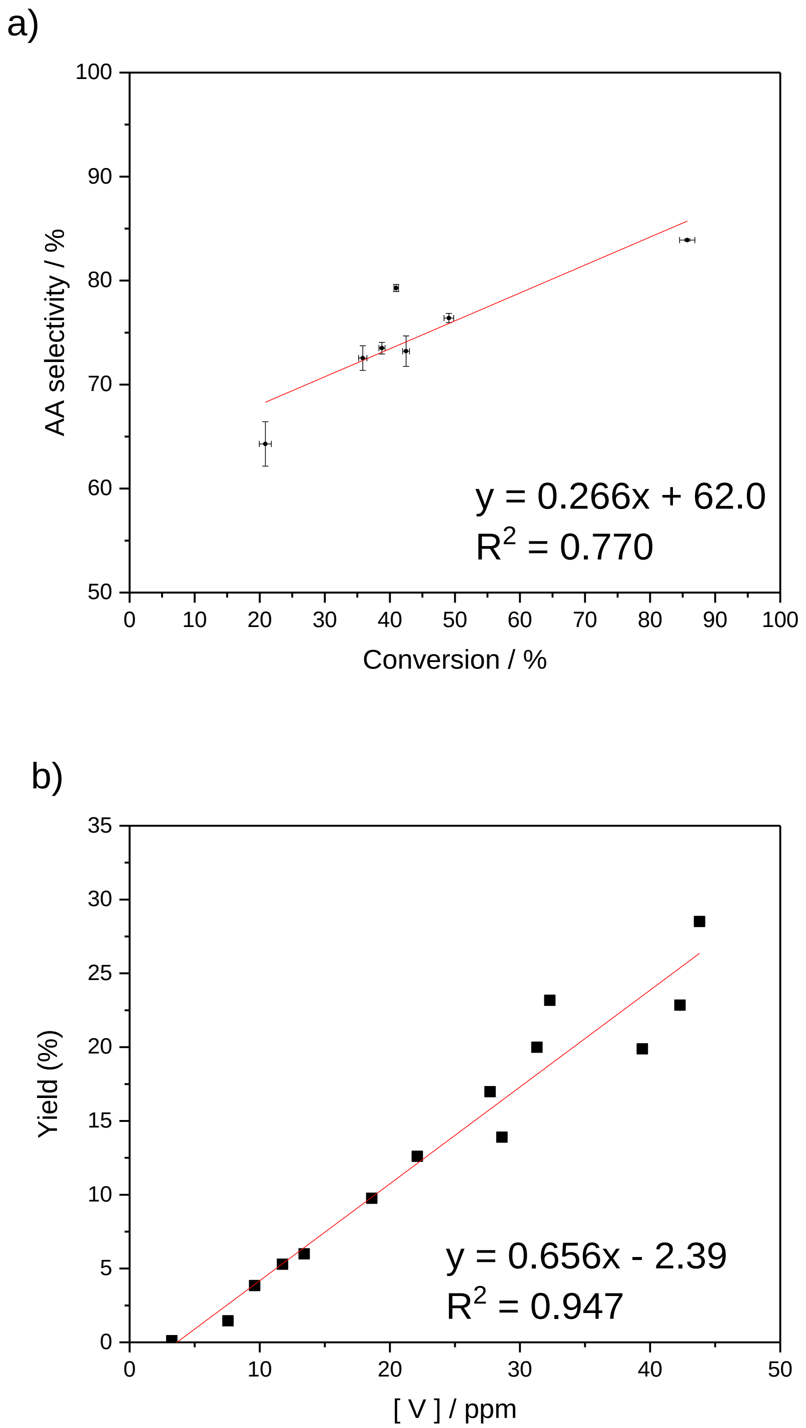

Figure 5-8 a) Effect of conversion on selectivity taken over reactions from 2 h to 22 h. **Reaction conditions:** 80 °C, 3 bar O_2, 5 ml 10000 ppm cyclohexanediol in water, 10 mg Pt/C, 2 mg vanadium catalyst b) Oxidation of 2-HCO to adipic acid using solutions of vanadium between 0 and 45 ppm. **Reaction conditions:** 80 °C, 3 bar O_2, 4 h, 4000 ppm 2-hydroxycyclohexanone in water (5 ml), vanadium added as a stock solution of 200 ppm V_2O_5 in water.

The effect of homogenous vanadium was analysed with more scrutiny in Figure 5-8b. In this study a solution of 4000 ppm 2-HCO in water was used as the starting reaction solution. The vanadium catalyst was added from a stock solution of vanadium consisting of a concentration of 200 ppm and passed through a 45 µm filter. This was inserted into the reaction to achieve concentrations in the range of 0 to 45 ppm. The concentrations of post-reaction solutions were then analysed using MP-AES. These solutions only contained homogeneous vanadium and therefore any activity observed would be a result of these species. Figure 5-8b demonstrates that at these low concentrations of vanadium, there is a linear trend between vanadium in solution and yield to AA. Interestingly, this set of reactions also demonstrate that only a small amount of vanadium is required to provoke a reaction to adipic acid. This effect was observed with only 7.6 ppm being sufficient, achieving a yield of 2.0 %. Since only a small amount of vanadium is necessary to encourage a reaction, it would suggest that even minor leaching from the vanadium materials would result in catalytic activity. Despite this linear relationship and the low concentrations required for a reaction, it can be determined that the vanadium species are acting catalytically and not as stoichiometric oxidants.

Table 5-9 Vanadium stoichiometry ratio for the oxidation of 2-hydroxycylohexanone to adipic acid **Reaction conditions:** 80 °C, 3 bar O_2, 4 h, 4000 ppm 2-hydroxycyclohexanone in water (5 ml), vanadium added as a stock solution of 200 ppm V_2O_5

Vanadium concentration / ppm	**Moles of vanadium / mmol L^{-1}**	**Concentration of product (AA) / ppm**	**Moles of Product (AA) / mmol L^{-1}**	**Stoichiometry ratio (V:AA)**
3.3	0.064	5.39	0.037	1.731
7.6	0.148	68.3	0.468	0.317
9.6	0.189	177.5	1.215	0.155
11.8	0.231	242.4	1.659	0.139
13.4	0.263	271.7	1.859	0.142
18.6	0.366	431.0	2.949	0.124
22.1	0.434	546.5	3.739	0.116
28.6	0.562	592.2	4.052	0.139
27.7	0.544	710.8	4.864	0.112
31.3	0.614	822.8	5.630	0.109
32.3	0.634	937.8	6.417	0.099
39.4	0.773	778.5	5.327	0.145
42.3	0.830	880.4	6.024	0.138
43.8	0.860	1081.4	7.400	0.116

This conclusion can be seen more clearly in Table 5-9, with a stoichiometry ratio as low as *ca.* 0.1 in the majority of reactions. This set of reactions only reached a maximum concentration of 43.8 ppm, despite seeing a concentration of 168 ppm previously when using V_2O_5 as catalyst in the cyclohexanediol oxidations. The high concentrations observed above 50 ppm seemed to be only attainable under certain reaction conditions, which were not present in the study of 4000 ppm 2-HCO.

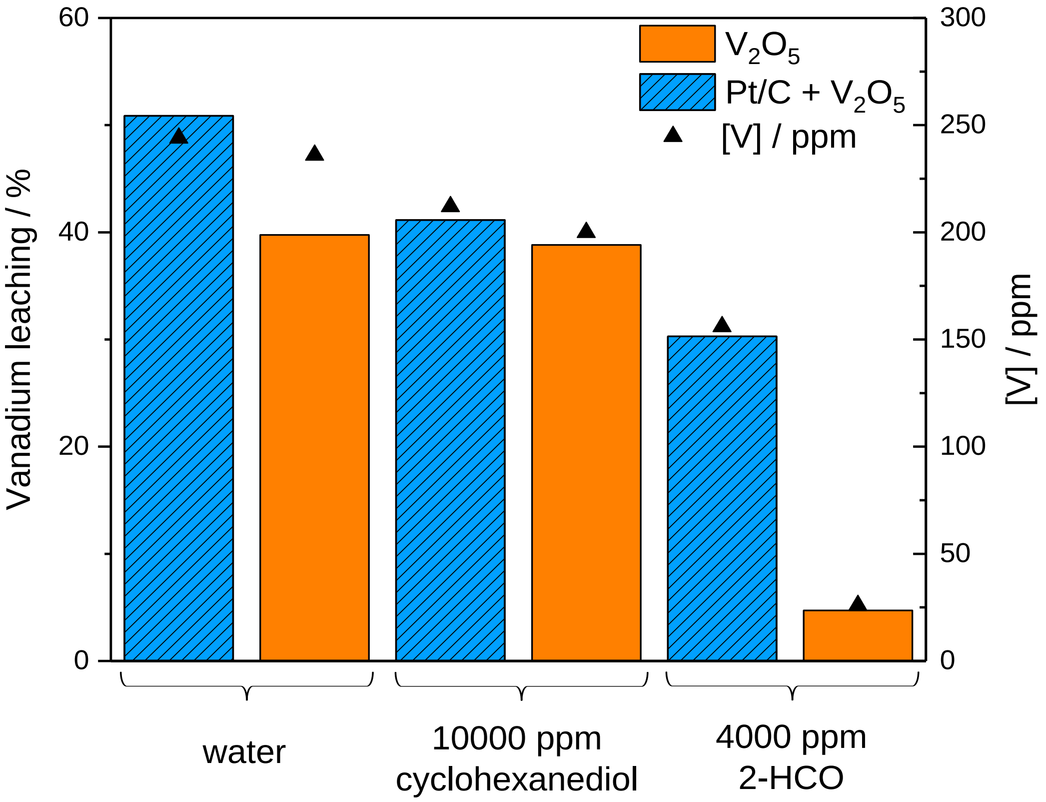

Figure 5-9 Leaching of vanadium as induced by differing sets of reaction conditions. **Reaction conditions:** 80 °C, 3 bar O_2, 4 h, 5 ml reaction solution (as specified), 10 mg Pt/C (when required), 5 mg V_2O_5 (when required)

Figure 5-9 shows a study undertaken to investigate whether the observation of a reduced amount of leaching is dependent on the reaction mixture. It can be seen that leaching is consistently higher when Pt/C is involved (blue columns) compared to the solely V_2O_5 counterparts (orange columns). This effect is true for water, 10 000 ppm cyclohexanediol and 4000 ppm 2-HCO. This effect that Pt/C has on the leaching may have been due to the Pt activating the oxygen causing it to destabilise the vanadium structure and promote leaching of the V_2O_5 more readily. The 4000 ppm 2-HCO solutions also show the lowest amount of leaching which may be due to a difference in polarity of the reaction matrix. In this solution, where only V_2O_5 was present, there was a low leaching of 4.7 % of the total vanadium. This is compared to 38.8 % under the same conditions but with 10000 ppm cyclohexanediol. Again, the main reason for this could be the polarity of the different substrates affecting the solubility of vanadium.

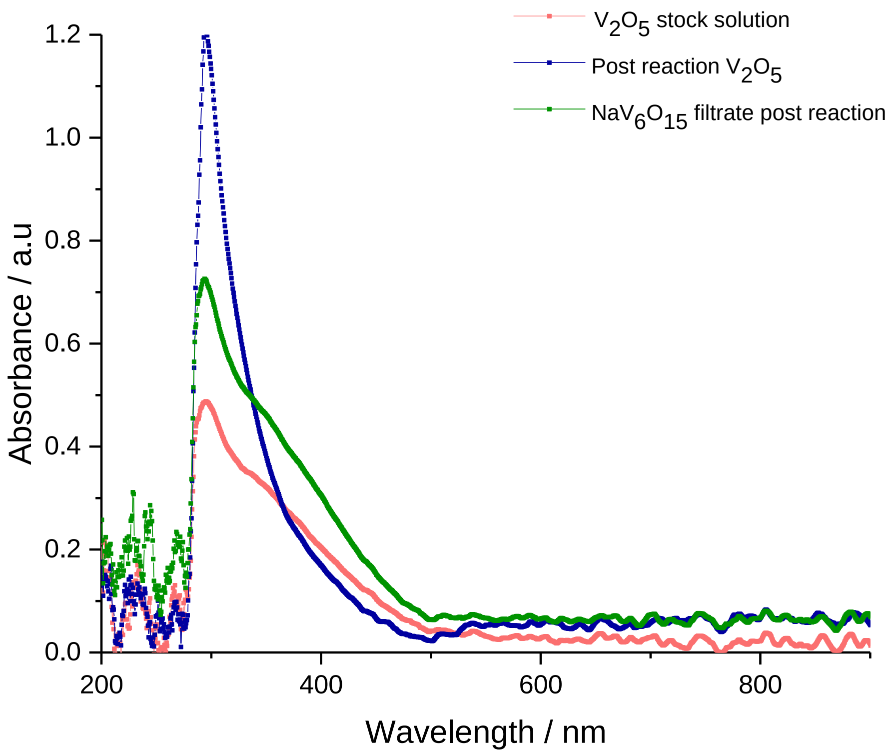

Figure 5-10 UV-vis spectra of reaction filtrate from bronze reactions showing presence of only vanadium +5

Since the selectivity to AA was largely influenced by homogeneous vanadium species, investigations to determine the speciation were undertaken. The analytical techniques taken to ascertain the speciation were UV-vis and ^{51}V NMR. Firstly, the UV-vis is displayed in Figure 5-10, and shows the reaction filtrate from NaVO2 (green), the V_2O_5 reaction mixture (blue) as well as the V_2O_5 stock solution (pink) used for the vanadium homogeneous reactions (Table 5-9). The absorbance in the UV-vis spectra shows a strong absorbance from 300 to 390 nm, which only corresponds to a V (V) species, with no overlapping of other oxidation states within this region.[36] The absence of either V(III) or V(IV) suggests the catalytic V(V) must have a closed catalytic cycle. The analysis of the homogeneous V by UV-vis is accompanied by ^{51}V NMR studies, which are shown in Figure 5-11. These spectra can be compared to data published by Anderson *et al.*[37] where these peaks can be identified as a vanadium decavanadate. To confirm the spectrum of a vanadium decavanadate, a sample was prepared from an acidified solution of sodium orthovanadate, which would form the decavanadate.[38–40] This vanadium compound has 3 chemical environments, as signified by the spectra in Figure 5-11a. These 3 chemical shifts can be observed at -424 ppm, -508 ppm, -526 ppm for Vc, Vb and Va respectively. The location of these vanadium environments on the compound are illustrated in Figure 5-11c. An additional signal, which can be observed at -549 ppm, can be attributed to the monovanadate species.[39] The two spectra show an almost perfect alignment, with the signal for Va differing slightly between each spectrum. There is a difference of 3 ppm in these spectra with a small shift from -526 ppm to -529 ppm for the reaction filtrate and the acidified sodium orthovanadate V_{10} species, respectively. A shift of this size could be consistent with a binding of reaction products to Va, however if there was a binding to the Vb as well then a merging of these peaks would be expected.[41] The other difference between the spectra is that there appears to be a stronger monovanadate peak in the ^{51}V NMR spectrum of V_{10}, which may be a consequence of the lower pH of this sample. The pH of the V_{10} sample is 2.0 compared to the reaction sample which was 3.8.

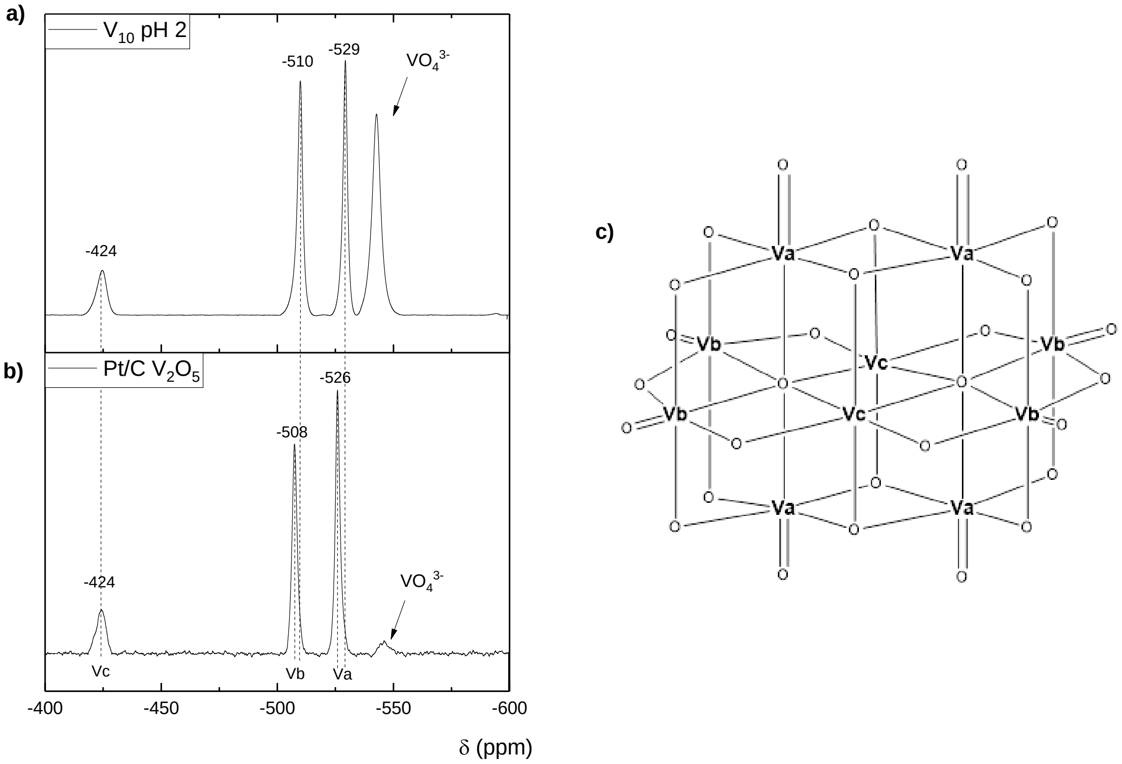

Figure 5-11 ^{51}V NMR of a) vanadium decavandate which is present at low pH with presence of monovanadate also b) Reaction sample of Pt/C and V_2O_5 with 4000 ppm 2-HCO solution c) V_{10} compound with labelled vanadium sites corresponding to the shifts shown in the NMR spectra

5.3.10 Alternative catalysts

5.3.10.1 Tungsten catalysts

As shown in the previous results, even low levels of vanadium leaching can have significant effects on AA selectivity. For this reason, other catalysts were investigated for their viability for the cleavage of CHD. Tungsten containing compounds have shown potential in cyclohexene epoxidations, as shown by work in the Hutchings group and by Ovoschnikov *et al*. as stated in Chapter 3.[1,42] Use of tungsten containing polyoxometalates have also shown high selectivity for adipic acid when using hydrogen peroxide.[43–46] The use of tungsten is most renowned in work by Sato *et al*. using Na_2WO_4 to produce AA in high yields using H_2O_2.[47] Due to the potential of tungsten systems in cyclohexene epoxidations and also AA synthesis, WCl_6, WO_3 and Au / $Cs_3P_3W_{12}O_{40}$ were used as catalysts in the oxidation of cyclohexanediol as shown in Table 5-10.

Table 5-10 Reaction data for the oxidation of cyclohexanediol. **Reaction conditions:** 80 °C, 3 bar O_2, 4 h, 10 000 ppm cyclohexanediol in water (5 mL), 5 mg 5 % Pt/C, 2 mg tungsten catalyst

	Catalyst	**Conv. / %**	**Selectivity / %**					**M. B / %**
			AA	2-HCO	GA	SA	Unknowns	
1	Au / $Cs_3P_3W_{12}O_{40}$	2.0	0.0	0.0	0.0	0.0	0.0	98
2	WO_3	0.1	0.0	0.0	0.0	0.0	0.0	100
3	WO_3 + Pt/C	33	3.0	73	1.0	2.0	0.3	95
4	WCl_6 + Pt/C	32	3.0	63	2.0	5.0	3.0	93

It is evident that these tungsten compounds are not active when used as the sole catalyst. This is illustrated by entries 1 and 2 where no products were observed after 4 h of reaction. Au / $Cs_3PW_{12}O_{40}$ had shown potential as an oxidation catalyst for cyclohexene and the presence of gold on the surface of the catalyst may increase any capability to activate oxygen and generate activity with these catalysts. However, no activity is observed for this polyoxometalate catalyst or for WO_3. As with the vanadium catalysts, Pt/C is required to convert CHD into 2-HCO before conversion to AA is detected, as can be seen in entries 3 and 4. A WO_3 catalyst combined with Pt/C as reported in entry 3 gives 3.0 % selectivity to adipic acid demonstrating that tungsten has potential for this reaction. However, selectivity to AA is also accompanied by the presence of unwanted side products such as GA and SA. The presence of these side products in their quantities relative to adipic acid call into question its viability as a catalyst. WCl_6 shows similar selectivities to WO_3 when combined with Pt/C, after 4 h of reaction. A selectivity of 3.0 % for AA alongside 2.0 % for GA and 5.0 % SA is exhibited. Longer reaction times may be needed to determine if selectivity to AA would increase given a longer time. These results give evidence to suggest that tungsten could be a viable element to start testing a wider array of catalysts for this reaction, however the heterogenous nature of WO_3 in entry 3 would need to be analysed by MP-AES as leaching could also result in the activity observed.

5.3.10.2 Silver catalysts

Silver has demonstrated potential in homogeneous oxidations, notably in work by Zhou *et al*. where silver carbonate exhibited high selectivity for the cleavage of 1,2-diols under mild conditions.[48] More specifically, terminal diols have demonstrated higher activity for these reactions , albeit with the requirement of 3 equivalents of sodium methoxide. This has been demonstrated using AgOTf and 3 equivalents of base to cleave a terminal diol into the corresponding carboxylic acids, achieving 88 % yield under 1 atm O_2 and a 12 h reaction time. Ag_2CO_3 was also used in these studies for a terminal diol using similar conditions as described previously, with Ag_2CO_3 51 % yield of the corresponding carboxylic acid being observed. Due to the suitability of Ag catalysts in oxidative cleavages of vicinal diols, Ag_2CO_3 was analysed as a catalyst for the oxidation of cyclohexanediol as shown in Table 5-11.

Table 5-11 Reaction data for the oxidation of cyclohexanediol. **Reaction conditions:** 80 °C, 3 bar O_2, 4 h, 10 000 ppm cyclohexanediol in water (5 mL), 10 mg 5 % Pt/C, 2 mg silver catalyst. ***Reaction conditions:** 80 °C, 3 bar O2, 4 h, 4000 ppm 2-hydroxycyclohexanone

	Catalyst	**Conv. / %**	**Selectivity / %**					**M. B / %**
			AA	2-HCO	GA	SA	Unknowns	
1	Ag_2CO_3	3.0	61	11	0.0	0.0	0.0	99
2	Ag_2CO_3 + Pt/C	12	4.0	63	0.0	0.0	0.0	96
3	Ag/AC	2.0	0.0	0.0	0.0	0.0	0.0	98
4	Ag/AC*	8.0	0.0	-	0.0	7.0	69	98

Much like with the tungsten catalysts there is minimal conversion when Pt/C is not involved in the reaction. However, when Ag_2CO_3 is the sole catalyst, a selectivity to adipic acid of 61 % is observed albeit at a low conversion of 3.0 % which can add to the error of this result. There were also no side products observed with this reaction. When Ag_2CO_3 is used in tandem with Pt/C conversion increases to 12 % with the selectivity to adipic acid overwhelmed by the presence of 2-HCO. This experiment showed that Ag was a capable catalyst for adipic acid synthesis but Ag_2CO_3 was a homogeneous catalyst so an alternative of Ag on activated carbon was prepared. The silver was deposited onto the carbon using an *aqua regia* impregnation. This preparation method has been used previously in the Hutchings' group for preparing Au catalysts for acetylene hydrochlorination.[49] However, in these reactions the Ag/AC catalysts exhibit minimal activity. Even with the use of 2-HCO as the starting material, no conversion to adipic acid is observed with mainly unknown compounds observed.

5.4 Conclusions

In this investigation a range of vanadium bronzes were prepared and the effect of the alloying metal was studied. The alloying metals studied were Na, Cu, Ag and Co due to a reported success in aqueous phase applications. Their structures and compositions were then confirmed by XRD, XPS and MP-AES. These bronzes were then assessed for their activity in the oxidation of CHD to adipic acid, showing promising activity which was comparable to the work by Obara *et al.*[4] The highest conversion achieved was with NaVO1 generating a selectivity of 70 % and a conversion of 41 %. However, the promising activity was accompanied by high levels of leaching, particularly with the NaVO catalysts where 36.8 % of total V was found to leach into solution.

To alleviate this leaching other metals such as Cu or Ag, were proven to significantly mitigate this leaching to as low as 5.0 %. Dissapointingly, the low levels of leaching observed with $Cu_{0.33}V_2O_6$ and $AgVO_3$ were accompanied by a lower activity of 28 % and 18 % respectively. In subsequent studies, the effect of the homogenous V was analysed, exhibiting a significant impact on the reaction. Even low levels of homogenous V observed with $Cu_{0.33}V_2O_6$ and $AgVO_3$, had an ability to enable the conversion of 2-HCO to adipic acid. Therefore, only a catalyst which displayed no leaching would be an acceptable heterogeneous catalyst but further attempts to create a stable V catalyst, such as, alloying with Co or the use of CN supports did not improve the stability.

Studies into the effect of homogeneous vanadium demonstrated that even trace levels of homogeneous vanadium have a great influence on the reaction with 7.6 ppm V resulting in the conversion of 2-HCO to AA. The vanadium in solution was revealed to be in the +5 oxidation state and subsequent ^{51}V NMR studies determined the species present in the reaction to be a vanadium decavanadate with was unbound to other reaction products or metals.

The possibility of omitting V from the reaction started with investigations into catalysts containing silver or tungsten. These catalysts showed promising but limited activity, particularly with Ag_2CO_3 and WO_3. Furthermore, these catalysts also required the addition of Pt/C as a co-catalyst to form 2-HCO, before any significant yield to adipic acid was observed. This activity was still limited to 1.0 % with a WO_3 + Pt/C system. Attempts to heterogenise the Ag system through its supporting onto activated carbon were unsuccessful in generating an active catalyst. However, further optimisation of W and Ag catalysts may result in a heterogeneous alternative for this reaction.

5.5 Future work

Since the vanadium catalysts did not show adequate stability in aqueous solutions, a further in-depth study into the effect that alloying metals have could be instigated to determine why metals, such as, Cu and Ag have a greater influence on stability. Further characterisation, such as, UV-vis would be a useful technique to analyse the effect that different metals can have on the environment of vanadium centres. In addition to this, FTIR and Raman spectroscopy would be useful to further understand the structural units that compose the bronzes.[50–52]

A focus should also be place on studying metals other than vanadium which are capable of vicinal diol cleavage. The studies into tungsten and silver as alternative catalysts showed they can both have some activity in this reaction, albeit with limited activity and some selectivity to unwanted side products. However, Ag_2CO_3 was soluble and the leaching of WO_3 was not measured so the contributions of both materials could be viewed as homogeneous. In these tests, Pt is required to generate a high concentration of 2-HCO, therefore, in any future catalyst Pt nanoparticles would be immobilised on the same support if a 1-catalyst system is desired.

PdFe nanoparticles have been explored for the vicinal diol cleavage of ethylene glycol displaying good activity and tunable selectivity depending on Fe content. Although this activity was demonstrated with a linear chain, it could be transferable to a cyclic system.[53] In another study, the aerobic oxidative cleavage of 1,2-diols was also achieved by atomically dispersed Co supported on N-doped carbon. The substrates tested in this study consisted mainly of internal diols rather than cyclic diols but the substrate scope of this catalyst could possibly be extended for adipic acid synthesis. In addition, the catalyst required a HF treatment which may make it impractical to prepare.[54] A similar approach could prove fruitful for a Ag catalyst, with an atomically dispersed Ag/CN prepared in work by Chen *et* al.[55] This preparation could be more successful than the *aqua regia* impregnation utilisied in this investigation for Ag/AC.

Further investigations into W catalysts may give some insight into any other active forms of W. It may also be necessary to support the tungsten alongside platinum since neither tungsten catalyst that was tested on its own showed much activity. If a tungsten catalyst is active in the solid state then a tungsten bronze could also be prepared and Pt nanoparticles deposited onto it, removing the requirement to have two catalysts in this system.

5.6 References

1 D. S. Ovoshchnikov, B. G. Donoeva, B. E. Williamson and V. B. Golovko, *Catal. Sci. Technol.*, 2014, **4**, 752.

2 P. Blach, Z.Böstrom, S. Franceschi-Messant, A. Lattes, E. Perez and I. Rico-Lattes, *Tetrahedron*, 2010, **66**, 7124–7128.

3 M. Vennat, P. Herson, J.-M. Brégeault and G. B. Shul, *Vanadium-Catalysed Aerobic Cleavage of CC Bonds in Substituted Cyclohexanones To Afford Carboxylic Acids: Two Model Complexes with Tetrahedral Geometry around Vanadium(V)*, .

4 N. Obara, S. Hirasawa, M. Tamura and Y. Nakagawa, *ChemCatChem*, 2016, **8**, 1732–1738.

5 Y.-K. Masumoto, R. Hamada, K. Yokota, S. Nishiyama and S. Tsuruya, *Liquid-phase oxidation of benzene to phenol by vanadium catalysts in aqueous solvent with high acetic acid concentration*, 2002, vol. 184.

6 M. Ziolek, in *Catalysis Today*, 2004, vol. 90, pp. 145–150.

7 M. D. Soriano, A. Vidal-Moya, E. Rodríguez-Castellón, F. V. Melo, M. T. Blasco and J. M. L. Nieto, *Catal. Today*, 2016, **259**, 237–244.

8 H. T. Evans and J. M. Hughes, *Crystal chemistry of the natural vanadium bronzes*, 1990, vol. 75.

9 L. Ruiz-Rodríguez, T. Blasco, E. Rodríguez-Castellón and J. M. L. Nieto, *Catal. Today*, 2018, **333**, 237–244.

10 J. Zhang, N. Wang, C. Zhao, J. Li and T. Zhang, *Cailiao Yanjiu Xuebao/Chinese J. Mater. Res.*, 2018, **32**, 555–560.

11 C. J. Patridge, C. Jaye, H. Zhang, A. C. Marschilok, D. A. Fischer, E. S. Takeuchi and S. Banerjee, *Inorg. Chem.*, 2009, **48**, 3145–3152.

12 H. Liu, Y. Wang, L. Li, K. Wang, E. Hosono and H. Zhou, *J. Mater. Chem.*, 2009, **19**, 7885–7891.

13 V. Bondarenka, Z. Martunas, S. Kaciulis and L. Pandolfi, *J. Electron Spectros. Relat. Phenomena*, 2003, **131**–**132**, 99–103.

14 C. Xia, J. Guo, P. Li, X. Zhang and H. N. Alshareef, *Angew. Chemie*, 2018, **130**, 4007–4012.

15 R. Konta, H. Kato, H. Kobayashi and A. Kudo, *Phys. Chem. Chem. Phys.*, 2003, **5**, 3061–3065.

16 S. K. Ghosh, R. Saha and B. Saha, *Res. Chem. Intermed.*, 2015, **41**, 4873–4897.

17 W. Guo, W. D. Chemelewski, O. Mabayoje, P. Xiao, Y. Zhang and C. B. Mullins, *J. Phys. Chem. C*, 2015, **119**, 27220–27227.

18 Z. Xie, J. Lai, X. Zhu and Y. Wang, *ACS Appl. Energy Mater.*, 2018, **1**, 6401–6408.

19 G. T. Zhou, X. Wang and J. C. Yu, *Cryst. Growth Des.*, 2005, **5**, 969–974.

20 P. Hu, T. Zhu, X. Wang, X. Wei, M. Yan, J. Li, W. Luo, W. Yang, W. Zhang, L. Zhou, Z. Zhou and L. Mai, *Nano Lett.*, 2018, **18**, 1758–1763.

21 L. I. Ivleva, K. V Zakutailov, E. E. Dunaeva and V. V Osiko, *Dokl. Phys. Chem.*, 2013, **451**, 176–179.

22 Y. Xu, X. Han, L. Zheng, W. Yan and Y. Xie, *J. Mater. Chem.*, 2011, **21**, 14466–14472.

23 L. Mai, L. Xu, Q. Gao, C. Han, B. Hu and Y. Pi, *Nano Lett.*, 2010, **10**, 2604–2608.

24 M. Xing, L. Bin Kong, M. C. Liu, L. Y. Liu, L. Kang and Y. C. Luo, *J. Mater. Chem. A*, 2014, **2**, 18435–18443.

25 L. Huang, X. Zhao, L. Zhang, L. Shi, J. Zhang and D. Zhang, *Nanoscale*, 2015, **7**, 2743–2749.

26 G. Ding, W. Wang, T. Jiang, B. Han, H. Fan and G. Yang, *ChemCatChem*, 2013, **5**, 192–200.

27 A. N. Kharat, S. Moosavikia, B. T. Jahromi, A. Badiei, A. Nemati Kharat, S. Moosavikia, B. Tamaddoni Jahromi, A. Badiei, A. N. Kharat, S. Moosavikia, B. T. Jahromi, A. Badiei, A. Nemati Kharat, S. Moosavikia, B. Tamaddoni Jahromi and A. Badiei, *J. Mol. Catal. A Chem.*, 2011, **348**, 14–19.

28 M. Woolery, in *Kirk-Othmer Encyclopedia of Chemical Technology*, American Cancer Society, 2005.

29 M. T. H. Bhuiyan, M. A. Rahman, M. A. Rahman, R. Sultana, M. R. Mostafa, A. H. Tania and M. A. R. Sarker, *Cogent Phys.*, 2016, **3**, 1265778.

30 G. Silversmit, D. Depla, H. Poelman, G. B. Marin and R. De Gryse, *Surf. Sci.*, 2006, **600**, 3512–3517.

31 D. Briggs, *XPS: Basics principles, spectral features and qualitative analysis*, IM Publications, Chichester, 2003.

32 M. C. Biesinger, L. W. M. Lau, A. R. Gerson and R. S. C. Smart, *Appl. Surf. Sci.*, 2010, **257**, 887–898.

33 G. Silversmit, D. Depla, H. Poelman, G. B. Marin and R. De Gryse, *J. Electron Spectros. Relat. Phenomena*, 2004, **135**, 167–175.

34 Y. Sang, L. Kuai, C. Chen, Z. Fang and B. Geng, *ACS Appl. Mater. Interfaces*, 2014, **6**, 5061–5068.

35 J. Mendialdua, R. Casanova and Y. Barbaux, *J. Electron Spectros. Relat. Phenomena*, 1995, **71**, 249–261.

36 C. Choi, S. Kim, R. Kim, Y. Choi, S. Kim, H. young Jung, J. H. Yang and H. T. Kim, *Renew. Sustain. Energy Rev.*, 2017, **69**, 263–274.

37 I. Andersson, S. Angus-Dunne, O. Howarth and L. Pettersson, *J. Inorg. Biochem.*, 2000, **80**, 51–58.

38 M. Adam and J. E. Hileman, *51V FT-nmr investigations of metavanadate ions in aqueous solutions*, .

39 D. Rehder, T. Polenova and M. Bühl, *Annu. Reports NMR Spectrosc.*, 2007, **62**, 49–114.

40 N. Samart, Z. Arhouma, S. Kumar, H. A. Murakami, D. C. Crick and D. C. Crans, *Front. Chem.*, 2018, **6**, 1–16.

41 L. Pettersson and K. Elvingson, *ACS Symp. Ser.*, 1998, **711**, 30–50.

42 O. Rogers, S. Pattisson, J. Macginley, R. Engel, K. Whiston, S. Taylor and G. Hutchings, *Catalysts.*, , DOI:https://doi.org/10.3390/catal8080311.

43 E. Rozhko, K. Raabova, F. Macchia, A. Malmusi, P. Righi, P. Accorinti, S. Alini, P. Babini, G. Cerrato, M. Manzoli and F. Cavani, *ChemCatChem*, 2013, **5**, 1998–2008.

44 J. C. S. Soares, A. H. A. Gonçalves, F. M. Z. Zotin, L. R. R. de Araújo and A. B. Gaspar, *Catal. Today*, , DOI:10.1016/j.cattod.2020.07.052.

45 J. C. S. Soares, A. H. A. Gonçalves, F. M. Z. Zotin, L. R. R. de Araújo and A. B. Gaspar, *Mol. Catal.*, 2018, 0–1.

46 S. Boudjema, H. Rabah and A. Choukchou-Braham, *Acta Phys. Pol. A*, 2017, **132**, 469–472.

47 K. Sato, M. Aoki and R. Noyori, *Sci. 281*, 1998, **281**, 1646–1648.

48 Z. Z. Zhou, M. Liu, L. Lv and C. J. Li, *Angew. Chemie - Int. Ed.*, 2018, **57**, 2616–2620.

49 G. Malta, S. J. Freakley, S. A. Kondrat and G. J. Hutchings, *Chem. Commun.*, 2017, 53, 11733–11746.

50 Y. Ma, S. Ji, H. Zhou, S. Zhang, R. Li, J. Zhu, W. Li, H. Guo and P. Jin, *RSC Adv.*, 2015, **5**, 90888–90894.

51 M. Safrany Renard, N. Emery, E. M. Roginskii, R. Baddour-Hadjean and J.-P. Pereira-Ramos, *J. Solid State Chem.*, 2017, **254**, 62–68.

52 M. Prześniak-Welenc, M. Nadolska, B. Kościelska and K. Sadowska, *Materials (Basel).*, , DOI:10.3390/ma12203446.

53 F. Liao, T. W. B. Lo, D. Sexton, J. Qu, C. T. Wu and S. C. E. Tsang, *Catal. Sci. Technol.*, 2015, **5**, 887–896.

54 H. Luo, L. Wang, S. Shang, J. Niu and S. Gao, *Commun. Chem.*, 2019, **2**, 17.

55 Z. Chen, S. Pronkin, T.-P. Fellinger, K. Kailasam, G. Vilé, D. Albani, F. Krumeich, R. Leary, J. Barnard, J. M. Thomas, J. Pérez-Ramírez, M. Antonietti and D. Dontsova, *ACS Nano*, 2016, **10**, 3166–3175.

6 General conclusions and future work

6.1 Aerobic oxidation of cyclohexene to cyclohexanediol

6.1.1 Conclusions

Adipic acid (AA) production can be accomplished using a feedstock of cyclohexene, which is a more reactive substrate than the currently used cyclohexane. This higher reactivity lends itself to be oxidised by greener oxidants such as molecular oxygen or H_2O_2. The utilisation of O_2 would be the most desirable oxidant from an industrial perspective since it is cheaper and could be switched with air. In addition, epoxidations are commonly achieved using stoichiometric oxygen donors such as chromates, permanganates, and periodates, which could result in complex heat management needs and by-products that are harmful to the environment. Peroxides are also commonly used to act as radical initiators or stoichiometric oxidants; however, these can increase the cost of the process and produce unwanted waste. The aerobic oxidation of alkenes using Au has been studied in the Hutchings group showing they are active for selective epoxidations of cycloalkenes.[1–5]

Chapter 3 represents an investigation utilising O_2 and Au catalysts, supported on graphite or graphene. These catalysts showed high activity for cyclohexene oxidation, however, it was not selective for the desired epoxide or diol product. Selectivity to cyclohexene oxide and CHD could be enhanced using WO_3 reaching a maximum yield of 10 %. This was achieved using a Au / graphite catalyst with WO_3 after 24 h at 3 bar O_2. This catalyst was prepared *via* sol immobilisation (SI), which consistently exhibited higher activity than their wet impregnation analogues. The enhanced activity of the SI catalysts was most likely due to the narrow size distribution and high dispersion, as confirmed by TEM imaging. The selectivity to epoxidation products is inhibited by mechanistic restrictions, which limit the selectivity to 50 %. In addition, there are also mass transfer limitations caused by the formation of polar products and the generation of in-situ water, which create a biphasic mixture. The issue with increasing conversion due to mass transfer issues could be resolved using a solvent. However, to maximise the atom economy of the reaction, it is more favourable to use solventless conditions. The use of a solvent would also create a need to separate the products, which may also be economically undesirable.

This investigation was extended to a metal-free approach using graphitic oxides, although with a primary focus on allylic oxidation. These catalysts were used because of their prior activity in the epoxidation of 1-decane as demonstrated by Pattisson *et al*. Similarly, the activity of these catalysts correlates strongly with the amount of surface oxygen across their surface albeit to a lesser extent in cyclohexene. However, this difference may be associated with the lower temperature which could result in a lower proportion of surface peroxy species. These surface oxygen species are likely to be responsible for the initiation of the radical reaction. This reaction over extended periods of time can lead to the build-up of polymeric species which affect the mass balance of both blank and catalysed reactions. This effect is also observed in the Au/C reactions.

6.1.2 Future work

The limitations in selectivity caused by mechanistic constraints make it unlikely that the aerobic oxidation of cyclohexene will offer an industrially viable alternative. The epoxide is formed in an equimolar ratio of the allylic alcohol, which is an unwanted by-product. Therefore, this process would suffer from a poor atom economy with an unsustainable cost of handling waste material.

A previously patented approach has used acetaldehyde as a co-reactant to provide the hydroperoxy reactant, which can react with cyclohexene to form the epoxide (Figure 6-1). The by-product of this process would be acetic acid which has its own value as a commodity chemical if it can be separated easily. This reaction was noted to be accomplished using a wide range of metals, such as, vanadium, tungsten, molybdenum, osmium and ruthenium. These catalytic compounds are oxidised under reaction conditions to form the active catalytic state. In addition, an inorganic nitrate salt can be included as a co-catalyst to aid in the reoxidation of spent metal catalyst. The most success was achieved using an ammonium metavanadate catalyst which would be homogeneous under the reaction conditions. Achieving a yield of 23 % after 16 h at a low temperature of 30 °C.[6] However, the aldehydes used in this reaction can also be expensive to use as stoichiometric reagents.

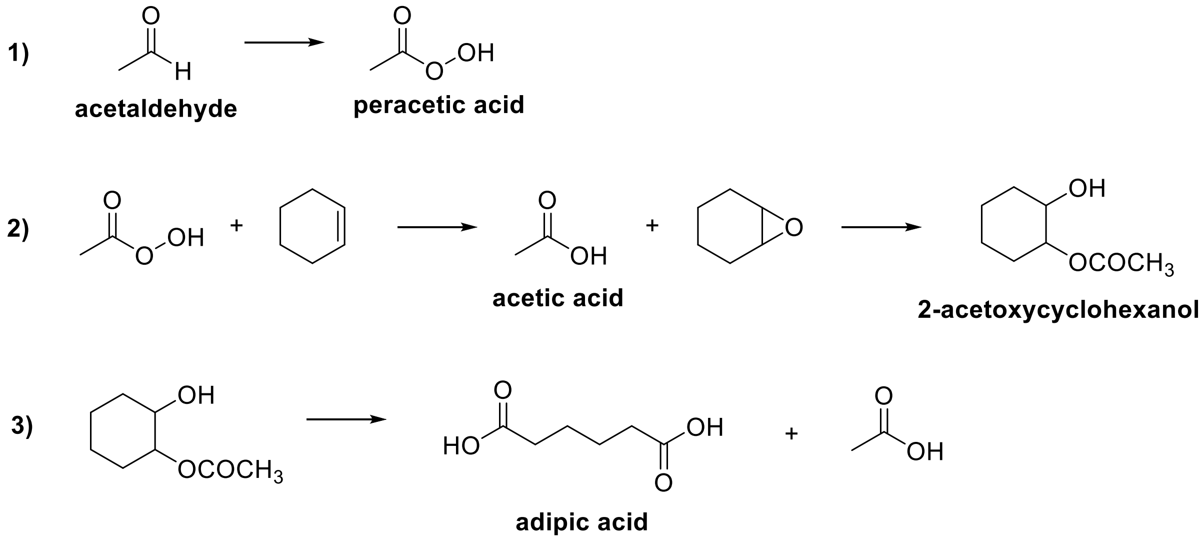

Figure 6-1 Aerobic oxidation of cyclohexene to form adipic acid with acetaldehyde acting as co-reactant and solvent, adapted from US3701804A.[6]

Improvements to this system could start with the testing of heterogeneous catalyst, possibly of the form of the cobalt-molybdenum catalyst, which has been studied by Sebastian *et al.*[7] In this approach the use of cobalt-molybdenum catalysts in addition to an ethylbenzene solvent which can also act as a sacrificial reactant, similar to the use of acetaldehyde. Oxidation of the solvent can form an ethylbenzenehydroperoxide, which can transfer an oxygen atom to cyclohexene in a reaction catalysed by Mo sites. This system achieved a cy-oxide selectivity of 59 % at a 33 % conversion and can subsequently be transformed into the diol in a hydrolysis step. The solvent could also be regenerated through a hydrogenation, which would help satisfy the green principles and help maintain a good atom economy.

6.2 Oxidation of cyclohexene to cyclohexanediol using H_2O_2

6.2.1 Conclusions

Hydrogen peroxide offers a more environmentally attractive proposition to alkyl hydroperoxides, chlorates, and permanganates due to water being the only by-product of its decomposition. Its benefits over O_2 are in its ability to directly oxidise the double bond to form the epoxide and avoid formation of the allylic hydroperoxide as occurs with O_2. However, the oxidation of cyclohexene to AA would require a 4:1 ratio of oxidant to substrate, which would increase the cost to an economically unfeasible amount. A solventless synthesis of AA from cyclohexene was first reported by Sato *et al.*[8] However, this may be a relatively expensive route to execute industrially because of the high requirement of H_2O_2 and the use of a quaternary ammonium salt, which is also not environmentally benign.[9] Despite these drawbacks, this research laid the foundations for future research into solventless H_2O_2 mediated oxidations of cyclohexene.

In chapter 4 $Au/Cs_XH_{3-x}PW_{12}O_{40}$ and $Au/Cs_XH_{4-x}SiW_{12}O_{40}$ catalysts were studied for their suitability as a cyclohexene oxidation catalyst using H_2O_2. Reactions were performed under mild conditions and using a stoichiometric amount of H_2O_2 to produce CHD, which could then be aerobically oxidised to AA. This would remove the need for high amounts of H_2O_2 in the reaction. In the investigation, solvated conditions were utilised leading to a stark contrast in the reactivities of phosphotungstic and silicotungstic acid catalysts, with the Si analogues appearing to be inactive. The use of 1-butanol as solvent proved problematic as it caused a nucleophilic ring-opening of the epoxide intermediate, which was further confirmed by GC-MS. This problem was solved using MeCN as solvent, which aided in confirming the high selectivity of the catalysts to epoxidation products. The immobilisation of Au onto the polyoxometalates resulted in an increase in conversion from 21 % to 24 % for $Au/Cs_3PW_{12}O_{40}$. However, this small gain in conversion did not represent economic sense due to the increased cost of adding Au to the catalyst. Another discovery in this investigation was the improvement to the selectivity caused by a sequential addition of H_2O_2, which exhibited a 5.0 % increase in CHD yield. This addition could be performed at a slower rate with the aid of a HPLC pump and possible mass losses to the atmosphere could be alleviated using an autoclave. However, work on this was not commenced in this investigation.

The disadvantages associated with using a phase transfer catalyst were addressed in the final part of this investigation. A silica-carbon hybrid was prepared as a support for $Cs_3PW_{12}O_{40}$, this material has previously been used to form a Pickering emulsion in work by Wei *et al.*[10] However, in solventless cyclohexene oxidations they were found to be inactive. The hybrid material could require a further reduction step to ensure that the reduced graphitic oxide did not retain any hydrophilic character, as this would hinder the formation of a Pickering emulsion. In addition, a catalyst containing 50 wt. % and 60 wt. % carbon to silica could be prepared to observe if a Pickering emulsion could be successfully created with more hydrophobic character. Furthermore, a greater weight loading of the material in the reaction may also be necessary for a successful reaction.

6.2.2 Future work

Improvements to the current work would entail the use of an autoclave and HPLC pump to improve mass balance and enhance the efficiency of H_2O_2 uptake. These improvements would make a stoichiometric oxidation of cyclohexene to cyclohexanediol (CHD) a possibility at a high selectivity and conversion, making it a more attractive proposition for industry. In addition, recent advancements to the formation of in-situ H_2O_2 would make cyclohexene an appealing substrate for this approach. Pd and Au can be substituted into the polyoxometalate materials used in this project, which are metals that are frequently used in the formation of H_2O_2 from H_2 and O_2.[11,12] The study on polyoxometalates could be extended to the group of molybdovanadates, which has shown activity in the oxidation of cyclohexene and has also been successfully supported on materials such as SBA-15 and MCM-41.[13,14] Molybdovanadates may also exhibit some activity in the second oxidation step involving the oxidative cleavage of CHD to AA, possibly allowing the use of the same catalyst in a two-step reaction.

Currently the nitric acid process for producing AA from cyclohexane is economically attractive. An alternative approach from cyclohexene may become more feasible with reducing costs to the Asahi partial dehydrogenation of benzene which is extracted from crude oil. Using H_2O_2 can provide an environmental benefit to the cyclohexene approach, however the current expense of providing this as an oxidant make it unfeasible that it could replace the nitric acid process. Although, if a stoichiometric amount of H_2O_2 could be used for the first oxidation step, it might provide more incentive since the second step can be achieved aerobically as discussed in Chapter 5. Realistically, a reasonable alternative could be if in-situ H_2O_2 technologies were developed enough to provide high yields of AA. Other bio-renewable approaches have proved successful enough to reach commercialisation and possibly provide a more attractive and sustainable route to AA than cyclohexene or cyclohexane routes. However, these approaches can prove to be highly risky and are dependent on oil prices which can be fairly volatile.

6.3 Oxidation of cyclohexanediol to adipic acid

6.3.1 Conclusions

The second step of the oxidation of cyclohexene to AA, requires an oxidative cleavage of CHD, which can be achieved aerobically. The effectiveness of V_2O_5 was studied by Obara *et al*. achieving a 90 % yield to AA in a 2-catalyst system containing Pt/C and V_2O_5.[15] It was found that Pt/C converted CHD to 2-HCO and the addition of V_2O_5 catalysed the conversion of 2-HCO to AA. The V_2O_5 encountered significant leaching with 50 % remaining in the solid catalyst, the remaining catalyst was stated to be responsible for the reaction. If the reaction was heterogeneously catalysed, then the development of a vanadium catalyst which exhibited minimal leaching would be beneficial.

This investigation proceeded with the preparation of a range of vanadium bronzes, which were incorporated with alloying metals such as, Na, Cu, Ag and Co. These metals were aimed at stabilising the mixed metal oxide structure against leaching and had shown previous success in aqueous applications. The incorporation of Cu and Ag significantly improved the stability of the catalyst whereby leaching was observed at a low value of 5.0 %. Na was less successful in stabilising the material with 36.8 % of the total V found to leach into solution. Interestingly, yield of AA correlated with catalysts demonstrating higher leaching. This led to a study into the effect of homogeneous vanadium, utilising a solution of V_2O_5, which could be inserted into the reactions. The reactions started with 2-HCO as the starting material, negating the necessity of a Pt/C co-catalyst. Only 7.6 ppm V was required to observe a 2.0 % yield of AA, which increased with increasing soluble V. The homogeneous vanadium species was discovered to be in the +5 oxidation state and ^{51}V NMR studies determined that the predominant species was a decavanadate molecule which was unbound to other reaction products or metals.

Ag was considered as an alternative to V owing to its promise in oxidative carbon cleavages demonstrated by other groups, notably by Zhou *et al.* for the selective cleavage of 1,2-diols under mild conditions.[16] Ag_2CO_3 demonstrated promising but limited activity with conversion limited to 3.0 % but selectivity achieving 61 % to AA. To obtain higher conversions and selectivities to AA it may be necessary to use a base such as sodium methoxide, which was applied in the studies by

Zhou *et al.*[16] The selectivity of a WO_3 and Pt/C system was also limited as were attempts with WCl_6 which exhibited low yields of AA. Longer reaction times may result in higher yields of AA, however unwanted products such as glutaric and succinic acid were also observed under the original reaction conditions.

6.3.2 Future work

The catalysis in this reaction was largely homogeneous so an emphasis should be focused on an investigation into metals other than vanadium, which can catalyse a vicinal diol cleavage. This was evidenced by various attempts to stabilise the vanadium catalysts and form a truly heterogenous material. However, small amounts of leaching were still detected in each case. It was confirmed that even low ppm (ca 7 ppm) was enough to catalyse the reaction in solution. Therefore, despite the high activity of vanadium, other more stable metals were investigated. This investigation into alternative metals was commenced with tungsten and silver catalysts; however, they exhibited a limited activity and some selectivity to unwanted side products. Among those tested were Ag_2CO_3 which was soluble and acted as a homogeneous catalyst. Attempts to synthesise an active heterogeneous catalyst from Ag was unsuccessful, however the study could be extended to analyse different nanoparticle sizes, which may prove to be more effective. Other catalysts which have displayed potential in vicinal diol cleavages are PdFe nanoparticles[17] and Co supported on N-doped carbon;[18] however, their effectiveness in cyclic diol cleavages is not clear. A further complication of the cyclic diol cleavage may be a requirement to include Pt as part of the catalyst due to its ability to form 2-HCO. Ideally, the Pt would be immobilised on the same support as the vicinal diol cleavage catalyst to negate the necessity to include two catalysts. This may be achievable for an alloyed PtAg catalyst, which would possibly perform the reaction in a concerted mechanism, without the need for desorption of 2-HCO and movement to another site.

An ambition of this project is to be able to complete the oxidation of cyclohexene to AA in a one-pot synthesis (Figure 6-2). The first step could be achieved with H_2O_2 under solventless conditions, preferentially under N_2 to avoid any aerobic oxidation. If a high selectivity could be achieved, then this would result in CHD solvated in H_2O resulting from the decomposition of H_2O_2. A second step could be accomplished with an atmosphere of O_2 and a vicinal diol cleavage catalyst. This approach would offer a greener alternative to the current cyclohexane based nitric acid approach and could be achieved under milder conditions. However, economically there would be the additional cost of using cyclohexene as a feedstock and with using H_2O_2 as an oxidant. If the cost of these materials was to significantly reduce, then this process may become more viable.

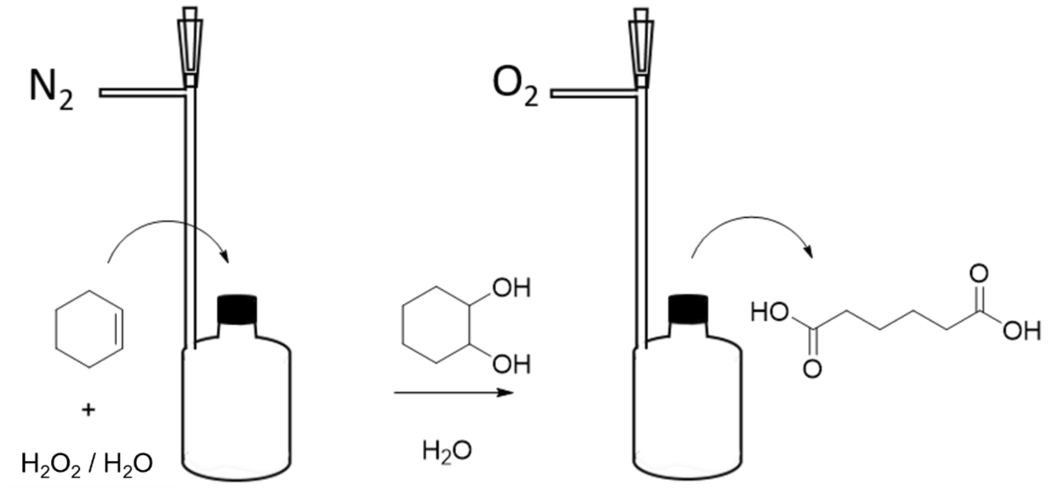

Figure 6-2 Prospective one-pot reaction cyclohexene to form adipic acid.

6.4 References

1 S. Bawaked, Q. He, N. F. Dummer, A. F. Carley, D. W. Knight, D. Bethell, C. J. Kiely and G. J. Hutchings, *Catal. Sci. Technol.*, 2011, **1**, 747–759.

2 S. Bawaked, N. F. Dummer, D. Bethell, D. W. Knight and G. J. Hutchings, *Green Chem.*, 2011, **13**, 127–134.

3 M. D. Hughes, Y.-J. Xu, P. Jenkins, P. Mcmorn, P. Landon, D. I. Enache, A. F. Carley, G. A. Attard, G. J. Hutchings, F. King, E. H. Stitt, P. Johnston, K. Griffin and C. J. Kiely, *Nature*, 2005, **437**, 1132–1135.

4 S. Bawaked, N. F. Dummer, N. Dimitratos, D. Bethell, Q. He, C. J. Kiely and G. J. Hutchings, *Green Chem.*, 2009, **11**, 1037–1044.

5 M. Álvaro, C. Aprile, A. Corma, B. Ferrer and H. García, *J. Catal.*, 2007, **245**, 249–252.

6 W. H. Knoth and G. W. Parshall, *Process for adipic acid manufacture*, US Patent, 1971.

7 J. Sebastian, K. M. Jinka and R. V. Jasra, *J. Catal.*, 2006, **244**, 208–218.

8 K. Sato, M. Aoki and R. Noyori, *Sci. 281*, 1998, **281**, 1646–1648.

9 Y. Deng, Z. Ma, K. Wang and J. Chen, *Green Chem.*, 1999, **1**, 275–276.

10 X. R. Wei, J. Liu, Y. Yang and L. Deng, *RSC Adv.*, 2014, **4**, 35744–35749.

11 E. N. Ntainjua, M. Piccinini, S. J. Freakley, J. C. Pritchard, J. K. Edwards, A. F. Carley and G. J. Hutchings, *Green Chem.*, 2012, **14**, 170–181.

12 S. J. Freakley, R. J. Lewis, D. J. Morgan, J. K. Edwards and G. J. Hutchings, *Catal. Today*, 2015, **248**, 10–17.

13 A. M. Khenkin, R. Neumann, A. B. Sorokin and A. Tuel, *Catal. Letters*, 1999, **63**, 189–192.

14 N. K. K. Raj, S. S. Deshpande, R. H. Ingle, T. Raja and P. Manikandan, *Catal. Letters*, 2004, **98**, 217–223.

15 N. Obara, S. Hirasawa, M. Tamura and Y. Nakagawa, *ChemCatChem*, 2016, **8**, 1732–1738.

16 Z. Z. Zhou, M. Liu, L. Lv and C. J. Li, *Angew. Chemie - Int. Ed.*, 2018, **57**, 2616–2620.

17 F. Liao, T. W. B. Lo, D. Sexton, J. Qu, C. T. Wu and S. C. E. Tsang, *Catal. Sci. Technol.*, 2015, **5**, 887–896.

18 H. Luo, L. Wang, S. Shang, J. Niu and S. Gao, *Commun. Chem.*, 2019, **2**, 17.